BNL-NCS-17541
(ENDF-201)
3rd EDITION (ENDF/B-V) SUPPLEMENT I

# ENDF-201 SUPPLEMENT I
# ENDF/B-V.2 SUMMARY DOCUMENTATION

Compiled and Edited by
B.A. Magurno
Brookhaven National Laboratory
and P.G. Young
Los Alamos National Laboratory

January 1985

NATIONAL NUCLEAR DATA CENTER

BROOKHAVEN NATIONAL LABORATORY
ASSOCIATED UNIVERSITIES, INC.
UPTON, LONG ISLAND, NEW YORK 11973

UNDER CONTRACT NO. DE-AC02-76CH00016 WITH THE
UNITED STATES DEPARTMENT OF ENERGY

Printed in the United States of America
Available from
National Technical Information Service
U.S. Department of Commerce
5285 Port Royal Road
Springfield, VA 22161

NTIS price codes:
Printed Copy: A10; Microfiche Copy: A01

Table of Contents

Table of Contents (cont.)

Contributors

| | |
|---|---|
| E. Arthur | Los Alamos National Laboratory |
| R. Boicourt | Los Alamos National Laboratory |
| G. de Saussure | Oak Ridge National Laboratory |
| R. J. Howerton | Lawrence Livermore National Laboratory |
| D. Larson | Oak Ridge National Laboratory |
| R. E. Mac Farlane | Los Alamos National Laboratory |
| D. G. Madland | Los Alamos National Laboratory |
| B. A. Magurno | Brookhaven National Laboratory |
| F. M. Mann | Hanford Engineering Development Laboratory |
| S. F. Mughabghab | Brookhaven National Laboratory |
| C. Philis | Centre D'Etude de Bruyere-le-Châtel |
| A. Prince | Brookhaven National Laboratory |
| P. F. Rose | Brookhaven National Laboratory |
| R. E. Schenter | Hanford Engineering Development Laboratory |
| R. Sher | Stanford University |
| A. B. Smith | Argonne National Laboratory |
| N. Steen | Bettis Atomic Power Laboratory |
| L. Stewart | Los Alamos National Laboratory |
| L. W. Weston | Oak Ridge National Laboratory |
| R. Q. Wright | Oak Ridge National Laboratory |
| P. G. Young | Los Alamos National Laboratory |

# I INTRODUCTION

# INTRODUCTION

The utilization of new versions of the Evaluated Nuclear Data File, ENDF/B, which is directed by the Cross Section Evaluation Working Group (CSEWG) and issued through the National Nuclear Data Center (NNDC), is greatly enhanced by the availability on a timely basis of appropriate supporting documentation. Because comprehensive reports describing new evaluations are sometimes delayed in time, it is the practice of the CSEWG and NNDC to collect shorter summary documents from contributing evaluators and to provide this information for new issues of ENDF/B libraries. The summaries are intended to be at least as (but preferably more) detailed as the (File 1) comments contained in the computer readable data files, but not as comprehensive as the formal reports describing the evaluations.

The purpose of the present publication is to provide the summary documentation for Revision 2 of the General Purpose File of ENDF/B-V. Revision 2 embodies a series of updates for important materials in the ENDF/B-V libraries in advance of the more comprehensive changes that will accompany a complete version change to ENDF/B, Version VI. The most curent edition of the ENDF/B library is therefore comprised of the Revison 2 updated materials, the Revision 1 materials modified earlier, and the original ENDF/B-V, Rev. 0 materials that thus far have not been modified.

The Revision 1 release consisted of two parts; a) the issuance of three new materials and b) corrections of minor bookkeeping errors. The three new materials issued were Sulfur (MAT 1347), Gallium (MAT 1358) and Bismuth (MAT 1375). The Sulfur documentation was completed in time to be included in ENDF-201[1]. The documentation for Bismuth was completed and issued as an ANL[2] report. The Gallium documentation is included in Section II of this report.

The Revision 2 summaries were written by members of the CSEWG Evaluation Committee responsible for the various evaluations. The materials included for Revision 2 are those on ENDF/B Version V tapes 556 to 563 (General Purpose File). Revision 2 also includes partial evaluations of Special Purpose files for actinide, dosimetry, activation and fission-product data, but documentation for these files will appear elsewhere.

Section II contains summary documents for the evaluations that were completely or extensively modified during Revision 2. Much of the data in these evaluations differs significantly from ENDF/B-V, Revision 0, and these files should be reprocessed before using in any applied problems. Less extensive changes were made to the evaluations in Section III. Complete reprocessing of these materials may not be necessary for all applications, depending on the sensitivity of specific problems to the changes described in Section III. Section IV describes modifications that were made to the fission energy release parameters (ENDF/B File 1) for the fissionable nuclei. These changes were necessary to provide an internally consistent data file and to facilitate documentation of the file. Finally, Section V summarizes a series of modifications made to the covariance files of the major fissionable nuclei, including cross correlation information.

For additional information concerning the evaluated files as well as the corresponding experimental data, contact:

National Nuclear Data Center
Brookhaven National Laboratory
Upton, New York 11973

1. "ENDF/B Summary Documentation", BNL-NCS-17541 (ENDF-201), compiled by R. R. Kinsey, July 1979.

2. "Measured and Evaluated Neutron Cross Sections of Elemental Bismuth", ANL/NDM-51, A. B. Smith, P. Guenther, D. Smith and J. Whalen, Argonne National Laboratory and R. Howerton, Lawrence Livermore Laboratory, April 1980.

## II SUMMARY OF MAJOR REVISIONS

# SUMMARY DOCUMENTATION FOR $^{7}$Li

by

Phillip G. Young
Los Alamos National Laboratory
Los Alamos, New Mexico 87545

## I. SUMMARY

The Revision 2 evaluation for ENDF/B-V is based primarily upon a covariance analysis of the neutron-induced data that was available by Summer, 1981 (Yo81). The evaluation also includes a complete reanalysis of all elastic and inelastic angular distribution data, a division of the (n,nt) cross section into a series of excitation energy bins that permit inclusion of accurate energy-angle correlations for emission neutrons, and complete covariance files for all cross-section data and (n,nt) neutron emission spectra.

## II. COVARIANCE ANALYSIS

The evaluation utilized the GLUCS code system, developed by Hetrick and Fu (He80), to perform covariance analyses of each of the major cross-section types for which experimental data exist. That is, GLUCS was used to determine evaluated cross sections and covariances for each reaction type from inputted experimental cross sections and covariances. The results of the GLUCS analysis were then combined using the ALVIN (Ha75) code under the constraint that all partial reactions sum to the total cross sections, with full account being taken of all covariances.

Using a constant 49-point energy grid, independent covariance analyses were carried out with GLUCS for the following four reactions or combinations of reactions:

1. total cross section (MT1);
2. elastic plus (n,n$'_1$) cross section to the first excited state of $^{7}$Li (MT2 + MT51);
3. (n,nt) cross sections (sum of MT52 + MT53 + ... + MT82);
4. (n,2n) plus (n,2nd) plus (n,3np) plus (n,d) cross sections (MT16 + MT24 + MT25 + MT104).

The GLUCS results for reactions 2-4, which sum to the total cross section, were then combined with the results of 1 using the ALVIN code.

The elastic plus (n,n$'_1$) was treated together because most of the available elastic scattering measurements do not resolve the first excited state. A separate GLUCS analysis was carried out for the extensive $^{7}$Li(n,n'$\gamma$) data that are available, which corresponds to the (n,n$'_1$) cross section. These results were used to separate the (n,n$'_1$) cross section from the combined elastic plus (n,n$'_1$) cross section determined in the main GLUCS/ALVIN analysis. Similarly, the combined (n,2n) plus (n,d) results from the GLUCS/ALVIN analysis were split into the constituent (n,2n), (n,2nd), and (n,d) reactions using ENDF/B-V data.

To perform this analysis, it was necessary to obtain covariance matrices for each experimental data measurement. In some instances, sufficient information was available to directly infer the correlations in the experimental data. In most cases, however, it was necessary to make simple generic assumptions regarding the correlations present in different types of measurements. For example, modern total cross-section measurements were generally assumed to have a normalization error of the order of 0.5% due to sample thickness and composition uncertainty. Greater normalization uncertainty was assumed for older measurements. The final GLUCS/ALVIN cross sections were not found to be highly sensitive to the exact assumptions made, although it was observed that significant overestimates of correlations could distort results, especially in energy regions where measured data are scarce.

All available experimental data for which error estimates were possible were used in the GLUCS analyses. A simple error doubling procedure was followed for measurements that differed by more than two standard deviations from trial results from GLUCS. Such a procedure was necessary for some 12 experiments out of the 56 used in the work. A total of 4200 data points were included in the analysis.

The only experimental data available in the energy range 15-20 MeV are the total and (n,n'γ) cross sections. Therefore, in order to permit an accurate separation of the partial cross sections at these energies, an optical-model analysis was performed covering the energy range 10-20 MeV. The elastic angular distribution measurements of Hogue et al. (Ho79) at 10, 12, and 14 MeV and the evaluated total cross section from 10-20 MeV were fit using the SCATOPT code (Be80). The resulting spherical optical parameters are given in Table I. These results were used to compute elastic cross sections from 16-20 MeV for inclusion in the GLUCS analysis.

TABLE I

SPHERICAL OPTICAL MODEL PARAMETERS FOR n + $^{7}$Li
INTERACTIONS WITH $10 \leqq E_n \leqq 20$ MeV

| | r(fm) | a(fm) |
|---|---|---|
| V (MeV) = 42.94 - 0.35 E | 1.206 | 0.718 |
| $W_{SD}$ (MeV) = 3.974 - 0.027 E | 1.05 | 0.757 |
| $V_{SO}$ (MeV) = 5.500 | 1.15 | 0.57 |

The adjustment factors from the ALVIN analysis, that is, the factors required to multiply the ALVIN input cross sections (output cross sections from the GLUCS analysis) in order to minimize the composite $\chi^2$ of the entire cross section/covariance system are shown in Table II for the full analysis grid. As expected, the adjustment factors for the total cross section are nearly unity because of the generally high accuracy of these measurements. The largest adjustments are seen for the elastic + (n,n$'_1$) below the (n,nt) threshold and for the (n,2n) + (n,d) reaction. In both cases, the input experimental data are generally older and the errors larger. The adjustments for the elastic + (n,n$'_1$)

TABLE II

ADJUSTMENT FACTORS FOR n + $^{7}$Li CROSS SECTIONS
DETERMINED IN ALVIN ANALYSIS

| E (MeV) | F (Total) | F (n,n+n,n'$_1$) | F (n,nt) | F (n,2n+n,d) |
|---|---|---|---|---|
| 0.10 | 0.9911 | 1.1482 | | |
| 0.14 | 0.9993 | 1.1953 | | |
| 0.18 | 0.9979 | 1.2689 | | |
| 0.22 | 1.0103 | 0.7534 | | |
| 0.24 | 0.9997 | 0.9518 | | |
| 0.26 | 0.9990 | 1.1489 | | |
| 0.28 | 0.9966 | 1.1931 | | |
| 0.30 | 0.9958 | 1.0712 | | |
| 0.34 | 1.0034 | 0.9673 | | |
| 0.40 | 1.0001 | 0.9920 | | |
| 0.50 | 1.0004 | 0.9601 | | |
| 0.60 | 0.9997 | 1.0056 | | |
| 0.75 | 1.0000 | 0.9859 | | |
| 0.90 | 0.9995 | 1.0302 | | |
| 1.00 | 0.9995 | 1.0700 | | |
| 1.20 | 0.9985 | 1.0861 | | |
| 1.40 | 0.9988 | 1.0553 | | |
| 1.80 | 1.0003 | 1.0187 | | |
| 2.20 | 0.9979 | 1.0625 | | |
| 2.60 | 0.9997 | 1.0779 | 1.0000 | |
| 3.00 | 0.9993 | 1.0466 | 1.0055 | |
| 3.40 | 1.0006 | 0.9747 | 0.9214 | |
| 3.80 | 1.0002 | 0.9661 | 0.9926 | |
| 4.20 | 1.0004 | 0.9865 | 0.9161 | |
| 4.40 | 0.9999 | 0.9795 | 0.9997 | |
| 4.60 | 1.0002 | 0.9815 | 0.9945 | |
| 5.00 | 0.9996 | 0.9906 | 1.0055 | |
| 5.40 | 1.0012 | 0.9519 | 0.7032 | |
| 5.60 | 1.0000 | 0.9825 | 0.9976 | |
| 5.80 | 0.9985 | 1.0090 | 1.0581 | |
| 6.00 | 0.9994 | 1.0029 | 1.0407 | |
| 6.50 | 1.0008 | 0.9748 | 0.9221 | |
| 7.00 | 0.9995 | 1.0008 | 0.9994 | |
| 7.50 | 0.9981 | 1.0210 | 1.0427 | |
| 8.00 | 1.0004 | 0.9537 | 0.9869 | 1.0000 |
| 8.50 | 0.9999 | 1.0075 | 0.9983 | 1.0000 |
| 9.00 | 1.0000 | 0.9909 | 0.9942 | 0.9917 |
| 9.50 | 0.9999 | 0.9507 | 1.0031 | 0.9998 |
| 10.00 | 1.0008 | 0.9763 | 0.9533 | 0.8757 |
| 11.00 | 0.9998 | 0.9956 | 0.9927 | 1.0152 |
| 12.00 | 0.9996 | 0.9993 | 1.0110 | 1.1895 |
| 13.00 | 0.9996 | 1.0030 | 1.0061 | 1.1973 |
| 14.00 | 0.9983 | 1.0304 | 1.0070 | 1.0046 |
| 15.00 | 0.9999 | 1.0307 | 0.9979 | 0.4575 |
| 16.00 | 0.9997 | 1.0353 | 1.0673 | 1.0214 |
| 17.00 | 0.9997 | 1.0432 | 1.0933 | 1.0311 |
| 18.00 | 0.9997 | 1.0506 | 1.1127 | 1.0393 |
| 19.00 | 0.9995 | 1.0568 | 1.1783 | 1.0645 |
| 20.00 | 0.9994 | 1.0569 | 1.2218 | 1.0826 |

and for the (n,nt) reaction above the latter's threshold differ from unity by generally less than 5%, highlighting the consistency of the total and partial cross sections from the GLUCS analysis. An exception is the 0.70 adjustment factor for the (n,nt) reaction at 5.4 MeV. At this energy, however, the (n,nt) reaction is changing rapidly with energy, and the large adjustment probably indicates a slight inconsistency between the energy scales of the total and (n,nt) measurements.

The adjusted points from the ALVIN analysis of the total cross sections vary smoothly with energy and were used directly to generate the final evaluated data file. The (n,nt) results, however, are not as smooth because of the smaller and less consistent experimental data base that went into the analysis. It was therefore necessary to smooth the (n,nt) results for the final cross-section evaluation. The smoothed curve is compared to the ALVIN results (points with error bars) in Fig. 1.

RESULTS

The final evaluated total and elastic + $(n,n_1')$ cross sections from 2-16 MeV are compared with selected experiments and to ENDF/B-V in Fig. 2. Similarly, the evaluated $^7Li(n,nt)$ cross section is compared with the measurements used in the analysis and with ENDF/B-V in Fig. 3. It is readily seen from Figs. 2 and 3 that the major difference between these results and ENDF/B-V is a lowering of the (n,nt) cross section between 6-20 MeV and a corresponding increase in the elastic plus $(n,n_1')$ cross section. The (n,nt) cross section is in excellent agreement with the recent measurement by Smith et al. (Sm81) between 7-9 MeV but is significantly higher than the Swinhoe data (Sw79). The (n,nt) results are 15% lower than ENDF/B-V at 10 MeV and 9% lower at 14 MeV.

The evaluated elastic and inelastic neutron angular distributions were obtained from a Legendre coefficient analysis of all the available experimental data. The experiments of Lane et al.(La61), Knitter and Coppola (Kn68), Knox et al. (Kn79), Knox and Lane (Kn81), and Hogue et al. (Ho79) were emphasized in the elastic angular distribution evaluation. Figure 4 compares the measurements of Hogue et al. at four energies to the new evaluation. Because there are no elastic angular distribution data above 14.1 MeV, the spherical optical model calculation described above was used to extrapolate the angular distributions to 20 MeV.

Because the customary representations used for ENDF/B evaluations do not permit inclusion of energy-angle correlation effects in secondary neutron emission data from (n,xn) reactions, we used an excitation-energy binning technique to represent the $^7Li(n,nt)$ reaction. With this technique the continuum neutrons from (n,nt) reactions are described as a series of lumped, discrete scattering levels, each representing a bin of excitation energy in the residual nucleus and each with a separate energy-dependent cross section and angular distribution. When these data are processed into multigroup form, the kinematic energy-angle correlations are automatically preserved.

The evaluation of the (n,nt) data into excitation energy bins was based upon the neutron emission spectrum measurements of Lisowski et al. (Li80), using monoenergetic neutrons from the Los Alamos Tandem Van de Graaff at 6, 10, and 14 MeV. The results are compared in Fig. 5 with the spectra measured at the Oak Ridge Electron Linear Accelerator (ORELA) by Morgan (Mo78) at 55° and 125°

for an incident neutron energy bin of 12.45-14-95 ($\bar{E}$ = 13.7) MeV. The broad peaks at higher energy are from elastic scattering, and the lower energy spectra result from the (n,nt) reaction.

Complete covariance files for the major cross-section types and for the excitation energy bins are included in the evaluation. The latter data determine the correlated errors in the neutron emission spectra from the (n,nt) reaction. Covariances for the cross sections were taken directly from the GLUCS-ALVIN analysis, when possible, and are based on those results for all major reaction types. The errors and cross correlations for the emission spectra were estimated from the Lisowski (Li80) experimental errors, but the final results were adjusted via the ALVIN code to be consistent with results from the independent GLUCS-ALVIN cross-section analysis.

## ENDF/B-V.2 FILES

### File 1.

MT=451. Descriptive data.

### File 2. Resonance Parameters

MT=151. Effective scattering radius = $0.28906 \times 10^{-12}$ cm.
Resonance parameters not included.

### File 3. Neutron Cross Sections

MT=1 Total Cross Section. ENDF/B-V.0 adopted below 0.1 MeV because no new experimental data available. Variance-covariance analysis above 0.1 MeV based on Me70, Go71, Ha78, Fo71, Ka57, Br58, Pe60, Co52, La79, and Hi68. Errors doubled near 260-keV resonance for Hi68, Me70 data.

MT=2 Elastic Cross Section. V-C analysis used data of Th56, Wi56, Kn68, Ba63A, Ho68, Li80, Co67, Wo62, Re66, Ar64, Hy68, La61, Kn81, Kn79, Ho79, La64. Errors tripled near 260-keV resonance for La61, La64 data. Optical model analysis of Ho79 data used to calculate cross sections above 14 MeV for V-C analysis.

MT=4 (n,n'γ) + (n,n') α-t. Sum of MT=51-82.

MT=16 (n,2n) Cross Section. V-C analysis of MT16 + MT24 used exp. data of As58, Mc61, Ma69. Separation of MT16 and MT24 follows the ratio of the ENDF/B-V.0 data.

MT=24 (n,2n) α-d Cross Section. See comment for MT16.

MT=25 (n,3n) α-p Cross Section. Smooth curve drawn above 14 MeV so as to approximately agree with Ma69, Ko71 data.

MT=51 (n,n'γ) Cross Section. Separate V-C analysis used data of Pr72, O180, Sm76, Di74, Mo78, Fr55, Kn81, Be60, Ba53, Ch61, Kn68, Gl63, Ho68, Ba63A. Errors doubled on Fr55, Be60, and tripled on Ch61.

MT=52-82 (n,n') α-t Cross Section. Except for MT56, excitation energy bins were constructed such that calculated neutron emission spectra agree with the measurements by Li80 at 5.96, 9.83, and 14.1 MeV incident energy. Interpolation of cross sections between energies based on linear interpolation of computed CM emission spectra, suitably contracted or expanded to conserve energy. Above 14.1 MeV, the exp. emission shape was used to infer the cross section, with the shapes again suitably expanded to conserve energy. MT=56 corresponds to a real state with $E_x$=4.63 MeV in Li-7. The MT56 result is based on a smooth curve through the resolved data of Li80, Ho68, Ba63A, Ho79, Co67, Yo65, Wo62, Re66, Hy68. At all incident energies, the sum of MT=52-82 was constrained to be the (n,nt) cross section from the V-C analysis.

MT=102 (n,γ) Cross Section. Adopted from ENDF/B-V.0

MT=104 (n,d) Cross Section. Adopted from ENDF/B-V.0. Data agree approximately with experiments of Ba53, Ba63B, Li73, and disagree with Mi61.

File 4. Neutron Angular Distributions.

MT=2 Legendre coefficients obtained by drawing smooth curve through fitted coefficients from measurements listed under MF3/MT2. Data of La61, Kn68, Kn79, Kn81, Ho79 emphasized. Optical model calculations used above 14 MeV.

MT=16 Tabulated distribution obtained by integrating three-body phase space calculation over secondary energy.

MT=24 Tabulated distribution obtained by integrating four-body phase space calculation over secondary energy.

MT=25 Tabulated distribution obtained by integrating five-body phase space calculation over secondary energy.

MT=51 Legendre coefficients obtained from R-matrix analysis of Kn81 below 6 MeV, joined smoothly to DWBA calculation above 8 MeV using DWUCK code and optical parameters from MT=2 analysis. Some use also made of Li7(p,p') data.

MT=52-71 Legendre coefficients obtained from analysis of Li80 experiment described in MF3 above (except MT56). Coefficients for MT=56 obtained by drawing smooth curves through fitted values from experiments listed above under MF3/MT56, especially Ho68 and Ho79.

MT=72-82 Isotropy assumed.

File 5. Neutron Energy Distributions

MT=16 Tabulated distribution obtained by integrating three-body phase space calculation over secondary angle.

MT=24 Tabulated distribution obtained by integrating four-body phase space calculation over secondary angle.

MT=25 Tabulated distribution obtained by integrating five-body phase space calculation over secondary angle.

File 12. Photon Multiplicities.

MT=51 Multiplicity is 1.0 everywhere since first level in Li7 is only known photon emitter.

MT=102 Adopted directly from ENDF/B-V.0. Due to the absence of data, the transitions are simply reasonable estimates.

File 14. Photon Angular Distributions.

MT=51 Isotropy assumed at all energies.

MT=102 Isotropy assumed for all gammas at all energies.

File 33. Neutron Cross Section Covariances.

MT=1 Below 100 keV, derived from MT2 + MT102. Above 100 keV, taken directly from GLUCS-ALVIN analysis.

MT=2 Below 100 keV, 5% correlated error assumed. Above 100 keV, derived from MT1-MT4-MT851 (MT16 + MT24 lump), which is the GLUCS-ALVIN analysis result.

MT=4 From GLUCS-ALVIN analysis [MT51 matrix combined with Reaction 3 (above) covariance matrix].

MT=16 Lump indicator only.

MT=24 Lump indicator only.

MT=25 Ad hoc estimate.

MT=51-82 Lump indicators only.

MT=102 Ad hoc estimate based on experimental spread and error below 1 MeV.

MT=104 Ad hoc estimate based on experimental errors.

MT=851 Lump of MT16 + MT24 errors. As determined in GLUCS-ALVIN analysis.

MT=852 Single lump of MT=51 error. Determined in independent GLUCS analysis of MT51 experimental data (see above).

MT=853 Lump of MT=52-55 errors. Determined in simultaneous analysis using ALVIN to constrain (adjust) the partial reaction covariances for MT=853-859 to be consistent with the total (n,nt) covariance (reaction 3 above) from the GLUCS-ALVIN analysis. Input covariances prior to the adjustment were estimated from experimental data described under MF=3 above.

MT=854 Single lump of MT=56 determined from scatter and errors of experimental data (see MF=3 description).

MT=855 Lump of MT=57-61 determined as described under MT=853.

MT=856 Lump of MT=62-66 determined as described under MT=853.

MT=857 Lump of MT=67-71 determined as described under MT=853.

MT=858 Lump of MT=72-76 determined as described under MT=853.

MT=859 Lump of MT=77-82 determined as described under MT=853.

***Note. The procedure used to determine MT=852-859 has the result that these matrices sum only approximately to MT=4. Therefore, it is recommended that MT=852-859 be used only for calculating neutron emission spectrum uncertainties and that MT=1, 2, 4, 25, 102, 104, 851 be used for calculating cross section uncertainties.

REFERENCES

Ar64 A. H. Armstrong et al., Nucl. Phys. 52, 505 (1964).
As58 V. J. Ashby et al., UCRL-5239 (1958).
Ba53 M. E. Battat, F. L. Ribe, Phys. Rev. 89, 80 (1983).
Ba63A R. Batchelor, J. H. Towle, Nucl. Phys. 47, 385 (1963).
Ba63B J. F. Barry, J. Nucl. Ener. A/B17, 273 (1963).
Be60 J. Benveniste, et al., UCRL-6074 (1960).
Be80 O. Bersillon, Bruyeres-le-Chatel, private comm. to E. D. Arthur, (1980).
Br58 A. Bratenahl et al., Phys. Rev. 110, 927 (1958).
Br63 F. Brown et al., J. Nucl. Ener. A/B17, 137 (1963).
Ch61 D. M. Chittenden, A-ARK-61, 1 (1961).
Co52 J. H. Coon et al., Phys. Rev. 88, 562 (1952).
Co67 J. A. Cookson et al., Nucl. Phys. A91, 273 (1967).
Di74 J. K. Dickens et al., ORNL-TM-4538 (1974).
Fo71 D. G. Foster, Jr., D. W. Glasgow, Phys. Rev. C3, 576 (1971).
Fr55 J. M. Freeman et al., Phil. Mag. 46, 17 (1955).
Gl63 N. P. Glzakov, Atomaya Energiya 15, 416 (1963).
Go71 C. A. Goulding et al., COO-3058-1 (1971).
Ha75 D. R. Harris et al., LA-5987 (1975).
He80 D. M. Hetrick, C. Y. Fu, ORNL/TM-7341 (1980).
Hi68 C. T. Hibdon, F. P. Mooring, Conf. Neut. Cross Sec. Tech., Washington (1968), p. 159.
Ha78 J. A. Harvey et al., DOE/NCD-12/U (1978), p. 229.
Ho68 J. C. Hopkins et al., Nucl. Phys. 107, 139 (1968).
Ho79 H. H. Hogue et al., Nucl. Sci. Eng. 69, 22 (1979).
Hy68 M. Hyakutake et al., EANDC(J)-10 (1968), p. 22.
Ka57 L. N. Katsaurov et al., Atom Ener. Suppl. 5, 90 (1957).
Kn68 H.-H. Knitter, M. Coppola, Conf. Neut. Cross Sec. Tech., Washington (1968), p. 827.
Kn79 H. D. Knox et al., Nucl. Sci. Eng. 69, 223 (1979).
Kn81 H. D. Knox, R. O. Lane, Nucl. Phys. A359, 131 (1981).
Ko71 K. F. Koral et al., Nucl. Phys. A175, 156 (1971).
La61 R. O. Lane et al., Ann. Physics 12, 135 (1961).
LA64 R. O. Lane et al., Phys. Rev. 136, B1710 (1964).
LA79 G. P. Lamaze et al., Bull. Am. Phys. Soc. 24, 862 (1979).
Li73 R. H. Lindsay, et. al., Nucl. Phys. A199, 513 (1973).
Li80 P. W. Lisowski, et al., LA-8342 (1980).
Li81 H. Liskien, A. Paulsen, Annals Nucl. Ener. 8, 423 (1981).
Ma69 D. S. Mather, L. F. Pain, AWRE-O-47/69 (1969).
Mc61 M. H. McTaggart, H. Goofellow (AWRE), pers. comm. to R. J. Howerton (1961).
Me70 J. W. Meadows, J. F. Whalen, Nucl. Sci. Eng. 41, 351 (1970).
Mi61 M. Mikhailini et al., Sov. Prog. Neut. Phys. (1961), p. 185.
Mo78 G. L. Morgan, ORNL/TM-6247 (1978).
Ol80 D. K. Olsen, et al., Nucl. Sci. Eng. 74, 219 (1980).
Os61 A. R. Osborn, H. W. Wilson, AWRE-NR/C-1/61 (1961).
Pe60 J. M. Peterson, et al., Phys. Rev. 120, 521 (1960).
Pr72 G. Presser, R. Bass, Nucl. Phys. A182, 321 (1972).
Re66 V. Regis, et al., J. Physique Suppl. C1-84 (1966).
Ro62 L. Rosen, L. Stewart, Phys. Rev. 126, 1150 (1962).
Sm76 D. L. Smith, Nucl. Sci. Eng. 61, 540 (1976).
Sm81 D. L. Smith, et al., Nucl. Sci. Eng. 78, 359 (1981).

Sw79 M. T. Swinhoe, C. A. Uttley, NBS Spec. Pub. 594, 246 (1980).
Th56 R. G. Thomas, et al., Phys. Rev. 101, 759 (1956).
Wi56 H. B. Willard, et al., Phys. Rev. 101, 756 (1956).
Wo62 C. Wong, et al., Nucl. Phys. 33, 680 (1962).
Wy58 M. E. Wyman, M. M. Thorpe, LA-2235 (1958).
Yo65 A. Yoshimura, et al. (Kyushu U.), Personal communication NNDC (1964).
Yo81 P. G. Young, Trans. Am. Nucl. Soc. 39, 272 (1981).

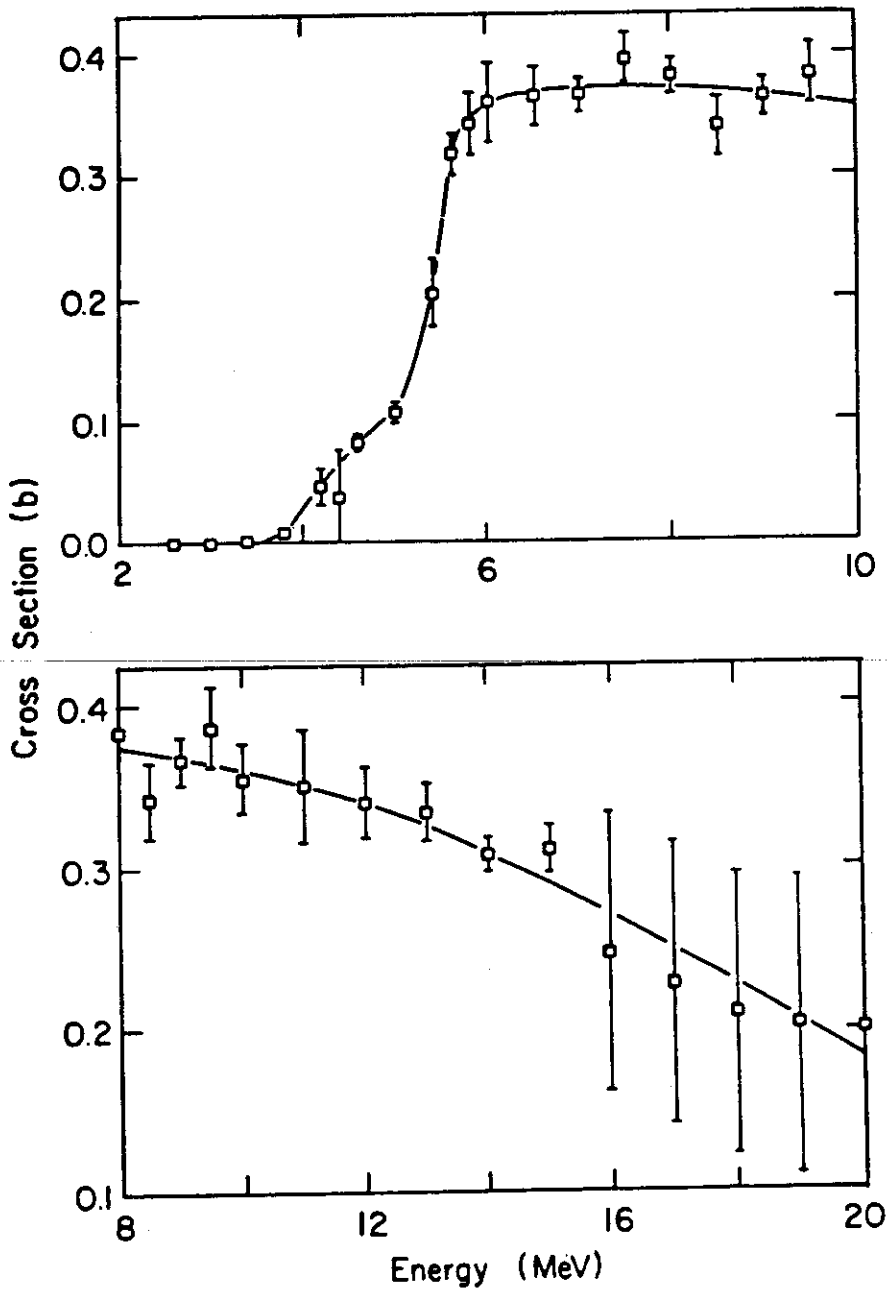


Fig. 1.

Comparison of smoothed evaluated $^{7}$Li(n,nt) cross section with fitted cross sections and standard deviations from the GLUCS/ALVIN analysis.

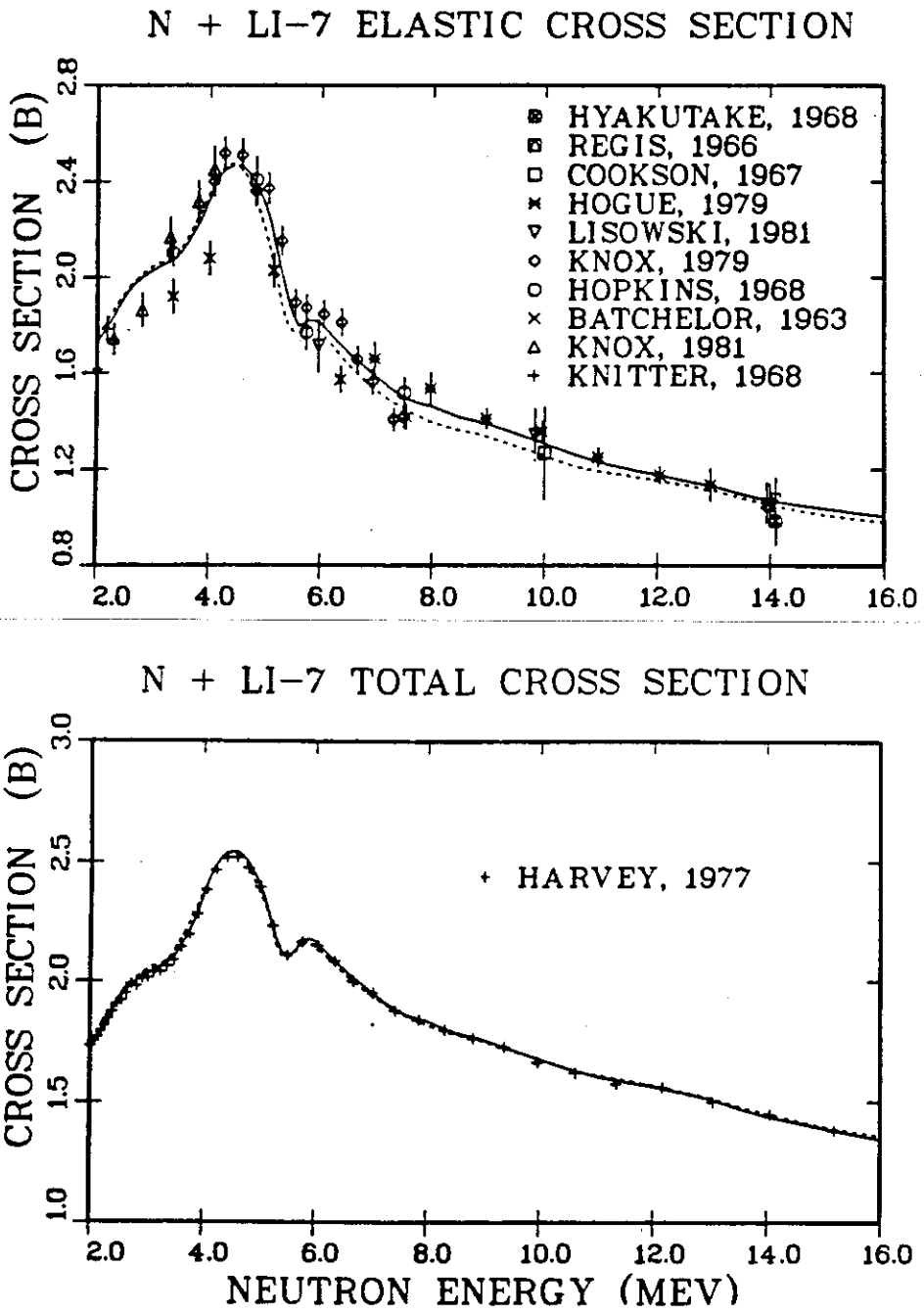


Fig. 2.

Evaluated and experimental n + $^{7}$Li elastic plus (n,n') (upper half) and total (lower half) cross sections. The solid curve is the present result and the dashed curve is ENDF/B-V.

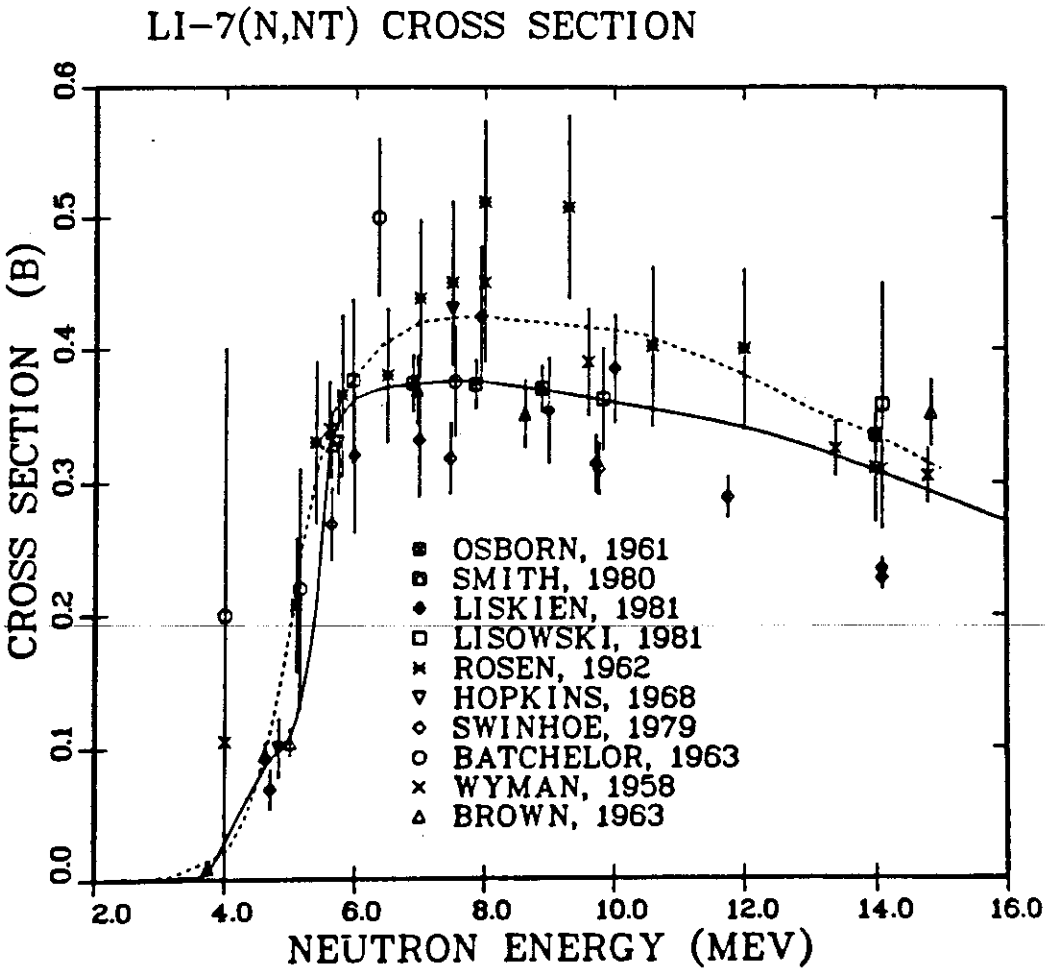


Fig. 3

Evaluated and experimental $^{7}$Li(n,nt) cross sections. The solid curve is the present result and the dashed curve is ENDF/B-V.

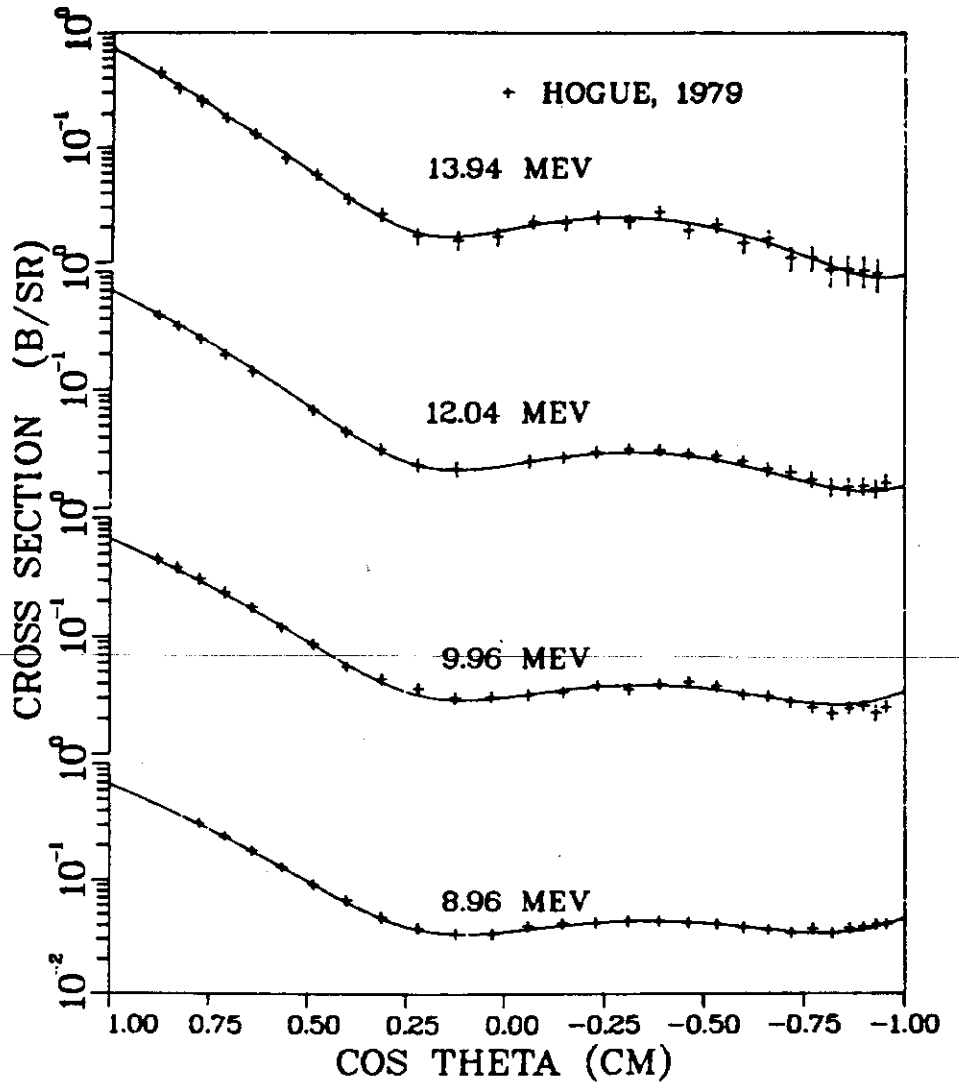


Fig. 4

Comparison of the n + $^{7}$Li elastic angular distribution measurement by Hogue et al. (Ho79) with the present evaluation. Both measurement and evaluation include the $^{7}$Li(n,n') reaction to the first excited state of $^{7}$Li.

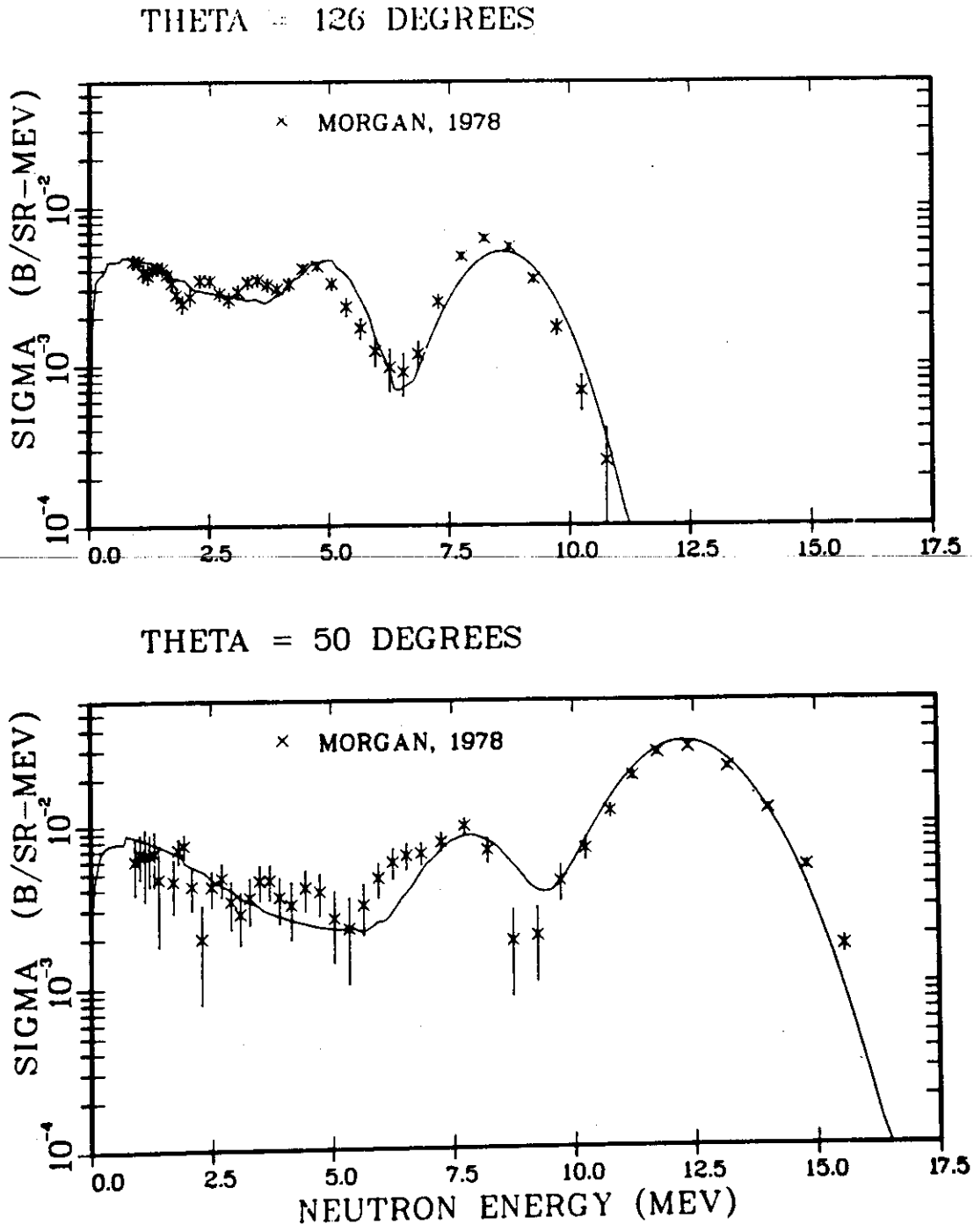


Fig. 5.

Measured (Mo78) and evaluated neutron emission spectra from n + $^{7}$Li reactions with 13.7-MeV incident neutrons.

# REVISION 2 OF ENDF/B-V CALCIUM

by

Duane Larson
Oak Ridge National Laboratory
Oak Ridge, Tennessee 37831

The following summary is condensed from Ref. 1.

A new calculation of neutron and gamma-ray production cross sections for calcium has been made from 8 MeV to 20 MeV to include precompound effects. Nuclear model calculations used for the previous evaluation[2] for calcium lacked the effects of precompound particle emission. Such effects are now known to be generally important above 5 or 10 MeV for nearly all reaction cross sections. The defect can be removed with the aid of an updated version of the model code TNG, now called TNG1, which accounts for particles emitted in the precompound reaction. To insure consistency, particlularly to maintain energy balance, all other reaction cross sections, including gamma-ray production cross sections and spectra, are reevaluated through calculation.

It should be emphasized here that our purpose is to remedy a major defect known to exist in the previous evaluation from 8 to 20 MeV. In this context, it is necessary to maintain continuity at 8 MeV for all reaction cross sections. For this reason, we made no efforts to update level energies, spins, parities, deformation parameters, etc., although we are aware of improvements in these areas. Also, it is not our intention to examine any new measured data.

In view of the lack of experimental data for many of the reaction channels which are open, this reevaluation could not have been performed without very extensive theoretical analyses. Parameters required as input to TNG1 were the same as determined previously.

TNG1 simultaneously calculated the binary-reaction, tertiary-reaction, and resulting gamma-ray production cross sections. TNG1 also computes the compound and precompound cross sections in a consistent fashion and conserves angular momentum in both compound and precompound reactions. The results from TNG1, found to agree reasonably with available data, were incorporated into the calcium evaluation for the energy range from 8 to 20 MeV.

The following MF/MT sections and subsections were changed from 8-20 MeV, and matched to the ENDF/B-V evaluation at 8 MeV: 3/1, 2, 3, 4, 22, 28, 52-69, 91, 103, 107, 108, 111, 112; 5/22, 28, 91; 12/4, 22, 28, 103, 107; and 15/4, 22, 28, 103, 107. Sections 3/70-73 were deleted. The user is encouraged to read Ref. 1 for futher details.

## REFERENCES

1. D. M. Hetrick and C. Y. Fu, "A Calculation of Neutron and Gamma-Ray Production Cross Sections for Calcium from 8 to 20 MeV," Oak Ridge National Laboratory Report ORNL/TM-7752, ENDF-308, June 1981.

2. C. Y. Fu, Atomic Data and Nucl. Data Tables 17, 127 (1976).

# REVISION 2 OF ENDF/B-V IRON

by

Duane Larson
Oak Ridge National Laboratory
Oak Ridge, Tennessee 37831

The following summary is condensed from Ref. 1. Revisions were made in four areas to the ENDF/B-V evaluation[2,3] for iron.

## INELASTIC SCATTERING IN $^{57}$Fe AND $^{58}$Fe

The cross sections for inelastic scattering to 21 levels in $^{57}$Fe and two levels in $^{58}$Fe were included and combined as 14 sections (MT numbers) as shown in Table 1. Corresponding gamma-ray production data (file 12) and covariance data (file 33) were also provided.

These cross sections were ignored in the ENDF/B-V file for natural iron because of their low abundances: 2.1% for $^{57}$Fe and 0.3% for $^{58}$Fe. However, for analyses[4,5] of shields or critical assemblies in which iron is the dominant component, the contribution of the low-lying levels of the minor iron isotopes to neutron slowing-down is important. This is mainly because $^{57}$Fe is an odd isotope whose levels are dense. In particular, its first four excited levels are below 846 keV which is the energy of the first excited state of $^{56}$Fe. It is therefore apparent that the low-lying levels of $^{57}$Fe cannot be ignored for slowing down of neutrons below 846 keV if there are little or no other materials in the system that have levels comparable in energy to those of $^{57}$Fe.

Sensitivity calculations by Kawai et al.[4] for the inelastic scattering cross sections of $^{57}$Fe and $^{58}$Fe were performed with a central source for a 100-cm-diam iron sphere. It was shown that a neutron flux below 10 keV at 30 cm from a 0.65-MeV source increased 60% after including the cross sections for inelastic scattering to the low-lying levels of $^{57}$Fe and $^{58}$Fe in the ENDF/B-IV file. Even for a 14-MeV source the increase still amounts to 20%. More recently, an analysis[5] of the Argonne iron benchmark, using the ENDF/B-V iron evaluation, showed that $k_{eff}$ was too low by about 0.7%. After incorporating calculated cross sections for inelastic scattering to the 12 lowest levels of $^{57}$Fe into the file, a repeat calculation raised $k_{eff}$ by 0.73%.

For the above reason, an update for MAT 1326 appeared worthwhile. Since no experimental data were available, the evaluation of the needed cross sections had to be based on model calculations. Level energies, spins, and parities were taken from the Table of Isotopes.[6] Optical model parameters were those found satisfactory for $^{54}$Fe and $^{56}$Fe by Arthur and Young.[7] Level density parameters were based on the formalism of Gilbert and Cameron.[8] The TNG1 code[9] was used for the calculation. The code was based on the Hauser-Feshbach formalism with a consistent treatment of width-fluctuation corrections for the discrete levels and the continuum.

Gamma-ray production cross sections for $E_n < 2.122$ MeV were based on the branching ratios given in the Table of Isotopes.[6] Some branching ratios were combined, particularly those for the lumped levels. Some weak gamma rays of similar energies were also combined. For $E_n > 2.122$ MeV, gamma-ray production data already present in the ENDF/B-V files were based on measurements made for natural iron, therefore containing the pertinent information for the minor isotopes.

Since all inelastic scattering cross sections for $^{57}Fe$ and $^{58}Fe$ were based on calculation, they were assumed to be fully correlated among the levels and for all energies with an estimated standard deviation of 20%.

## IMPROVED CROSS SECTIONS

The (n,2n), (n,d), (n,t) and (n,$^3$He) cross sections evaluated by Arthur and Young[7] were judged to be superior to the ENDF/B-V evaluation and were adopted. New data for (n,2n) and (n,d) were used in their evaluation.[7] The corresponding covariance data in file 33 were slightly adjusted to reflect the improved knowledge of these cross sections.

## ENERGY BALANCE AND GAMMA-RAY PRODUCTION

Energy imbalances reported by MacFarlane[10] were corrected for $E_n$ between 2.122 and 20 MeV by adjusting the total gamma-ray production cross sections in file 13 to reproduce the estimated values of heating per collision. The adjusted results approach those of ENDF/B-IV. The largest changes occurred for $E_n$ between 12 and 20 MeV.

A detailed calculation was made for the heating per collision using the new evaluated file that has the changes proposed above incorporated into it. The results are shown in Table 2 for some representative energies along with the values derived from our model calculations. The latter values may be good to 20%. The former values are substantially lower than the latter and some are negative, particularly near 14 MeV. It is apparent that the specific energies for either or both the outgoing neutrons and outgoing gamma rays need to be reduced. The specific energy is the energy of the outgoing particle times its production cross section. Examining all the available data, we found little room for changing either the neutron production cross sections, the secondary neutron energy distributions, or the secondary gamma-ray energy distributions. But as is evident from Fig. 1, there is some flexibility in reducing the gamma-ray production cross sections. Therefore, we adjusted the total gamma-ray production cross sections to reproduce the more desirable heating values derived from our model calculations. The adjusted results, also shown in Fig. 1 for $E_\gamma > 0.68$ MeV, approach those used in ENDF/B-IV and represent a compromise of all experimental data. The results also agree with the Arthur and Young evaluation.[7]

The total gamma-ray production cross sections in ENDF/B-V was replaced with the adjusted results as a plausible solution to the energy imbalance problem for $E_n > 2.122$ MeV.

For $E_n$ < 2.122 MeV, energy imbalances still exist. Here the gamma rays produced are from inelastic scattering and radiative capture. The problem was due to the neutron-energy-dependent capture gamma-ray spectra given in the file. For each neutron group, the gamma rays produced may be representative of just one isotope, having its own unique Q-value. Therefore, a single Q-value, as required by the ENDF/B-V formats, cannot adequately define the energy balance. This is the well-known "elemental Q-value problem," but solutions other than providing isotopic evaluations are still wanting.

RESONANCE PARAMETERS

Resonance parameters (file 2) and covariances (file 32) were revised so that the files and the corresponding report[3] are consistent. A few clerical errors were also corrected. However, changes were either very small or involved insignificant resonances.

REFERENCES

1. C. Y. Fu, "Summary of ENDF/B-V Evaluations for Carbon, Calcium, Iron, Copper, and Lead and ENDF/B-V Revision 2 for Calcium and Iron," ORNL/TM-8283, ENDF-325, Oak Ridge National Laboratory, Oak Ridge, Tenn., 1982.

2. C. Y. Fu and F. G. Perey, "Evaluation of Neutron and Gamma-Ray Production Cross Sections for Natural Iron (ENDF/B-V MAT 1326)," ORNL/TM-7523, ENDF-302, Oak Ridge National Laboratory, Oak Ridge, Tenn., September 1980.

3. C. M. Perey and F. G. Perey, "Evaluation of Resonance Parameters for Neutron Interaction with Iron Isotopes for Energies up to 400 keV," ORNL/TM-6405, ENDF-298, Oak Ridge National Laboratory, Oak Ridge, Tenn., September 1980.

4. M. Kawai, N. Yamano, and K. Koyama, "Request to Evaluating Neutron Cross Section of Structural Material for Shielding Application," p. 586 in Proc. Conf. Nucl. Cross Sections for Tech., NBS-SP-594, 1979.

5. A. B. Smith, Argonne National Laboratory, personal communication to C. Y. Fu, Oak Ridge National Laboratory, Oak Ridge, Tenn., 1980.

6. C. M. Lederer and V. S. Shirley, Table of Isotopes, 7th Edition, 1978.

7. E. D. Arthur and P. G. Young, "Evaluated Neutron-Induced Cross Sections for $^{54,56}$Fe to 40 MeV," LA-8626-MS, ENDF-304, Los Alamos Scientific Laboratory, 1980.

8. A. Gilbert and A. G. W. Cameron, Can. J. Phys. 43, 1446 (1965).

9. C. Y. Fu, "A Consistent Nuclear Model for Compound and Precompound Reactions with Conservation of Angular Momentum," ORNL/TM-7042, Oak Ridge National Laboratory, Oak Ridge, Tenn., May 1980.

10. R. E. MacFarlane, "Energy Balance of ENDF/B-V," Trans. Am. Nucl. Soc., 33, 681 (1979).

**Table 1. The energy levels of the iron isotopes as grouped for the MT numbers in ENDF/B-V Mod 2**

| MT | Fe-54 (keV) | Fe-56 (keV) | Fe-57 (keV) | Fe-58 (keV) |
|---|---|---|---|---|
| 51 | | | 14.4 | |
| 52 | | | 137 | |
| 53 | | | 367 | |
| 54 | | | 707 | |
| 55 | | | | 811 |
| 56 | | 846 | | |
| 57 | | | 1008 | |
| 58 | | | 1198,1255,1357 | |
| 59 | 1408 | | | |
| 60 | | | 1628,1725 | 1675 |
| 61 | | | 1975,1989 | |
| 62 | | 2084 | | |
| 63 | | | 2117 | |
| 64 | | | 2207 | |
| 65 | | | 2335,2355 | |
| 66 | | | 2454,2455,2506 | |
| 67 | | | 2565,2597 | |
| 68 ↓ | | 2654 ↓ | | |
| 90 | | 4505 | | |

**Table 2. Some typical heating values calculated from the modified ENDF/B-V ($H_5$), from model calculations ($H_c$), and the necessary adjustments in gamma-ray production cross sections**

| $E_n$ (MeV) | $H_5$ (MeV) | $H_c$ (MeV) | $\Delta G_\gamma$ (mb) |
|---|---|---|---|
| 3 | -0.075 | 0.063 | -426 |
| 5 | 0.087 | 0.117 | -76 |
| 7 | -0.019 | 0.194 | -440 |
| 9 | 0.13 | 0.301 | -280 |
| 11 | -0.003 | 0.44 | -588 |
| 14 | -0.463 | 0.70 | -1335 |
| 17 | 0.46 | 1.03 | -1353 |

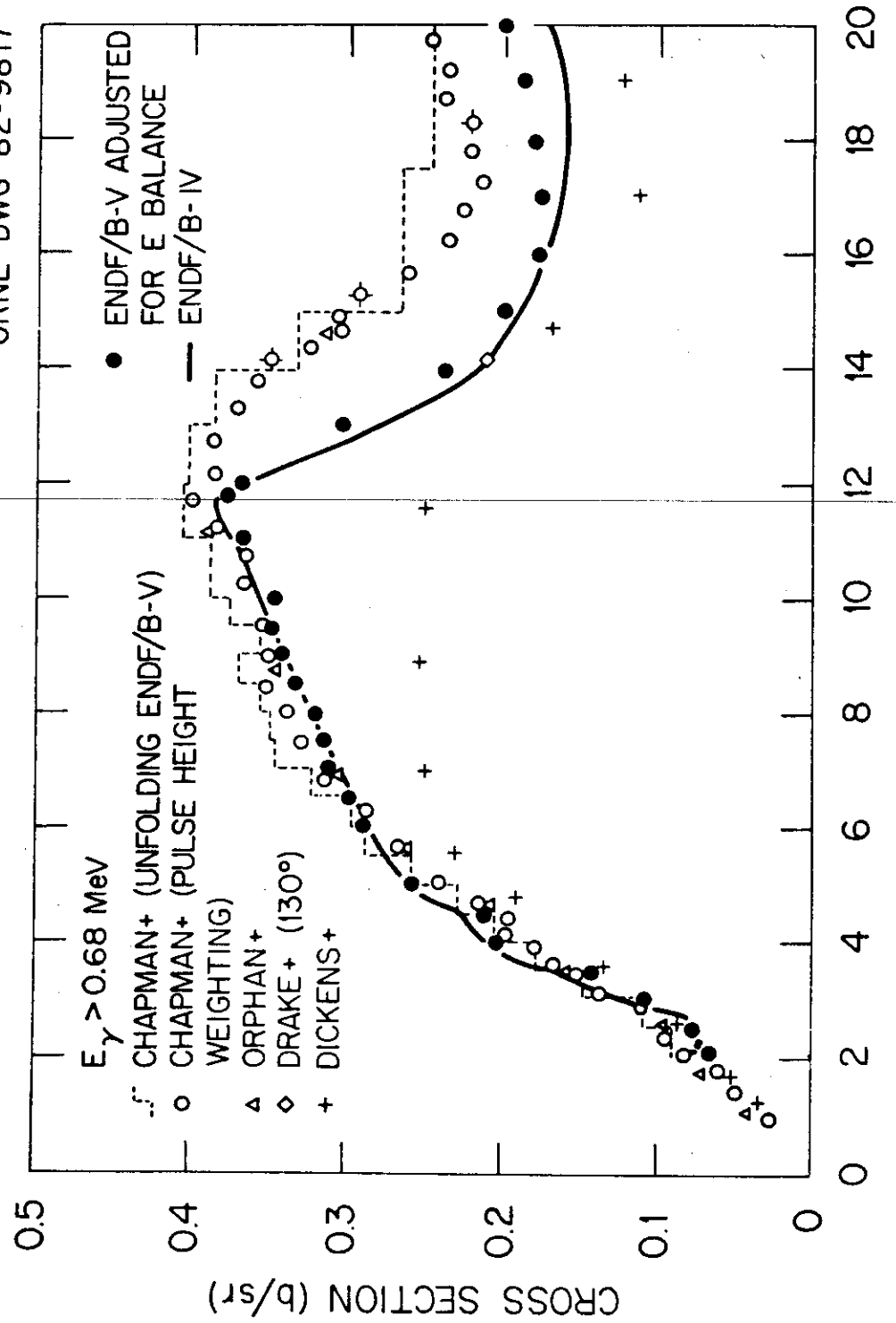


**Fig. 1. Various experimental and evaluated gamma-ray production cross sections for natural iron.**

# REVISION 2 OF ENDF/B-V COBALT

by

Said Mughabghab
Brookhaven National Laboratory
Upton, New York 11973

The hollerith description for Cobalt-59 ENDF/B-V.0 is a proper representation of the data and procedures used in the evaluation. Due to a summing error, the tabulated data in the ENDF/B-V.0 file contain errors in the total, File 3 (MT=1) and inelastic continuum cross sections, File 3 (MT=91).

Minor errors (mispunches) were found in File 12, MT=102 (record 2724) and File 15, MT=3 (records 2758, 2761).

A modification was made to the thermal capture cross section covariance value, MF=33, MT=102 (record 3296).

The errors in the tabulated data have been corrected and the file reissued in ENDF/B-V.2.

# SUMMARY DOCUMENTATION FOR Ga

by

Phillip G. Young
Los Alamos National Laboratory
Los Alamos, New Mexico 87545

and

Robert J. Howerton
Lawrence Livermore National Laboratory
PO Box 808, Livermore, Calif. 94550

## SUMMARY

Gallium is present in small amounts in certain fast critical benchmark experiments and should be included in calculations of those experiments. Before the present work, a gallium evaluation was not included in the ENDF/B-V data base. The present analysis is based on an earlier evaluation (ENDL-78),[1] which was updated to better represent more recent experimental data. Changes were made to the total, elastic, (n,γ), and (n,2n) cross sections. The effect of utilizing this evaluation in a calculation of the JEZEBEL benchmark experiments is to raise the calculated eigenvalue ($k_{eff}$) by 0.0039.[2] The present evaluation was included in Revision 1 of ENDF/B-V.

## REVISIONS TO ENDL-78

The neutron total cross section in ENDL-78 was revised to better describe the data of Walt et al.[3] from 0.3-3.0 MeV and the data of Foster and Glasgow[4] from 2.5 to 15 MeV. The new evaluation (solid curve) is compared with ENDL-78 (dashed curve) and experimental data[5] in Figs. 1 and 2.

The radiative capture cross section from 0.8 to 4 keV in the ENDL-78 evaluation was revised slightly to better agree with the measurement of Konks,[6] as shown in Figs. 3 and 4. More extensive changes were made between 20 keV and 5 MeV to improve agreement with the data of Dovbenko et al.[7] and Zaikin et al.[8]

The (n,2n) cross section was modified at all energies from threshold to 20 MeV on the basis of the data of Frehaut and Mosinski.[9] The result is compared with ENDL-78 (dashed curve) and Frehaut's data in Fig. 5.

The cross sections for all other neutron reactions with Ga we left unchanged from the ENDL-78 evaluation, with the exception of elastic scattering, which was adjusted to absorb our changes in the total, (n,γ), and (n,2n) cross sections. The neutron angular and energy distributions and all gamma-ray production data were simply translated from ENDL-78. The elastic angular distribution is shown at three energies between 3.2 and 14.7 MeV in Fig. 6.

ENDF/B-V.1 FILES

File 1. Miscellaneous Information.

MT =451. Descriptive Data

File 2. Resonance Parameters.

MT = 151. Effective scattering radius = $0.7192 \times 10^{-12}$ cm. Resonance parameters not included.

File 3. Neutron Cross Sections.

MT = 1. Total Cross Section.
Based on smooth curve through experimental data, especially data of Newson (Ref. 10) below 30 keV, Walt (Ref. 3) from .3-2 MeV, Foster (Ref. 4) from 2-15 MeV, and Peterson (Ref. 11) near 20 MeV.

MT = 2. Elastic Cross Section.
Taken as the difference between the evaluated total cross section and the sum of the evaluated nonelastic cross section.

MT = 16. (n,2n) Cross Section.
The n,2n threshold in $^{69}$Ga is 10.46 MeV, and the n,2n threshold in $^{71}$Ga is 9.44 MeV. In the n,2n evaluation for natural gallium, the threshold was set equal to 9.44 MeV. The evaluation is based on a smooth curve through the data of Frehaut (Ref. 9).

MT = 91. Inelastic Cross Section.
Based on integrated cross sections inferred from two sets of inelastic angular distributions, one for $^{69}$Ga and one for $^{71}$Ga (see Ref. 12). Pure continuum representation used to describe (n,n') reactions.

MT = 102. Radiative Capture Cross Section.
Based on a smooth curve through the available experimental data (see Ref. 13).

MT = 103. (n,p) Cross Section.
The n,p mass difference thresholds for $^{69}$Ga and $^{71}$Ga are 0.13 MeV and 2.05 MeV, respectively. In the n,p evaluation, an effective n,p threshold of 5 MeV was used. Evaluation based primarily on $^{71}$Ga experimental data (see Ref. 13).

MT = 107. (n,$\alpha$) Cross Section.
The n,$\alpha$ cross section in gallium is exoergic. In the evaluation, an effective (n,$\alpha$) threshold of 2 MeV was assumed. Evaluation based on experimental data (see Ref. 13) and nuclear systematics.

File 4. Neutron Angular Distributions.

MT = 2. Elastic Angular Distributions.
Angular distribution was assumed isotropic for neutron energies below 100 keV. At higher energies, the angular distributions were obtained from spherical optical model calculations using the best-fit optical model parameters of Ref. 14. Experimental data available only at 3.2 MeV (Ref. 15).

MT = 16, 19. (n,2n) and Inelastic Angular Distributions.
Assumed isotropic in the lab system for all incident neutron energies.

File 5. Neutron Energy Distributions.

MT = 16. (n,2n) Spectra.
Energy distributions of the secondary neutrons are presented in tabular form and are derived from temperature model calculations, with the assigned temperatures consistent with systematics (see Ref. 1).

MT = 91. Inelastic Spectra.
For energies below, the onset of the preequilibrium process at about 8 MeV, the energy distributions of the secondary neutrons were derived from a temperature model. For incident neutron energies above 8 MeV, the energy distributions of the secondary neutrons were characterized by a two-component model--a temperature component plus a preequilibrium and unresolved direct-interaction component. The method used in selecting the fraction of the inelastically scattered neutrons to be associated with the preequilibrium process is described in Ref. 1.

File 12. Photon Multiplicities.

MT = 102. (n,γ) Production Yield.
Photon multiplicity adjusted to conserve energy.

File 13. Photon Production Cross Sections.

MT = 3. (n,xγ) Production Cross Section.
There are no experimental n,xγ data for gallium. The evaluated n, xγ cross sections were calculated with the NXGAMEL code, using the systematics described in Ref. 16 and summarized in Ref. 1, pgs. 38-41. The evaluated n,xγ cross section is represented as a continuum that has a threshold at 0.4 MeV.

File 14. Photon Angular Distributions.

MT = 3, 102. (n,xγ) and (n,γ) Angular Distributions.
Assumed isotropic in the lab system.

File 15. Photon Energy Distributions.

MT = 3 (n,xγ) Spectra.
Photon energy distributions obtained from the systematics of Ref. 16.

MT = 102 (n,γ) Spectra.
The spectrum of photons from the neutron capture process at thermal neutron energies was taken from the measurements of Ref. 17. This spectrum was assumed to apply at all incident neutron energies up to 20 MeV, but the photon multiplicity was adjusted so as to conserve the total energy of the reaction.

REFERENCES:

1. R. J. Howerton, personal communication of ENDL-78; see also R. J. Howerton, D. E. Cullen, R. C. Haight, M. H. MacGregor, S. T. Perkins, and E. F. Plechaty, "The LLL Evaluated Nuclear Data Library (ENDL): Evaluation Techniques, Reaction Index, and Description of Individual Evaluations," Lawrence Livermore Laboratory report UCRL-50400 Vol. 15, Part A (Sept. 1975).

2. R. B. Kidman, "LASL Benchmarks," in Applied Nuclear Data Research and Development: January 1-March 31, 1980, compiled by C. I. Baxman and P. G. Young, Los Alamos Scientific Laboratory report LA-8418-PR (1980), p. 10.

3. W. Walt, R. L. Becker, A. Okazaki, and R. E. Fields, "Total Fast Neutron Cross Sections of Co, Ga, Se, Cd, Te, Pt, Au, Hg, and Th," Phys. Rev. 89, 1271 (1953).

4. D. G. Foster, Jr., and D. W. Glasgow, "Neutron Total Cross Sections, 2.5-15 MeV, Part 1 Experimental," Phys. Rev. C3, 576 (1971).

5. D. I. Garber and R. R. Kinsey, "Neutron Cross Sections Volume II, Curves," Brookhaven National Laboratory report BNL-325 (1976); data available from the CSISRS Experimental Data Library maintained by the National Nuclear Data Center at Brookhaven National Laboratory.

6. V. A. Konks, personal communication via National Nuclear Data Center, Brookhaven National Laboratory (1964).

7. A. G. Dovbenko, V. E. Kolesov, V. P. Koroleva, and V. A. Tolstikov, Atomnaya Eergiya 26, 67 (1969).

8. G. G. Zaikin, I. A. Korzh, M. V. Pasechnic, and N. T. Skljar, UKR. Fiz. Zh. 16, 1205 (1971).

9. J. Frehaut and G. Mosinski, "Measurement of (n,2n) and (n,3n) Cross Sections at Incident Energies Between 8 and 15 MeV," Proc. Conf. on Neutron Physics, Kiev (1975).

10. H. W. Newson et al., Phys. Rev. 105, 198 (1957).

11. J. M. Peterson et al., Phys. Rev. 120, 521 (1960).

12. D. E. Cullen et al., University of California Radiation Laboratory report UCRL-50400, Vol. 19 (1977).

13. D. E. Cullen et al., University of California Radiation Laboratory report UCRL-50400, Vol. 8, Rev. 1 (1976).

14. F. Becchetti and G. Greenlees, Phys. Rev. 182, 1190 (1969).

15. R. L. Becker et al., Nucl. Phys. 89, 154 (1966).

16. S. Perkins et al, Nucl. Sci. Eng. 57, 1 (1975).

17. V. Orphan et al., Gulf General Atomic report GA-10248 (1970).

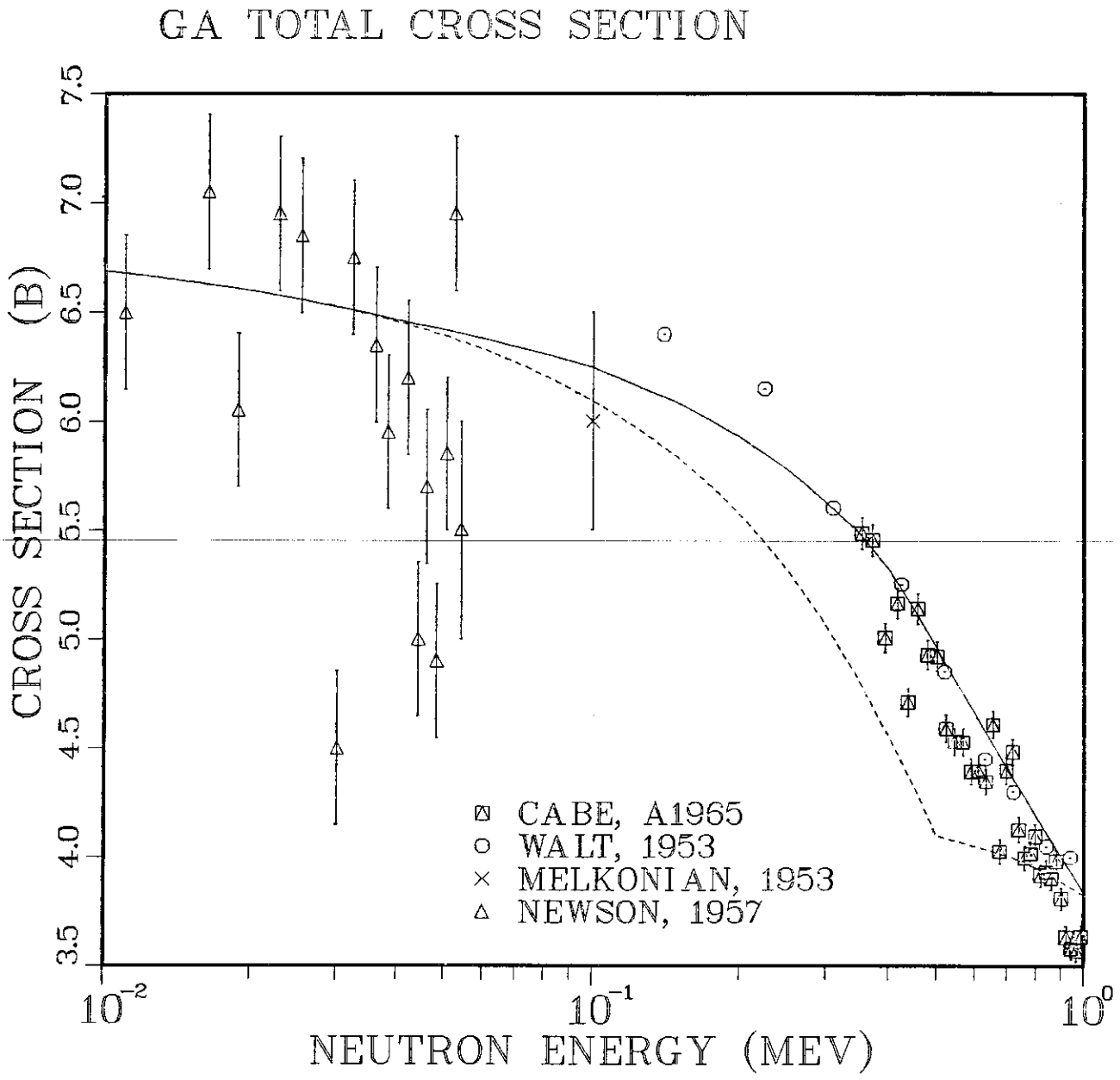


Fig. 1

Gallium total cross section from 0.01-1.0 MeV. The solid and dashed curves are the present and ENDL-78 (Ref. 1) evaluations, respectively. The experimental data are described in Ref. 5.

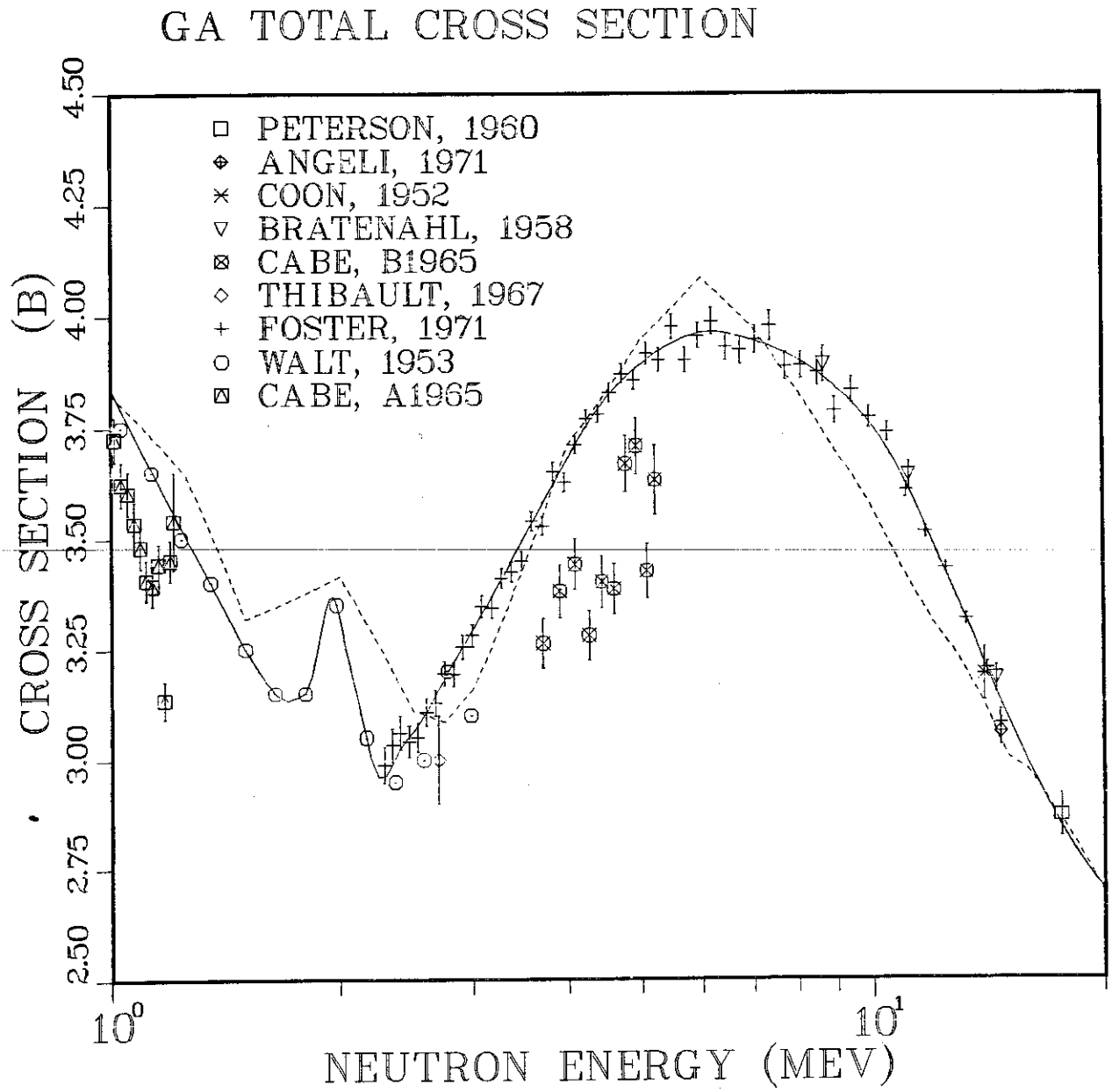


Fig. 2.

Gallium total cross section from 1-20 MeV. The solid and dashed curves are the present and ENDL-78 (Ref. 1) evaluations, respectively. The experimental data are described in Ref. 5.

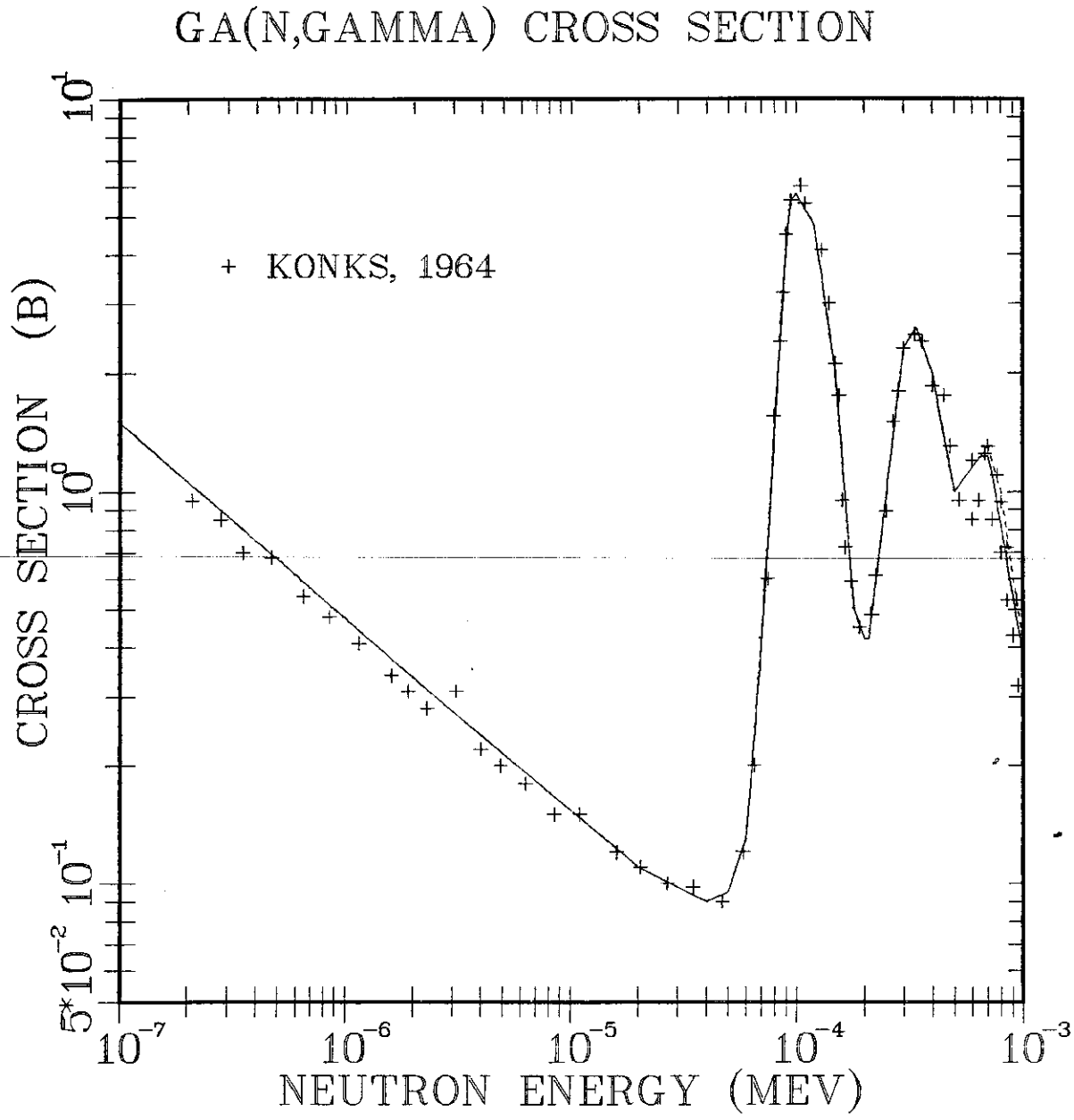


Fig. 3.

The Ga(n,γ) cross section from 0.1 eV to 10 keV. The solid curve is the present evaluation and the dashed curve is ENDL-78.

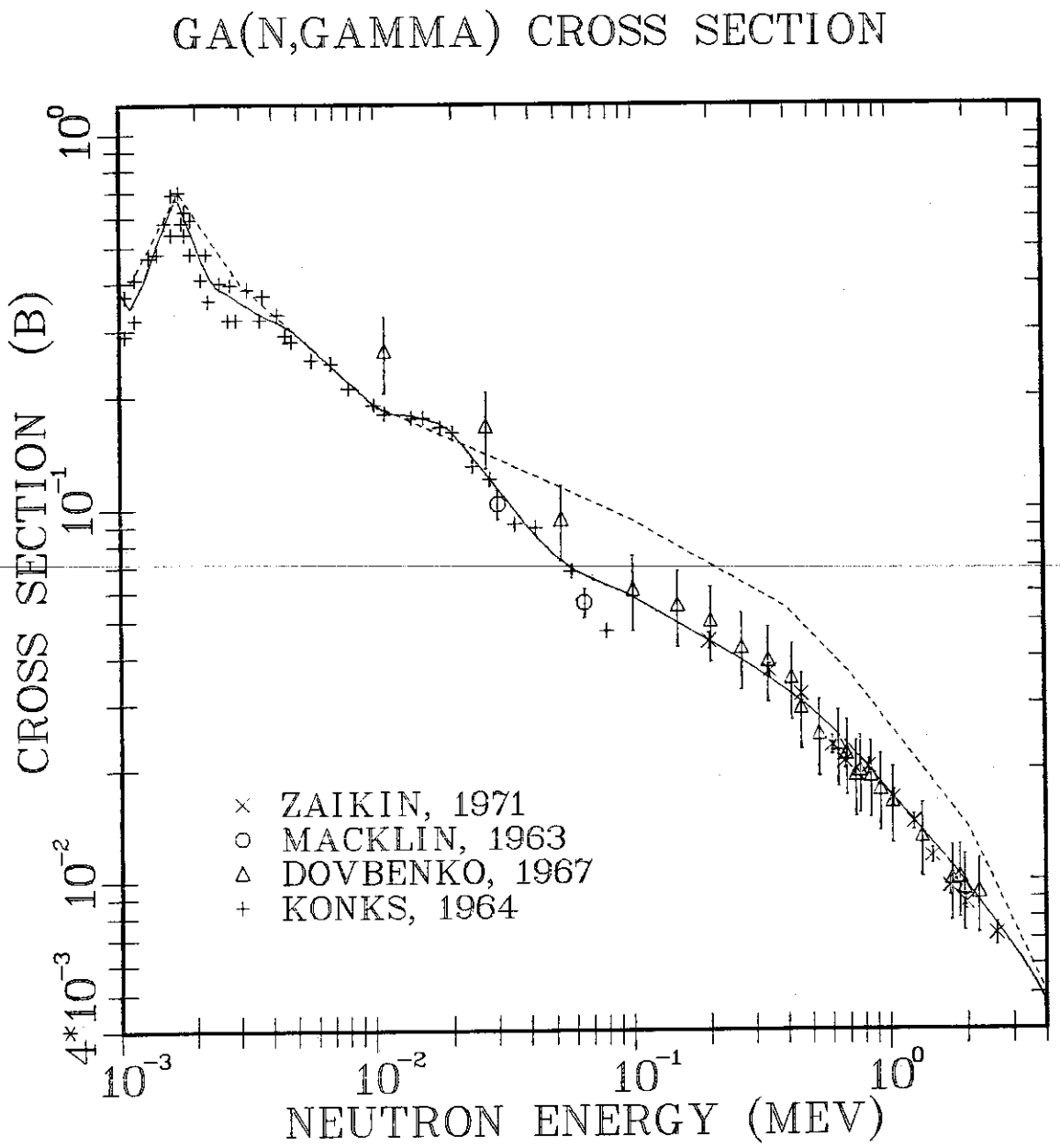


Fig. 4.

The Ga(n,γ) cross section from 1 keV to 4 MeV. The solid curve is the present evaluation and the dashed curve is ENDL-78.

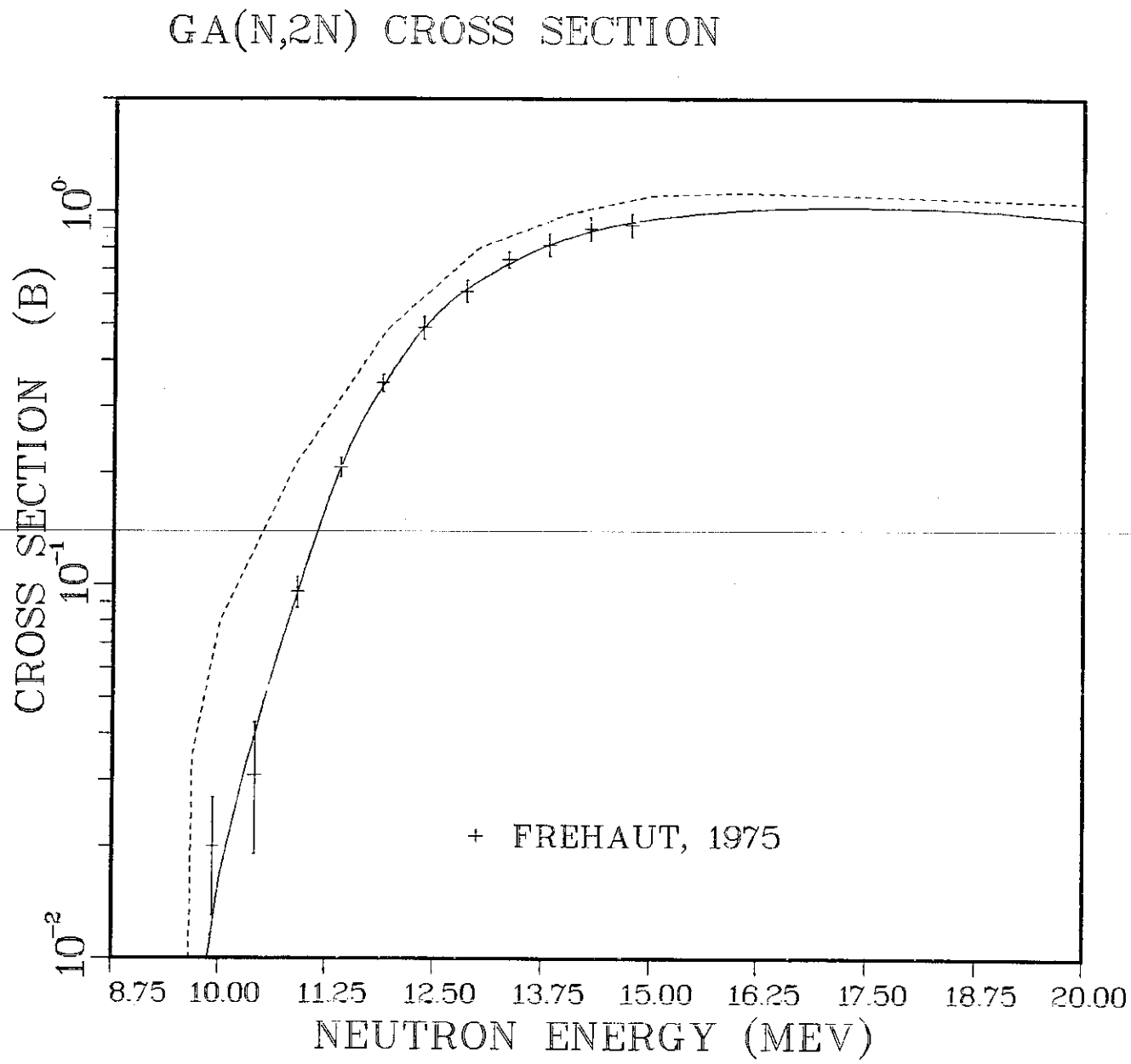


Fig. 5.

Gallium (n,2n) cross sections from threshold to 20 MeV. The solid and dashed curves are the present and ENDL-78 (Ref. 1) evaluations, respectively. The experimental data are from Ref. 9.

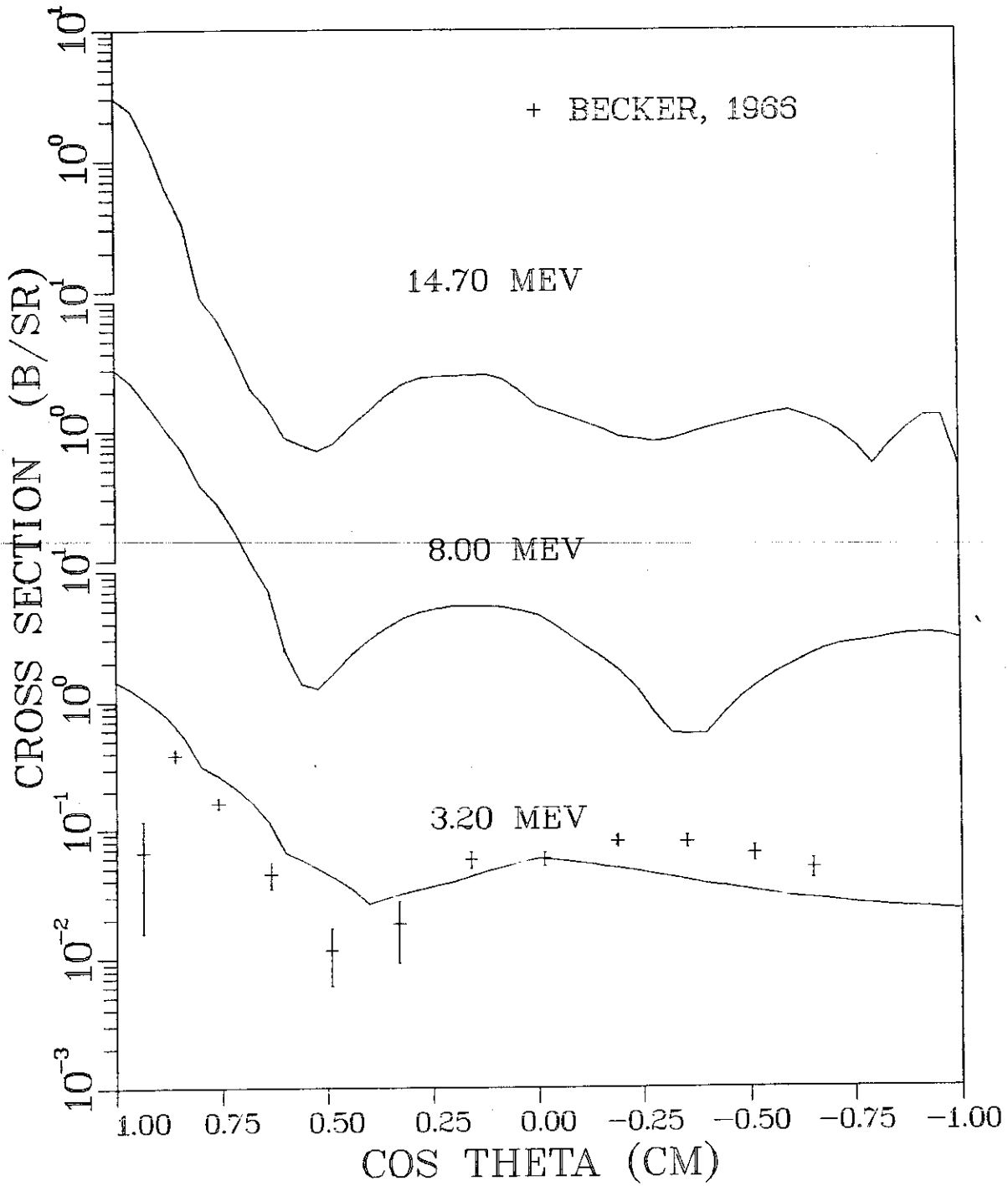


Fig. 6.

Elastic scattering angular distributions at 3.2, 8.0, and 14.7 MeV from the present evaluation. The experimental data at 3.2 MeV are from Ref. 15.

37-Rb- 85 BNL/BRC Eval-Oct79 A. Prince

Supersedes ENDF/B-IV Mat 153 by Schmittroth and Schenter (HEDL).

File 2. Resonance Parameters

Resonance Parameters based on recent publication of 'NEUTRON CROSS SECTION' Vol I (Z=1 to 60) S.F.Mughabghab et al., Academic Press N.Y. 1981.

L=0 number of resonances = 76.
Average total width = 4.36 eV.
Average gamma width = 0.205 eV.
S-wave strength function = 1.06-04.
Average level spacing = 241.5 eV.
L=1 number of resonances = 12.
Average total width = 0.240 eV.
Average gamma width = 0.217 eV.
P-wave strength function = 3.28-04.
Average level spacing = 225.1 eV.
0.253 eV capture cross section (calc.) = 0.48 b.
Resonance absorption integral = 5.5 b.
Effective scattering radius = 7.0 fm.

File 3. Neutron Cross Sections

Based on latest experimental results and nuclear model calcs.

MT = 1 Total cross sections in energy range from 0.3 to 1.0 MeV based on experimental data of ref. 1. From 2.0 MeV to 20.0 MeV the experimental data of ref. 2 was combined with model calcs. using OM code SCAT2 ref. 3.

MT = 2 Elastic cross sections derived from angle integrated data of ref. 1 for energies up to 1.0 MeV. At higher energies model calcs. from SCAT2 and COMNUC ref. 4 were combined to be consistent with total minus non-elastic cross sections.

MT = 3 Non-elastic cross sections determined from OM calcs. combined with available experimental data on partial reaction cross sections.

MT = 4 Inelastic cross sections based on exptl. data of ref.1 were combined with HAUSER-FESHBACH calcs. using COMNUC ref. 4.

MT = 16 (n,2n) cross sections were derived from exptl. data of refs. 5 to 14.

MT = 22,28,104-106 Calculated using code THRESH ref. 15.

MT = 51-55 Discrete inelastic cross sections calculated using HAUSER-FESHBACH theory with width fluctuation corrections were combined with exptl. data of ref. 1. Level excitation energies up to 0.868 MeV taken from refs. 16 to 18.

MT = 91 Continuum inelastic cross section taken as difference between total inelastic and discrete.

MT = 102 Radiative capture cross section calculated using COMNUC to obtain agreement with exptl. data of refs. 19 to 22 for energies up to 2.0 MeV. For higher energies COMNUC calcs. used along with normalization to 14.0 MeV exptl. data of ref. 22.

MT = 103 (n,proton) cross sections were determined from combined statistical - HAUSER-FESHBACH calcs. and exptl. data of refs. 23, 24 and refs. 6, 10.

MT = 107 (n,alpha) cross sections calculated in the same manner as MT=103 with normalization to 14.4 MeV exptl. data of ref. 10.

MT = 203-207 Total gas production cross sections obtained by adding appropriate reaction data for protons, alphas, deuterons, tritons and helium-3.

MT = 251-253 Same as ENDF/B-IV.

File 4. Angular Distribution of Secondary Neutrons

MT = 2,51-55 Based on COMNUC calcs.

MT = 16,22,28,91 Angular distributions were assumed to be isotropic.

File 5. Energy Distribution of Secondary Neutrons

MT = 16,22,28,91 Calculated using code SOEC 66 ref. 25.

## REFERENCES

1. E.Barnard et al., Z.Physik 260, 197 (1973)

2. D.G.Foster Jr. and D.W.Glasgow, Phys.Rev. C3, 576 (1971)

3. O.Bersillon, SCAT2, CEA, Bruyeres-le-Chatel (France), Private Comm. (1979)

4. C.L.Dunford, COMNUC, Rpt. AI-AEC 12931 (1970)

5. D.I.Garber and R.R.Kinsey BNL-325 Vol.2 (1976)

6. W.Augustyniak et al., J.Acta Phys.Pol. B7, 347 (1976)

7. M.Bormann et al., Z.Phys. A277, 203 (1976)

8. S.K.Ghorai et al., Nuc.Phys. A223, 118 (1974)

9. J.Araminowicz and J.Dresler, Rpt. INR-1464, 14 (1973)

10. P.Venugapola et al., Phys.Rev. C3, 629 (1971)

11. L.Husain et al., Phys.Rev. C1, 1233 (1970)

12. S.C.Mistra and J.C.Gupta, J.Phys.G,Nuc.Phys. 5, 855 (1979)

13. R.Voelpel, Nuc.Phys. A182, 411 (1972)

14. E.Rurarz et al., J.Acta.Phys.Pol. B2, 553 (1971)

15. S.Pearlstein, THRESH, NSE 23, 238 (1965)

16. R.C.Ragaini, Phys.Rev. C8, 988 (1973)

17. K.Krishna, Phys.Rev. C13, 2055 (1976)

18. P.D.Bond and G.J.Kumbartski, Nuc.Phys. A205, 239 (1972)

19. A.L.Rao and J.R.Rao, Phys.Rev. C6, 572 (1972)

20. D.C.Stupegia et al., INE 22, 267 (1968)

21. Yu.P.Popov, ZET 42, 988 (1962)

22. F.Rigaud et al., Nuc.Phys. A154, 243 (1970)

23. L.Husain et al., Phys.Rev. C1, 1233 (1970)

24. B.Erlandsson et al., Physica Scripta 19, 251 (1979)

25. G.Simon, CEA, Bruyeres-le-Chatel, Private Comm. (1979)

37-Rb- 87 BNL/BRC Eval-Oct79 A. Prince

Supersedes ENDF/B-IV MAT 156 by Schmittroth and Schenter (HEDL).

File 2. Resonance Parameters

Resonance parameters based on recent publication of 'NEUTRON CROSS SECTION' Vol I (Z=1 to 60) S.F.Mughabghab et al., Academic Press N.Y. 1981.

L=0 number of resonances =14.
L=1 number of resonances =1.
Average total width =0.457 eV.
Average gamma width =0.115 eV.
S-wave strength function =1.41-04.
Average level spacing = 1.807+03 eV.
0.253 eV capture cross section (calc)=0.115 b.
Resonance absorption integral (calc)=2.66 b.
Effective scattering radius = 7.0 fm.

File 3. Neutron Cross Sections

Based on latest experimental results and nuclear model calcs.

MT = 1 Total cross sections in energy range from 0.3 to 1.0 MeV based on experimental data of ref. 1. From 2.0 MeV to 20.0 MeV the experimental data of ref. 2 was combined with model calcs. using OM code SCAT2 ref. 3.

MT = 2 Elastic cross sections derived from angle integrated data of ref. 1 for energies up to 1.0 MeV. At higher energies model calcs. from SCAT2 and COMNUC ref. 4 were combined to be consistent with total minus non elastic cross sections.

MT = 3 Non elastic cross sections determined from OM calcs. combined with available experimental data on partial reaction cross sections.

MT = 4 Inelastic cross sections based on exptl. data of ref. 1 were combined with HAUSER-FESHBACH calcs. using COMNUC ref. 4.

MT = 16 (n,2n) cross sections were derived from exptl. data of refs. 5 to 12.

MT = 22,28,104-106 Calculated using code THRESH ref. 15.

MT = 51-60 Discrete inelastic cross sections calculated using HAUSER-FESHBACH theory with width fluctuations calculations were combined with exptl. data of ref. 1. Level excitation energies up to 0.868 MeV taken from refs. 13 to 15.

MT = 91 Continuum inelastic cross section taken as difference between total inelastic and discrete.

MT = 102 Radiative capture cross section calculated using COMNUC to obtain agreement with exptl. data of ref. 5 for energies up to 5.0 MeV. For higher energies COMNUC calcs. used.

MT = 103 (n,proton) cross sections were determined from combined statistical - HAUSER-FESHBACH calcs. and exptl. data of refs. 9,16 and 17.

MT = 107 (n,alpha) cross sections calculated in the same manner as MT=103 with normalization to 14.5 MeV exptl. data.

MT = 203-207 Total gas production cross sections obtained by adding appropriate reaction data for protons, alphas, deuterons, tritons and helium-3.

MT = 251-253 Same as ENDF/B-IV.

File 4. Angular Distribution of Secondary Neutrons

MT=2,51-55 Based on COMNUC calculations.

MT=16,22,28,91 Angular distributions were assumed to be isotropic.

File 5. Energy Distribution of Secondary Neutrons

MT=16,22,28,91 Calculated using code SOEC 66 ref. 19.

REFERENCES

1. E.Barnard et al., Z.Physik 260, 197 (1973)

2. D.G.Foster,Jr. and D.W.Glasgow, Phys.Rev. C3, 576 (1971)

3. O.Bersillon, SCAT2, CEA, Bruyeres-le-Chatel (France), Private Comm. (1979)

4. C.L.Dunford, COMNUC, Rpt. AI-AEC 12931 (1970)

5. D.I.Garber and R.R.Kinsey, BNL-325 Vol.2 (1976)

6. W.Augustyniak et al., J.Acta Phys.Pol B7, 347 (1976)

7. S.K.Ghorai et al., Nuc.Phys. A223, 118 (1974)

8. J.Araminowicz and J.Dresler, Rpt.INR-1464, 14 (1973)

9. P.Venugapola et al., Phys.Rev. C3, 629 (1971)

10. L.Husain et al., Phys.Rev. C1, 1233 (1970)

11. E.Rurarz et al., J.Acta.Phys.Pol. B2, 553 (1971)

12. S.Pearlstein, THRESH, NSE 23, 238 (1965)

13. Hoffman and Pinther, Z.Phys. A283, 85 (1977)

14. A.Shihab-Eldin et al., Nuc.Phys. A160, 33 (1970)

15. R.P.Torti et al., Phys.Rev. C6, 1686 (1972)

16. L.Husain et al., Phys.Rev. C1, 1233 (1970)

17. R.Prasad and D.C. Sarker, Nuovo Cimento 3A, 467 (1971)

18. E.B.Paul and R.L.Clarke, Can.J.Phys. 31, 267 (1953)

19. G.Simon, CEA, Bruyeres-le-Chatel (France) Private Comm. (1979)

# SUMMARY DOCUMENTATION FOR $^{90}Zr$, $^{91}Zr$, $^{92}Zr$, $^{94}Zr$ and $^{96}Zr$

by

Philip F. Rose
Brookhaven National Laboratory
Upton, New York 11973

## I. INTRODUCTION

For Revision 2 of ENDF/B-V, cross sections in the resonance energy range were updated. The evaluated data above the resonance region was unchanged from ENDF/B-V, Revision 0. The original evaluation is completely described by Drake, Sarges and Maung in EPRI NP-250.[1]

## II. RESONANCE RANGE CROSS SECTIONS

The resolved region resonance parameters were taken from the output of BNLNDF[2] which is based on the resonance parameters of Mughabghab, Divadeenam and Holden.[3] In order to eliminate negative scattering cross sections, the MLBW formalism was employed. Table 1 outlines the thermal capture cross sections and resonance integrals for the various isotopes.

Table 1 - Zr Resonance Data

| Isotope | MAT | Abundance | Thermal Capture Cross Section | Resonance Integral |
|---|---|---|---|---|
| Zr-90 | 1385 | 51.46 | 0.011 | 0.179 |
| Zr-91 | 1386 | 11.23 | 1.188 | 4.913 |
| Zr-92 | 1387 | 17.11 | 0.221 | 0.655 |
| Zr-94 | 1388 | 17.40 | 0.049 | 0.311 |
| Zr-96 | 1389 | 2.80 | 0.023 | 5.629 |

The upper boundary of the resolved resonance range was 90 keV for the even isotopes and 24.5 keV for Zr-91. For Zr-91 an additional unresolved resonance range was specified from 24.5 keV to 90 keV. The unresolved resonance parameters were evaluated from experimental data fits using the UR code of E. Pennington.[4]

## III. TOTAL CROSS SECTION

Total cross sections for the natural element were smoothly joined to the resonance range cross sections for the individual isotopes.

Between 90 keV and 500 keV the data of Seth[5] were used. Between 500 keV and 2 MeV the evaluated data were based on measurements of Green and Mitchell[6] and Stooksberry and Anderson.[7] The latter measurements were for Zr-90. Above 2 MeV, Green and Mitchell's data were combined with that of Foster and Glasgow[8], Carlson and Barschall[9] and Peterson et al.[10]

## IV. RADIATIVE CAPTURE CROSS SECTIONS

In the kilovolt energy region the (n,γ) cross sections were not well known since only a few measurements were available.

The results from only two measurements were available for $^{90}Zr$ and $^{91}Zr$.[11,12] The only data for $^{92}Zr$ was measured by Macklin, Inada and Gibbons.[12] In addition to the data from these references there were two additional measurements for $^{94}Zr$, i.e., Macklin, Lazar and Lyon[13] and Lyon and Macklin.[14] Three experimental points were available for $^{96}Zr$.[12,13,14] Because of the paucity of experiments, the semi-empirical data recommended by Benzi et al.[15] was employed for all isotopes.

## V. ELASTIC SCATTERING CROSS SECTION

The elastic scattering cross sections was taken to be the difference between the total cross section and the non-elastic cross section for the entire energy range.

The measurement by McDaniel et al.[16] for the elastic scattering cross sections of the even isotopes and the measurements by Guenther, Smith and Whalen[17] for energies between 0.9 and 4.0 MeV for $^{90}Zr$ and $^{94}Zr$ appear consistent with the evaluation.

## VI. INELASTIC SCATTERING CROSS SECTION

The inelastic scattering cross sections were described by levels up to 4 MeV. Above 3 MeV the experimentally measured non-elastic cross section was used in determining the inelastic scattering cross sections. The reference document by Drake et al.[1] summarizes all the levels considered in the evaluation. The inelastic cross sections were based on a previous evaluation by KAPL[18] and the experimental data of Tessler et al.,[19] Day,[20] McDaniel et al.,[16] Guenther, Smith and Whalen,[17] Lind and Day,[21] Tessler and Glickstein,[22] and Glazkov.[23] The energy distribution for the secondary neutrons was treated by specifying a nuclear temperature which was obtained from Anufrienko.[24]

## VII. (n,2n) CROSS SECTION

The (n,2n) cross section for Zr-90 is reasonably well known from measurements of Prestwood and Bayhurst[25] and Nethaway.[26] Only a few measurements exist for the other isotopes and recommended values were taken from statistical model estimates.[27]

## VII. (n,α) CROSS SECTION

The measurements of Bayhurst and Prestwood[28] were used for $^{92}Zr$ and $^{94}Zr$. Statistical model estimates provided by BNL[27] were used to supplement the experimental data. Statistical model estimates were used to determmine the slope and magnitude of the remaining isotopes. These estimates were found to be in agreement with the limited experimental data available for $^{91}Zr$ and $^{96}Zr$.

## VIII. (n,p) CROSS SECTION

The energy dependent measurements of Carroll and Stooksberry and Bayhurst and Prestwood[28] were used to obtain the recommended Zr-90 cross section. The (n,p) cross section for $^{91}$Zr was based on Carroll and Stooksberry[28] for neutron energies between 4 and 6 MeV. Near 14 MeV it was based on the measurement of Reed[30] and Levkovskii.[31] These measurements were used to normalize the slope obtained from statistical model estimates. A similar treatment was used for Zr-92 and Zr-94. Experimental measurements included those of Carroll and Stooksberry, Reed, Bramlitt and Fink,[32] Lu et al.,[33] Levkovskii,[31] Prasad and Sarkar[34] and Paul and Clarke.[35]

## IX. ANGULAR DISTRIBTIONS

The recommended angular distributors for elastically scattered neutron was based on the experimental data of Reitman et al.[36] and Guenther, Smith and Whalen[17] for neutron energies up to 4 MeV and for all isotopes. Above 4 MeV the evaluation by KAPL[18] was used.

## REFERENCES

1. M. K. Drake, D. A. Sargis and T. Maung, "Evaluated Neutron Cross Sections for Zirconium and Hafnium," EPRI NP-250 (1976).

2. S. F. Mughabghab, "Resonance Parameters of BNL-325 in the ENDF Format." To be published.

3. S. F. Mughabghab, M. Divadeenam and N. E. Holden, "Neutron Cross Sections" Fourth Edition Volume 1 "Neutron Resonance Parameters and Thermal Cross Sections Part A Z=1-60," New York, Academic Press (1981).

4. E. M. Pennington, Argonne National Laboratory, Private communication (1973).

5. K. K. Seth, Phys. Letters 16, 306 (1965).

6. L. Green and J. A. Mitchell, "Total Cross Section Measurements with a $^{252}$Cf Time-of-Flight Spectrometer," USAEC report, WAPD-TM-1073 (April 1973).

7. R. W. Stooksberry and J. H. Anderson, Nucl. Sci. and Eng. 51, 235 (1973).

8. D. G. Foster and D. W. Glasgow, Phys. Rev. C3, 576 (1971).

9. A. D. Carlson and H. H. Barschall, Phys. Rev. 158, 1142 (1967).

10. J. M. Peterson, A. Bratenahl and J. D. Storering, Phys. Rev. 120, 521 (1960).

11. S. P. Kapchigashev, Atomnaya Energiya 19, 194 (1965).

12. R. L. Macklin, T. Inada and J. H. Gibbons, Bull. Am. Phys. Soc. 8, 81 (1963).

13. R. L. Macklin, N. H. Lazar and W. S. Lyon, Phys. Rev. 107, 504 (1957).

14. W. S. Lyon and R. L. Macklin, Phys. Rev. 114, 1619 (1959).

15. V. Benzi, et al., "Fast Neutron Radiative Capture Cross Sections of Stable Nuclei with $29 < Z < 79$", Comitato Nazionale Energia Nucleare-Centro di Calcolo report CEC (71)9, November 1971.

16. F. D. McDaniel, J. D. Brandenberger and G. P. Glasgow, Phys. Rev. C10, 1087 (1974).

17. P. Guenther, A. Smith and J. Whalen, "$^{90}$Zr and $^{92}$Zr Neutron Total and Scattering Cross Sections", Argonne National Laboratory report-ANL/NDM-4, (1974).

18. J. T. Reynolds and C. J. Slavik, "Evaluated Neutron Cross Sections for the Zirconium Isotopes," Knolls Atomic Power Laboratory report KAPL-M-7078 (1970).

19. G. Tessler, S. S. Glickstein and E. E. Carroll, Jr., Phys. Rev. C2, 2390 (1970).

20. R. B. Day, private communication to the NNDC (1965).

21. D. A. Lind and R. B. Day, Annals of Phys. 12, 485 (1961).

22. G. Tessler and S. Glickstein, Bull. Am. Phys. Soc. 20, 174 (1975).

23. N. P. Glazkov, Atomnaya Energiya 15, 416 (1963).

24. V. B. Anufrienko, et al., Soviet J. Nucl. Phys. 2, 589 (1966).

25. R. J. Prestwood and B. P. Bayhurst, Phys. Rev. 121, 1438 (1961).

26. D. R. Nethaway, Nucl. Phys. A190, 635 (1972).

27. Private communication from the National Nuclear Data Center (1975).

28. B. P. Bayhurst and R. J. Prestwood, J. Inorg. Nucl. Chem. 23, 173 (1961).

29. E. E. Carroll and R. W. Stooksberry, Nucl. Sci. Eng. 25, 285 (1966).

30. C. H. Reed, "Absolute (n,2n), (n,pγ) and (n,αγ) Cross Sections for 14.1 MeV Neutrons in Zirconium and the Calibration of a Crystal Scintillation Spectrometer", UC-34, Univ. of Calif. (1960).

31. V. N. Levkovskii, Sov. Phys. JETP 18, 213 (1964).

32. E. T. Bramlitt and R. W. Fink, Phys. Rev. 131, 2649 (1963).

33. Weu-deh Lu, N. Rana Kumar and R. W. Fink, Phys. Rev. C1, 358 (1970).

34. R. Prasad and D. C. Sarkar, Nuovo Cimento 3A, 467 (1971).

35. E. B. Paul and R. L. Clarke, Can. J. Phys. 31, 268 (1953).

36. D. Reitman, C. A. Engelbrecht and A. B. Smith, Nucl. Phys. 48, 593 (1963).

# SUMMARY DOCUMENTATION FOR $^{NAT}Zr$

by

Philip F. Rose
Brookhaven National Laboratory
Upton, New York 11973

## I. INTRODUCTION

An elemental zirconium evaluation was constructed for Revision 2 of ENDF/B-V from the isotopic evaluations for $^{90,91,92,94,96}Zr$ described in the previous article. As in the case for the isotopic evaluations the evaluated data above the resonance region was unchanged from ENDF/B-V Revision 0. The original evaluation is completely described by Drake, Sarges and Maung in EPRI NP-250.[1]

## II. RESONANCE RANGE CROSS SECTIONS

The resolved region resonance parameters were taken from the output of BNLNDF[2] which is based on the resonance parameters of Mughabghab, Divadeenam and Holden.[3] Table 1 outlines the thermal capture cross sections and resonance integrals for the various isotopes and the natural element.

Table 1 - Zr Resonance Data

| Isotope | MAT | Abundance | Thermal Capture Cross Section | Resonance Integral |
|---|---|---|---|---|
| Zr-90 | 1385 | 51.46 | 0.011 | 0.179 |
| Zr-91 | 1386 | 11.23 | 1.188 | 4.913 |
| Zr-92 | 1387 | 17.11 | 0.221 | 0.655 |
| Zr-94 | 1388 | 17.40 | 0.049 | 0.311 |
| Zr-96 | 1389 | 2.80 | 0.023 | 5.629 |
| Zr (nat) | 1340 | --- | 0.186 | 0.965 |

The upper boundary of the resolved resonance range was 90 keV for the even isotopes and 24.5 keV for Zr-91. For Zr-91 an additional unresolved resonance range was specified from 24.5 keV to 90 keV. The unresolved resonance parameters were evaluated from experimental data fits using the UR code by E. Pennington.[4]

## III. TOTAL CROSS SECTION

Between 90 keV and 500 keV the data of Seth[5] was used. Between 500 keV and 2 MeV the evaluated data set was based on measurements of Green and Mitchell[6] and Stooksberry and Anderson.[7] Above 2 MeV, Green and Mitchell's data set was combined with those of Foster and Glasgow,[8] Carlson and Barschall,[9] and Peterson et al.[10]

## IV. RADIATIVE CAPTURE CROSS SECTIONS

In the kilovolt energy region the (n,γ) cross sections were not well known since only a few measurements were available. Radiative capture data for natural zirconium due to Kapchigashev[11] was available to 35 keV and by Stavisskii and Shapar[12] and Diven et al. [13] at higher energies to one MeV. The semi-emperical data recommended by Benzi et al.[14] was used. Benzi used experimental data along with a statistical model which included direct and semi-direct capture cross section estimates. His overall file was statistically acceptable relative to the available experimental data.

## V. ELASTIC SCATTERING CROSS SECTION

The elastic scattering cross section was taken to be the difference between the total cross section and the non-elastic cross section for the entire energy range. The experimental data of Engelbrecht and Smith,[15] Hans and Snowdon,[16] Kent et al.,[17] Walt and Beyster,[18] Gilboy and Towle,[19] and Clarke and Cross[20] were found to be consistent with the elemental evaluation.

## VI. INELASTIC SCATTERING CROSS SECTION

The inelastic cross sections were based on a previous evaluation by KAPL[21] and the experimental data of Tessler et al;[21] Day;[23] McDaniel et al;[24] Guenther, Smith and Whalen;[25] Lind and Day;[26] Tessler and Glickstein[27] and Glazkov.[28]

Nineteen level excitation cross sections and a continuum cross section were specified. Table 2 shows the energy levels considered in the evaluation. The energy distribution for the secondary neutrons was treated by specifying a nuclear temperature which was obtained from Anufrienko et al.[29]

Table 2

ENERGY LEVELS USED IN THE EVALUATION FOR ZIRCONIUM

| Level Number | Energy (MeV) | Isotope |
|---|---|---|
| 1 | 0.9182 | 94 |
| 2 | 0.9345 | 92 |
| 3 | 1.2049 | 91 |
| 4 | 1.30 | 94 |
| 5 | 1.383 | 92 |
| 6 | 1.46 | 91,92,94,96 |
| 7 | 1.669 | 94 |
| 8 | 1.7607 | 90,96 |
| 9 | 1.85 | 91,92,96 |
| 10 | 2.05 | 91,92,94 |
| 11 | 2.15 | 90,91,94,96 |
| 12 | 2.261 | 91 |
| 13 | 2.319 | 90 |
| 14 | 2.32 | 91 |
| 15 | 2.35 | 91,92,94 |
| 16 | 2.557 | 91 |
| 17 | 2.61 | 91,94 |
| 18 | 2.738 | 90,91 |
| 19 | 2.748 | 90 |

## VII. (n,2n) CROSS SECTION

The cross sections for the element were based on estimates for the various isotopes. Except for Zr-90 the results from statistical model calculations were used. The (n,2n) cross section for $^{90}$Zr was based on measurements by Prestwood and Bayhurst,[30] Nethaway,[31] and several measurements near 14 MeV.

## VIII. (n,α) CROSS SECTION

The recommended (n,α) cross section for natural zirconium was obtained by first evaluating the (n,α) cross sections for the isotopes.

The energy dependent isotopic measurements made by Bayhurst and Prestwood were primarily used,[32] as well as statistical model calculations, and several individual measurements made at 14 MeV.

## IX. (n,p) CROSS SECTION

An analysis procedure similar to that used for the (n,α) cross section was used to obtain the recommended (n,p) cross sections for natural zirconium. The energy dependent measurements of Carroll and Stooksberry[35] were used in evaluating Zr-90 and Zr-91. The (n,p) cross sections for Zr-92 and Zr-94 were based on measurements by Carroll and Stooksberry,[33] Reed,[34] Bramlitt and Fink,[36] Lu et al.,[37] Levkovskii,[35] Prasad and Sarkar[38] and Paul

and Clarke.[39] The resulting (n,p) cross sections for the element were found to be in close agreement with the KAPL[21] evaluation.

## X. ANGULAR DISTRIBUTIONS

The recommended angular distributions for elastically scattered neutrons was based on the experimental data of Reitman et al.[15] and Guenther, Smith and Whalen[25] for neutron energies up to 4 MeV. Above 4 MeV the KAPL[20] evaluation was used.

## REFERENCES

1. M. K. Drake, D. A. Sargis and T. Maung, "Evaluated Neutron Cross Sections for Zirconium and Hafnium," EPRI NP-250 (1976).

2. S. F. Mughabghab, "Resonance Parameters of BNL-325 in the ENDF Format." To be published.

3. S. F. Mughabghab, M. Divadeenam and N. E. Holden, "Neutron Cross Sections Fourth Edition Volume 1 Neutron Resonance Parameters and Thermal Cross Sections Part A Z=1-60, New York, Academic Press (1981).

4. E. M. Pennington, Argonne National Laboratory, Private Communication (1973).

5. K. K. Seth, Phys. Letters 16, 306 (1965).

6. L. Green and J. A. Mitchell, "Total Cross Section Measurements with a $^{252}$Cf Time-of-Flight Spectrometer," USAEC report, WAPD-TM-1073 (April 1973).

7. R. W. Stooksberry and J. H. Anderson, Nucl. Sci and Eng. 51, 235 (1973).

8. D. G. Foster, Jr. and D. W. Glasgow, Phys. Rev. C3, 576 (1971).

9. A. D. Carlson and H. H. Barschall, Phys. Rev. 158, 1142 (1967).

10. J. M. Peterson, A. Bratenahl and J. D. Storering, Phys. Rev. 120, 521 (1960).

11. S. P. Kapchigashev, Atomnaya Energiya 19, 294 (1965).

12. Yu. Ya. Stavisskii and A. V. Shapar, Atomnaya Energiya 15, 323 (1963).

13. B. C. Diven, J. Terrell and A. Hemmendinger, Phys. Rev. 120, 556 (1960).

14. V. Benzi, et al., "Fast Neutron Radiative Capture Cross Sections of STable Nuclei with 29<Z<79", Comitato Naxionale Energia Nucleare-Centro di Calcolo report CEC (71) 9, November 1971.

15. D. Reitman, C. A. Engelbrecht and A. B. Smith, Nucl. Phys. 48, 593 (1963).

16. H. S. Hans and S. C. Snowdon, Phys. Rev. 108, 1028 (1957).

17. D. W. Kent, et al., Phys. Rev. 125, 331 (1962).

18. M. Walt and J. R. Beyster, Phys. Rev. 98, 677 (1955).

19. W. H. Gilboy and J. H. Towle, Nucl. Phys. 42, 86 (1963).

20. R. L. Clarke and W. G. Cross, Nucl. Phys. A95, 320 (1967).

21. J. T. Reynolds and C. J. Slavik, "Evaluated Neutron Cross Sections for the Zirconium Isotopes," Knolls Atomic Power Laboratory report KAPL-M-7078 (1970).

22. G. Tessler, S. S. Glickstein and E. E. Carroll, Jr., Phys. Rev. C2, 2390 (1970).

23. R. B. Day, private communication to the NNDC (1965).

24. F. D. McDaniel, J. D. Brandenberger and G. P. Glasgow, Phys. Rev. C10, 1087 (1974).

25. P. Guenther, A. Smith and J. Whalen, "$^{90}$Zr and $^{92}$Zr Neutron Total and Scattering Cross Sections", Argonne National Laboratory report ANL/NDM-4, (1974).

26. D. A. Lind and R. B. Day, Annals of Phys. 12, 485 (1961).

27. G. Tessler and S. Glickstein, Bull. Am. Phys. Soc. 20, 174 (1975).

28. N. P. Glazkov, Atomnaya Energiya 15, 416 (1963).

29. V. B. Anufrienko, et al., Soviet J. Nucl. Phys. 2, 589 (1966).

30. R. J. Prestwood and B. P. Bayhurst, Phys. Rev. 121, 1438 (1961).

31. D. R. Nethaway, Nucl. Phys. A190, 635 (1972).

32. B. P. Bayhurst and R. J. Prestwood, J. Inorg. Nucl. Chem. 23, 173 (1961).

33. E. E. Carroll and R. W. Stooksberry, Nucl. Sci. Eng. 25, 285 (1966).

34. C. H. Reed, "Absolute (n,2n), (n,pγ), and (n,αγ) Cross Sections for 14.1 MeV Neutrons in Zirconium and the Calibration of a Crystal Scintillation Spectrometer", UC-34, Univ. of Calif. (1960).

35. V. N. Levkovskii, Sov. Phys. JETP 18, 213 (1964).

36. E. T. Bramlitt and R. W. Fink, Phys. Rev. 131, 2649 (1963).

37. Weu-deh Lu, N. Rana Kumar and R. W. Fink, Phys. Rev. C1, 358 (1970).

38. R. Prasad and D. C. Sarkar, Nuovo Cimento 3A, 467 (1967).

39. E. B. Paul and R. L. Clarke, Can. J. Phys. 31, 268 (1953).

# REVISION 2 OF ENDF/B-V SILVER-107

by

A. Prince
Brookhaven National Laboratory
Upton, New York 11973

R. E. Schenter
Hanford Engineering Development Laboratory
Richland, Washington 99352

The present work supersedes the ENDF/B-V evaluation, MAT-1371 by BNL/HEDL (Prince, Bhat, Mann, Johnson, Schenter and Schmittroth). The Summary of MAT 1371 is given on page 47-107-5 of ENDF-201 Summary Documentation. All the data were re-evaluated by A. Prince and completed in July 1980. R. Schenter updated the capture and elastic cross sections using recent capture measurements of Macklin (1982) and Poenitz (1982). The following file 1 comments for MAT 1407 summarize the evaluation.

47-Ag-107 BNL,HEDL Eval-Jun83 A.Prince, R.E.Schenter

Evaluation of A.Prince 7/80 which supersedes ENDF/V MAT 1371 by BNL/HEDL (Schenter, Bhat, Prince, and Johnson). Changes in the capture and elastic keeping the total cross section constant were also made by R.Schenter. These changes reflect the use of results of recent measurements by Macklin and Poenitz on isotopic and elemental capture, ref. 22 and ref. 23.

File 2. Resonance Parameters

Resonance Parameters based on new exptl. data, ref. 1.
L=0 number of resonances is 74.
Average total width = 2.3298-01 eV.
Average reduced neutron width = 2.82367-03 eV.
Average gamma width = 1.39069-01 eV.
Average level spacing = 3.65767+01 eV.
S-wave strength function = 3.7851-05.
0.025 eV capture cross section (calc)= 3.7616+01 barns.
Resonance absorption integral (0.5 eV cut-off) = 1.0487+02 b.
Effective scattering radius = 6.60 fm.

File 3. Neutron Cross Sections

All data re-evaluated based on latest experimental data and nuclear model calcs.

MT = 1 Total cross section in energy range 0.25 MeV to 4.5 MeV based on experimental data of ref. 2. From 4.5 to 20.0 MeV optical model calcs. combined with exptl. data from BNL-325.

MT = 2 Elastic cross sections derived from angle integrated exptl. data of ref. 2 and BNL 325 supplemented with optical model calcs. at higher energies (5.0 to 20.0 MeV). The elastic cross section was chosen to be consistent with total minus non-elastic exptl. data (BNL-325).

MT = 3 Non elastic cross sections determined from exptl. data of ref. 2 in region 0.25 to 4.5 MeV. From 5.0 to 20.0 MeV optical model calcs. combined with BNL-325 exptl data.

MT = 4 Total inelastic cross section based on exptl. data of ref. 2 and ref. 3 combined with HAUSER-FESHBACH calcs.

MT = 16 (n,2n) cross sections were determined from recent exptl. data of refs. 4 to 8 and BNL 325. In regions lacking exptl. data, model calcs were performed.

MT = 17 (n,3n) cross sections were based primarily on model calcs. normalized to exptl. data of refs. 7 and 9.

MT = 22,28,104,105,106 Determined from statistical model calcs.

MT = 51 - 63 Discrete inelastic cross sections, calculated using HAUSER-FESHBACH theory with width fluctuation. Corrections derived by refs. 10 and 11, were combined with exptl. data of refs. 2, 3 and 12. Level excitation energies up to 1.65 taken from refs. 13, 14 and 15.

MT = 91 Continuum inelastic cross section with 1.143 MeV cutoff taken as difference between total inelastic and discrete level excitations.

MT = 102 Radiative capture cross section using results mainly from ref. 22 and 23.

MT = 103 (n,proton) cross section; HAUSER-FESHBACH and statistical model calcs were normalized to 14.0 MeV data of ref. 18.

MT = 107 (n,alpha) cross section; calculated in same manner as MT = 103 and combined with exptl. data of refs. 19 and 20.

MT = 203, 204, 206, 207 Total gas production. Derived from results of H,D,T, He-3 and He-4 contained in MT = 103 to 107 and MT = 22, 28.

MT = 251 - 253 Same as BNL/HEDL ENDF/B-V 1979 evaluation ref. 17.

File 4. Angular Distribution of Secondary Neutrons

MT = 2 Same as BNL/HEDL ENDF/B-V 1979 evaluation ref. 17.

MT = 16,17,22,28,51 to 91 Angular distributions assumed to be isotropic.

File 5. Energy Distribution of Secondary Neutrons

MT = 16,17,22,28 and 91 Energy distributions presented as histogram based on calcs using nuclear temperatures determined from ref. 21.

Summary

Files 2 and 3 are completely new evaluations resulting from improved nuclear model calcs and the most recent experimental data.

File 4 remains the same as the earlier version except for 5 additional inelastic level excitations and the inclusion of MT = 17, 22 and 28.

File 5 also has been expanded to include MT = 17,22 and 28.

## Codes Used

1. CERBERO 2 improved version of the CERBERO computer code for calculation of nuclear reaction cross section. F.Fabbri et al., RT/FI(77)6 CNEN 1977.
2. ERINNI an optical model fortran IV code for the calculation of multiple cascading particle emissions. F.Fabbri and G.Reffo RT/FI(77)4 CNEN 1977.
3. SCAT4U modified version of SCAT2 an optical model program O.Bersillon- Bruyeres-le-Chatel (Private Comm.).
4. THRES2 modified version of THRESH- S.Pearlstein 1975 (Private Comm.).

## REFERENCES

1. S.Mughaghab, Private Comm. (1980)
2. A.Smith, et al., ANL/NDM-46 (Jan.1979)
3. E.Barnard, et al., Harwell Conf. (1978)
4. E.Rondaiah, J.Phys.a Math.-Nuc.Gen. 7 (12) 1457 (1974)
5. W.Mannhart and H.Vonach, Z.Phys. A272, 279 (1975)
6. W.Augustyniack, et al., Nucl.Phys. A247, 231 (1975)
7. B.P.Bayhurst, et al., Phys.Rev. C12, 451 (1975)
8. S.C.Misra and U.C.Gupta, J.Phys.G Nucl.Phys. 5, 855 (1979)
9. H.Liskien, Nucl.Phys. A118, 379 (1968)
10. J.W.Tepel, et al., Phys.Lett. 49B, 1 (1974)
11. H.M.Hoffman, et al., Ann.Phys. 90, 403 (1975)
12. W.G.Vonach and A.B.Smith, Nucl.Phys. 78, 389 (1966)
13. C.M.Lederer, et al., Table of Isotopes (7th-Ed.) Wiley (1978)
14. H-W.Schuh, et al., Zeit.f.Physik, A293, 301 (1979)
15. Z.Matumoto, et al., JAERI-M-7734 (1978)
16. Y.D.Harker, et al., Rpt.Tree 1259 (CFRMF) (1978)
17. R.E.Schenter, et al., ENDF/V Summary Documentation 47-107-1 (1979)
18. R.Prasad and D.C.Sarker, Nuovo Cim. 3A, 467 (1961)
19. A.Rubbind and D.Zubke, Nucl.Phys. 85, 606 (1966)
20. M.Bormann, et al., Nucl.Phys. A186, 65 (1972)

22. R.L.Macklin, Nucl.Sci. and Eng. 82, 400 (1982)

23. W.P.Poenitz, Spec.Meet. on Fast Capture, Anl-83-4, 239 (1982)

# REVISION 2 OF ENDF/B-V SILVER-109

by

A. Prince
Brookhaven National Laboratory
Upton, New York 11973

R. E. Schenter
Hanford Engineering Development Laboratory
Richland, Washington 99352

The present work supersedes the ENDF/B-V evaluation, MAT-1373 by BNL/HEDL (Prince, Bhat, Mann, Johnson, Schenter and Schmittroth). The Summary of MAT 1373 is given on page 47-109-4 of ENDF-201 Summary Documentation. All the data were re-evaluated by A. Prince and completed in July 1980. R. Schenter updated the capture and elastic cross sections using recent capture measurements of Macklin (1982) and Poenitz (1982). The following file 1 comments for MAT 1409 summarize the evaluation.

47-Ag-109 BNL,HEDL Eval-Jun83 A.Prince, R.E.Schenter

Evaluation of A.Prince 7/80 which supersedes ENDF/V MAT 1373 by BNL/HEDL (Schenter, Bhat, Prince and Johnson). Changes in the capture and elastic keeping the total cross section constant were also made by R.Schenter. These changes reflect the use of results of recent measurements by Macklin and Poenitz on isotopic and elemental capture, ref. 13 and ref. 14.

File 2. Resonance Parameters

Resonance parameters based on new exptl. data, ref. 1.
L = 0 number of resonances is 83.
Average total width = 2.11512-01 eV.
Average reduced neutron width = 2.80735-03 eV.
Average gamma width = 1.320-01 eV.
Average level spacing = 3.04977+01 eV.
S-wave strength function = 4.55065-05.
0.025 eV capture cross section = 9.0720+01 barns.
Resonance absorption integral (0.5 eV cut-off) = 1.4675+03 b.
Effective scattering radius = 6.60 fm.

File 3. Smooth Cross Sections

All data re-evaluated from latest exptl. data coupled with nuclear model calcs.

MT = 1 Total cross sections (energy range 0.25 MeV to 20.0 MeV) based on Ag-107 exptl. data of ref. 2, BNL-325 and optical model calcs.

MT = 2 Elastic scattering cross sections derived from angle integrated exptl. data of ref. 2, BNL-325 and optical model calcs.

MT = 4 Total inelastic cross section based on exptl. results of ref. 2,3 and HAUSER-FESHBACH calcs.

MT = 16 (n,2n) cross sections were determined primarily from the exptl. data of ref. 4., BNL-325 and statistical model calcs.

MT = 17,22,28,104,105,106 determined from statistical model calcs.

MT = 51 to 70 Discrete inelastic cross sections, calculated using HAUSER-FESHBACH Theory with width fluctuation corrections derived by refs. 5 and 6, were combined with exptl. data of refs. 2,3 and 7.

Level excitation information up to energy = 1.66 MeV taken from refs. 8, 9 and 10.

MT = 91 Continuum inelastic cross section with 0.911 MeV cutoff taken as difference between total inelastic and discrete level excitations.

MT = 102 Radiative capture cross section using results mainly from ref. 13 and 14.

MT = 103 (n,proton) cross sections- HAUSER-FESHBACH and evaporation model calcs. Were combined with exptl. data of ref. 4 and exptl data in BNL-325.

MT = 107 (n,alpha) cross section calcs. in same manner as MT = 103.

MT = 203,204,206,207 Derived from results of h,d,t,He-3 and He-4 contained in MT = 1-3 to 107 and MT = 22 and 28.

MT = 251 to 253 Same as BNL/HEDL ENDF/V 1979 evaluation ref. 1.

File 4. Angular Distribution of Secondary Neutrons

~~MT = 2 Same as BNL/HEDL evaluation ref. 11.~~

MT = 16,17,22,28,51 to 91 Angular distributions assumed to be isotropic.

File 5. Energy Distribution of Secondary Neutrons

MT = 16,17,22,28 and 91 Energy distributions presented as histograms based on calcs. using nuclear temperatures from ref. 12.

Summary

Files 1,2 and 3 are completely new evaluations resulting from the most recent exptl. data and improved model calcs.

File 4 includes 15 additional level excitations and the addition of MT = 17,22 and 28.

File 5 also expanded to include MT = 17,22 and 28.

Codes Used

1. CERBERO 2 improved version of the CERBERO computer code for calculation of nuclear reaction cross sections F.Fabbri, et al., RT/FI(77)6 CNEN 1977.
2. ERINNI an optical model Fortran IV code for the calculation of multiple cascading particle emissions F.Fabbri and G.Reffo RT/FI(77)4 CNEN 1977.
3. SCAT4U BNL modified version of SCAT2 an optical model program O.Bersillon- Bruyers-le-Chatel(Pri. Comm.) 1979.

4. THRES2 modified version of THRESH - S.Pearlstein BNL 1975 (Pri. Comm.).

REFERENCES

1. S.Mughabghab, BNL Private Comm.

2. A.B.Smith, et al., ANL/NDM-46 (Jan. 1979)

3. E.Barnard, et al., Harwell Conference (1978) Prol.-78-Ha

4. W.Augustyniak, et al., Nucl.Phys. A247, 231 (1975)

5. J.W.Tepel, et al., Phys.Lett. 49B, 1 (1974)

6. H.M.Hoffman, et al., Ann.Phys. 90, 403 (1975)

7. W.G.Vonach and A.B.Smith, Nucl.Phys. 78, 389 (1966)

8. C.M.Lederer, et al., Table of Isotopes (7th-Ed.) Wiley (1978)

9. H.-W.Schuh, et al., Zeit.F.Physik, A293, 301 (1979)

10. A.Matumato, et al., JAERI-M-7734 (1978)

11. R.E.Schenter, et al., ENDF/V Summary Documentation 47-107-1 HEDL (1979)

12. A.G.Gilbert and A.G.W.Cameron, Can.J.Phys. 43, 1446 (1965)

13. R.L.Macklin, Nucl.Sci. and Eng. 82, 400 (1982)

14. W.P.Poenitz, Spec.Meet. on Fast Capture, ANL-83-4, 239 (1982)

# SUMMARY DOCUMENTATION FOR EUROPIUM

The Europium evaluation (MAT 1463) presented in the ENDF/B-V.2 library is a composite of Eu-151 (MAT 1357) and Eu-153 (MAT 1359). The isotopes Eu-151 and Eu-153 were evaluated by S. F. Mughabghab for ENDF/B-V (see ENDF 201 (ref. 1) for documentation of the isotopes). The composite Eu-natural was generated by S. Pearlstein (ref. 2) for ENDF/B-V.2 using the code COMBO (ref. 3).

## REFERENCES

1. R. R. Kinsey, ENDF/B-V Summary Documentation, BNL-NCS-17541 (ENDF 201) 3rd Ed., July 1979.

2. S. Pearlstein, Synthesized ENDF material Europium using the code COMBO, Private Communication to NNDC, August 1981.

3. S. Pearlstein, COMBO - A code to generate natural elements using available isotopes, Private Communication to NNDC, January 1979.

# SUMMARY DOCUMENTATION FOR $^{182}W$, $^{183}W$, $^{184}W$, AND $^{186}W$

by

E. D. Arthur, P. G. Young, A. B. Smith* and C. Philis**

## I. SUMMARY

The ENDF/B-V, Revision-2 evaluations of neutron-induced reactions on the major tungsten isotopes are based on extensive new experimental data and theoretical analyses above neutron energies of 100 keV. Only the resonance regions and the (n,p) and (n,α) cross section files were retained from ENDF/B-V, Revision 0.

## THEORETICAL ANALYSIS

The analysis involved use of a deformed optical model to calculate neutron transmission coefficients, total and reaction cross sections, a giant-dipole-resonance model to determine gamma-ray transmission coefficients, and Hauser-Feshbach statistical theory to calculate partial reaction cross sections.

The deformed optical model calculations were performed with the ECIS78 coupled-channel code.[1] Cross sections were calculated for neutron inelastic scattering to the $2^+$ and $4^+$ states in $^{182,184,186}W$ and the $3/2^-$, $5/2^-$, $7/2^-$, and $9/2^-$ states in $^{183}W$. In addition, ECIS78 was used to provide shape elastic scattering cross sections, total cross sections above 15 MeV and at all energies for $^{183}W$, and neutron transmission coefficients for the Hauser-Feshbach statistical-theory calculations.

The Hauser-Feshbach statistical theory calculations were performed with the COMNUC[2] and GNASH[3] reaction theory codes. The COMNUC cross section calculations include width-fluctuation corrections, important at lower energies, and the GNASH calculations incorporate preequilibrium effects, which become significant at higher energies. COMNUC was used to calculate all cross sections below 6 MeV, whereas GNASH was used for cross sections above 6 MeV and for all spectra calculations. Both codes use the Gilbert and Cameron[4] level density formulation and the Cook[5] tabulation of level density parameters, modified slightly (within ± 10%) in some cases. A maximum amount of experimental information on discrete energy levels was incorporated into the calculations, and the constant temperature part of the Gilbert and Cameron level density was matched to the discrete level data for each residual nucleus in the analysis. Gamma-ray strength functions ($f_{E1}$) were determined from analyses of $^{182,183,184,186}W(n,\gamma)$ data and are generally consistent with the experimentally determined $f_{E1}$ values of Joly.[6]

---

* A. B. Smith, Argonne National Laboratory, Argonne, Illinois
**C. Philis, Centre d'Études de Bruyères-le-Châtel, France

The deformed optical model parameterization that was used is a modification[7] of a set originally derived by Delaroche et al.[8] The original parameterization was based on neutron total cross sections from 0.1-15 MeV, elastic scattering angular distributions up to 4 MeV, and inelastic scattering angular distributions for $2^+$ and $4^+$ states, primarily at 3.4 MeV. In addition, 16 MeV (p,p') data on $^{182\ 184\ 186}W$, as well as s- and p-wave neutron strength functions and the potential scattering radius, were reasonably fit by the Delaroche analysis. It was not possible, however, for us to fit the $^{184}W$(n,2n) and $^{186}W$(n,2n) cross sections using the original parameters. Therefore, we modified the parameters somewhat in order to achieve good fits to all the experimental results, including (n,xn) results, as well as the data that Delaroche et al. included in their analysis.

The resulting optical parameters appear in Table I. They are similar in form to the Delaroche set but generally involve small adjustments in the geometrical parameters for the real and imaginary well depths. The form of the energy dependence of the surface derivative imaginary well depth was changed to include a linear dependence on energy (instead of $\sqrt{E}$). Also, the energy at which a transition in the form of the surface imaginary well depth occurred was altered. For the $^{186}W$ calculations, the $\beta_2$ value was decreased from the Delaroche result of 0.203 ± 0.006 to 0.195.[2] These parameter changes did not significantly alter the agreement obtained to the neutron total, differential elastic and inelastic data, and to the (p,p') results described above. An improvement in the calculated (n,2n) cross section did occur as shown for $^{184}W$(n,2n) in Fig. 1, where the solid curve is the results obtained using the parameters of Table I and the dashed curve is from the Delaroche parameter set. The experimental data in Fig. 1 are those of Frehaut et al.[9]

## EVALUATION RESULTS

The analysis described above was combined with experimental data and with ENDF/B-V (Rev. 0) below 0.1 MeV to produce evaluated data files for $^{182,183,184\ 186}W$ spanning the incident neutron energy range from $10^{-5}$ eV to 20 MeV.

Evaluated total cross sections were obtained for the even-even tungsten isotopes through use of experimental data, particularly recent measurements[10,11] made in the energy region from 0.2 to 5 MeV as well as guidance from the deformed optical-model calculations. Figure 2 compares the evaluated total cross sections for $^{182}W$ to available data. The evaluated total cross section below 1 MeV is based on the new Argonne results of Ref. 10. For $^{182}W$, these new measurements are consistent with previous measurements by Martin.[12] However, for $^{184}W$ and $^{186}W$ (see Fig. 3), the new Argonne data do not agree with the Martin data so that the evaluated total cross section differs substantially from the ENDF/B-V values below 2 MeV. Because no experimental total cross sections exist above 15 MeV for the tungsten isotopes, theoretical results from coupled-channel calculations were used between 15 and 20 MeV. Similarly, because of the complete absence of experimental data, evaluated total cross sections for $^{183}W$ are based exclusively on the calculations between 0.1 and 20 MeV.

For inelastic scattering to discrete levels, we used only those levels whose properties (excitation energy, spin, parity) have been fully identified. At excitation energies where knowledge of such discrete levels becomes sparse

TABLE I

OPTICAL PARAMETERS FOR TUNGSTEN ISOTOPES*

| | r | a |
|---|---|---|
| $^{182}W$ | | |
| $V = 46.8 - 0.4E$ | 1.26 | 0.61 |
| $W_{vol} = -1.8 + 0.2E$ | 1.26 | 0.61 |
| $V_{SO} = 7.5$ | 1.26 | 0.61 |
| $W_{SD} = 3.68 + 0.76E$ | 1.24 | 0.45 |
| Above 4.75 MeV | | |
| $W_{SD} = 7.29 - 0.1E$ | | |
| $\beta_2 = 0.223$, $\beta_4 = -0.054$ | | |
| $^{183}W$ | | |
| $V = 46.7 - 0.4E$ | 1.26 | 0.61 |
| $W_{vol} = -1.8 + 0.2E$ | 1.26 | 0.61 |
| $V_{SO} = 7.5$ | 1.26 | 0.61 |
| $W_{SD} = 3.54 + 0.76E$ | 1.24 | 0.45 |
| Above 4.63 MeV | | |
| $W_{SD} = 7.055 - 0.1E$ | | |
| $\beta_2 = 0.22$, $\beta_4 = -0.055$ | | |
| $^{184}W$ | | |
| $V = 46.6 - 0.4E$ | 1.26 | 0.61 |
| $W_{vol} = -1.8 + 0.2E$ | 1.26 | 0.61 |
| $V_{SO} = 7.5$ | 1.26 | 0.61 |
| $W_{SD} = 3.4 + 0.76E$ | 1.24 | 0.45 |
| Above 4.5 MeV | | |
| $W_{SD} = 6.82 - 0.1E$ | | |
| $\beta_2 = 0.209$, $\beta_4 = -0.056$ | | |
| $^{186}W$ | | |
| $V = 46.6 - 0.4E$ | 1.26 | 0.61 |
| $W_{vol} = -1.8 + 0.2$ | 1.26 | 0.61 |
| $V_{SO} = 7.5$ | 1.26 | 0.61 |
| $W_{SD} = 3.12 + 0.76E$ | 1.24 | 0.45 |
| Above 4.25 MeV | | |
| $W_{SD} = 6.35 - 0.1E$ | | |
| $\beta_2 = 0.195$, $\beta_4 = -0.057$ | | |

*All well depths are in MeV, geometrical parameters are in fm.

or fragmented, we used a continuum representation rather than employing fictitious levels. By doing so, we preserved a continuity in the calculated results over the entire incident energy range. Note that the continuum cross section, denoted by MT=91 in the ENDF/B files, generally has a threshold lying much lower than those of of the uppermost discrete level. In these cases MT=91 includes contributions from the (n,γn') process that has non-negligible cross-section values, at least until incident energies where the continuum (n,n') process dominates.

Figures 4-11 compare the evaluation to selected experimental results for reaction types that dominate within the 1- to 20-MeV energy range. Since the evaluated results were obtained from nuclear-model calculations, such comparisons illustrate how well these techniques can reproduce varied data in a consistent manner. The evaluated elastic cross sections for $^{184}W$ and $^{186}W$ appear in Fig. 4, and the inelastic cross sections to low-lying states in $^{182}W$ are shown in Figs. 5-7. The $^{182}W$ elastic angular distributions measured between 1.5 and 1.9 MeV by Guenther et al.[10] are compared with the evaluation in Fig. 8; similarly, the 3.4-MeV angular distribution measurements by Delaroche et al.[8] for the $0^+$, $2^+$, and $4^+$ states of $^{186}W$ are compared with the evaluation in Fig. 9. In the instances of Figs. 4, 5, 8, and 9, both Hauser-Feshbach and coupled-channel direct-reaction models govern the calculated results.

The calculated (n,γ) cross sections for $^{183}W$ and $^{184}W$ are compared with the available experimental data in Fig. 10. At higher energies a direct-semi-direct model was included in the calculation, producing a characteristic enhancement in the cross section near 15 MeV. The (n,2n) cross sections for $^{182}W$ and $^{183}W$ from our analysis (solid curve) are compared with experiment in Fig. 11. Similar agreement was obtained for the $^{184}W$ and $^{186}W$(n,2n) cross sections.

## ENDF/B-V.2 FILE FOR $^{182}$W (MAT 1475)

File 1. General Information

MT=451. Descriptive Data

Atomic mass and Q-values taken from Ref. 13.

File 2. Resonance Parameters

MT=151. (A) Resolved Resonances Evaluation

Potential scattering cross section = 8.0 ± 1.0 b at $E_n$=0.

2200 m/s Cross Sections (barns)

| | CALC | MEAS (Ref. 14) |
|---|---|---|
| CAP | 20.5 | 20.7 ± 0.5 |
| SCAT | 11.6 | |

Resolved Resonance Parameters

| | |
|---|---|
| - 100 eV | from fit to capture |
| 4.16 eV | from Ref. 14 |
| 5 - 250 eV | from evaluation, Refs. 14, 15 and 16 |
| 250 -1250 eV | from evaluation, Refs. 15 and 16 |
| 1250 -4500 eV | from Ref. 16 |
| 1920 -2198 eV | from Ref. 15 |

MT=151. (B) Unresolved Resonances Evaluation

Potential scattering cross section = 8.5 ± 1.0 b at $E_n$=0.
Total cross section = 8.85 b at $E_n$=100 keV (calculated).

Unresolved resonance parameters from automated optimized fit to the evaluated measured capture cross section.

AV L=0 level spacing ($E_n$=0) = 57.45 eV, energy dep. from Ref. 17.
AV Capture level width = 0.0901 eV, energy independent
L=0 Strength function = 1.8E-4 eV, energy independent
L=1 Strength function = 0.272E-4 eV, energy independent
L=2 Strength function = 0.0

Average capture cross section uncertainty at energy E

| E (keV) | Uncertainty (%) |
|---|---|
| 100 | 15 |
| 90 | 10 |
| 10 | 10 |
| 4.5 | 17 |

Resonance integral (capture) 596 b calculation, 590 ± 10 b measurement (Ref. 18).

File 3. Neutron Cross Sections

MT=1 Total Cross Section

The evaluated total cross section relies upon the experimental results of Lister et al. (Ref. 19) from 0.1 to 0.65 MeV. (Below 0.1 MeV the ENDF/B-V results in the unresolved resonance range were used directly). From 0.65 to 2.3 MeV the newly measured results of Guenther et al (Ref. 10) were used because these data are consistent with both higher and lower energy data (Refs. 12, 19, 20). From 2.3 to 5.0 MeV the Guenther results and those of Foster and Glasgow (Ref. 20) were averaged to produce the evaluated data. Between 5 and 15 MeV the evaluation relied on the Foster results. No experimental data exist above 15 MeV so that results from calculations using the coupled channels code ECIS (Ref. 1) were adopted. The optical parameters used (Ref. 7) gave good agreement to data in the energy range from 0.1 to 15 MeV.

MT=2 Elastic Cross Section

The evaluated elastic cross section was obtained by subtracting the non-elastic cross section from the evaluated total cross section. The evaluated data are in good agreement with recent measurements at energies below 4 MeV (Ref. 10).

MT=4 Total Inelastic Cross Section.

Equal to the sum of the inelastic level excitation and continuum cross sections.

MT=16 (n,2n) Cross Sections.

Multistep Hauser-Feshbach calculations with preequilibrium corrections were made using the GNASH code (Ref. 3) and deformed optical model transmission coefficients from the ECIS coupled-channels code. The results agree well with the isotopic data of Frehaut et al. (Ref. 9) measured from threshold to 15 MeV.

MT=17 (n,3n) Cross Sections.

Obtained from preequilibrium Hauser-Feshbach calculations made with the GNASH code.

MT=28 (n,pn) and (n,np) Cross Sections.

ENDF/B-V values modified to fit QAIM (1975) systematics.

MT= 51, 52 Inelastic Cross Sections for Excitation of the First and Second Excited States.

Calculated values were used for these cross sections. The ECIS coupled channels code was used for direct-reaction contributions while compound nucleus contributions were obtained using the COMNUC Hauser-Feshbach code (Ref. 2) with width-fluctuation corrections. Both calculations employed deformed neutron optical model parameters based on a modification (Ref. 7) of the set developed by Delaroche et al. (Ref. 8). These calculated data agree well with the measured results of Ref. 10.

MT=53-69 Inelastic Scattering Cross Sections to the Third through Nineteenth Excited States in $^{182}W$.

Cross sections for inelastic scattering from the third through nineteenth excited states in $^{182}W$ were calculated using the COMNUC Hauser-Feshbach code so only compound-nucleus contributions were included. Above 6 MeV such cross sections were set to zero and were added to the continuum cross section.

MT=91 Inelastic Scattering to the Continuum.

At low energies this cross section represents contributions from the (n,γ,n) process calculated using the COMNUC code. At higher energies this cross section is dominated by inelastic scattering to the continuum that was calculated using the COMNUC code and, where preequilibrium effects are important, with the GNASH code.

MT=102 Radiative Capture Cross Sections.

At energies below 0.1 MeV, the ENDF/B-V results were used directly. From 0.1 to 6 MeV, COMNUC/GNASH calculations were made. At energies greater than 1 MeV, a full treatment of the gamma-ray cascade was included. Above 6 MeV a simple model based on the preequilibrium emission of gamma rays was used to account for direct-semidirect effects. Results from this model were normalized to data (Ref. 21) at 14 MeV. The calculated capture cross sections between 0.5 and 3 MeV agree well with the recent measurements of Grenier (Ref. 22).

MT=103, 107 (n,p) and (n,α) Cross Sections.

Taken directly from ENDF/B-V.

File 4. Neutron Angular Distributions.

MT=2 Elastic Scattering Angular Distributions.

Angular distributions obtained from ECIS coupled-channel calculations are expressed in terms of Legendre coefficients in the center-of-mass system.

MT=16, 17 Angular Distributions of Neutrons from (n,2n) and (n,3n) Reactions.

Angular distributions were obtained using the Kalbach-Mann systematics (Ref. 23) that require knowledge of the preequilibrium emission fraction and the average energy of the emitted neutron. The results are expressed in terms of Legendre polynomial coefficients in the laboratory system.

MT=28 Angular Distributions of Neutrons from (n,np) and (n,pn) Reactions.

These are assumed isotropic in the laboratory system.

MT=91 Angular Distributions of Neutrons from Continuum Inelastic Scattering.

Legendre coefficients obtained from the Kalbach-Mann systematics are given in the laboratory system.

File 5. Neutron Energy Distributions.

MT=16, 17 Neutron Emission Spectra from (n,2n) and (n,3n) Reactions.

Histograms are given of emission spectra calculated using the GNASH preequilibrium statistical model code.

MT=28 Neutron Spectra from (n,np) and (n,pn) Reactions.

For these spectra, ENDF/B-V results were used directly.

MT=91 Neutron Spectra from the Continuum Emission of Inelastically Scattered Neutrons.

Histograms are given of emission spectra that include preequilibrium effects as obtained from GNASH calculations.

File 12. Photon Multiplicities.

MT=102 Multiplicities for Gamma-Ray Production from Radiative Capture.

Below 0.1 MeV the multiplicities were taken directly from ENDF/B-V. At higher energies multiplicities were obtained from COMNUC and GNASH statistical model calculations.

File 13. Photon Production Cross Sections.

MT=4, 16, 17 Gamma-Ray Production Cross Sections from Inelastic, (n,2n) and (n,3n) Reactions.

The cross section for discrete photons occurring through inelastic scattering are based on the level excitation cross sections in MF=3, MT=51-69. For gamma-ray cross sections from continuum inelastic, (n,2n) and (n,3n) reactions, GNASH results were used directly.

File 14. Photon Angular Distributions.

MT=4, 16, 17, 102 Angular Distributions of Gamma-Rays from Inelastic Scattering, (n,2n), (n,3n), and Radiative Capture Reactions.

All gamma rays are assumed isotropic in the laboratory system.

File 15. Photon Energy Distributions.

MT=16, 17, 91 Energy Spectra of Gamma-Rays from (n,2n), (n,3n), and Continuum Inelastic Reactions.

The spectra at all energies are based directly on preequilibrium Hauser-Feshbach calculations made using the GNASH nuclear model code.

MT=102 Energy Spectra of Gamma-Rays from Radiative Capture.

Below 0.1 MeV the spectra are taken from ENDF/B-V. From 0.1 to 10 MeV, the spectra are taken from GNASH statistical model calculations. Above 10 MeV, a simple preequilibrium-like model was used to calculate the spectra.

## ENDF/B-V.2 FILE FOR $^{183}$W (MAT 1476)

File 1. General Information

MT=451. Descriptive Data

Atomic mass and Q-values taken from Ref. 13.

File 2. Resonance Parameters

MT=151. (A) Resolved Resonances Evaluation

Potential scattering cross section = 8.0 ± 1.0 b at $E_n$ = 0.

2200 m/s Cross Sections (barns)

| | CALC | MEAS (Ref. 14) |
|---|---|---|
| CAP | 10.0 | 10.2 ± 3.0 |
| SCAT | 3.4 | |

Resolved Resonance Parameters

| | | |
|---|---|---|
| -1.5 eV | from | fit to capture |
| 0 - 150 eV | from | Ref. 14 |
| 150 - 175 eV | from | evaluation, Refs. 14 and 15 |
| 175 - 760 eV | from | Ref. 15 |

MT=151. (B) Unresolved Resonances Evaluation

Potential scattering cross section = 8.5 ± 1.0 b at $E_n$=0.
Total cross section = 11.3 b at $E_n$=45 keV (calculated).

Unresolved resonance parameters from automated optimized fit to the evaluated measured capture cross section. The competitive reaction width for L=2, J=1 is for the L to L-2 elastic scattering process.

AV L=0 level spacing ($E_n$=0) = 12.53 eV, energy dep. from Ref. 17.
AV Capture level width = 0.0801 eV, energy independent
L=0 Strength function = 2.124E-4 eV, energy independent
L=1 Strength function = 0.227E-4 eV, energy independent
L=2 Strength function = 2.56E-4 eV, energy independent

Average capture cross section uncertainty at energy E

| E (keV) | Uncertainty (%) |
|---|---|
| 45 | 11 |
| 10 | 12 |
| 5 | 20 |
| 2.5 | 40 |

Resonance integral (capture) 355 b calculation, 380 ± 15 b measurement (Ref. 18).

File 3. Neutron Cross Sections

MT=1 Total Cross Section

No experimental data exist for $^{183}W$, so coupled-channel calculations were made between 0.1 and 20 MeV using the ECIS (Ref. 1) code and optical parameters (Ref. 7) that gave good agreement to $^{182,184,186}W$ isotopic total cross section data as well as to $^{183}W$ elastic scattering data at 3.4 MeV (Ref. 8). Below 0.1 MeV, ENDF/B-V results in the unresolved region were used directly.

MT=2 Elastic Cross Section

The evaluated elastic cross section was obtained by subtracting the nonelastic cross section from the evaluated total cross section. The evaluated data are in good agreement with recent measurements at energies below 4 MeV (Ref. 10).

MT=4 Total Inelastic Cross Section

Equal to the sum of the inelastic level excitation and continuum cross sections.

MT=16 (n,2n) Cross Sections

Multistep Hauser-Feshbach calculations with preequilibrium corrections were made using the GNASH code (Ref. 3) and deformed optical model transmission coefficients from the ECIS coupled-channels code. The results agree well with the isotopic data of Frehaut et al. (Ref. 9) measured from threshold to 15 MeV.

MT=17 (n,3n) Cross Sections

Obtained from preequilibrium Hauser-Feshbach calculations made with the GNASH code.

MT=28 (n,pn) and (n,np) Cross Sections

These values were taken directly from ENDF/B-V.

MT=51, 52, 53, 56 Inelastic Cross Sections for Excitation of the First, Second, Third, and Sixth Excited States in $^{183}W$.

Calculated values were used for these cross sections. The ECIS coupled channels code was used for direct-reaction contributions while compound nucleus contributions were obtained using the COMNUC Hauser-Feshbach code (Ref. 2) with width-fluctuation corrections. Both calculations employed neutron optical model parameters based on a modification (Ref. 7) of the set developed by Delaroche et al. (Ref. 8). These calculated data agree well with the measured results of Ref. 10.

MT=54, 55, 57-64 Inelastic Scattering Cross Sections to the Fourth, Fifth, and Seventh through Fourteenth Excited States in $^{183}W$.

Cross sections for inelastic scattering from the fourth, fifth, and seventh through fourteenth excited states in $^{183}W$ were calculated using the COMNUC Hauser-Feshbach code so only compound-nucleus contributions were included. Above 6 MeV such cross sections were set to zero and were added to the continuum cross section (MT=91).

MT=91 Inelastic Scattering to the Continuum.

At low energies this cross section represents contributions from the (n,γn) process calculated using the COMNUC code. At higher energies this cross section is dominated by inelastic scattering to the continuum which was calculated using the COMNUC code and, where preequilibrium effects are important, with the GNASH code.

MT=102 Radiative Capture Cross Section.

At energies below 0.1 MeV the ENDF/B-V results were used directly. From 0.1 to 6 MeV, COMNUC/GNASH calculations were made. At energies greater than 1 MeV, a full treatment of the gamma-ray cascade was included. Above 6 MeV, a simple model based on the preequilibrium emission of gamma rays was used to account for direct-semidirect effects. Results from this model were normalized to data (Ref. 21) at 14 MeV. The calculated capture cross sections between 0.5 and 3 MeV agree well with the recent measurements of Grenier (Ref. 11).

MT=103, 107 (n,p) and (n,α) Cross Sections.

(n,p) based on ENDF/B-V renormalized to fit QAIM (1975) systematics. (n,α) taken directly from ENDF/B-V.

File 4. Neutron Angular Distributions.

MT=2 Elastic Scattering Angular Distributions.

Angular distributions obtained from ECIS coupled-channel calculations are expressed in terms of Legendre coefficients in the center-of-mass system.

MT=16, 17 Angular Distributions of Neutrons from (n,2n) and (n,3n) Reactions.

Angular distributions were obtained using the Kalbach-Mann systematics (Ref. 23) that require knowledge of the preequilibrium emission fraction and the average energy of the emitted neutron. The results are expressed in terms of Legendre polynomial coefficients in the laboratory system.

MT=28 Angular Distributions of Neutrons from (n,np) and (n,pn) Reactions.

These are assumed isotropic in the laboratory system.

MT=91 Angular Distributions of Neutrons from Continuum Inelastic Scattering .

Legendre coefficients obtained from the Kalbach-Mann systematics are given in the laboratory system.

File 5. Neutron Energy Distributions

MT=16, 17 Neutron Emission Spectra from (n,2n) and (n,3n) Reactions.

Histograms are given of emission spectra calculated using the GNASH pre-equilibrium statistical model code.

MT=28 Neutron Spectra from (n,np) and (n,pn) Reactions.

For these spectra ENDF/B-V results were used directly.

MT=91 Neutron Spectra from the Continuum Emission of Inelastically Scattered Neutrons.

Histograms are given of emission spectra that include preequilibrium effects as obtained from GNASH calculations.

File 12. Photon Multiplicities.

MT=102 Multiplicities for Gamma-ray Production from Radiative Capture.

Below 0.1 MeV, the multiplicities were taken directly from ENDF/B-V. At higher energies, multiplicities were obtained from COMNUC and GNASH statistical model calculations.

File 13. Photon Production Cross Sections.

MT=4, 16, 17 Gamma-ray Production Cross Sections from Inelastic, (n,2n), and (n,3n) Reactions.

The cross section for discrete photons occurring through inelastic scattering are based on the level excitation cross sections in MF=3, MT=51-64. For Gamma-ray cross sections from continuum inelastic, (n,2n), and (n,3n) reactions, GNASH results were used directly.

File 14. Photon Angular Distributions.

MT=4, 16, 17, 102 Angular Distributions of Gamma-rays from Inelastic Scattering, (n,2n), (n,3n), and Radiative Capture Reactions.

All gamma rays are assumed isotropic in the laboratory system.

File 15. Photon Energy Distributions.

MT=16, 17, 91 Energy Spectra of Gamma Rays from (n,2n), (n,3n) and Continuum Inelastic Reactions.

The spectra at all energies are based directly on preequilibrium Hauser-Feshbach calculations made using the GNASH nuclear model code.

MT=102 Energy Spectra of Gamma Rays from Radiative Capture.

Below 0.1 MeV, the spectra are taken from ENDF/B-V. From 0.1 to 10 MeV, the spectra are taken from GNASH statistical model calculations. Above 10 MeV, a simple preequilibrium-like model was used to calculate the spectra.

## ENDF/B-V.2 FILE FOR $^{184}$W (MAT 1477)

File 1. General Information

MT=451. Descriptive Data

Atomic mass and Q-values taken from Ref. 13.

File 2. Resonance Parameters

MT=151. (A) Resolved Resonance Evaluation

Potential scattering cross section = 8.0 ± 1.0 b at $E_n$=0.

2200 m/s Cross Sections (barns)

| | CALC | MEAS (Ref. 14) |
|---|---|---|
| CAP | 1.8 | 1.8 ± 0.2 |
| SCAT | 3.9 | |

Resolved Resonance Parameters

| | |
|---|---|
| -11.76 eV | from fit to capture |
| 102 eV | from evaluation, Refs. 14 and 15 |
| 150 - 2060 eV | from evaluation, Refs. 14, 15, and 16 |
| 2080 - 2110 eV | from Ref. 15 |
| 2200 - 2650 eV | from Ref. 16 |

MT=151. (B) Unresolved Resonances Evaluation

Potential scattering cross section = 8.5 ± 1.0 b at $E_n$=0.
Total cross section = 9.1 b at $E_n$=100 keV (calculated).

Unresolved resonance parameters from automated optimized fit to the evaluated measured capture cross section.

| | |
|---|---|
| AV L=0 level spacing ($E_n$=0) | = 80.3 eV, energy dep. from Ref. 17. |
| AV Capture level width | = 0.0731 eV, energy independent |
| L=0 Strength function | = 2.3E-4 eV, energy independent |
| L=1 Strength function | = 0.18E-4 eV, energy independent |
| L=2 Strength function | = 1.45E-4, energy independent |

Average capture cross section uncertainty at energy E

| E (keV) | Uncertainty (%) |
|---|---|
| 100 | 15 |
| 90 | 10 |
| 10 | 10 |
| 4.5 | 20 |

Resonance integral (capture) 16.2 b calculation, 13 ± 12 b measurement (Ref. 18).

File 3. Neutron Cross Sections

MT=1 Total Cross Section

The evaluated total cross section relies upon the experimental results of Lister et al. (Ref. 19) from 0.1 to 0.65 MeV. (Below 0.1 MeV the ENDF/B-V results in the unresolved resonance range were used directly). From 0.65 to 2.3 MeV the newly measured results of Guenther et al (Ref. 10) were used because these data are consistent with both higher and lower energy data (Refs. 12, 19, 20). From 2.3 to 5.0 MeV the Guenther results and those of Foster and Glasgow (Ref. 20) were averaged to produce the evaluated data. Between 5 and 15 MeV the evaluation relied on the Foster results. No experimental data exist above 15 MeV so that results from calculations using the coupled channels code ECIS (Ref. 1) were adopted. The optical parameters used (Ref. 7) gave good agreement to data in the energy range from 0.1 to 15 MeV.

MT=2 Elastic Cross Section

The evaluated elastic cross section was obtained by subtracting the non-elastic cross section from the evaluated total cross section. The evaluated data are in good agreement with recent measurements at energies below 4 MeV (Ref. 10).

MT=4 Total Inelastic Cross Section.

Equal to the sum of the inelastic level excitation and continuum cross sections.

MT=16 (n,2n) Cross Sections.

Multistep Hauser-Feshbach calculations with preequilibrium corrections were made using the GNASH code (Ref. 3) and deformed optical model transmission coefficients from the ECIS coupled-channels code. The results agree well with the isotopic data of Frehaut et al. (Ref. 9) measured from threshold to 15 MeV.

MT=17 (n,3n) Cross Sections.

Obtained from preequilibrium Hauser-Feshbach calculations made with the GNASH code.

MT=28 (n,pn) and (n,np) Cross Sections.

These values were taken directly from ENDF/B-V.

MT= 51, 52 Inelastic Cross Sections for Excitation of the First and Second Excited States.

Calculated values were used for these cross sections. The ECIS coupled channels code was used for direct-reaction contributions while compound nucleus contributions were obtained using the COMNUC Hauser-Feshbach code (Ref. 2) with width-fluctuation corrections. Both calculations employed deformed neutron optical model parameters based on a modification (Ref. 7) of the set developed by Delaroche et al. (Ref. 8). These calculated data agree well with the measured results of Ref. 10.

MT=53-68 Inelastic Scattering Cross Sections to the Third through Eighteenth Excited States in $^{184}W$.

Cross sections for inelastic scattering from the third through eighteenth excited states in $^{184}W$ were calculated using the COMNUC Hauser-Feshbach code so only compound-nucleus contributions were included. Above 6 MeV such cross sections were set to zero and were added to the continuum cross section.

MT=91 Inelastic Scattering to the Continuum.

At low energies this cross section represents contributions from the (n,γ,n) process calculated using the COMNUC code. At higher energies this cross section is dominated by inelastic scattering to the continuum that was calculated using the COMNUC code and, where preequilibrium effects are important, with the GNASH code.

MT=102 Radiative Capture Cross Sections.

At energies below 0.1 MeV, the ENDF/B-V results were used directly. From 0.1 to 6 MeV, COMNUC/GNASH calculations were made. At energies greater than 1 MeV, a full treatment of the gamma-ray cascade was included. Above 6 MeV a simple model based on the preequilibrium emission of gamma rays was used to account for direct-semidirect effects. Results from this model were normalized to data (Ref. 21) at 14 MeV. The calculated capture cross sections between 0.5 and 3 MeV agree well with the recent measurements of Grenier (Ref. 22).

MT=103, 107 (n,p) and (n,α) Cross Sections.

ENDF/B-V normalized to fit QAIM (1975) values.

File 4. Neutron Angular Distributions.

MT=2 Elastic Scattering Angular Distributions.

Angular distributions obtained from ECIS coupled-channel calculations are expressed in terms of Legendre coefficients in the center-of-mass system.

MT=16, 17 Angular Distributions of Neutrons from (n,2n) and (n,3n) Reactions.

Angular distributions were obtained using the Kalbach-Mann systematics (Ref. 23) that require knowledge of the preequilibrium emission fraction and the average energy of the emitted neutron. The results are expressed in terms of Legendre polynomial coefficients in the laboratory system.

MT=28 Angular Distributions of Neutrons from (n,np) and (n,pn) Reactions.

These are assumed isotropic in the laboratory system.

MT=91 Angular Distributions of Neutrons from Continuum Inelastic Scattering.

Legendre coefficients obtained from the Kalbach-Mann systematics are given in the laboratory system.

File 5. Neutron Energy Distributions.

MT=16, 17 Neutron Emission Spectra from (n,2n) and (n,3n) Reactions.

Histograms are given of emission spectra calculated using the GNASH preequilibrium statistical model code.

MT=28 Neutron Spectra from (n,np) and (n,pn) Reactions.

For these spectra, ENDF/B-V results were used directly.

MT=91 Neutron Spectra from the Continuum Emission of Inelastically Scattered Neutrons.

Histograms are given of emission spectra that include preequilibrium effects as obtained from GNASH calculations.

File 12. Photon Multiplicities.

MT=102 Multiplicities for Gamma-Ray Production from Radiative Capture.

Below 0.1 MeV the multiplicities were taken directly from ENDF/B-V. At higher energies multiplicities were obtained from COMNUC and GNASH statistical model calculations.

File 13. Photon Production Cross Sections.

MT=4, 16, 17 Gamma-Ray Production Cross Sections from Inelastic, (n,2n) and (n,3n) Reactions.

The cross section for discrete photons occurring through inelastic scattering are based on the level excitation cross sections in MF=3, MT=51-68. For gamma-ray cross sections from continuum inelastic, (n,2n) and (n,3n) reactions, GNASH results were used directly.

File 14. Photon Angular Distributions.

MT=4, 16, 17, 102 Angular Distributions of Gamma-Rays from Inelastic Scattering, (n,2n), (n,3n), and Radiative Capture Reactions.

All gamma rays are assumed isotropic in the laboratory system.

File 15. Photon Energy Distributions.

MT=16, 17, 91 Energy Spectra of Gamma-Rays from (n,2n), (n,3n), and Continuum Inelastic Reactions.

The spectra at all energies are based directly on preequilibrium Hauser-Feshbach calculations made using the GNASH nuclear model code.

MT=102 Energy Spectra of Gamma-Rays from Radiative Capture.

Below 0.1 MeV the spectra are taken from ENDF/B-V. From 0.1 to 10 MeV, the spectra are taken from GNASH statistical model calculations. Above 10 MeV, a simple preequilibrium-like model was used to calculate the spectra.

## ENDF/B-V.2 FILE FOR $^{186}$W (MAT 1478)

File 1. General Information

MT=451. Descriptive Data

Atomic mass and Q-values taken from Ref. 13.

File 2. Resonance Parameters

MT=151. (A) Resolved Resonances Evaluation

Potential scattering cross section = 8.0 ± 1.0 b at $E_n$=0.

2200 m/s Cross Sections (barns)

| | CALC | MEAS (Ref. 14) |
|---|---|---|
| CAP | 37.5 | 38 ± 2 |
| SCAT | 0.39 | |

Resolved Resonance Parameters

| | | |
|---|---|---|
| 18.81 eV | from | evaluation of Refs. 14 and 16 plus adjustment from fit to capture cross section |
| 100 - 250 eV | from | evaluation of Refs. 14-16 |
| 250 - 3200 eV | from | evaluation of Refs. 15, 16. |

MT=151. (B) Unresolved Resonance Evaluation

Potential scattering cross section = 8.5 ± 1.0 b at $E_n$=0.
Total cross section = 9.1 b at $E_n$=100 keV (calculated).

Unresolved resonance parameters from automated optimized fit to the evaluated measured capture cross section.

| | | |
|---|---|---|
| AV L=0 level spacing ($E_n$=0) | = 99.1 eV, | energy dep. from Ref. 17. |
| AV Capture level width | = 0.0530 eV, | energy independent |
| L=0 Strength function | = 2.2E-4, | energy independent |
| L=1 Strength function | = 0.252E-4, | energy independent |
| L=2 Strength function | = 1.45E-4, | energy independent |

Average capture cross section uncertainty at energy E

| E (keV) | Uncertainty (%) |
|---|---|
| 100 | 11 |
| 90 | 8 |
| 45 | 8 |
| 22.5 | 14 |
| 10 | 11 |
| 4.5 | 17 |

Resonance integral (capture) 522 b calculation, 490 ± 50 b measurement (Ref. 18).

File 3. Neutron Cross Sections

MT=1 Total Cross Section

The evaluated total cross section relies upon the experimental results of Lister et al. (Ref. 19) from 0.1 to 0.65 MeV. (Below 0.1 MeV the ENDF/B-V results in the unresolved resonance range were used directly). From 0.65 to 2.3 MeV, the newly measured results of Guenther et al (Ref. 10) were used because these data are consistent with both higher and lower energy data (Refs. 12, 19, 20). From 2.3 to 5.0 MeV, the Guenther results and those of Foster and Glasgow (Ref. 20) were averaged to produce the evaluated data. Between 5 and 15 MeV the evaluation relied on the Foster results. No experimental data exist above 15 MeV so that results from calculations using the coupled channels code ECIS (Ref. 1) were adopted. The optical parameters used (Ref. 7) gave good agreement to data in the energy range from 0.1 to 15 MeV.

MT=2 Elastic Cross Section

The evaluated elastic cross section was obtained by subtracting the non-elastic cross section from the evaluated total cross section. The evaluated data are in good agreement with recent measurements at energies below 4 MeV (Ref. 10).

MT=4 Total Inelastic Cross Section.

Equal to the sum of the inelastic level excitation and continuum cross sections.

MT=16 (n,2n) Cross Sections.

Multistep Hauser-Feshbach calculations with preequilibrium corrections were made using the GNASH code (Ref. 3) and deformed optical model transmission coefficients from the ECIS coupled-channels code. The results agree well with the isotopic data of Frehaut et al. (Ref. 9) measured from threshold to 15 MeV.

MT=17 (n,3n) Cross Sections.

Obtained from preequilibrium Hauser-Feshbach calculations made with the GNASH code.

MT=28 (n,pn) and (n,np) Cross Sections.

These values were taken directly from ENDF/B-V.

MT= 51, 52 Inelastic Cross Sections for Excitation of the First and Second Excited States.

Calculated values were used for these cross sections. The ECIS coupled channels code was used for direct-reaction contributions while compound nucleus contributions were obtained using the COMNUC Hauser-Feshbach code (Ref. 2) with width-fluctuation corrections. Both calculations employed deformed neutron optical model parameters based on a modification (Ref. 7) of the set developed by Delaroche et al. (Ref. 8). These calculated data agree well with the measured results of Ref. 10.

MT=53-68 Inelastic Scattering Cross Sections to the Third through Eighteenth Excited States in $^{186}W$.

Cross sections for inelastic scattering from the third through eighteenth excited states in $^{186}W$ were calculated using the COMNUC Hauser-Feshbach code so only compound-nucleus contributions were included. Above 6 MeV such cross sections were set to zero and were added to the continuum cross section.

MT=91 Inelastic Scattering to the Continuum.

At low energies this cross section represents contributions from the (n,γ,n) process calculated using the COMNUC code. At higher energies this cross section is dominated by inelastic scattering to the continuum that was calculated using the COMNUC code and, where preequilibrium effects are important, with the GNASH code.

MT=102 Radiative Capture Cross Sections.

At energies below 0.1 MeV, the ENDF/B-V results were used directly. From 0.1 to 6 MeV, COMNUC/GNASH calculations were made. At energies greater than 1 MeV, a full treatment of the gamma-ray cascade was included. Above 6 MeV a simple model based on the preequilibrium emission of gamma rays was used to account for direct-semidirect effects. Results from this model were normalized to data (Ref. 21) at 14 MeV. The calculated capture cross sections between 0.5 and 3 MeV agree well with the recent measurements of Grenier (Ref. 22).

MT=103, 107 (n,p) and (n,α) Cross Sections.

ENDF/B-V normalized to fit QAIM (1975) values.

File 4. Neutron Angular Distributions.

MT=2 Elastic Scattering Angular Distributions.

Angular distributions obtained from ECIS coupled-channel calculations are expressed in terms of Legendre coefficients in the center-of-mass system.

MT=16, 17 Angular Distributions of Neutrons from (n,2n) and (n,3n) Reactions.

Angular distributions were obtained using the Kalbach-Mann systematics (Ref. 23) that require knowledge of the preequilibrium emission fraction and the average energy of the emitted neutron. The results are expressed in terms of Legendre polynomial coefficients in the laboratory system.

MT=28 Angular Distributions of Neutrons from (n,np) and (n,pn) Reactions.

These are assumed isotropic in the laboratory system.

MT=91 Angular Distributions of Neutrons from Continuum Inelastic Scattering.

Legendre coefficients obtained from the Kalbach-Mann systematics are given in the laboratory system.

File 5. Neutron Energy Distributions.

MT=16, 17 Neutron Emission Spectra from (n,2n) and (n,3n) Reactions.

Histograms are given of emission spectra calculated using the GNASH preequilibrium statistical model code.

MT=28 Neutron Spectra from (n,np) and (n,pn) Reactions.

For these spectra, ENDF/B-V results were used directly.

MT=91 Neutron Spectra from the Continuum Emission of Inelastically Scattered Neutrons.

Histograms are given of emission spectra that include preequilibrium effects as obtained from GNASH calculations.

File 12. Photon Multiplicities.

MT=102 Multiplicities for Gamma-Ray Production from Radiative Capture.

Below 0.1 MeV the multiplicities were taken directly from ENDF/B-V. At higher energies multiplicities were obtained from COMNUC and GNASH statistical model calculations.

File 13. Photon Production Cross Sections.

MT=4, 16, 17 Gamma-Ray Production Cross Sections from Inelastic, (n,2n) and (n,3n) Reactions.

The cross section for discrete photons occurring through inelastic scattering are based on the level excitation cross sections in MF=3, MT=51-68. For gamma-ray cross sections from continuum inelastic, (n,2n) and (n,3n) reactions, GNASH results were used directly.

File 14. Photon Angular Distributions.

MT=4, 16, 17, 102 Angular Distributions of Gamma-Rays from Inelastic Scattering, (n,2n), (n,3n), and Radiative Capture Reactions.

All gamma rays are assumed isotropic in the laboratory system.

File 15. Photon Energy Distributions.

MT=16, 17, 91 Energy Spectra of Gamma-Rays from (n,2n), (n,3n), and Continuum Inelastic Reactions.

The spectra at all energies are based directly on preequilibrium Hauser-Feshbach calculations made using the GNASH nuclear model code.

MT=102 Energy Spectra of Gamma-Rays from Radiative Capture.

Below 0.1 MeV the spectra are taken from ENDF/B-V. From 0.1 to 10 MeV, the spectra are taken from GNASH statistical model calculations. Above 10 MeV, a simple preequilibrium-like model was used to calculate the spectra.

REFERENCES

1. J. Raynal, "Optical Model and Coupled-Channel Calculations in Nuclear Physics," International Atomic Energy Agency report IAEA-SMR-9/8 (1972).

2. C. L. Dunford, "A Unified Model for Analysis of Compound Nucleus Reactions," Atomics International report AI-AEC-12931 (July 1970).

3. P. G. Young and E. D. Arthur, "GNASH" A Preequilibrium Statistical Nuclear Model Code for Calculations of Cross Sections and Emission Spectra," Los Alamos Scientific Laboratory report LA-6947 (November 1977).

4. A. Gilbert and A. G. W. Cameron, "A Composite Nuclear-Level Density Formula with Shell Corrections," Can. J. Phys. 43, 1446 (1965).

5. J. L. Cook, H. Ferguson, and A. R. Musgrove, Aust. J. Phys. 20, 477 (1967).

6. S. Joly, Bruyeres-le-Chatel, personal communication (1980).

7. E. D. Arthur, et al., Los Alamos National Laboratory report LA-8630-PR (1980), p. 2.

8. J. P. Delaroche, G. Haouat, J. Lachkar, Y. Patin, J. Sigaud, and J. Chardine, "Coherent Optical and Statistical Model Analysis of $^{182,183,184}$ $^{186}$W Neutron Cross Sections," Proc. Int. Conf. Nuclear Cross Sections for Technology, Knoxville, Tenn. (1979) [NBS Special Publ. 594, p. 336 (1980)].

9. J. Frehaut, A. Bertin, R. Bois, and J. Jary, "Status of (n,2n) Cross Section Measurements at Bruyeres-le-Chatel," Proc. Symp. on Neutron Cross Sections from 10 to 50 MeV, May 1980, BNL-NCS-51245, Vol. 1, p. 399 (1980).

10. P. T. Guenther and A. B. Smith, Phys. Rev. C26, 2433 (1982).

11. A. B. Smith, Argonne National Laboratory, personal communication (1980). (See also Ref. 10.)

12. R. C. Martin, P. F. Yergin, R. H. Auguston, N. N. Kaushal, H. A. Medicus, and E. J. Winhold, "MeV Neutron Total Cross Sections of Ta and W Isotopes," Bull. Am. Phys. Soc. 12, 106 (1967).

13. A. H. Wapstra and K. Bos, At. Data and Nucl. Data Tables 19, 177 (1977).

14. M. Goldberg et al., Brookhaven National Laboratory report BNL-325, 2nd Edition, Supplement 2, (1966).

15. Z. M. Bartolome et al, Nucl. Sci. Eng. 37, p. 137 (1969).

16. F. J. Rahn and H. Camarda, personal communication, Columbia (1970).

17. J. L. Cook et al., AAEC/TM-392 (1967).

18. M. Drake, (1968) for American Institute of Physics Handbook (1972).

19. D. Lister et al., Phys. Rev. 162, 1077 (1967).

20. D. G. Foster, Jr., and D. Glasgow, Phys. Rev. C3, 576 (1971).

21. M. Budnar et al., INDC (YUG)-6/2 (1979).

22. G. Grenier, J. P. Delaroche, S. Joly, Ch. Lagrange, and J. Voignier, "Neutron Capture Cross Sections of Y, Nb, Gd, W, and Au Between 0.5 and 3.0 MeV," Proc. Int. Conf. on Nuclear Cross Sections for Technology, Knoxville, Tenn. (1979); [NBS Spec. Pub. 594, p. 323 (1980)].

23. C. Kalbach and F. M. Mann, "Phenomenology of Preequilibrium Angular Distributions," Proc. Symp. on Neutron Cross Sections from 10 to 50 MeV," Brookhaven National Laboratory (1980); [BNL-NCS-51245, Vol. 2, p. 689 (1980)].

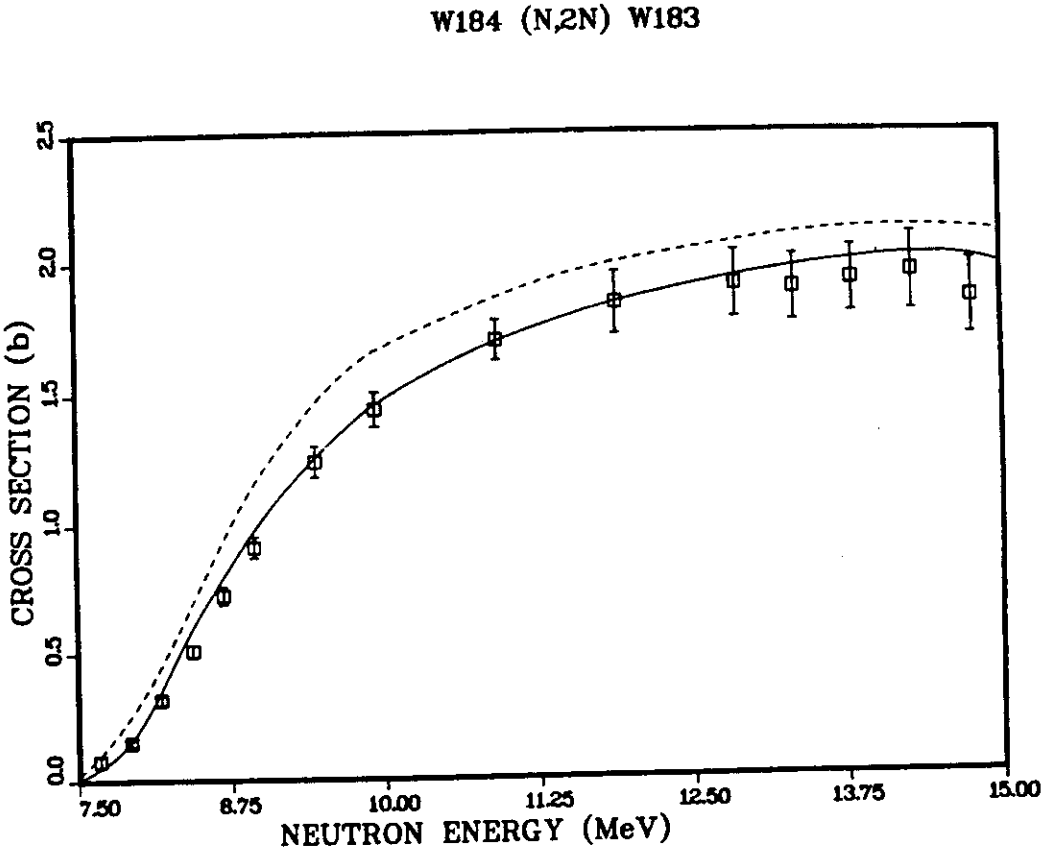


Fig. 1.

Calculated values of the $^{184}W(n,2n)$ cross section using the parameters of Table I (solid curve) are compared with the Frehaut data.[9] The dashed curve indicates results obtained with the Delaroche parameters.[8]

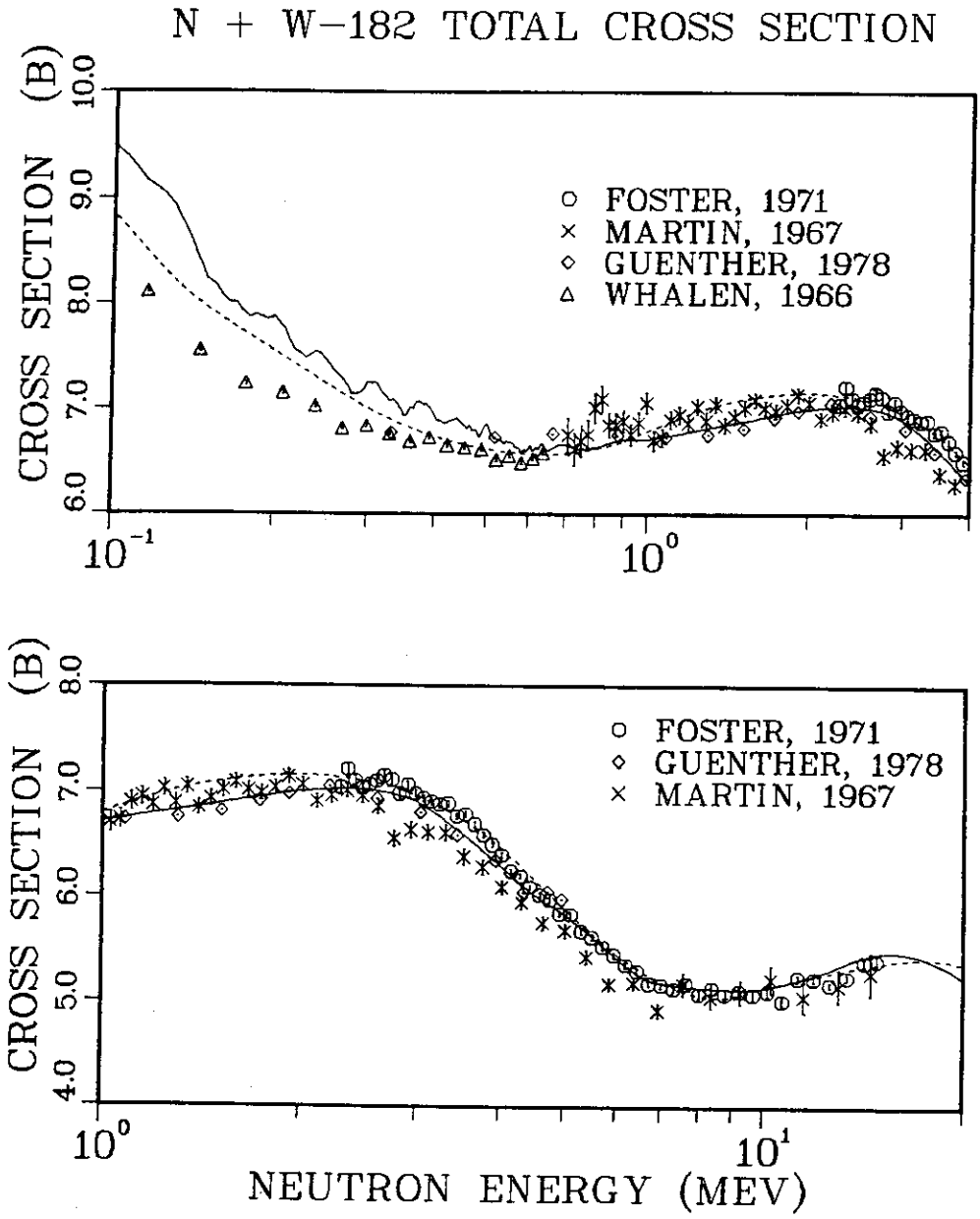


Fig. 2.

Evaluated (solid curve) and experimental values for the $^{182}W$ total cross section. The dashed curve is ENDF/B-V, Rev. 0.

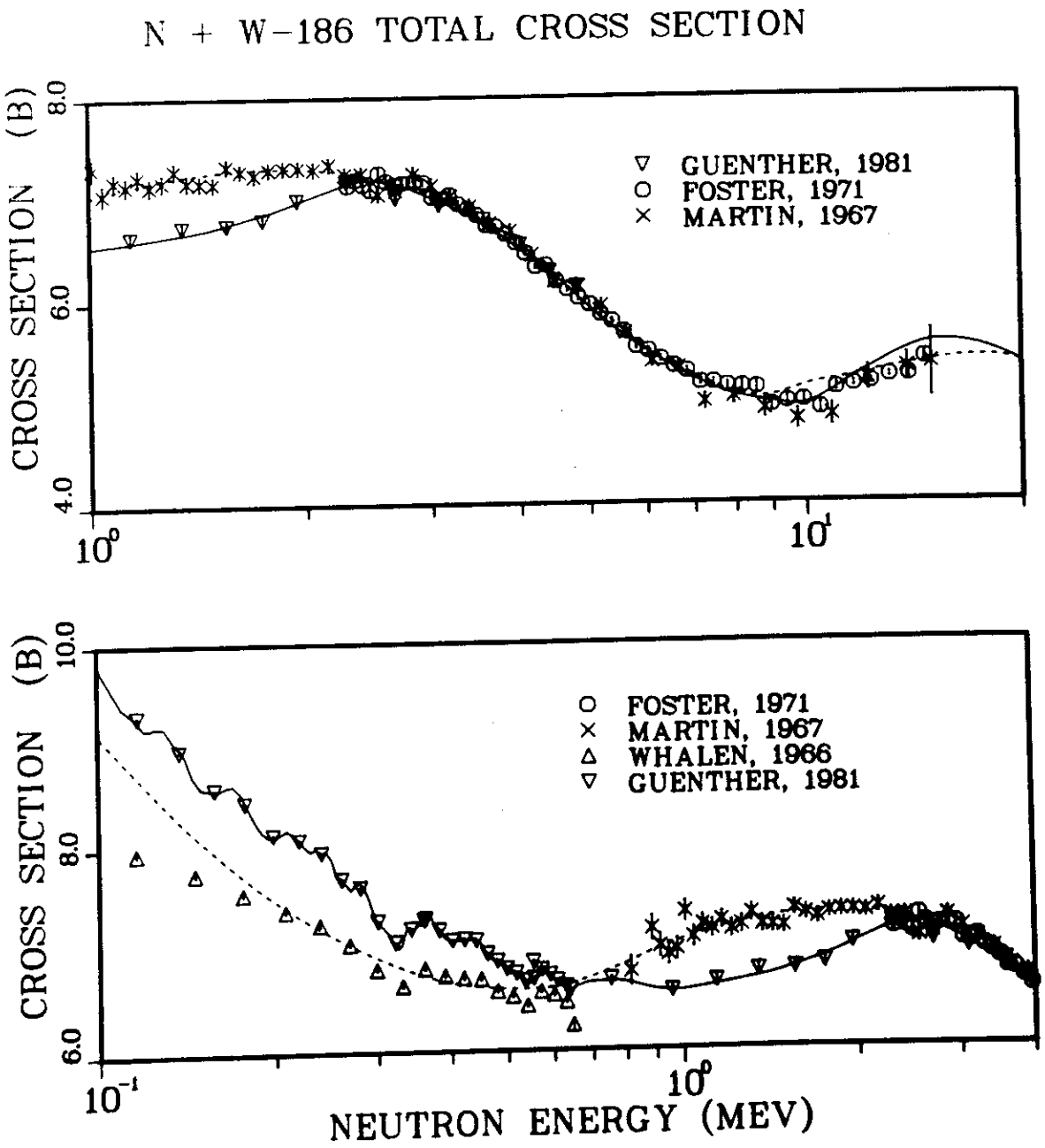


Fig. 3.

Evaluated (solid curve) and experimental values for the $^{186}W$ total cross section. The dashed curve is ENDF/B-V, Rev. 0.

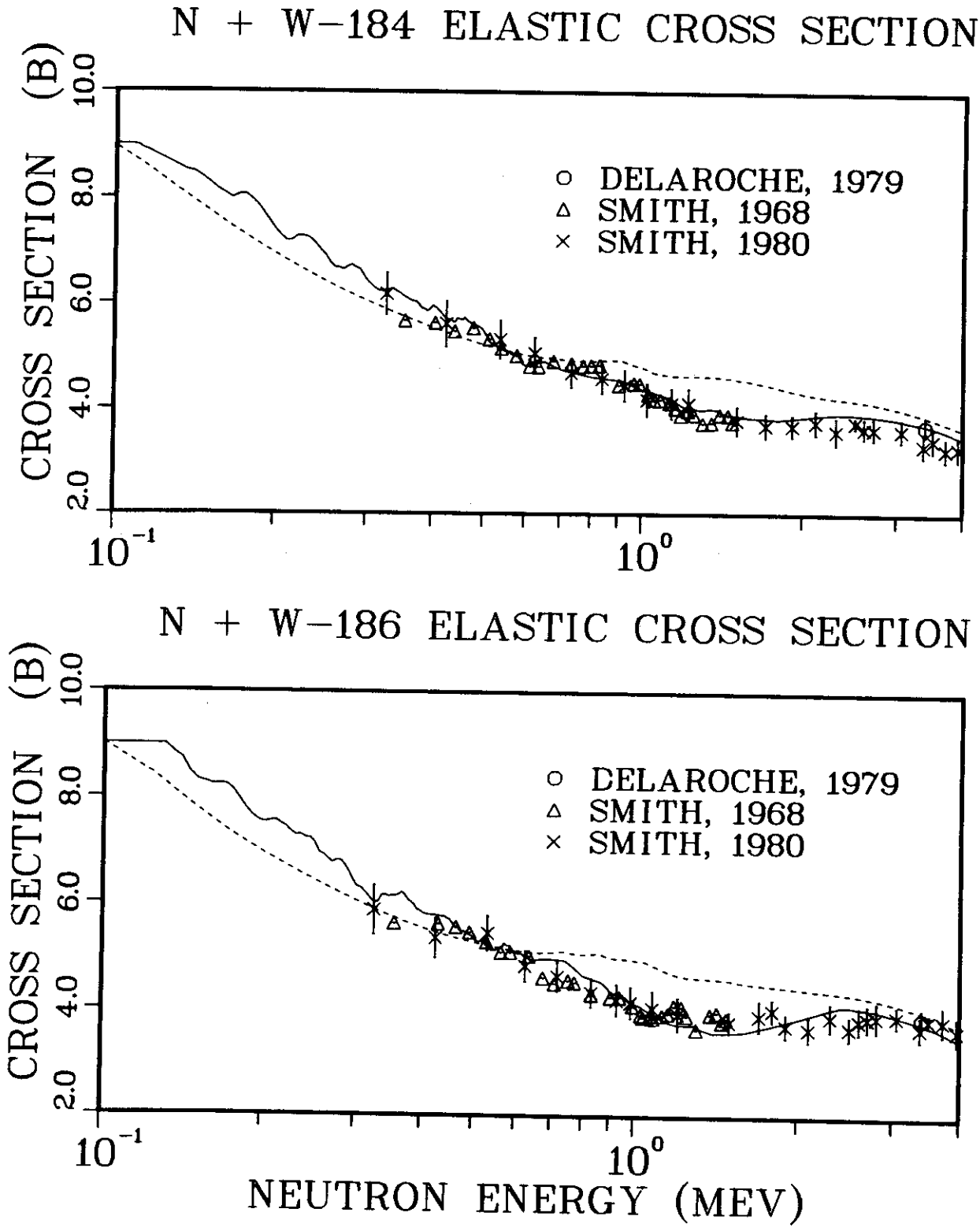


Fig. 4.

The evaluated elastic cross section is compared with experimental data available for $^{184}W$ and $^{186}W$. ENDF/B-V, Rev. 0, is the dashed line.

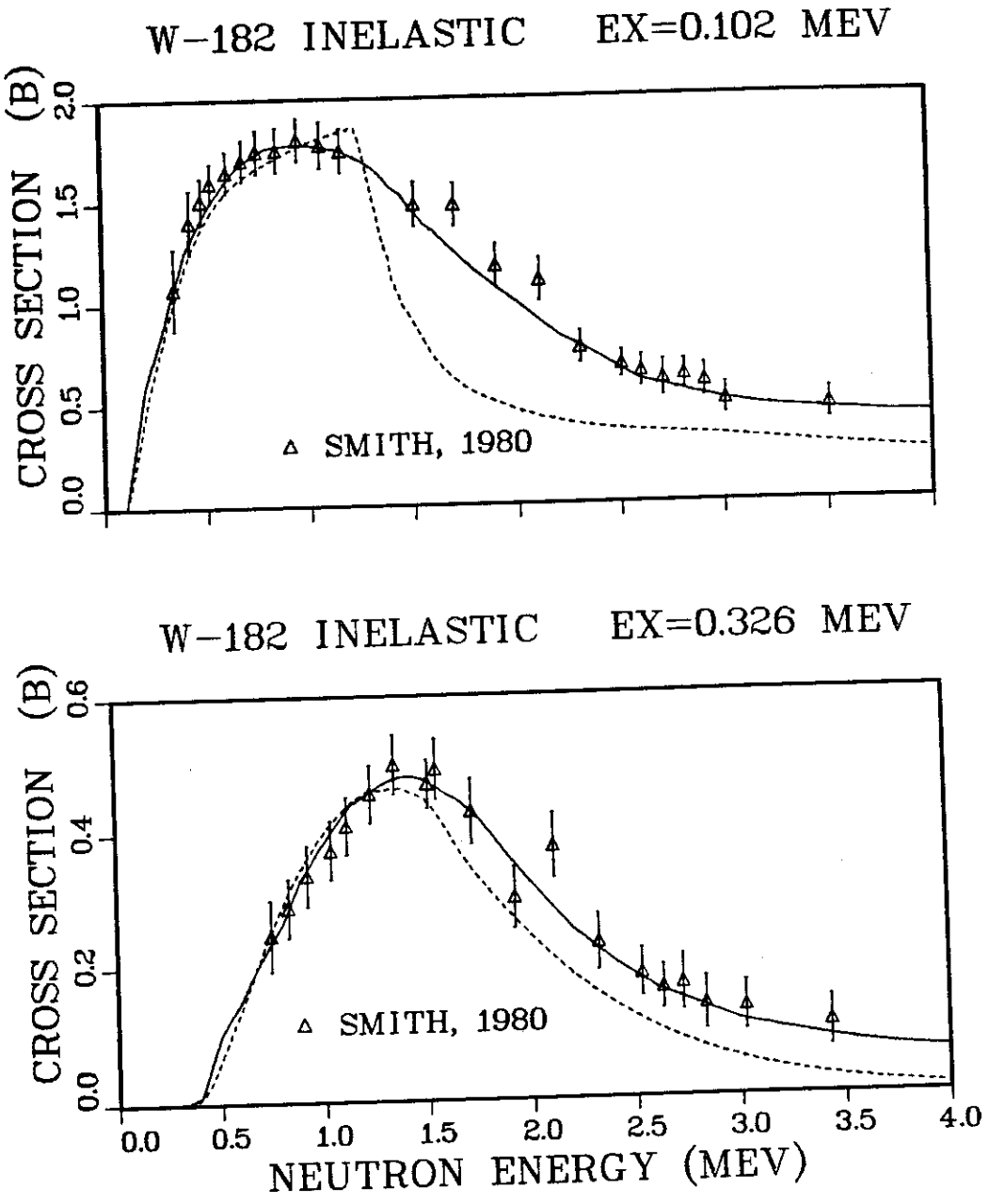


Fig. 5.

A comparison of the evaluated and experimental cross sections for neutron inelastic scattering from the $2^+$ and $4^+$ rotational states in the $^{182}W$. (Dashed lines are ENDF/B-V, Rev. 0).

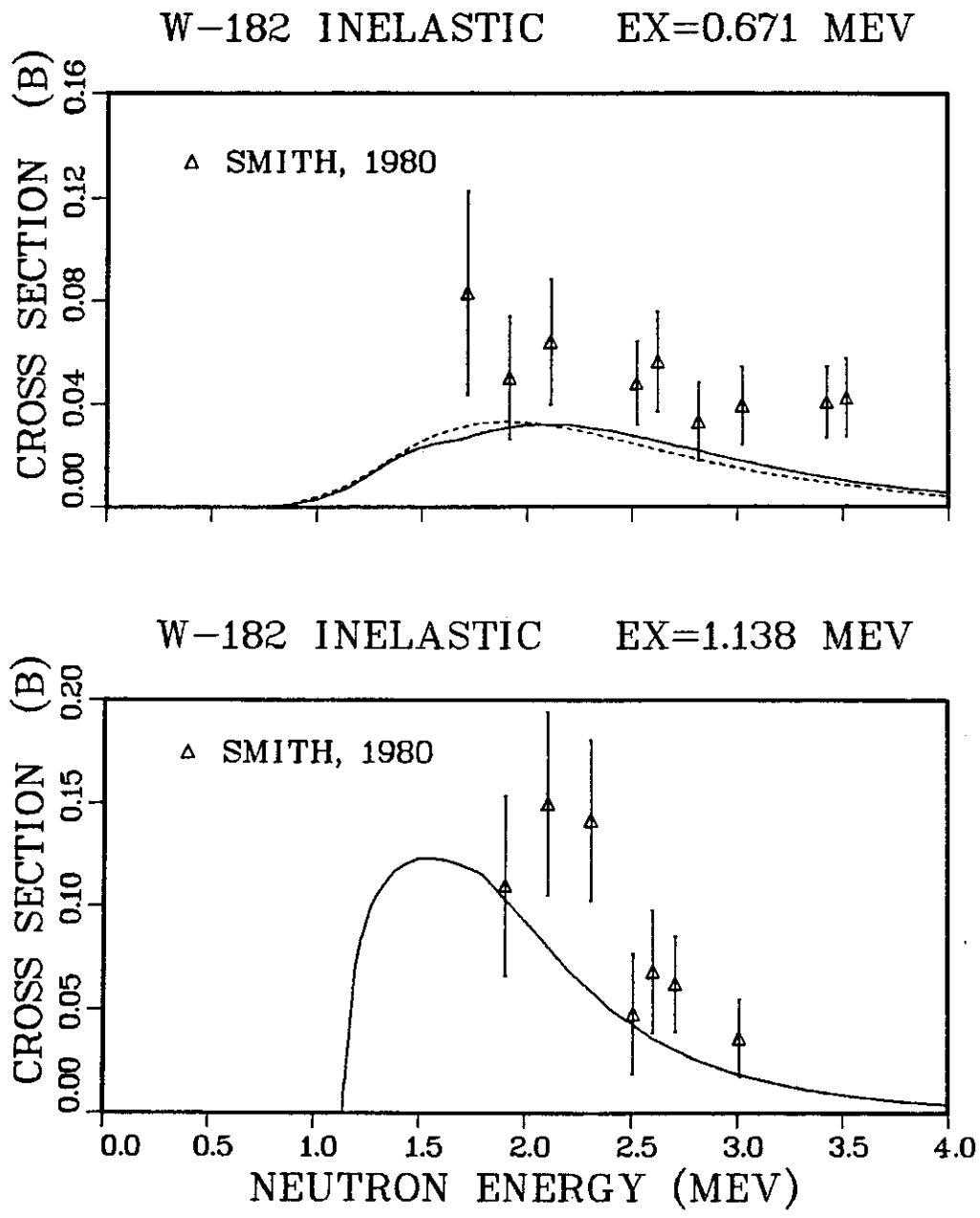


Fig. 6.

Evaluated and experimental cross sections for $^{182}W(n,n')$ reactions to $^{182}W$ states at 0.671 and 1.138 MeV excitation energies. The dashed curve is ENDF/B-V, Rev. 0.

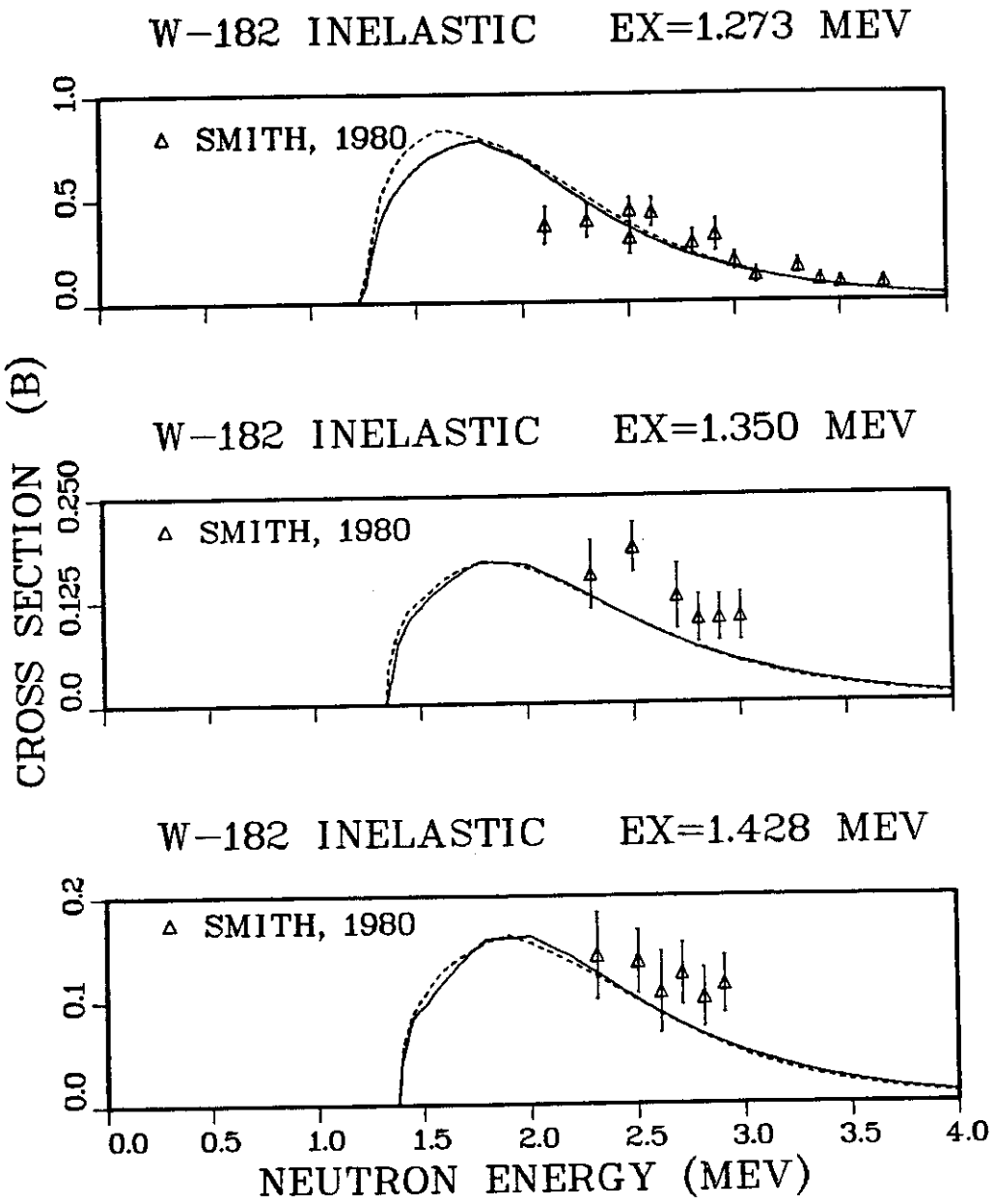


Fig. 7.

Evaluated and experimental cross sections for $^{182}W(n,n')$ reactions to $^{182}W$ states at 1.273, 1.350, and 1.428 MeV. The dashed curve is ENDF/B-V, Rev. 0.

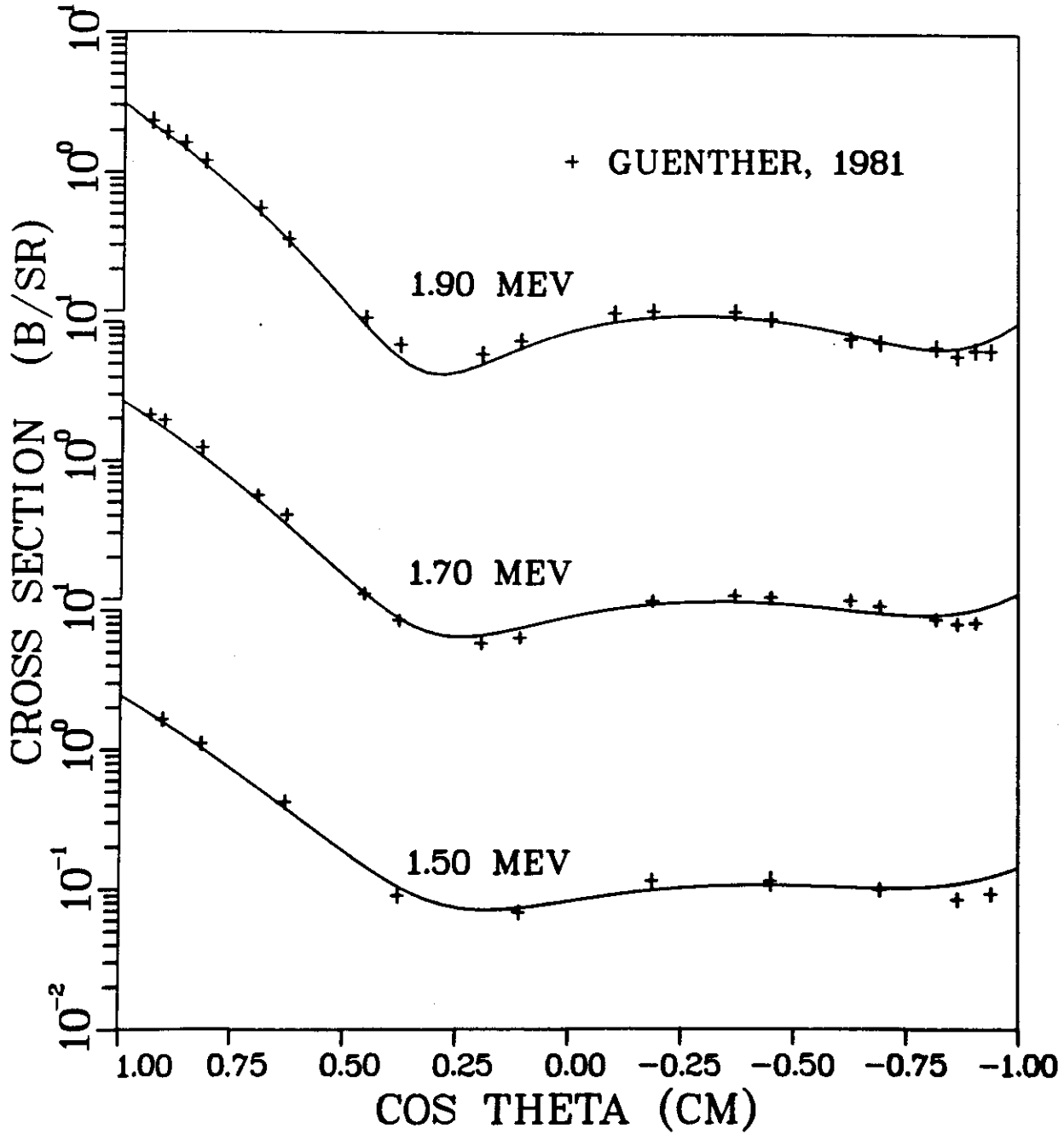


Fig. 8.

Elastic scattering angular distributions for n + $^{182}W$ interactions between 1.5 and 1.9 MeV.

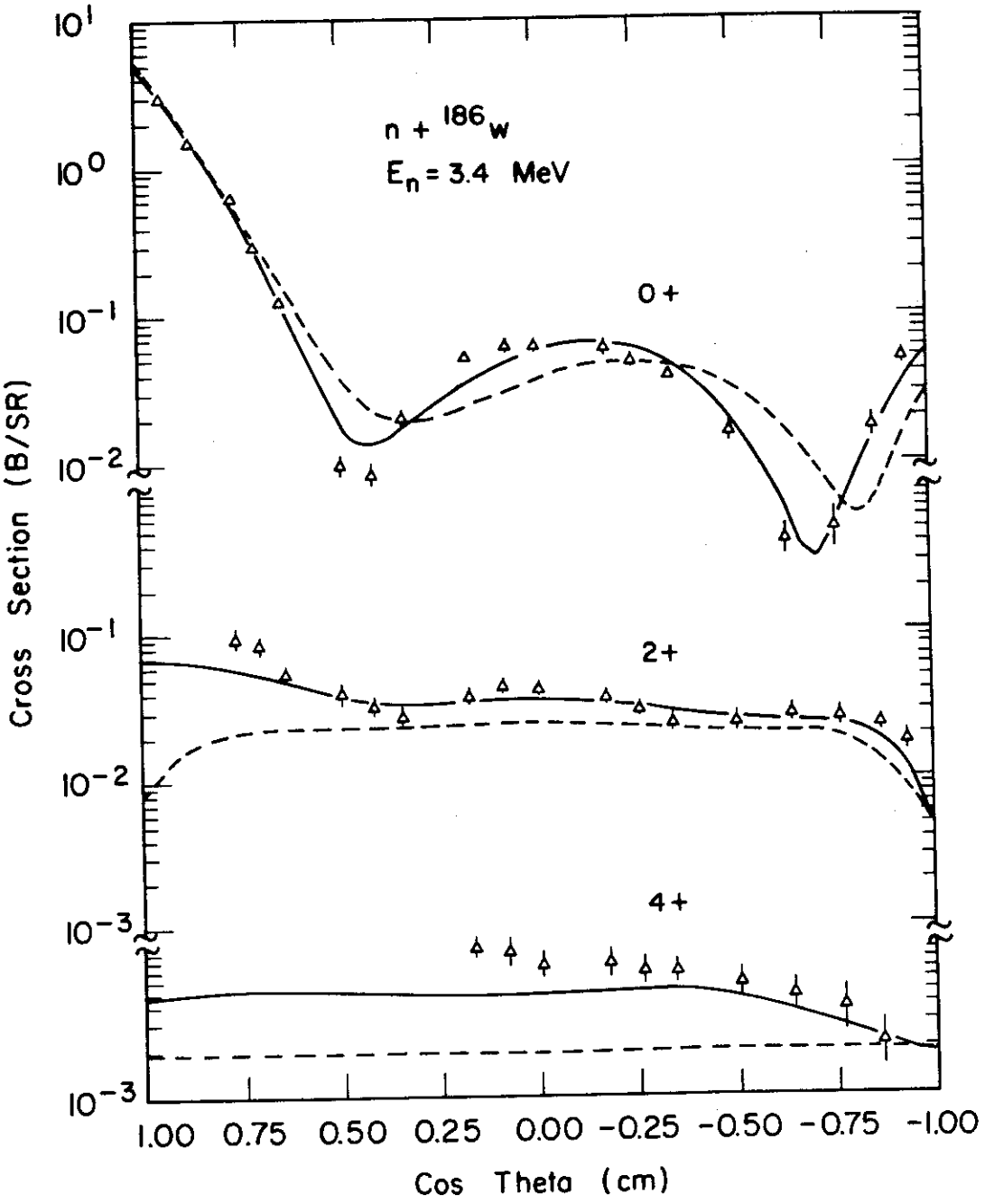


Fig. 9.

Elastic and inelastic neutron angular distributions to the $0^+$, $2^+$, and $4^+$ states in $^{186}W$ for 3.4-MeV neutrons. The solid curves are the present analysis; the dashed curve is ENDF/B-V, Rev. 0.

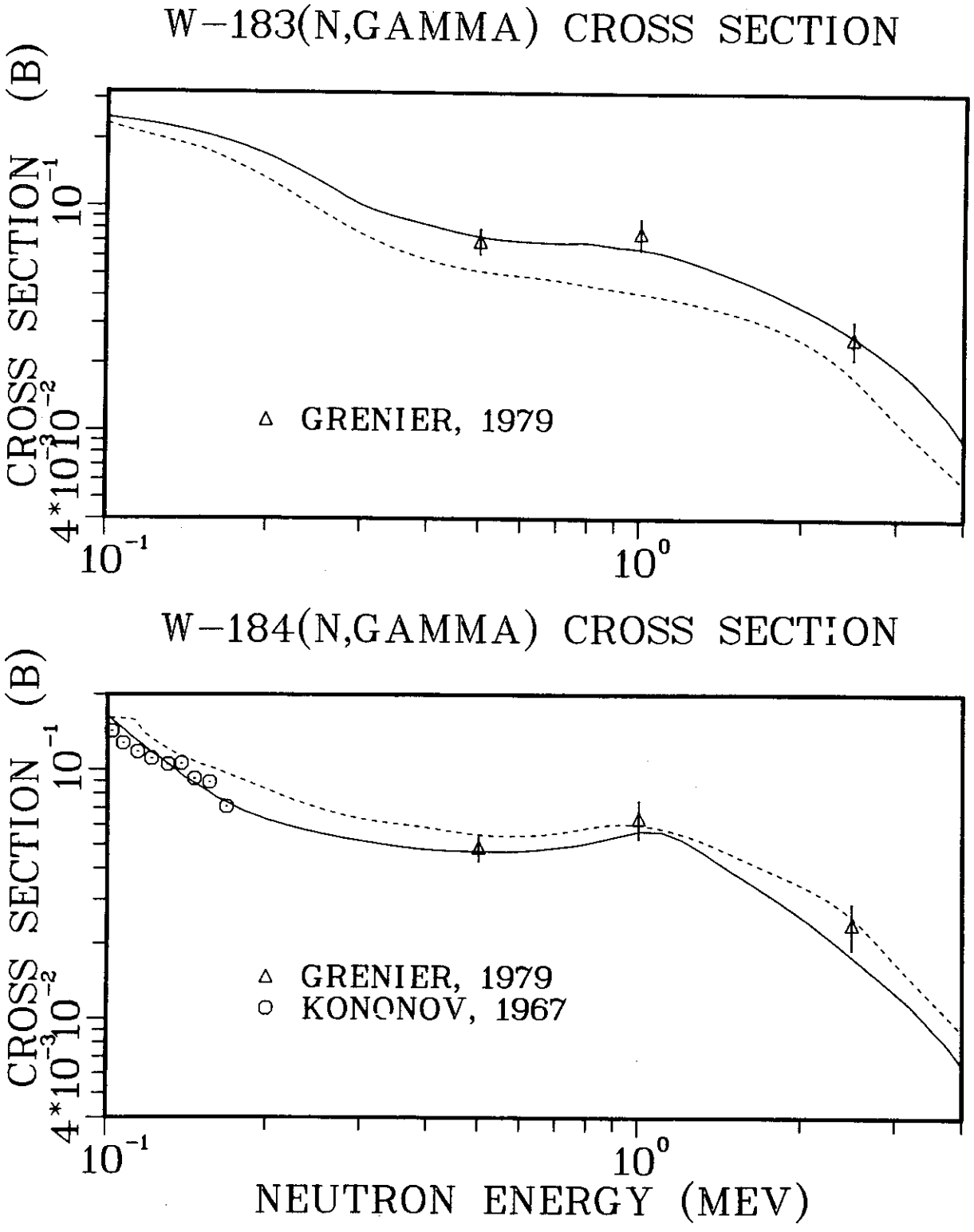


Fig. 10.

Evaluated and measured cross sections for the (n,γ) reaction on $^{183}W$ and $^{184}W$. The dashed curve is ENDF/B-V, Rev. 0.

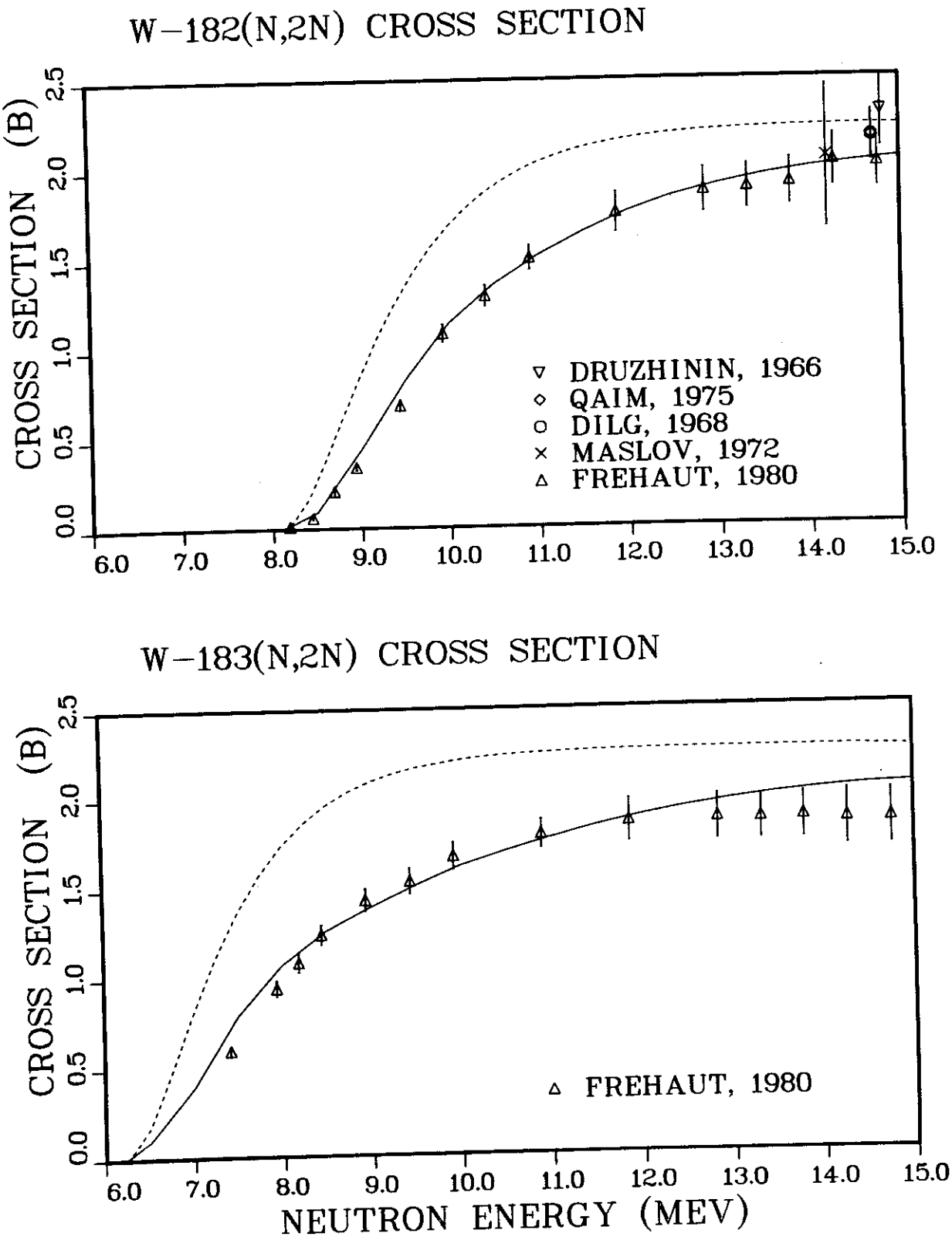


Fig. 11.

Measured and evaluated cross sections for (n,2n) reactions on $^{182}W$ and $^{183}W$. The dashed curve is ENDF/B-V, Rev. 0.

# SUMMARY DOCUMENTATION FOR $^{NAT}W$

by

E. D. Arthur, P. G. Young, and R. Boicourt
Los Alamos National Laboratory
Los Alamos, New Mexico 87545

## SUMMARY

An elemental tungsten evaluation was constructed for Revision 2 of ENDF/B-V from the isotopic evaluations for $^{182,183,184,186}W$ described in the previous article. As is the case for the isotopic evaluations, the elemental data above a neutron energy of 100 keV are based on new theoretical calculations and include several recent measurements. The evaluated data in the resonance region are unchanged from ENDF/B-V, Revision 0.

## COMPARISONS WITH EXPERIMENT

Because the elemental tungsten evaluated data file was constructed through use of the isotopic evaluations, which were, in turn, based on extensive model calculations, a direct link does not always exist between this new natural evaluation and data measured for natural tungsten. We have instead relied on the quality and consistency of the isotopic experimental data along with constraints introduced through our application of the relevant nuclear models. The success of this technique is illustrated through comparison of the evaluation to experimental data available for the major reaction channels of natural tungsten.

Figure 1 compares our evaluated total cross section (solid curve) with experimental data and with the ENDF/B-V Rev. 0 evaluation* (dashed curve). A similar comparison is shown in Fig. 2 for the elastic cross section. Numerous experimental measurements have been made of neutrons elastically scattered from natural tungsten, but some of the more recent and complete sets of such measurements are those of Kinney.[1] We compare the evaluation to these angular distributions in Fig. 3. Within these comparisons there is general agreement between our evaluation and experimental total and elastic cross-section data. Such agreement, along with isotopic data, implies realistic values for the total reaction cross section.

Major components of the reaction cross section are (n,γ) radiative capture, (n,n') inelastic scattering, and (n,xn) reactions at higher energies. Figure 4 compares the Revision 2 evaluated cross sections with the available experimental data for capture (lower part) and inelastic scattering (upper part). Similarly, experimental data for the (n,2n) and (n,3n) reactions on natural tungsten are compared with the evaluated cross sections in Fig. 5. Again, reasonable agreement is obtained.

---

*Obtained from the ENDF/B-V.0 isotopic evaluations for $^{182,183,184,186}W$.

A major deficiency of the ENDF/B-V evaluation was the significant underprediction of portions of the neutron emission spectrum caused by failure to consider the influence of preequilibrium processes at incident energies above 10 MeV. In the present evaluation this deficiency has been rectified as shown in Fig. 6 where the evaluated spectrum is compared to several neutron emission measurements performed around 14 MeV. The agreement is good particularly with the precise data measured by Vonach.[2]

Comparisons to the gamma-ray production data of Dickens[3] between $E_n$=5.7 and 7.3 MeV are shown in Fig. 7. The evaluated gamma-ray production cross sections were obtained from the nuclear model calculations to ensure overall energy conservation in the evaluated data files. There are some disagreements to the measurements, however, particularly for gamma rays resulting from continuum inelastic scattering. To some extent this disagreement represents an inconsistency among available neutron cross-section measurements and is discussed in detail in Ref. 4. We achieve better agreement in this neutron energy range with the more recent gamma-ray production measurements of Savin,[5] as shown in Fig. 8, as well as with the data measured by Drake[6] that is shown in Fig. 9.

Comparisons of measured gamma-ray emission spectra with the evaluation at neutron energies above 10 MeV are given in Figs. 10 and 11. The disagreement between the evaluation and Dickens' data in Fig. 10 is not as severe as was the case for lower neutron energies. The comparison with Budnar's data[7] in Fig. 11, which covers emission gamma-ray energies between 8 and 24 MeV, is somewhat better although uncertainties on the data are larger. The enhancement in the calculated spectrum near $E_\gamma$ = 15 MeV results from the direct-semi-direct model that was used.

## ENDF/B-V.2 FILE

The ENDF/B-V.2 file for $^{NAT}W$ was constructed mainly using the NJOY/MIXR code[8] with appropriate isotopic weighting of the Revision-2 evaluations for $^{182,183,184,186}W$. The detailed descriptions of the isotopic data files included in the previous article therefore apply for the $^{NAT}W$ file. The main deviation from a strict abundance-weighted combination of the isotopic data occurs for the inelastic data in Files 3-5, MT=51-91. In this instance, it was not possible to include every single discrete (n,n') cross section from the isotopic files because of the ENDF/B limit of 40 such reactions. Therefore, some of the highest excitation (n,n') reactions from the isotopic files were lumped into the (n,n') continuum data given under MT=91.

## REFERENCES

1. W. E. Kinney and F. G. Perey, "Tungsten Neutron Elastic- and Inelastic-Scattering Cross Sections from 4.34 to 8.56 MeV," Oak Ridge National Laboratory report ORNL-4803 (1973).

2. H. Vonach, A. Chalupka, F. Wenninger, G. Staffel, "Measurement of the Angle-Integrated Secondary Neutron Spectra from the Interaction of 14 MeV Neutrons with Medium and Heavy Nuclei," Proc. Symp. on Neutron Cross-Sections from 10 to 50 MeV, Brookhaven National Laboratory, 1980, BNL-NCS-51245, Vol. 1, p. 343.

3. J. K. Dickens, T. A. Love, and G. L. Morgan, "Gamma-Ray Production due to Neutron Interactions with Tunsten for Incident Neutron Energies between 1. and 20 MeV," Oak Ridge National Laboratory report ORNL-4847 (1973).

4. E. D. Arthur, "Gamma-Ray Production Cross Section Calculations for the Tungsten Evaluation," and E. D. Arthur, P. G. Young, A. B. Smith, and C. A. Philis, "$^{181,183,184,186}$W Evaluations," in Los Alamos National Laboratory report LA-8757-PR, pp. 3 and 6 (March 1981).

5. M. B. Savin, In. A. Khoklov, I. N. Paramonova, V. A. Chirkin, V. N. Lunin, and N. N. Zalialov, "Total Gamma-Ray Production Cross Sections from the Interaction of 1-10 MeV Neutrons with Tungsten Nuclei," Proc. 4th All Union Conf. Neutron Physics, Kiev, 1978, Vol. 2, p. 103.

6. D. M. Drake, J. C. Hopkins, C. S. Young, and H. Condé, "Gamma-Ray Production Cross Sections for Fast Neutron Interactions with Several Elements," Nucl. Sci. Eng. 40, 194 (1970).

7. M. Budnar, F. Cvelbar, E. Hodgson, A. Hudoklin, V. Ivkovic, A. Likar, M. V. Mihailovic, R. Martincic, M. Najzer, A. Perdan, M. Potokav, and V. Ramsak, INDC(YUG)-6/L (1979).

8. R. E. MacFarlane, Los Alamos National Laboratory, personal communication (1984).

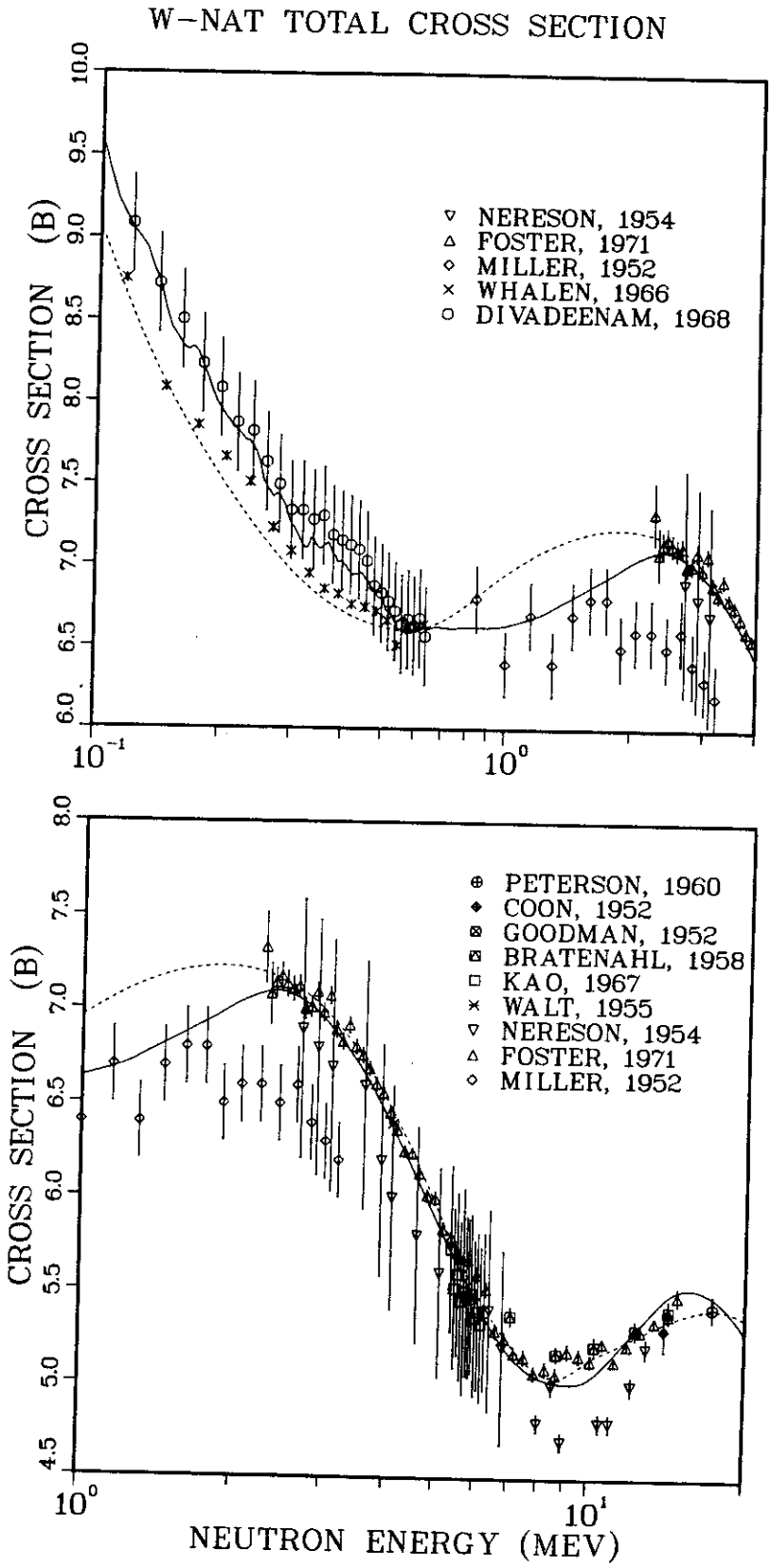


Fig. 1.

Evaluated total cross sections for natural tungsten. The dashed curve is ENDF/B-V.0.

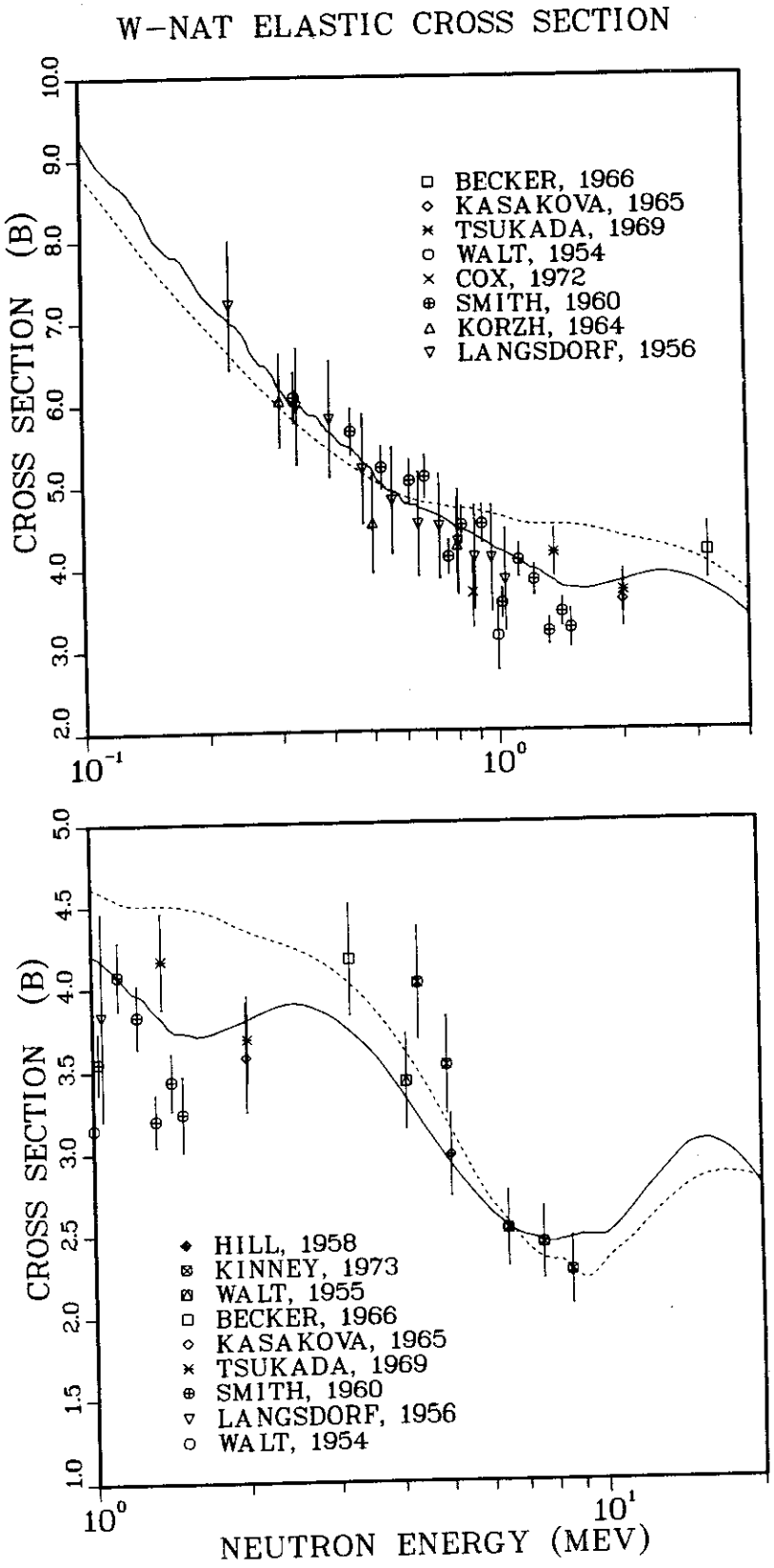


Fig. 2.

Evaluated elastic cross sections for natural tungsten. The dashed curve is ENDF/B-V.0.

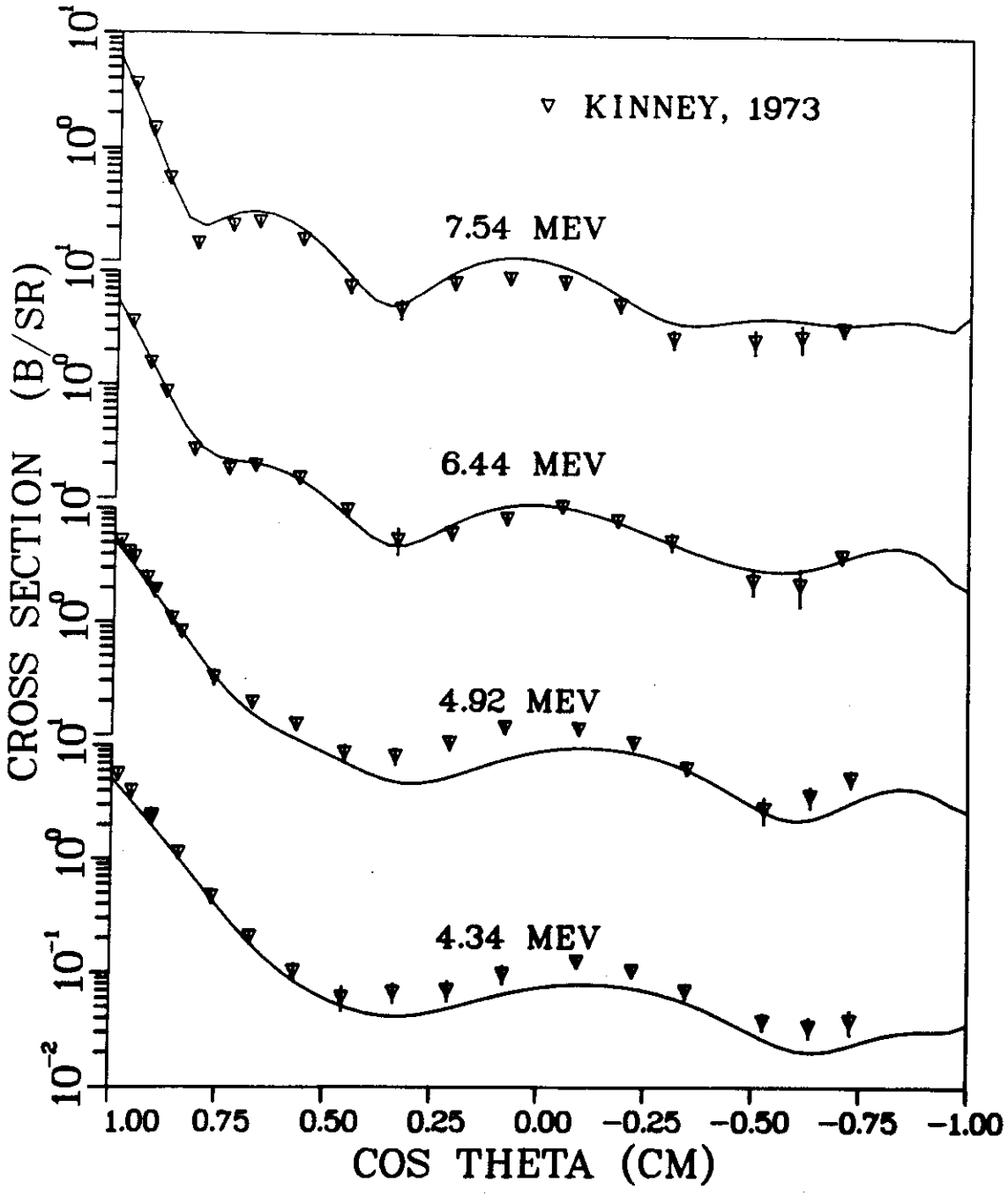


Fig. 3.

Comparison of the evaluated angular distributions for elastic scattering (and inelastic scattering producing excitations < 0.1 MeV), and the Kinney measurements.

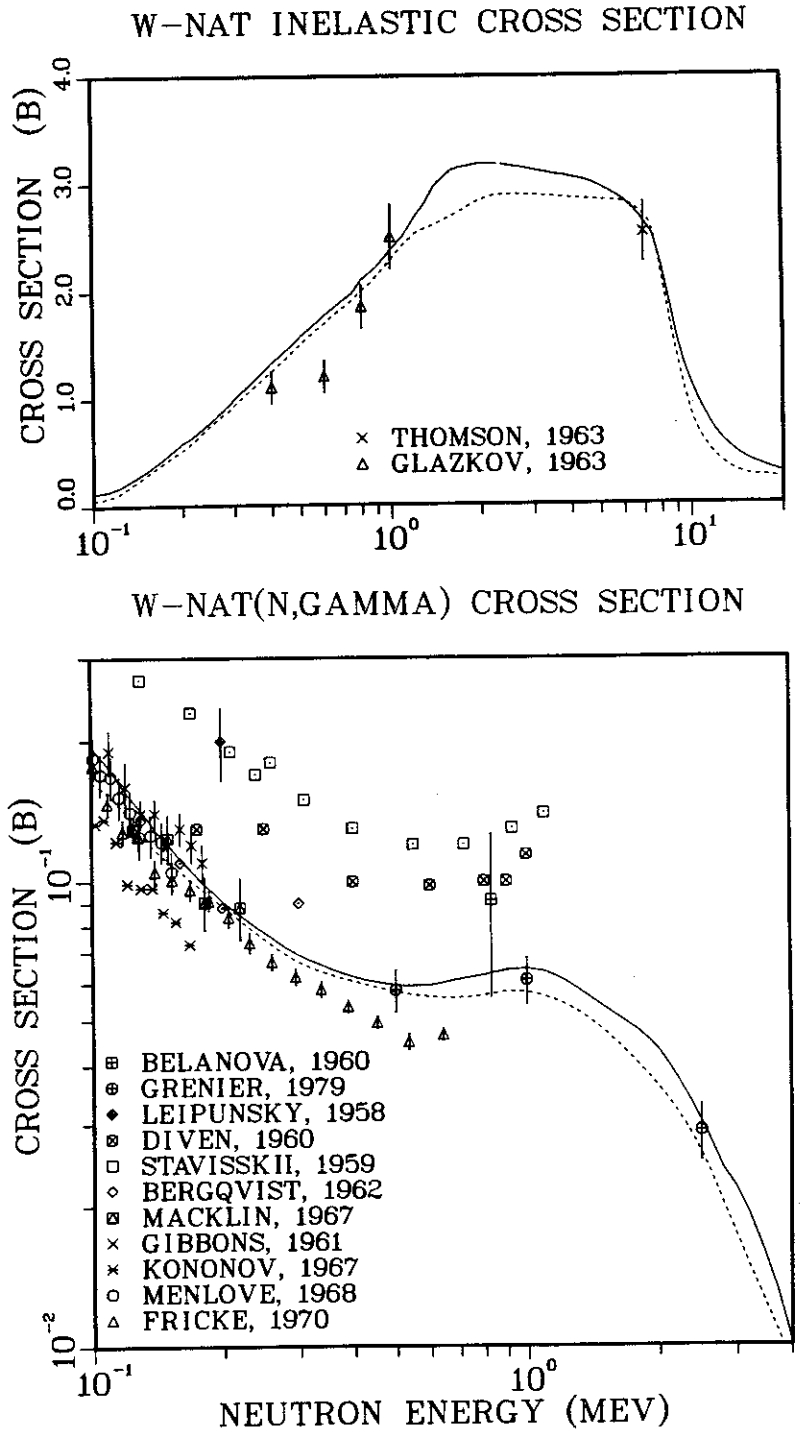


Fig. 4.

Comparison of measured and evaluated cross sections for radiative capture (lower) and inelastic scattering (upper) of neutrons on natural W. The solid curve is Revision 2, and the dashed curve is ENDF/B-V, Revision 0.

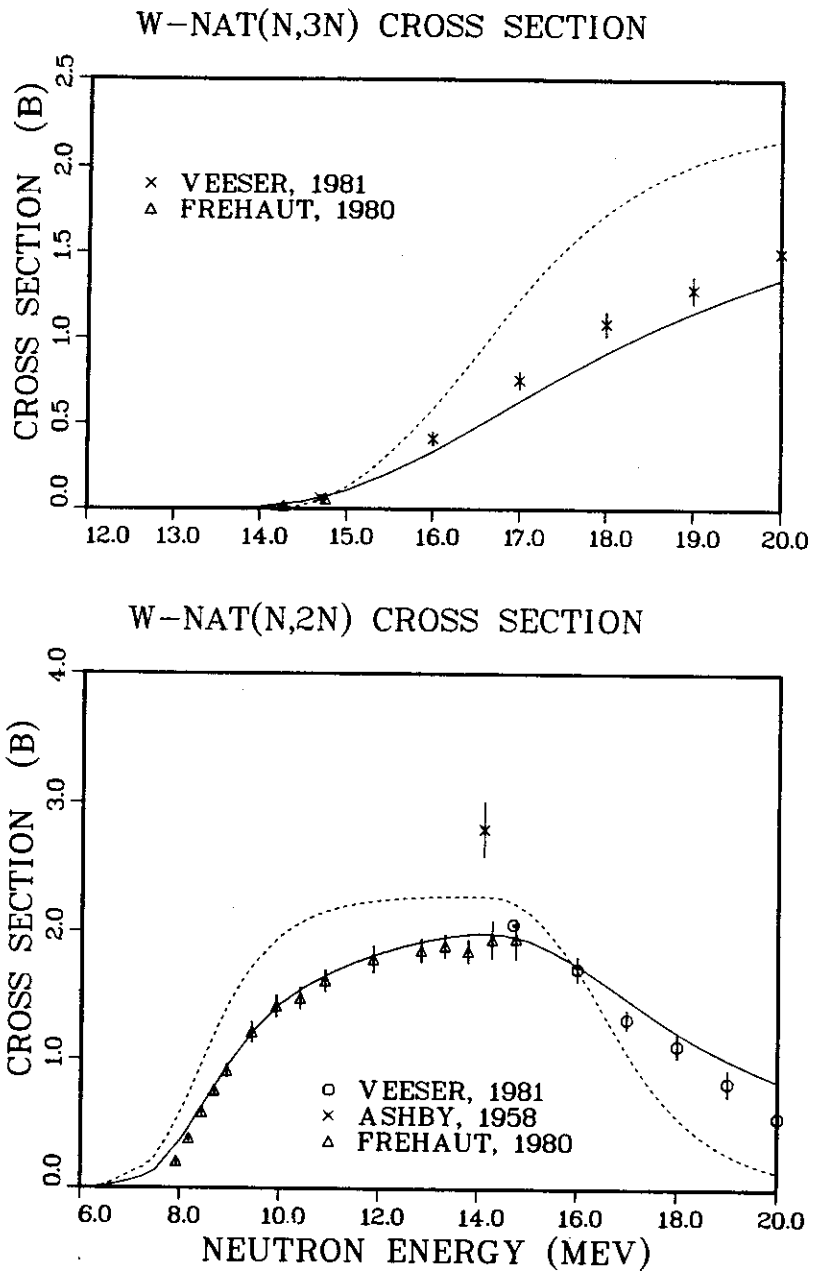


Fig. 5.

Evaluated (n,2n) and (n,3n) cross sections are compared with recent experimental data. Again, the solid curve is the present effort; the dashed curve is ENDF/B-V.

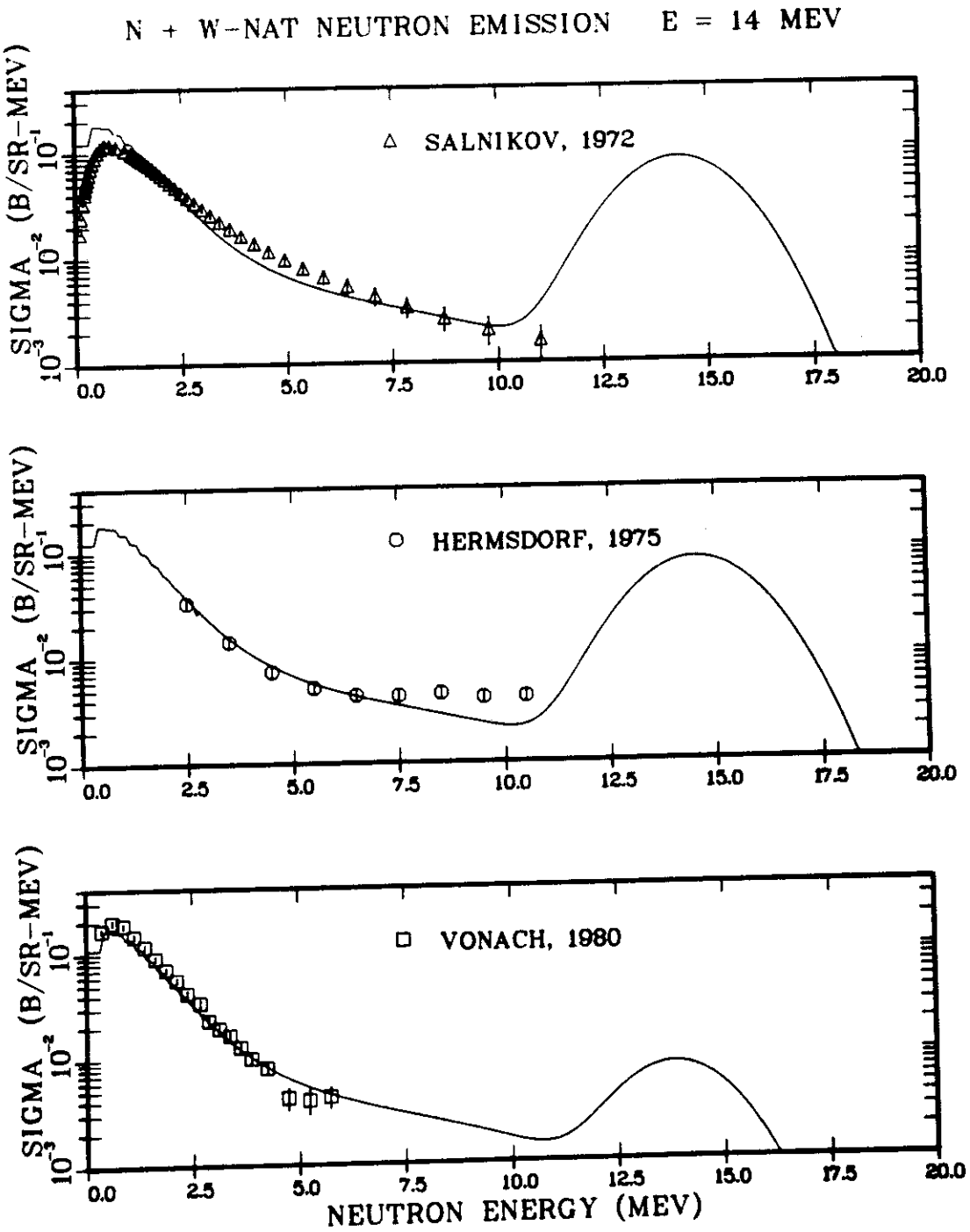


Fig. 6.

The evaluated neutron emission spectrum produced by 14-MeV neutrons is compared with experimental results.

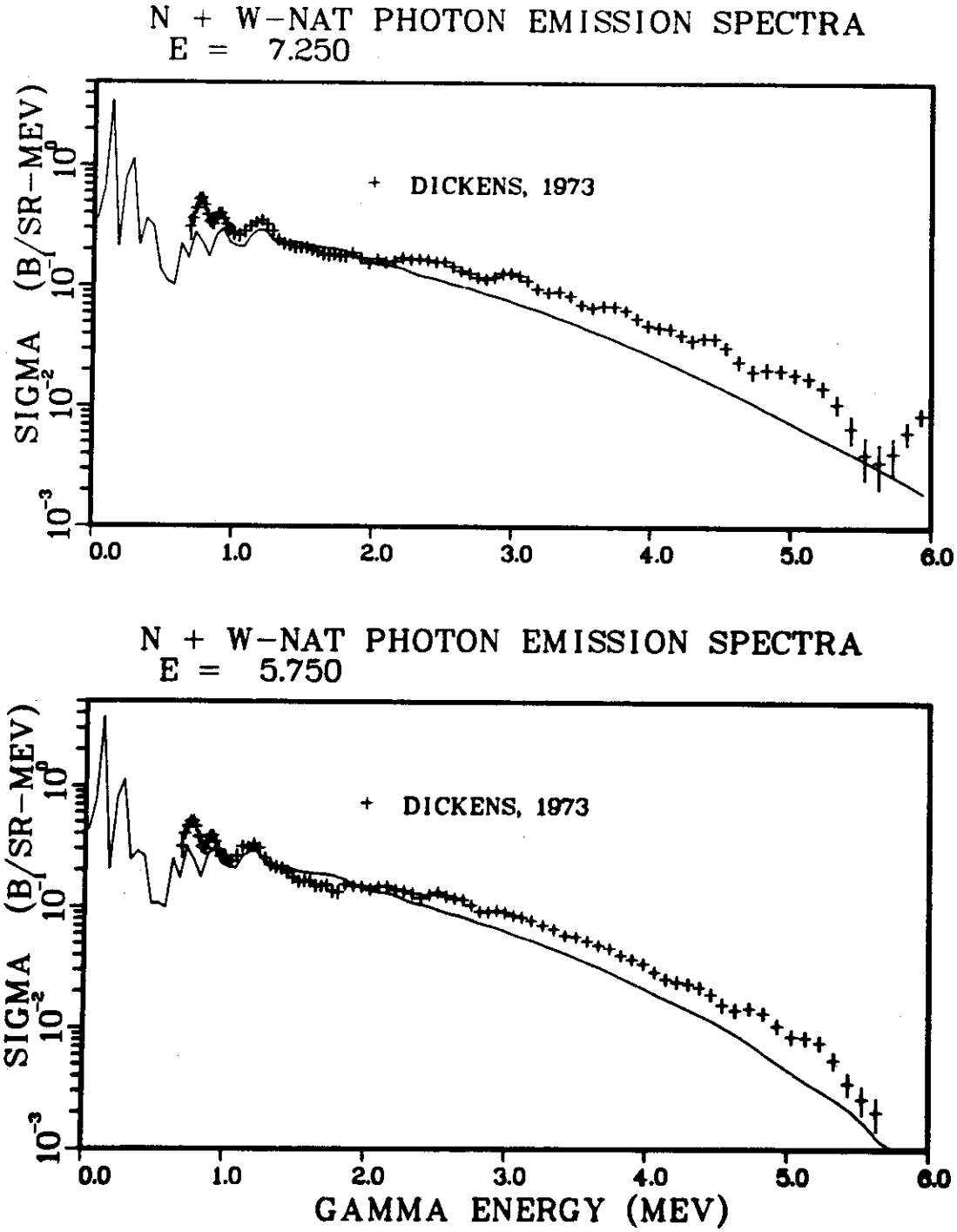


Fig. 7.

The evaluated gamma-ray production spectrum obtained in the present effort is compared with Dickens' experimental results[3] for incident neutron energies of 5.75 and 7.25 MeV.

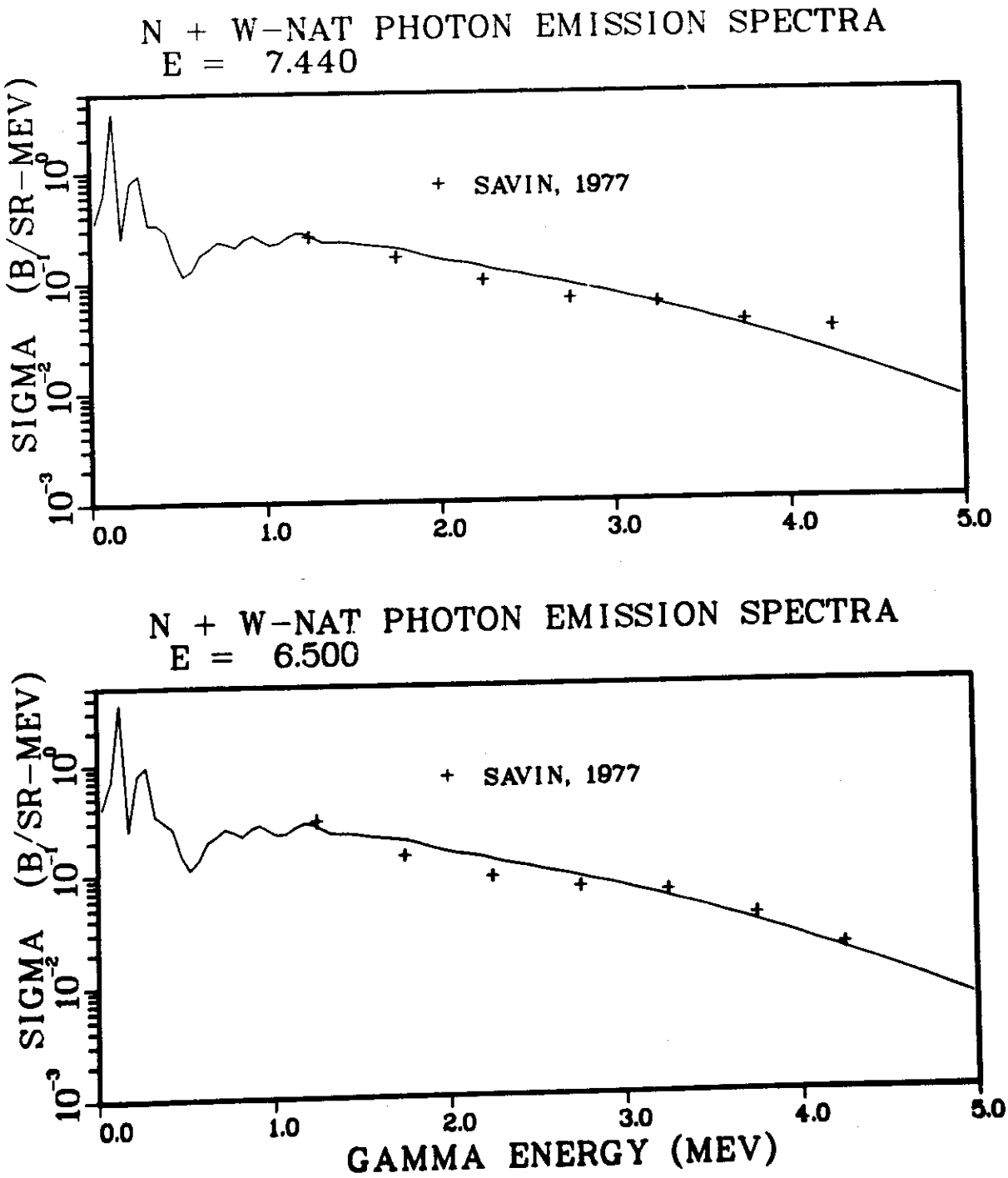


Fig. 8.

A comparison of the present evaluation with recent gamma production spectra measured by Savin[5] at incident neutron energies of 6.50 and 7.44 MeV.

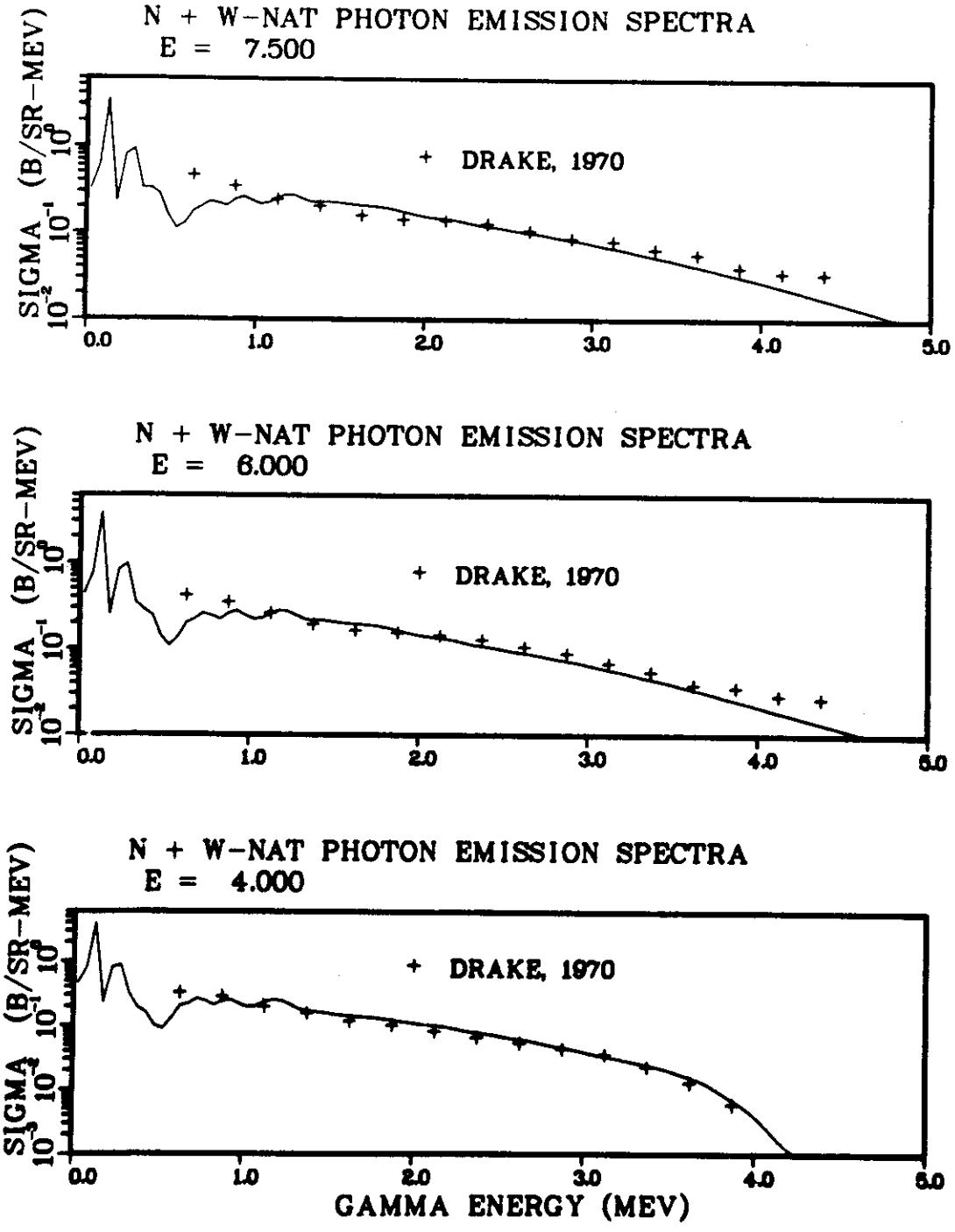


Fig. 9.

The present evaluation is compared with the gamma-ray production spectra measured by Drake et al.[6] at incident neutron energies of 4.0, 6.0, and 7.5 MeV.

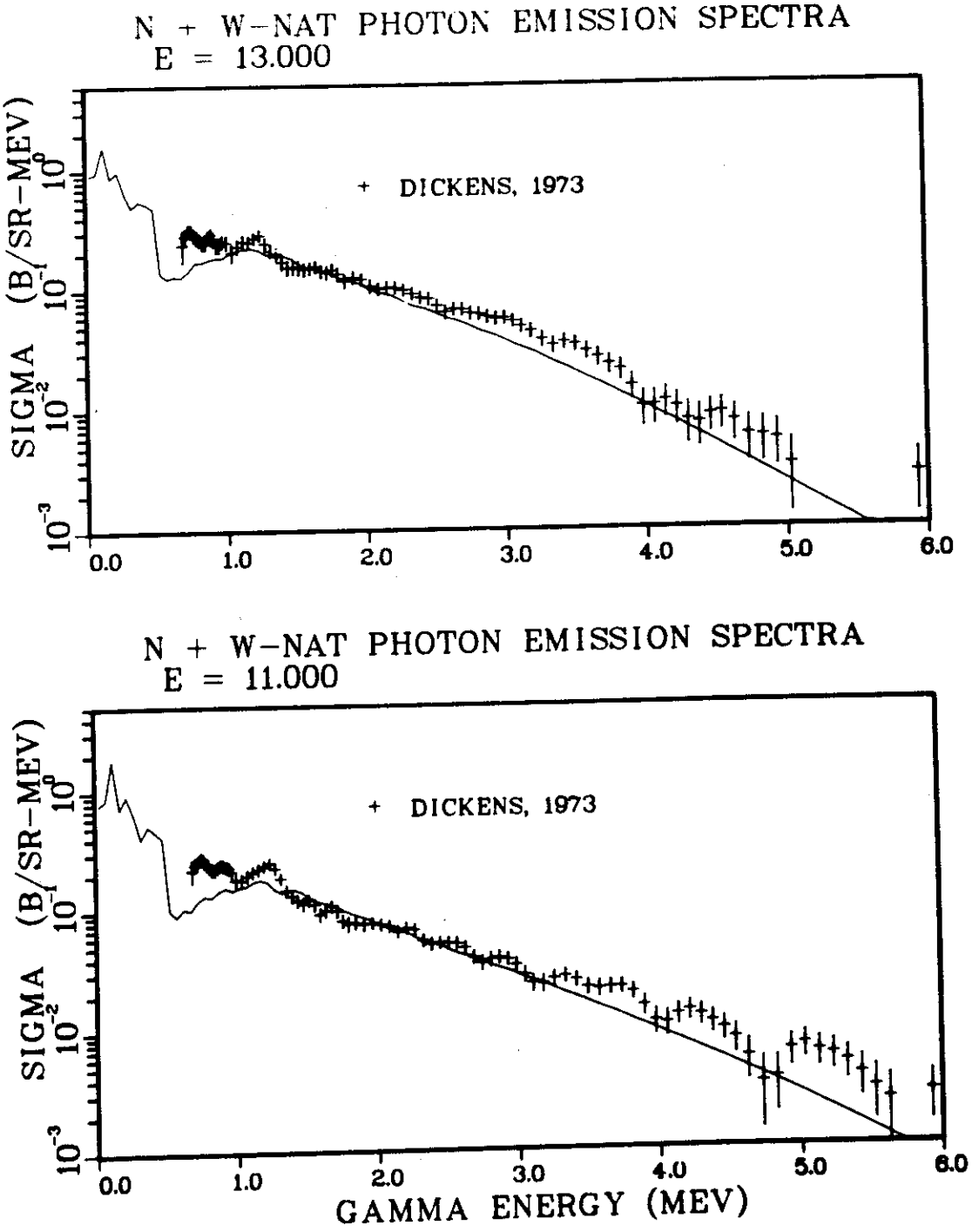


Fig. 10.

The evaluated gamma-ray production spectrum obtained in the present effort is compared with Dickens' experimental results[3] at $E_n$=11 and 13 MeV.

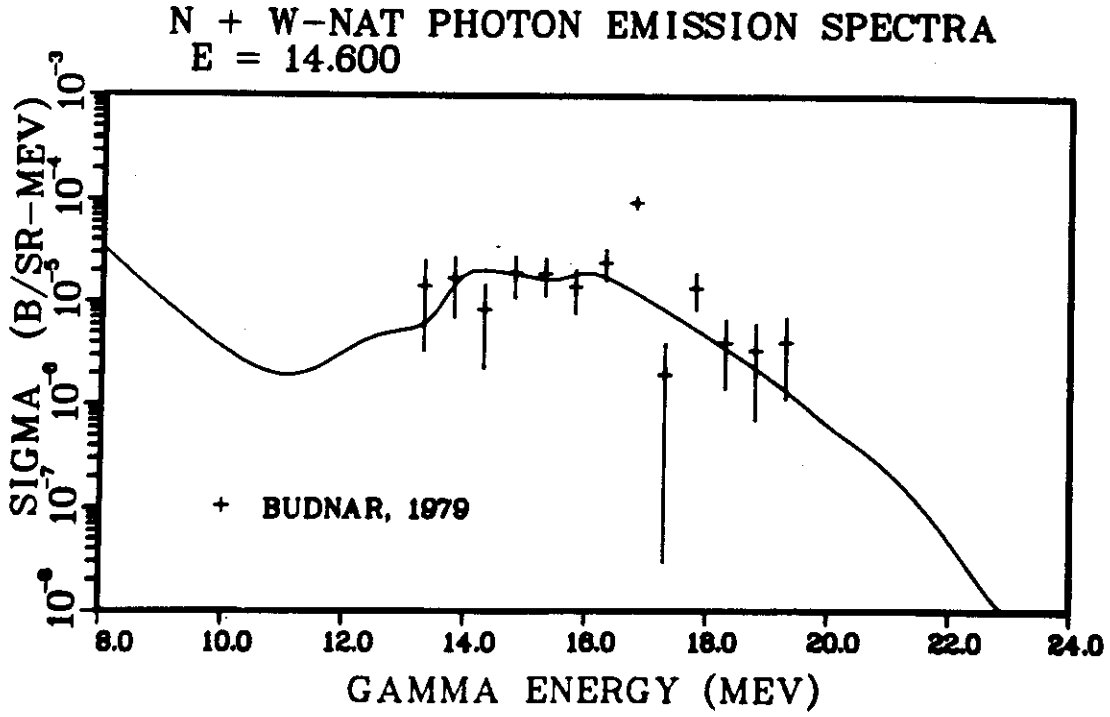


Fig. 11.

Comparison of the present evaluated gamma-ray emission spectra at $E_n$ = 14.6 MeV with the measurements of Budnar.[7]

90-TH-232 BNL Eval-Dec-77; Revised Mar-82

Principal evaluators- J.W.Meadows, W.P.Poenitz,A.B.Smith, D.L.Smith, and J.F.Whalen (ANL)
R.J.Howerton (LLL)
B.R.Leonard et.al., (BNW)
M.R.Bhat (BNL)
G.de Saussure, R.L.Macklin and R.Gwin (ORNL)
D.K.Olsen (ORNL)

This evaluation assembled by M.R.Bhat (BNL) using the following evaluations.

Nu-bar (prompt) - R.Gwin (ORNL), ref. 4.

Delayed neutrons - R.E.Kaiser and S.G.Carpenter (ANL), ref. 5.

Energy release in fission - R.Sher et al., (Stanford), ref. 6.

Thermal range - B.R.Leonard Jr. et al., ref. 2 with changes by M.R.Bhat, ref. 31.

Resolved resonance region - D.K.Olsen, ref. 37.

Unresolved resonance region - G.de Saussure and R.L.Macklin, ref. 3 with changes by M.R.Bhat, ref. 31.

Smooth cross-sections 50 keV to 20 MeV.

Total - A.B.Smith (ANL), ref. 1.

Fission - W.P.Poenitz (ANL), ref. 1.

Capture - W.P.Poenitz (ANL), ref. 1.

Inelastic and other cross-sections.
J.W.Meadows et al., (ANL), ref. 1.

Fission neutron spectrum - M.R.Bhat (BNL), ref. 31.

Radioactive decay data - C.W.Reich (E.G.and G,Idaho,Inc).

Fission products yields - F.P.Yields Subcommittee.

Gamma-ray production - R.J.Howerton (LLL).

File 1. General Information

MT = 452 Nu-bar total consistent with MT = 455 and MT = 456.

MT = 455 Delayed neutron yields, Kaiser and Carpenter (ANL), ref. 5.

MT = 456 Prompt nu-bar based on Cf-252 nu-bar (prompt) = 3.757.

Evaluation by Gwin (ORNL) based on a straight line least-squares fit to the available data listed in ref. 4.

MT = 458 Energy release in fission evaluation by R.Sher et al., (Stanford), ref. 6.

File 2. Resonance Parameters

Resolved resonance region - D.K.Olsen, ref. 37 resonance parameters are uncertainty weighted average of available data and the two bound resonances of ref. 2 with MF = 3 files for truncation, missed p-waves, 1/v capture, and smooth connection to the end of the thermal region cross sections at 5 eV. Average capture width = 2.44 x 10-2 eV, s-wave strength function = 0.826 x 10-4, p-wave strength function assumed = 1.6 x 10-4, 5 to 4000 eV. Infinitely dilute capture resonance integral = 81.58 b.

Unresolved resonance region - G.de Saussure and R.L.Macklin, ref. 3 evaluation of capture cross section used from 4 to 25 keV. Above 25 keV this was joined smoothly to the Poenitz evaluation from 40 keV to 50 keV. These were then fitted using the code UR ref. 30 to give the unresolved resonance parameters. In this fit the s- and d-wave parameters were kept constant at the values given by de Saussure and Macklin, the p-wave gamma width was increased to 2.52E-02 eV and the p-wave reduced neutron width varied to fit the capture cross-section.

The capture cross-section input used to extract the unresolved resonance parameters in file 2/151 are given here from 4 keV to 50 keV at 1 keV intervals. These are: 1.130,0.982,0.908,0.850,0.803,0.764,0.730, 0.702,0.677,0.655,0.636,0.618,0.601,0.585,0.571,0.557, 0.545,0.533,0.521,0.511,0.500,0.491,0.482,0.473,0.465, 0.459,0.452,0.448,0.443,0.439,0.435,0.431,0.429,0.426, 0.424,0.422,0.420,0.420,0.420,0.420,0.417,0.414,0.411, 0.407,0.401,0.395,0.390.

File 3. Neutron Cross Sections

Thermal region (1.0 E-05 to 5.0 eV) - mainly based on Leonard ref. 2 evaluation with the following changes. The capture cross section in ref. 2 normalised to 7.40 b at 2.53E-02 eV and used from 1.0E-05 eV to 2.53E-02 eV. From 2.60E-02 eV to 14 eV the fit to their capture data by Chrien and Liou ref. 32 used. The scattering cross-section was changed to accommodate changes in capture using total slightly modified from that given in ref. 2. These small changes are described in ref. 31.

2.53 E-02 eV cross-section capture 7.4 b.
Dilute capture resonance integral 86.1 b (0.5 to 2.0E+07 eV).

Total cross section from 50 keV to 20 MeV - A.B.Smith (ANL), ref. 1; mainly based on ref. 9-13 from 0.025 to 1 MeV, from 1 to 5 MeV based on ref. 9-11, 14-16. From 5 to 15 MeV evaluation based on ref. 11, 15, 17. From 15 to 20 MeV evaluation based on nuclear model calculations described in ref. 18 and 19. Total cross section modified by about 3 per-cent between 50 to 150 joined smoothly with that calculated from unresolved resonance parameters below 50 kev.

Elastic scattering cross section from 50 keV to 20 MeV obtained as the difference between total and other partial cross sections.

Fission cross section up to 20 MeV - W.P.Poenitz. Details of the evaluation and the data sets used are ref. 1. Fission cross section changed to be consistent with U-235(n,f) evaluation given in ref. 33.

Capture cross section 50 keV - 20 MeV - W.P.Poenitz. Details of the evaluation and the data sets used are given in ref. 1. Capture cross section changed to be consistent with U-235(n,f) evaluation given in ref. 33.

Inelastic scattering cross sections - J.W.Meadows et al., ref. 1 evaluation based mainly on the data in ref. 20-25. Interpolated between experimental data and extrapolated to 20 MeV using coupled channel nuclear model calculations of ref. 26.

(n,2n) and (n,3n) cross sections - J.W.Meadows et al., experimental data used (ref. 1) renormalised to a common set of standards before evaluation.

File 4. Angular Distributions of Secondary Neutrons

Elastic angular distributions - J.W.Meadows et al., ref. 1 evaluation based on experimental data to 2.5 MeV ref. 1 and nuclear model calculations from 2.5 to 20 MeV ref. 26.

Inelastic angular distributions - J.W.Meadows et al., ref. 1 angular distributions based on coupled channel nuclear model calculated and experimental data for incident energies less or equal to 2.5 MeV and on model calculations ref. 26 from 2.5 to 20 MeV.

MT = 16,17,18 Assumed to be isotropic.

File 5. Energy Distributions of Secondary Neutrons

MT = 16,17 - J.W.Meadows et al., ref. 1.
These determined using the statistical model of Segev ref. 27 with a precompound component.

MT = 18 The variation of the mean energy of the fission was calculated using the method of Howerton and Doyas, ref. 28 and normalized to the 14.3 MeV data of Vasil'ev et al., ref. 29 to give a mean energy of 2.255 MeV at 14 MeV and the corresponding Watt spectrum shape parameters obtained.

MT = 91 - J.W.Meadows et al., ref. 1.
Evaluation based on the measured evaporation temperatures of ref. 23 and 25. In addition, a harder precompound component varying from 0.0 at 6 MeV to 20 per-cent at 20 MeV patterned after U-238 was added.

MT = 455 Evaluation by Kaiser and Carpenter, ref. 5.

File 8. Radioactive Decay and Fission Product Yield Data

MT = 454 and 459 Inserted into file at BNL by R.Kinsey 9/78.

ENDF/B-V Yield Data

Fission product yield data for phase one review set 1978. Values obtained from the recommendations of the yields subcommittee, T.R.England (Chairman), D.M.Gilliam, Y.Harker, J.R.Liaw, W.J.Maeck, D.G.Madland, V.McLane May, P.L.Reeder, B.F.Rider, R.E.Schenter, B.I.Spinrad, J.P.Unik, A.Wahl, W.Walker, B.W.Wehring, K.Wolfsberg.

Uncertainties are based on the total yield to each ZA. When there is an isomeric state, the independent nuclide yield to each state has a larger uncertainty than the total yield in state distributions (uncertainties average approximately 50 percent but can be larger). Any yield having a large uncertainty (45-64 percent) may be a model estimate or a value assigned to the yields on the wings or valley of the mass yield distribution. These small yields may only be accurate to within a factor of 2.

MT = 454 Contains direct yields before delayed neutron emission.

MT = 459 Contains cumulative yields along each isobaric chain after delayed neutron emission.

Direct and cumulative yields are normalized by the same factors based on B.F.Rider evaluation. The isomeric state model, LA-6595-Ms (ENDF-241), and delayed neutron emission branchings (pn values) for 102 emitters, LA-UR-78-688, and pairing effects, LA-6430-Ms (ENDF-240), have been incorporated.

Data prepared for files by T.R.England
(LASL LTR. T-2-1-2891).

MT = 457 Radioactive decay data

INEL Eval-Apr78 Reich
Data added to the file at BNL by R.Kinsey 04-May-78.

References Q(alpha)-1974 version of Wapstra-Bos-Gove mass table. other- M.R.Schmorak, Nuclear Data Sheets 20, No. 2, 165 (1977). See also, Table of Isotopes, 7th. ed. (preliminary data, Priv. Comm. from C.M.Lederer).

Note: The energies of the two most intense alpha-particle groups are the recommended values of A.Rytz, At. Data and Nucl. Data Tables 12, No.5, 479 (1973).

Note: Separate listings of the x-ray and the conversion-electron spectra are not given. However, their contribution to the average photon and electron energies has been calculated and included.

Translated into ENDF/B-V format by Mann and Schenter (HEDL) 4/78.

File 12. Photon Production Multiplicities and Transition Probability Arrays

MT = 18 For all incident energies the multiplicity of photons from fission was derived from the data of ref. 34 which reported the photon spectrum and total photon energy for thermal fission of U-235. It was assumed that the multiplicity is independent of incident neutron energy.

MT = 102 For all incident neutron energies photon production from neutron capture is represented by an energy dependent multiplicity to be applied to the (n,gamma) cross section and by an energy independent spectrum. The spectrum used was based on an undocumented measured spectrum for U-238 with a minor adjustment for small Q-value difference between Th-232 and U-238. The average energy of the assumed spectrum was then divided into the Q-value to obtain a multiplicity at zero neutron energy. The multiplicity at 20 MeV was obtained, ref. 35 by use of the formula M(E) = M0(En+Q)/Q where M0 is the multiplicity at zero neutron energy as described above.

File 13. Photon Production Cross Sections

MT = 3 Explicit representation of three photons (.04971, .1632 and .3344 MeV) from inelastic scattering was derived from file 3 data and known branching ratios. For incident neutron energies > .7251 MeV the method of ref. 36 was used to calculate photon production

cross sections and spectra from all reactions except photons from the first three inelastic groups, neutron capture and neutron-induced fission.

File 14. Photon Angular Distributions

MT = 3,18,102 All photons were assumed to be isotropic.

File 15. Continuous Photon Energy Spectra

MT = 3 Photon spectra were obtained using the method of ref. 36.

MT = 18 The measured photon spectrum of ref. 34 was used for all incident neutron energies because there are no experimental data for Th-232.

MT = 102 The spectrum used was based on an undocumented measured photon spectrum at thermal neutron energy for U-238 with a minor adjustment for the small Q-value difference between U-238 and Th-232. It was assumed that the spectrum remained unchanged for all incident neutron energies.

File 31. Covariances of the Average Number of Neutrons Per Fission

MT = 452 By R.Gwin, ref. 4.

File 33. Covariances of Neutron Cross Sections

MT = 18,102 Based on error estimates in these cross sections in ref. 32,1.

REFERENCES

1. J.W.Meadows, W.P.Poenitz, A.B.Smith, D.L.Smith, J.F.Whalen and R.J.Howerton, ANL/NDM-35 (Feb. 1978)

2. D.F.Newman, B.R.Leonard Jr., et al., EPRI Np-222 (May 1977)

3. G.de Saussure and R.L.Macklin, ORNL/TM-6161, ENDF-255 (Dec. 1977)

4. R.Gwin, ORNL/TM-6245, ENDF-262 (May 1978)

5. R.E.Kaiser and S.G.Carpenter, (ANL-West) Private Comm. (March 1978) Data inserted into file at BNL by R.Kinsey (4/18/78)

6. R.Sher + C.Beck, EPRI 1771/81 + Rev. (1/83) + Private Comm. to Magurno (2/83)

7. S.F.Mughabghab and D.I.Garber, BNL-325, 3rd Edition (1973)

8. H.Derrien, NEANDC(E) 163(U) (1975)

9. J.F.Whalen and A.B.Smith, Nuc.Sci. and Eng. 67, 129 (1978)

10. J.Meadows, A.Smith and J.Whalen, Private Comm. (1977)

11. U.Fasoli, et al., Nucl.Phys. A151, 369 (1970)

12. M.Divadeenam, et al., Diss.Abs. 28, 3834 (1968)

13. C.Uttley, et al., 66 Paris, 1, 165 (1966)

14. L.Green, et al., Proc.Conf. on Nucl. Cross-Sections and Technology, Knoxville, 1, 325 (1971)

15. D.Foster, et al., Private Comm. (1967)

16. R.Batchelor, et al., Nucl.Phys. 65, 236 (1956)

17. J.Coon, et al., Phys.Rev. 88, 562 (1952)

18. P.Guenther, et al., Nuc.Sci. and Eng. (1977)

19. C.Philis, et al., ANL/NDM-28 (1977)

20. A.Smith, Phys.Rev. 126, 718 (1962)

21. W.McMurray, et al., Southern Univ. Nuclear Inst. Report SUNI-41 (1975)

22. J.Haouat, et al., Proc.Iner.Conf. on Interactions of Neutrons with Nuclei, CONF-760715 (1976)

23. R.Batchelor and J.Towle, Nucl.Phys. 65, 236 (1965)

24. R.Batchelor and J.Towle, Proc.Phys.Soc. 73, 193 (1959)

25. A.Smith, Private Comm. (1970 and 1977)

26. A.Smith, et al., Nuc.Sci. and Eng. (1977)

27. M.Segev, et al., Trans.Am.Nucl.Soc, 22, 679 (1975) and Private Comm. (1976)

28. R.J.Howerton and R.J.Doyas, Nucl.Sci and Eng, 46, 414 (1971)

29. Yu.A.Vasil ev, et al., Physics of Nuclear Fission, N.A.Perfilov and V.P.Eismont, (Eds), Israel Program of Sci.Trans. Jerusalem (1964)

30. E.M.Pennington, Private Comm. (1973)

31. M.R.Bhat, ENDF-268 (to be published)

32. R.E.Chrien and H.Liou, (1978) (to be published)

33. W.P.Poenitz, ANL/NDM-45 (1978) (to be published)

34. R.W.Peele and F.C.Maienschein, Nucl.Sci.Eng. 40, 485 (1970)

35. R.J.Howerton, D.E.Cullen, R.C.Haight, M.H.MacGregor, S.T.Perkins and E.F.Plecharty, "The LLL Evaluated Nuclear Data Library (ENDL): Evaluation techniques, reaction index, and descriptions of individual evaluations," UCRL-50400, Vol.15, Part A, Lawrence Livermore Laboratory, (1975)

36. S.T.Perkins, R.C.Haight and R.J.Howerton, Nucl.Sci.Eng. 57, 1 (1975)

37. D.K.Olsen, ORNL/TM-8056 (1982), ENDF-319

# SUMMARY DOCUMENTATION FOR $^{233}U$

by

L. Stewart, D. G. Madland, and P. G. Young
Los Alamos National Laboratory
Los Alamos, New Mexico

and

L. Weston, G. de Saussure, and R. Q. Wright
Oak Ridge National Laboratory
Oak Ridge, Tennessee

and

F. Mann
Hanford Engineering and Development Laboratory
Richland, Washington

and

N. Steen
Bettis Atomic Power Laboratory
West Mifflin, Pennsylvania

## ABSTRACT

Version V, Revision 2

The Revision-2 evaluation for Version V is identical to Revision-0 for the neutron files and was based on data available prior to 1978. The Revision-2 evaluation includes gamma-ray production data (cross sections, energy, and angular distributions). These were added in November 1981 and distributed in March 1983. In summary, Files 2, 3, 4, 5, and 8 remain unchanged and Files 12, 13, 14, and 15 were added resulting in necessary additions to File 1, MT = 451.

## I. SUMMARY

A new evaluation of neutron-induced reactions on $^{233}U$ was carried out for Version V of ENDF/B (MAT 1393). The analysis was divided among several laboratories. The thermal data evaluation was performed at BAPL and LASL, the resolved and unresolved resonance regions were evaluated at ORNL and HEDL, and evaluation of the data from 10 keV to 20 MeV and assembly of the composite file were carried out at LANL. In addition, fission product yield data were provided by the CSEWG Yield Subcommittee (T. England, chairman), and radioactive decay data by C. Reich (INEL). Partial documentation of the evaluation is

provided in LA-7200-PR[3] and in Ref. 16. The evaluation covers the energy range $10^{-5}$ eV to 20 MeV. Gamma-ray production data were added in the Revision-2 Version (November 1981). Covariance data may be included at a later date. This evaluation was based on experimental data available to November 1978.

II. ENDF/B-V FILES

File 1. General Information

MT=451. Descriptive data.

MT=452. $\bar{\nu}$ Total

Sum of prompt plus delayed $\bar{\nu}$. Used thermal value recommended by CSEWG Standards Subcommittee of 2.4947 on 5-27-78. This value is 1% larger than recommended by Lemmel[1] and 0.13% smaller than Version IV.

MT=455. $\bar{\nu}$ Delayed

The delayed yields and spectra were evaluated by Kaiser and Carpenter at ANL-Idaho (see Ref. 2 for technical details). The same six-group yields appear in Version IV but the spectra have been changed for Version V.

MT=456. $\bar{\nu}$ Prompt

The energy dependence of prompt $\bar{\nu}$ is changed significantly from Version IV. Although the thermal value is slightly lower, the value around 1.5 MeV is significantly higher and has a different shape with three slightly different slopes. The evaluation relies heavily on the measurements with respect to $^{235}U$ and $^{252}Cf$ using the CSEWG recommended standards. In particular, the data of Boldeman, Sergachev, Nurpeisov, and Block[5-7] were weighted at all energies while the Mather[8] measurements were relied upon only at high energies. Smirenkin, Flerov, and Protopopov[9-11] also contributed in the high-energy range. This evaluation decouples the thermal value based on $\eta$ measurements from the fast range. Otherwise, the $\bar{\nu}$-$\eta$ discrepancy would be perpetuated to 20 MeV.

MT=458. Energy Release in Fission

These values were taken directly from an evaluation by R. Sher[12] (Stanford).

File 2. Resonance Parameters

MT=151. (a) Resolved Resonance Region

Resolved range extends to 60 eV. Multi-level parameters provided by de Saussure (ORNL) in Adler-Adler formalism from analysis by Reynolds (KAPL). Version IV used single-level Breit-Wigner representation but had large fluctuations in fission in File 3 background.

(b) Unresolved Resonance Region

Unresolved range extends to 10 keV. Version IV was pointwise over this range. A reevaluation of the point-wise cross sections begun by Mann (HEDL) were used as the starting point by Weston (ORNL), who obtained new average cross sections for fission and capture that require no File 3 backgrounds. Cross sections based on Carlson and Behrens,[4] Weston,[17] Cao,[18] and Nizamuddin[19] for fission. Weston's data[20] were used for capture using a potential scattering radius of 0.9893. Reasonable agreement with Pattenden's total cross section[21] was obtained, especially below 1 keV. New measurements are needed in this range.

File 3. Neutron Cross Sections

Thermal Range

The 2200 m/s ($E_n$=0.0253 eV) data are as follows:

| | | | |
|---|---|---|---|
| Eta | 2.2959 | Capture | 45.76 b |
| Alpha | 0.0866 | Fission | 528.45 b |
| $\bar{\nu}$ Prompt | 2.4873 | Absorption | 574.21 b |
| $\bar{\nu}$ Total | 2.4947 | Elastic | 12.6 b |
| | | Total | 586.81 b |

The capture and fission cross sections were renormalized by N. Steen (BAPL). The elastic scattering in the thermal range changed significantly from Version IV to conform to Leonard's thermal and Weston's evaluation in unresolved range. The total was adjusted accordingly. Elastic and total changes made by LANL.

10 keV - 20 MeV

Much of the File 3 data above 50 keV relied heavily on model calculations performed by Madland (LANL). Calculations were particularly important for this isotope since experimental information was often insufficient if not completely missing. A detailed description of the methods used can be found in Ref. 3. Note that for convenience, many of the specific references found in BNL-325 are not repeated here.

MT=1. Total Cross Section

No measurements exist from 10 to 40 keV; therefore, an extrapolation was made to give reasonable agreement with recent ANL data[13] above 40 keV and cross sections predicted by Madland. The present evaluation is based on recent ANL measurements[13] and earlier work of Green (Bettis) and Foster (Hanford). See BNL-325 (Ref. 5). No measurements exist above 15 MeV. This reevaluation resulted in an increased total cross section up to 7 MeV, the increase near 1.6 MeV being as large as 8%. Use of the Foster data resulted in a decrease of 4.8% near 14 MeV.

MT=2. Elastic Cross Section

(Obtained from total minus reaction). The increased total cross section required a significant increase in the elastic cross section over the energy range to 7 MeV. At 14 MeV the elastic was decreased due to the decrease in the total.

MT=4. Inelastic Cross Section

Sum of MT=51-54 and MT=91. These data were taken from model calculations of discrete and continuum compound inelastic scattering and coupled-channel direct inelastic scattering.

MT=16, 17. (n,2n) and (n,3n) Cross Sections

Taken from Hauser-Feshbach statistical model calculations performed by Madland.

MT=18. (n,f) Cross Sections

Data from 10 keV to 100 keV are sparse and reasonably discrepant. Above 100 keV, we relied heavily on the ratio measurements of Carlson and Behrens[4] and those of Meadows,[14] normalized to Version V $^{235}U$ fission. The absolute data of Poenitz[15] were also employed, although good agreement among the sets was lacking. The evaluated curve was drawn as smoothly as possible due to the magnitude of the discrepancy among the sets.

MT=51-54. Discrete Inelastic Cross Sections

Taken from compound and direct inelastic scattering model. More than four discrete levels are needed to improve the evaluations.

MT=102. Radiative Capture Cross Section

No data exist above 10 keV except for the $\alpha$ measurements of Diven and Hopkins (see Ref 5) that extend to 1 MeV. Extrapolated to 20 MeV assuming a rise due to direct capture.

MT=251, 252, 253, $\mu_L$, $\xi$, $\gamma$

Calculated from MF=3 and 4 data and input by Kinsey at BNL.

File 4. Neutron Angular Distributions

All neutron angular distributions isotropic in laboratory system except for the elastic (MT=2) which was taken from Version IV. The elastic and direct inelastic should be modified in the next update.

File 5. Neutron Energy Distributions

MT=16, 17. (n,2n), (n,3n) Energy Distributions

Represented by an evaporation spectrum with LF=9.

MT=18. (n,f) Neutron Energy Distributions

Represented by an energy-dependent Watt spectrum with an average energy at thermal of 2.073 MeV. This spectrum based on Grundl ratio data to $^{235}U$ and $^{239}Pu$.

MT=91. Inelastic Continuum Energy Distributions

Represented by an evaporation spectrum with LF=9.

MT=455. Delayed Neutron Spectra

Evaluated in six time groups by Kaiser and Carpenter[2] at ANL-Idaho.

File 8. Fission Product Yields and Decay Data

MT=454. Individual Fission Product Yields

Direct yields before neutron emission.

MT=459. Cumulative Yields

Cumulative yields along each isobaric chain after neutron emission taken from set 5D.3/78. Values recommended by CSEWG Yields Subcommittee (England, chairman).

Note: Both direct and cumulative yields are normalized by the same factors based on B. F. Rider's evaluation. The isomeric state model, LA-6595-MS (ENDF-241), and delayed neutron emission branchings (Pn values) for 102 emitters, and pairing effects, LA-6430-MS (ENDF-240), have been incorporated.

Uncertainties are based on the total yield to each ZA. When there is an isomeric state, the independent nuclide yield to each state has a larger uncertainty than the total yield in state distributions. (Uncertainties average 50% but can be larger). Any yield with an uncertainty of 45-64% may be model estimate or a value assigned in the wings of the mass distribution. These small yields may be accurate only within a factor of two.

Data prepared for ENDF/B-V by T. R. England (Ref. LA-UR-78-687).

MT=457. Radioactive Decay Data

Evaluated by C. Reich (INEL)

Q (ALPHA) - 1974 Version of Wapstra-Bos-Gove mass tables.

Half-life - Average of Values by Vaninbroukx[22] and Jaffy et al.[23]

Alpha Energies and Intensities - Are based mainly on the results of Ellis[24] with a few deletions based on level-scheme considerations. Energies and intensities of the two most prominent alpha groups are those recommended by Rytz.[25]

Gamma-Ray Energies and Intensities - Based on results of Kroger and Reich.[26]

Gamma-Ray Multipolarities - Taken from level scheme considerations (see Ref. 26).

General Note. The decay data (MT=457) were translated into the ENDF/B-V format by Mann and Schenter at HEDL. Also much of the above data provided by other laboratories were first input in the file by Bob Kinsey at BNL and then sent to LANL. His help was significant and is gratefully acknowledged in assembling this file.

File 12.

MT=4. Transition probabilities used for four discrete levels assuming 60%-40% split. Continuum added above 300 keV. Due to the fact that only four levels are involved, the continuum probability is large. MT=4 is zero above 1.09 MeV.

MT=18. Multiplicities taken from Hoffman and Hoffman.[21]

MT=102 Multiplicities guessed. No data available.

File 13.

MT=3. Above 1.09 MeV, all gammaray production represented by the nonelastic cross section. Data for $^{239}$Pu were modified for this cross section as taken from work by Hunter and Stewart[27] and by Hunter, Stewart, and Hirons[28].

File 14.

MT=3, MT=4, MT=18, MT=102: all assumed isotropic in laboratory system.

File 15.

MT=3. Spectra for MT=3 taken from $^{239}$Pu, MAT 1399.

MT=4. Continum spectra taken from $^{239}$Pu, MAT 1399.

MT=18. Taken from $^{239}$Pu, MAT 1399.

MT=102. Taken from $^{239}$Pu, MAT 1399 after adjustment for energy differences.

REFERENCES

1. H. D. Lemmel, Proc. Symp. Neutron Standards and Applications, National Bureau of Standards, Washington, D.C., March 28-31, 1977. (See p. 170).

2. Kaiser and Carpenter, private communication to BNL (1978).

3. D. G. Madland and P. G. Young, Los Alamos Scientific Laboratory report LA-7200-PR (1978), pp. 11 and 13.

4. G. W. Carlson and J. W. Behrens, Nucl. Sci. Eng. 66, 205 (1978).

5. D. I. Garber and R. R. Kinsey, Brookhaven National Laboratory report BNL-325, Vol. 11 (1976).

6. J. W. Boldeman, J. Nucl. Ener. 25, 321 (1971), and Boldeman, Bertram, and Walsh, Nucl. Phys. A 265, 337 (1976).

7. L. Reed, R. W. Hockenbury, and R. C. Block, Rensselaer Polytechnic Inst. report COO-3058-39, p. 9 (September 1973).

8. D. S. Mather, Nucl. Phys. 66, 149 (1965).

9. G. N. Smirenkin, At. Ener. 4, 88 (1958).

10. N. N. Flerov, At. Ener. 10, 86 (1961).

11. A. N. Protopopov, At. Ener. 5, 71 (1958).

12. R. Sher and C. Beck, EPRI NP-1771/81, Rev 1/83, P. C. to NNDC 2/83.

13. W. P. Poenitz, J. F. Whalen, P. Guenther, and A. B. Smith, Nucl. Sci. Eng. 68, 358 (1978).

14. J. W. Meadows, Nucl. Sci. Eng. 54, 317 (1974).

15. W. P. Poenitz, Argonne National Laboratory report ANL-NDM-36 (1978).

16. L. Stewart, D. Madland, and P. Young, Trans. Am. Nucl. Soc. 28, 721 (1978).

17. L. Weston et al., Nucl. Sci. Eng. 42, 143 (1970).

18. M. Cao et al., J. Nucl. Ener. 24, 111 (1970).

19. S. Nizamuddin and J. Blons, Nucl. Sci. Eng. 54, 116 (1974).

20. L. Weston et al., Nucl. Sci. Eng. 34, 1 (1968).

21. N. Pattenden et al., Nucl. Sci. Eng. 17, 404 (1963).

22. R. Vaninbroukx et al., Phys. Rev. C 13, 315 (1976).

23. A. H. Jaffy et al., Phys. Rev. C 9, 1991 (1974).

24. Y. A. Ellis, Nucl. Data Sheets B 6, No. 3, 257 (1971).

25. A. Rytz, At. Data and Nucl. Data Tables 12, No. 5, 479 (1973).

26. L. A. Kroger and C. W. Reich, Nucl. Phys. A 259, 29 (1976).

27. R. E. Hunter and L. Stewart, Los Alamos Scientific Laboratory report LA-4901 (1972).

28. R. E. Hunter, L. Stewart, and T. J. Hirons, Los Alamos Scientific Laboratory report LA-5172 (1973).

93-Np-237 HEDL,SRL,+ Eval-Apr78: revised 1981; Mann, Benjamin, Smith, Stein, Reich

| | |
|---|---|
| HEDL | Eval-Apr78 Mann and Schenter (Fast) |
| SRL | Eval-Oct75 Benjamin |
| INEL | Eval-Aug78 Reich (Decay) |
| ANC,LASL | Eval-Jun73 J.R.Smith (ANC), W.E.Stein (LASL) |

The basic changes from the version III evaluation are
1. A new fission evaluation by W.E.Stein, from 40 keV to 20 MeV.
2. New resonance parameters, both resolved and unresolved.
3. Revised capture cross sections.
4. Renormalized (n,2n) and (n,3n) data.
5. Readjustment of the inelastic cross sections to accommodate the above changes.

Cross section values at E=0.0253 eV are

| | |
|---|---|
| Total | 195.06 barns |
| Scatter | 14.13 barns |
| Capture | 180.91 barns |
| Fission | 18.45 millibarns. |

File 1. General Information

MT = 452 Based on ref. 1.

MT = 458 Energy from fission based on Sher, ref. 22.

File 2. Resonance Parameters

MT = 151 Below 10-eV resubmitted by Mann (HEDL) reentered by Magurno (BNL) for ENDF/B-V.2. Resolved parameters below 10-eV are taken from the eval. of Derrien et al., ref. 23. The thermal gamma cross section is 181 bns. From 10-130 eV, resolved parameters of Paya, ref. 2 are used with fission widths multiplied by 0.625 in keeping with the renormalization recommended by Paya in a Private Communication. Unresolved parameters were fitted by J.R.Smith and M.K.Bhat to the Paya data from 130 eV to 5 keV, using the UR code developed by E.Pennington (ANL). The unresolved parameters are designed to yield histograms in the fission cross section, with areas equal to those of the -class 2- resonance areas determined by Paya (renormalized by factor 0.625).

File 3. Neutron Cross Sections

MT = 1 From 1.0-05 eV to 40 keV the resolved and unresolved parameters yield the total cross section, with a small correction for inelastic scattering beginning at 33.34 keV. From 40 keV to 1 MeV the total is the sum of the partials. Above 1 MeV, the total is also the sum of the partials, but all cross sections have

been constrained to keep the total close to the recent measurements made at RPI ref. 3.

MT = 2 A 10.5 barn potential scattering cross section is assumed. Above the resonance range the elastic cross section follows an extrapolation of the unresolved calculation to 1 MeV, above which it follows a curve based on cross sections of neighboring nuclei.

MT = 4 The inelastic cross sections for ENDF/B-I were based on a calculation by D.T.Goldman, ref. 4. They have been progressively modified since.
For version III the inelastic cross sections were reduced so the total cross section would be consistent with measurements on neighboring nuclei above 1 MeV.

For version IV the inelastic cross sections have been again adjusted to insure that the total inelastic was equal to the sum of its parts, and to accommodate reevaluated (n,2n),(n,3n), and capture cross sections in the constrained total cross section.
For version V, the cross sections were smoothly continued above 1.0 MeV (Stewart and Young, LASL).

MT = 16 - 17 Both (n,2n) and (n,3n) cross sections are based on calculations made by S.Pearlstein, ref. 4. The (n,2n) cross section was normalized to the integral measurement of Paulson and Hennelly ref. 6, to obtain cross section to short lived state and of Myers et al., ref. 7, to obtain ratio of short-lived to long-lived state. MT = 16 contains (n,2n) only to states which populate Np-236. Such an evaluation differs from differential measurements of Lindeke et al., ref. 8 and of Landrum et al., ref. 9 as well as HAUSER-FESHBACH calculations, ref. 10.

The (n,3n) cross section keeps the Pearlstein shape and was renormalized to a maximum value of .203 barn to maintain the constraints on the total cross section.

MT = 18 Below 40 keV the cross section is calculated from resolved and unresolved resonance parameters.
Above 40 keV the data is an average of experimental data, ref. 11-19.

MT = 51 - 61,91 See comment under MT = 4.

MT = 102 The thermal capture cross section = 181 b. From 1.0-05 eV to 40 keV the capture is given by the resolved and unresolved resonance parameters.
From 120 keV to 20 MeV the capture is from a smooth curve drawn through the measurements of Nagle et al., ref. 20. Between 40 and 120 keV the capture is pointwise, taken from an unresolved calculation which had been extended to 120 keV using parameters

adjusted to yield the evaluated capture cross section at that point. The Nagle measurements are appreciably lower than the Stupegia data on which previous ENDF/B files were based, and tie in much more smoothly with the extrapolation of the unresolved calculation.

File 4. Angular Distributions of Secondary Neutrons

MT = 2 Angular distributions were supplied by H.Alter, then of AI, based on optical model calculations made on neighboring nuclei.

All other reactions, i.e. MT = 16,17,18,51-61,91 are assumed isotropic.

File 5. Energy Distributions of Secondary Neutrons

MT = 16-17 Nuclear temp calculated for Maxwell dist, LF = 9. Calc. of temp distribution follows prescription used for the Pu-240 file of ENDF/B-I.

MT = 18 Fission spectrum has Maxwellian density with the temp based on Terrells prescription, ref. 20.

MT = 91 Inelastic secondaries based on D.T.Goldman data, ref. 11. Both discrete level and evaporation spectra are included.

File 8. Radioactive Decay and Fission Product Yield Data

MT = 16 Based on ENDF/B-V decay data of Np-237(s) and (1).

MT = 454,459 Fission yield data set 5e,7/78.
Values obtained from the recommendations of the yields subcommittee, T.R.England (Chairman), D.M.Gilliam, Y.Harker, J.R.Liaw, W.J.Maeck, D.G.Madland, V.McLane May, P.L.Reeder, B.F.Rider, R.E.Schenter, B.I.Spinrad, J.P.Unik, A.Wahl, W.Walker, B.W.Wehring, and K.Wolfsberg.

Uncertainties are based on the total yield to each ZA. When there is an isomeric state, the independent nuclide yield to each state has a larger uncertainty than the total yield in state distributions (uncertainties average approximately 50 percent but can be larger). Any yield having a larger uncertainty (45-64 percent) may be a model estimate or a value assigned to the yields on the wings or valley of the mass yield distribution. These small yields may only be accurate to within a factor of 2.

MT 454 contains direct yields before delayed neutron emission.

MT 459 contains cumulative yields along each isobaric chain after delayed neutron emission.

Direct and cumulative yields are normalized by the same factors based on B.F.Rider evaluation. The isomeric state model, LA-6595-MS (ENDF-241), and delayed neutron emission branchings (pn values) for 102 emitters, LA-UR-78-688, and a pairing effects, LA-6430-MS (ENDF-240), have been incorporated.

Data prepared for files by T.R.England (LASL LTS. T-2-1-2891). Data for 93-Np-237 decays by Reich inserted into file at BNL by R.Kinsey in Sep 1978.

MT = 457 Radioactive decay data references.

Q(alpha)-1974 version of Wapstra-Bos-Gove Mass Table other- see Y.A.Ellis, Nuclear Data Sheets 6, No. 6, 539 (1971) and also Table of Isotopes, 7th ed. (preliminary data, Priv. Comm. from C.M.Lederer).

The gamma-ray energy and relative-intensity values are those of M.Skalsey and R.D.Connor, Can. J. Phys. 54, 1409 (1976).

Note The data on the more prominent alpha groups are those recommended by A.Rytz, At. Data and Nucl. Data Tables 12, No. 5, 479 (1973).

Note The k x-ray intensities represent measured values translated into ENDF/B-V format by Mann and Schenter (HEDL) 8/78.

File 9. Multiplicities for Production of Radioactive Nuclides

MT = 16 Based on Meyers et al., ref. 35. HAUSER-FESHBACH calculations ref. 38 give energy dependent ratios.

## REFERENCES

1. Keyworth and Vesser, LASL Memo P-3-2080(U) (1976)

2. D.Paya, Thesis, University of Paris-South, Center D-Orsay (1972)

3. R.C.Block, Private Comm.

4. D.T.Goldman, Trans.Am.Nucl.Soc. Vol.7, 84 (1964)

5. S.Pearlstein, Nucl.Sci.Engr. Vol.23, 238 (1965)

6. C.K.Paulson and E.J.Hennelly, Nucl.Sci.Eng. 55, 24 (1974)

7. W.A.Myers, M.Linder, and R.S.Newbury, J.Inorg.Nucl.Chem. 37, 637 (1975)

8. K.Lindeke, S.Specht, and H.-J.Born, Phys.Rev. C12, 1507 (1975)

9. J.H.Landrum, R.J.Nagle, and M.Linder, Phys.Rev. C8, 1938 (1975)

10. F.M.Mann, Private Comm. (1977)

11. P.H.White, et al., Phys. and Chem. of Fission, 219 IAEA, Salzburg (1965)

12. E.D.Klema, Phys.Rev. Vol.72, 88 (1947)

13. W.E.Stein, et al., Conf-660303, 623 Washington (1966)

14. V.M.Pankratov, Sov.Journ.Atomic Energy, Vol.14, 197 (1963)

15. P.H.White and G.P.Warner, J.Nucl.Energy, Vol.21, 671 (1967)

16. W.K.Brown, D.R.Dixon, and D.M.Drake, Nucl.Phys. A156 (1970), La-4372 (1970)

17. R.J.Jiacoletti, W.K.Brown, and H.G.Olson, Nucl.Sci. and Eng. 48, 412 (1972)

18. K.Kobayashi, I.Kimura, H.Gotoh, and H.Yagi, EANDC(J) 26L, 39 (1972)

19. S.Plattard, Y.Pranal, J.Blons, and C.Mazur, Kiev Conference (1975)

20. J.J.Nagle, et al., Conf-710301, V1, 259 Knoxville (1971)

21. J.Terrell, Phys.Chem. of Fission, Vol.2, 3 IAEA, Vienna (1965)

22. Sher + Beck, EPRI NP-1771/81 + Rev 1/83 + Private Comm. to Magurno (2/83)

23. H.Derrien, J.P.Dont, E.Fort, and D.Lafond, INDC(FR)-42/L (1980)

# SUMMARY DOCUMENTATION FOR $^{239}$Pu

by

E. D. Arthur, P. G. Young, D. G. Madland, and R. E. MacFarlane
Theoretical Division, Los Alamos National Laboratory
Los Alamos, New Mexico 87545

## SUMMARY

A major revision of the ENDF/B-V evaluation for $^{239}$Pu covering neutron energies between 8 keV and 20 MeV was completed for Revision 2 of ENDF/B-V. The most important changes to the evaluation include incorporation of a comprehensive new theoretical analysis based on recent experimental data to replace part of the total cross-section file and all of the elastic and inelastic cross sections and secondary distributions, reevaluation of the prompt and total average neutron multiplicities from fission for incident energies between 0.4 and 11.5 MeV to correct discrepancies of almost 3% with new experimental data, and the replacement of all secondary neutron energy spectra from fission with improved shapes based on approximations to a new theoretical method. The results have been validated by calculating measured quantities for five fast critical assemblies. The evaluation and theoretical calculations are described in detail in Ref. 1.

## THEORETICAL ANALYSIS

The theoretical analysis involved application of two main reaction models: a coupled-channel optical model to describe direct-reaction contributions to inelastic scattering from collective states and Hauser-Feshbach statistical theory to calculate compound-nucleus contributions to the reactions. The neutron transmission coefficients required for the Hauser-Feshbach calculations were obtained from the coupled-channel analysis, thereby ensuring consistency between the compound-nucleus and direct-reaction parts of the calculations. At incident energies above ~ 10 MeV, preequilibrium theory was employed to correct the statistical theory calculations for nonequilibrium effects.

The ECIS computer code[2] was used for coupled-channel deformed optical model calculations. The first six states of the $^{239}$Pu ground state rotational band ($1/2^+$, $3/2^+$,..., $11/2^+$) were coupled in the calculation. The optical potential was represented in a standard manner,[3] and the coupling form factors needed in the expansion of the optical parameters were assumed complex. We used neutron optical parameters based on the Bruyères-le-Châtel analysis,[4] which relied mainly on fits to actinide total, elastic, and inelastic cross sections as well as s- and p-wave strength functions. Slight modifications were made to the optical parameters to produce better agreement with the $^{239}$Pu total cross-section measurements of Poenitz et al.,[5] particularly around 1 MeV. The resulting optical and deformation parameters appear in Table I.

The reaction theory code[6] COMNUC, which includes width-fluctuation corrections, was used for the Hauser-Feshbach statistical theory calculations below 5 MeV, and the GNASH code,[7] which includes preequilibrium corrections, was employed at higher energies. Both codes utilized the phenomenological level density model of Gilbert and Cameron[8] along with the parameters of Cook et al.[9] A

maximum amount of experimental information on discrete levels was included for each nucleus appearing in the calculation. Such data were used to adjust the constant temperature level density parameters so as to reproduce the cumulative number of levels at low excitation energies while joining smoothly to the Fermi-gas form at higher energies. Gamma-ray transmission coefficients were calculated using a Brink-Axel expression[10,11] that utilized two Lorentzian forms to represent the split giant dipole resonance. The gamma-ray transmission coefficients were normalized to reproduce measured $2\pi\langle\Gamma_\gamma\rangle/\langle D\rangle$ data[12] available for s-wave resonances near the neutron binding energy. From such data, gamma-ray strength function parameterizations were obtained and were used to describe gamma-ray emission from unstable compound systems in the calculations.

TABLE I

OPTICAL MODEL AND DEFORMATION PARAMETERS USED IN THE CALCULATIONS[a]

| | | | r | a |
|---|---|---|---|---|
| V | = 46.2 - 0.3E | | 1.26 | 0.615 |
| $W_{VOL}$ | = -1.2 + 0.15E | E ≧ 8 MeV | 1.26 | 0.615 |
| $W_{SD}$ | = 3.6 + 0.4E | E ≦ 7 MeV | 1.24 | 0.50 |
| $W_{SD}$ | = 6.4 - 0.1(E-7) | E > 7 MeV | 1.24 | 0.50 |
| $V_{SO}$ | = 6.2 | | 1.12 | 0.47 |

$\beta_2$ = 0.21 $\beta_4$ = 0.065

[a]The well depths and energies are in MeV; geometrical parameters are in fm. A Woods-Saxon form factor is used throughout.

Although we relied on experimental data (as represented in ENDF/B-V.0) for the total fission cross section in the evaluation, the ability to calculate the fission channel reliably (better than ±5%) provides an important constraint on the Hauser-Feshbach calculation of other channels. For our calculation we introduced a double-humped barrier model into the COMNUC and GNASH codes using two uncoupled oscillators for the barrier representation. The fission model and calculations are described in detail in Ref. 1.

## RESULTS FOR TOTAL, ELASTIC, AND INELASTIC REACTIONS

A number of modifications were incorporated into the ENDF/B-V, Revision 0, data file on the basis of the above theoretical calculations:

1. The total cross section was significantly modified in the range of $E_n$ = 0.025 to 1.5 MeV.

2. The inelastic scattering cross sections and angular distributions were completely replaced from threshold to 20 MeV.

3. The continuum inelastic cross section and secondary neutron energy spectra were significantly revised to match the calculations.

4. The elastic cross section and angular distributions were completely replaced from the inelastic threshold ($E_n$ = 7.8932 keV) to 20 MeV. (The actual elastic cross sections in the file were determined by subtracting the nonelastic cross section from the total, but these values were constrained by the analysis described above to closely approximate the theoretical results.)

The revised total cross section below 2 MeV is compared in Fig. 1 with the ENDF/B-V evaluation (dashed curve) and with experimental results. The lower energy cutoff of the curve (25 keV) is the upper boundary of the unresolved resonance region in ENDF/B-V, which we did not modify. The older data of Schwartz et al.[13] and Smith et al.[14] were available for version V, but the more recent measurements of Poenitz et al.[5] were not. As mentioned previously, the Poenitz data were considered in our theoretical calculations. As is evident in Fig. 1, significant modifications were made in the total cross-section evaluation between 25 and 500 keV, with changes as large as 7% being required. Large changes in the elastic cross section also resulted in this energy region, reaching ~ 11% near 1.6 MeV.

Calculated elastic and inelastic scattering angular distributions for 0.7-MeV incident neutrons are shown in Fig. 2 with the experimental data of Haouat et al.[4] for the ground state band members of $^{239}$Pu. At this energy, compound contributions can be significant, so that both the direct and compound-nucleus calculations are tested by this comparison. Overall, the agreement with experiment is good, although the calculation somewhat underpredicts the cross section for the $7/2^+$ state.

Figure 3 presents a comparison of the calculated results with a scattering measurement by Smith and Guenther[15] for 2.5-MeV incident neutrons. This measurement includes elastic as well as inelastic neutrons from states in $^{239}$Pu up to an excitation energy of $E_x$ = 0.2 MeV. Smith and Guenther also used their results, together with total and fission cross-section data, to infer total inelastic scattering cross sections for levels above a given excitation-energy threshold. A comparison of our calculated inelastic cross sections (solid curve) with their inferred results is given in Fig. 4 with the excitation-energy threshold for the results ranging from $E_x$ = 0.08 to 0.3 MeV. The dashed curve in Fig. 4 represents the ENDF/B-V evaluation, which lies substantially above both the experimental data and our calculations at higher energies.

The evaluated inelastic excitation cross sections for the lowest three levels in $^{239}$Pu are compared with ENDF/B-V in Fig. 5. These comparisons illustrate the large differences that exist between the present (n,n') results and version V, with discrepancies of factors > 2 being common. In the cases of the lowest five levels, the differences largely reflect the fact that direct reactions were included in our calculations but not in ENDF/B-V. For some of the levels, it also appears that shapes characteristic of lower spin states were assumed for the version V results.

The overall effect on the total inelastic cross section of our revisions is shown by the comparison with ENDF/B-V in Fig. 6. Again, large differences from version V (up to a factor of ~ 2) are apparent, particularly over the 0.01-3.0-MeV range and above 7 MeV. Most of the increased cross section in the 0.01- to 3.0-MeV range results from the inclusion of direct-reaction contributions to low-lying states of $^{239}$Pu, which were neglected in ENDF/B-V. Above 7 MeV the larger cross section reflects inclusion of preequilibrium effects in the present calculation. Both these additions result in hardening of the spectra of emitted neutrons.

## PROMPT FISSION NEUTRON MULTIPLICITY REVISION

The ENDF/B-V evaluation of the prompt neutron multiplicity from fission, $\bar{\nu}_p(E_n)$, in the mega-electron-volt range was influenced strongly by the experimental results of Frehaut et al.[16,17] These data resulted from a measurement reported earlier[18] that was revised to correct for suspected backgrounds thought to be higher than originally reported. In the years that followed publication of the "corrected" data, however, the background problem was studied further and measurements repeated. The result is that the higher background was not confirmed, and final data from the experiments, including the new measurements, have been issued by Frehaut et al.[19] showing significant disagreement (~1 to 3%) with ENDF/B-V in the mega-electron-volt region.

In addition to the Frehaut results, a second $\bar{\nu}_p(E_n)$ measurement of high accuracy (approximately ±0.5%) was completed by Gwin et al.[20] after the issuance of version V. This new measurement, which covers the incident neutron energy range from below thermal to 10 MeV, is in substantial agreement with Frehaut's latest results above 1 MeV and with ENDF/B-V at lower energies (aside from the thermal region).

Of the older measurements, only one experiment (Savin et al.[21]) supports the withdrawn French results[16,17] and version V in the 2- to 10-MeV region. The measurements of Hopkins and Diven,[22] Mather et al.,[23] and Condé et al.[24] are all consistent with the new results of Frehaut et al.[19] and Gwin et al.[20] Therefore, as an interim correction before a more thorough covariance analysis is made, we revised the version V $\bar{\nu}_p$ evaluation by constructing simple linear line segments that pass through the Frehaut and Gwin data, joining version V at 0.4 and 11.5 MeV, with a break in slope at 3.6 MeV. The total neutron multiplicity ($\bar{\nu}_t$) was also appropriately revised using the ENDF/B-V evaluation of delayed neutron multiplicities.

The revised $\bar{\nu}_p(E_n)$ evaluation (solid curve) is compared in Fig. 7 with ENDF/B-V (dashed curve) and with the experimental data of Frehaut et al.[19] and Gwin et al.[20] between 0.1 and 10 MeV.* Two different flight paths (20 and 85 m) were used in the Gwin measurements and these are depicted by different symbols in Fig. 7. Figure 8 compares the evaluations over the same energy range with the older experimental data of Hopkins and Diven,[22] Mather et al.[23] Condé et al.,[24] and Savin et al.[21] As pointed out earlier, the Savin measurement is the only one that now supports version V.

---

*All $\bar{\nu}_p$ measurements relative to $^{252}$Cf were renormalized in our analysis using the value $\bar{\nu}_p(^{252}\text{Cf}) = 3.758 \pm 0.004$ from Ref. 25.

Note that in the thermal region, some revision of the ENDF/B-V $\bar{\nu}_p(E_n)$ evaluation also appears to be warranted by the Gwin measurements, especially near the dip at 0.3 eV. We have deferred such a revision, however, until a more careful study of data in the thermal region can be made, hopefully coupled through a covariance analysis with other reactions and nuclei. Gwin's data at low energies are compared with the ENDF/B-V evaluation in Fig. 9.

## NEUTRON ENERGY SPECTRA FROM FISSION

In 1982, an improved theoretical treatment for calculating neutron energy spectra from fission was published by Madland and Nix.[26] The two features of the new method that are most significant for applied data usage are that it permits the use of physics information other than direct measurements in inferring fission neutron spectra, and it results in a more solidly grounded theoretical spectrum that differs from both the usual Maxwellian or Watt shapes used in data evaluations, particularly for secondary energies higher than ~8 MeV. This latter feature is obviously important for any applications sensitive to the high-energy tail of the fission spectrum.

Using the constant inverse cross section form of the Madland-Nix formalism, the three basic input parameters required to calculate the first-chance fission spectrum are $E_f^L$ and $E_f^H$ (the average kinetic energies per nucleon of the average light and heavy fission fragments, respectively), and $T_m$ (the maximum temperature of the fission-fragment residual nuclear-temperature distribution). The quantities $E_f^L$ and $E_f^H$ are assumed independent of incident neutron energy and can be determined from measurements of the total average fission-fragment kinetic energy[27,28] together with a knowledge of the fission-fragment mass distribution.[27,28] For the present evaluation, the values $E_f^L$ = 1.0360 MeV and $E_f^H$ = 0.52857 MeV were used, as determined in Appendix C of Ref. 26.

The $T_m$ parameter is a function of incident neutron energy and depends on several fission-related quantities, on parameters of the compound fissioning nucleus, and on an effective level density parameter $a_{eff}$. The scope of the present work did not permit reevaluation of all fission spectrum measurements in terms of the Madland-Nix theory. Therefore, as an interim procedure, the parameter $a_{eff}$ was simply adjusted so that the fission spectrum calculated for thermal incident neutrons resulted in the same average neutron energy as does ENDF/B-V. This value of $a_{eff}$ was then used in the Madland-Nix theory to calculate $T_m(E_n)$ up to the threshold for second-chance fission, defined to be 5.68 MeV in the $E_n$ evaluation. The $T_m(E_n)$ at incident energies $\geq$ 14 MeV were determined by requiring the same average first-chance fission neutron energy as is given by the ENDF/B-V evaluation. Between 5.68 and 14 MeV, the $T_m$ points were joined by a linear line segment.

The fission neutron spectrum that results from thermal incident neutrons is compared in Fig. 10 with the ENDF/B-V evaluation. The solid curve is the ratio of the present Madland-Nix spectrum to the Watt spectrum from version V. Although both spectra result in the same average neutron energy ($\langle E' \rangle$ = 2.1120 MeV), there is a marked difference in the two above a secondary neutron energy of 8 MeV. At lower energies the ratio oscillates somewhat but never differs from unity by more than ±1.8%.

To calculate fission spectra above the threshold for second-chance fission, additional assumptions were required and are described in Ref. 1. The

average fission neutron energy that results from our treatment is plotted as a function of incident neutron energy (solid curve) in Fig. 11. Also shown are the ENDF/B-V values that result from total fission (dashed curve) and from the sum of first-, second-, third-, and fourth-chance fission (dotted curve). The dashed and dotted curves should in principle be the same, but an approximate form was used in ENDF/B-V to simplify the representation for the total neutron spectrum. In the present evaluation, the total fission spectrum is consistent with the sum of the parts. The structure appearing in Fig. 11 corresponds to the onset of second-, third-, and fourth-change fission and is determined by the fission-spectrum parameters we have assumed as well as the relative magnitudes of the multichance fission cross sections taken from ENDF/B-V.

## INTEGRAL TESTING WITH FAST CRITICAL MEASUREMENTS

In the course of these revisions, calculations were made for several critical assemblies,[29] including the bare plutonium sphere JEZEBEL (95% $^{239}$Pu), the liquid-metal fast breeder reactor benchmark ZPR-6/7 (13% $^{239}$Pu), the "dirty" plutonium sphere JEZEBEL-PU (20% $^{240}$Pu), the uranium-reflected plutonium sphere FLATTOP-PU, and the thorium-reflected plutonium sphere THOR. Eighty-group cross-section libraries based on the ENDF/B-V evaluations and the present revision were generated using the TRANSX code[30] with MATXS libraries produced by the NJOY nuclear data processing system.[31]

The impact of the Revision-2 evaluation is shown in Table II. The changes in $k_{eff}$ and the $^{238}$U to $^{235}$U fission ratio ($f^{28}/f^{25}$) relative to ENDF/B-V are quite dramatic for the four small assemblies in Table II. The $^{238}$U fission ratios show a definite and consistent improvement, due mainly to hardening of the $^{239}$Pu inelastic spectra. The deviation of the eigenvalues from unity is reduced significantly in Table II, resulting from changes in both $\bar{\nu}_p(E_n)$ and the inelastic neutron spectra. Only for the JEZEBEL-PU assembly was the eigenvalue calculation worsened, which might indicate problems with the ENDF/B-V $^{240}$Pu evaluation. The changes to ZPR-6/7 are smaller due to its lower $^{239}$Pu concentration and softer spectrum. In all cases, however, the changes to the inelastic cross section and fission neutron emission spectra have hardened the spectra of emitted neutrons. Overall, the Revision-2 data file offers significant improvements over ENDF/B-V, Revision 0.

TABLE II

CRITICAL ASSEMBLY PERFORMANCE PARAMETERS FOR $^{239}Pu$
USING THE FINAL REVISION RESULTS

| Parameter | ENDF/B-V | Revision 2 | Assembly |
|---|---|---|---|
| $k_{eff}$ | 1.0068 | 0.9982 | JEZEBEL[c] |
| $f^{28}/f^{25}$ (C/E)[a] | 0.917 | 0.959 | |
| $f^{23}/f^{25}$ (C/E) | 0.987 | 0.985 | |
| $f^{37}/f^{25}$ (C/E) | 0.989 | 1.001 | |
| $f^{49}/f^{25}$ (C/E) | 0.972 | 0.975 | |
| $f^{25}/f^{49}$ (C/E)[b] | 1.028 | 1.026 | |
| $f^{28}/f^{49}$ (C/E)[b] | 0.943 | 0.984 | |
| $k_{eff}$ | 0.9980 | 0.9917 | JEZEBEL-PU[c] |
| $f^{28}/f^{25}$ | 0.923 | 0.958 | |
| $f^{37}/f^{25}$ | 1.016 | 1.027 | |
| $k_{eff}$ | 1.0093 | 1.0050 | FLATTOP-PU[c] |
| $f^{28}/f^{25}$ | 0.941 | 0.973 | |
| $f^{37}/f^{25}$ | 1.014 | 1.017 | |
| $k_{eff}$ | 1.0228 | 1.0070 | THOR[c] |
| $f^{28}/f^{25}$ | 0.901 | 0.948 | |
| $f^{37}/f^{25}$ | 0.944 | 0.970 | |
| $k_{eff}$ | 0.9956 | 0.9958 | ZPR-6/7[d] |
| $f^{25}/f^{49}$ (C/E) | 1.018 | 1.018 | |
| $f^{28}/f^{49}$ (C/E) | 1.010 | 1.020 | |
| $c^{28}/f^{49}$ (C/E) | 1.078 | 1.077 | |
| Average $k_{eff}$ | 1.007 | 1.000 | |
| Spread in $k_{eff}$ | 0.027 | 0.015 | |

[a] Calculated result divided by the experimental result.

[b] Derived from benchmark's C/E values.

[c] Transport-corrected $P_3S_{16}$ (with no other corrections).

[d] Diffusion theory with corrections specified for the benchmark.

ENDF/B-V.2 FILES

This section describes the specific reactions that we modified in the Revision-2 evaluation. All other reactions were left unchanged from ENDF/B-V, Revision 0.

File 1. General Information.

MT=452, 456. Prompt and Total $\bar{\nu}$. Revised from 0.4 to 11.5 MeV using experimental data, as described above. The delayed $\bar{\nu}$ values from ENDF/B-V.0 were retained at all energies.

MT=458. Energy Release per Fission. Based on the work of R. Sher, ref. 32.

File 3. Neutron Cross Sections.

MT=1. Total Cross Section. Revised from 0.025-1.50 MeV, as described above, mainly on basis of new measurements.

MT=2. Elastic Cross Section. Revised in energy range 0.025-20 MeV, as described above. Obtained by subtracting nonelastic cross section from the total.

MT=18, 19, 20. Fission Cross Section. The Q value listed is the value ER = ET-ENU (the total energy less the energy of the neutrino) taken from R. Sher, ref. 32.

MT=51-68. Discrete Inelastic Cross Sections. Changed from threshold to 20 MeV on the basis of the theoretical calculations described above.

MT=91. Continuum Inelastic Cross Section. Changed from threshold to 20 MeV on the basis of the theoretical calculations described above.

File 4. Neutron Angular Distributions.

MT=2. Elastic Angular Distributions. Changed from 0.025-20 MeV on the basis of ECIS calculations described above.

MT=51-68, 91. Discrete and Continuum Inelastic Angular Distributions. Changed from threshold to 20 MeV on basis of the ECIS COMNUC, and preequilibrium calculations described above.

File 5. Neutron Energy Distributions.

MT=18-21, 38. Total, First-, Second-, Third-, and Fourth-Chance Fission Energy Distributions. Modified from $10^{-5}$ eV to 20 MeV to use the shape calculated from the Madland-Nix formalism, as described above.

MT=91. Continuum Inelastic Energy Distribution. Modified from threshold to 20 MeV on basis of the Hauser-Feshbach statistical theory analysis described above.

REFERENCES

1. E. D. Arthur, P. G. Young, D. G. Madland, and R. E. MacFarlane, "Evaluation and Testing of n + $^{239}$Pu Nuclear Data for Revision 2 of ENDF/B-V," Nucl. Sci. Eng. 88, 56 (1984).

2. J. Raynal, "Optical Model And Coupled-Channel Calculations in Nuclear Physics," International Atomic Energy Agency report IAEA SMR-9/8 (1970).

3. C. M. Perey and F. G. Perey, "Compilation of Phenomenological Optical-Model Parameters: 1954-1975," At. Data and Nucl. Data Tables 17, 1 (1976).

4. G. Haouat, J. Lachkar, Ch. Lagrange, J. Jary, J. Sigaud, and Y. Patin, "Neutron Scattering Cross Sections for $^{232}$Th, $^{233}$U, $^{235}$U, $^{238}$U, $^{239}$Pu, and $^{242}$Pu between 0.6 and 3.4 MeV," Nucl. Sci. Eng. 81, 491 (1982).

5. W. P. Poenitz, J. F. Whalen, and A. B. Smith, "Total Neutron Cross Sections of Heavy Nuclei", Nucl. Sci. Eng. 78, 333 (1981).

6. C. L. Dunford, "A Unified Model for Analysis of Compound Nucleus Reactions", Atomics International report AI-AEC-12931 (1970).

7. P. G. Young and E. D. Arthur, "GNASH: A Preequilibrium-Statistical Nuclear Model Code for Calculations of Cross Sections and Emission Spectra", Los Alamos Scientific Laboratory report LA-6947 (1977).

8. A. Gilbert and A. G. W. Cameron, "A Composite Nuclear-Level Density Formula with Shell Corrections", Can. J. Phys. 43, 1446 (1965).

9. J. L. Cook, H. Ferguson, and A. R. Musgrove, "Nuclear Level Densities in Intermediate and Heavy Nuclei", Aust. J. Phys. 20, 477 (1967).

10. D. M. Brink, "Individual Particle and Collective Aspects of the Nuclear Photoeffect," Nucl. Phys. 4, 215 (1957).

11. P. Axel, "Electric Dipole Ground State Transition Width Strength Function", Phys. Rev. 126, 671 (1962).

12. S. F. Mughabghab and D. I. Garber, "Neutron Cross Sections, Volume 1, Resonance Parameters," Brookhaven National Laboratory report BNL-325, 3rd Ed. Vol. 1 (1973).

13. R. B. Schwartz, R. A. Schrack, and H. T. Heaton II, "Total Neutron Cross Sections of $^{235}$U, $^{238}$U, and $^{239}$Pu from 0.5 to 15 MeV", Nucl. Sci. Eng. 54, 322 (1974).

14. A. B. Smith, P. Guenther, and J. Whalen, "Total and Elastic Scattering Neutron Cross Sections of $^{239}$Pu", J. Nucl. En. 27, 317 (1973).

15. A. B. Smith and P. T. Guenther, "On the Neutron Inelastic-Scattering Cross Sections of $^{232}$Th, $^{233}$U, $^{235}$U, $^{238}$U, $^{239}$Pu, and $^{240}$Pu", Argonne National Laboratory report ANL/NDM-63 (1982).

16. J. Frehaut, G. Mosinski, and M. Soleilhac, "Recent Results in $\bar{\nu}_p$ Measurements between 1.5 and 15 MeV," European-American Nuclear Data Committee report EANDC(E)-154 (1973) p. 67.

17. J. Frehaut, G. Mosinski, and M. Soleilhac, "Recent Results in $\bar{\nu}_p$ Measurements between 1.5 and 15 MeV," Proc. Second National Soviet Conf. on Neutron Physics, Kiev, May 28 - June 1, 1973 [Fiziko-Energeticheskij Institut (1973)] p. 153.

18. M. Soleilhac, J. Frehaut, and J. Gauriau, "Energy Dependence of $\bar{\nu}_p$ for Neutron-Induced Fission of $^{235}U$, $^{238}U$, and $^{239}Pu$ from 1.3 to 15 MeV," J. Nucl. En. 23, 257 (1969).

19. J. Frehaut, G. Mosinski, and M. Soleilhac, "Recent Results on Prompt Nubar Measurements between 1.5 and 15 MeV", communicated to the National Nuclear Data Center at Brookhaven National Laboratory in 1980, available as SCISRS accession number 20490.

20. R. Gwin, R. R. Spencer, R. W. Ingle, J. H. Todd, and H. Weaver, "Measurements of the Average Number of Prompt Neutrons Emitted per Fission of $^{239}Pu$ and $^{235}U$", Oak Ridge National Laboratory report ORNL/TM-6246 (1978).

21. M. V. Savin, Ju. A. Khokhlov, Ju. S. Zamjatnin, and I. N. Paramonova, "The Average Number of Prompt Neutrons in Fast Neutron-Induced Fission of $^{235}U$, $^{239}Pu$, and $^{240}Pu$," Proc. Second IAEA Conf. on Nucl. Data for Reactors, Helsinki, June 15-19, 1970 [International Atomic Energy Agency, Vienna (1970)] V. II, p. 157.

22. J. C. Hopkins and B. C. Diven, "Prompt Neutrons from Fission", Nucl. Phys. 48, 433 (1963).

23. D. S. Mather, P. Fieldhouse, and A. Moat, "Measurement of Prompt $\nu$ for the Neutron-Induced Fission of $^{232}Th$, $^{233}U$, $^{234}U$, and $^{239}Pu$," Nucl. Phys. 66, 149 (1965).

24. H. Conde', J. Hansen, and M. Holmberg, "Prompt $\bar{\nu}$ in Neutron-Induced Fission of $^{239}Pu$ and $^{241}Pu$," J. Nucl. En. 22, 53 (1968).

25. J. R. Stehn, M. Divadeenam, and N. E. Holden, "Evaluation of the Thermal Neutron Constants for $^{233}U$, $^{235}U$, $^{239}Pu$, and $^{241}Pu$," Proc. Int. Conf. on Nuclear Data for Science and Tech., Antwerp, Sept. 6-10, 1982 [K. H. Bockhoff, Ed., Reidel Pub. Co., Dordrecht, Holland (1983)] p. 685.

26. D. G. Madland and J. R. Nix, "New Calculation of Prompt Fission Neutron Spectra and Average Prompt Neutron Multiplicities", Nucl. Sci. Eng. 81, 213 (1982).

27. J. P. Unik, J. E. Gindler, L. E. Glendenin, K. F. Flynn, A. Gorski, and R. K. Sjoblom, "Fragment Mass and Kinetic Energy Distributions for Fissioning Systems Ranging from Mass 230 to 256," Proc. Third IAEA Sym. on Physics and Chemistry of Fission, Rochester, New York, Aug. 13-17, 1973 [International Atomic Energy Agency, Vienna (1974)] V. II, p. 19.

28. D. C. Hoffman and M. M. Hoffman, "Post-Fission Phenomena," Ann. Rev. Nucl. Sci. 24, 151 (1974).

29. H. Alter, R. B. Kidman, R. J. LaBauve, R. Protsik, and B. A. Zolotar, "ENDF-202: Cross Section Evaluation Working Group Benchmark Specifications," Brookhaven National Laboratory report BNL 19302 [ENDF-202] (November 1974) and references therein; see also R. B. Kidman, "Los Alamos Benchmarks: Calculations Based on ENDF/B-V Data," Los Alamos National Laboratory report LA-9037-MS (1981).

30. R. J. Barrett and R. E. MacFarlane, "The MATXS-TRANSX System and the CLAW-IV Nuclear Data Libr Proc. of Int. Conf. on Nuclear Cross Sections for Technology, Oct. 22-26, 1979, Knoxville, Tn. (NBS Special Publication 594, 1980) p. 213.

31. R. E. MacFarlane, D. W. Muir, and R. M. Boicourt, "The NJOY Nuclear Data Processing System, Volume I: User's Manual," Los Alamos National Laboratory report LA-9303-M, Vol. I (ENDF-324) (1982).

32. R. Sher and C. Beck, EPRI NP-1771/81, Rev 1/83, P. C. to NNDC 2/83.

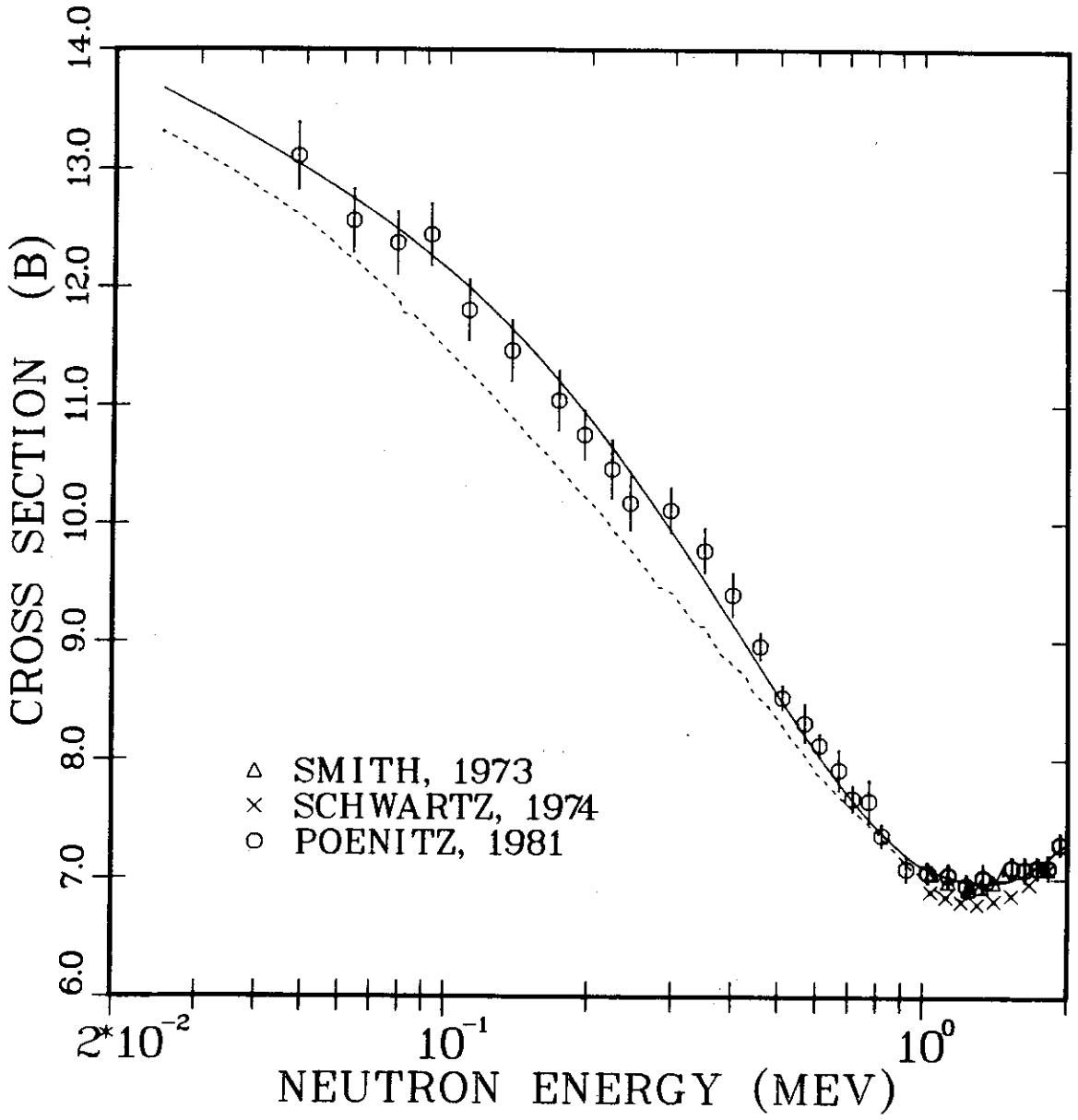


Fig. 1.

Evaluated and measured (Refs. 5, 13, and 14) total cross sections for n + $^{239}$Pu interactions between 25 keV and 2 MeV. The solid curve is the present calculation, and the dashed curve is the ENDF/B-V evaluation.

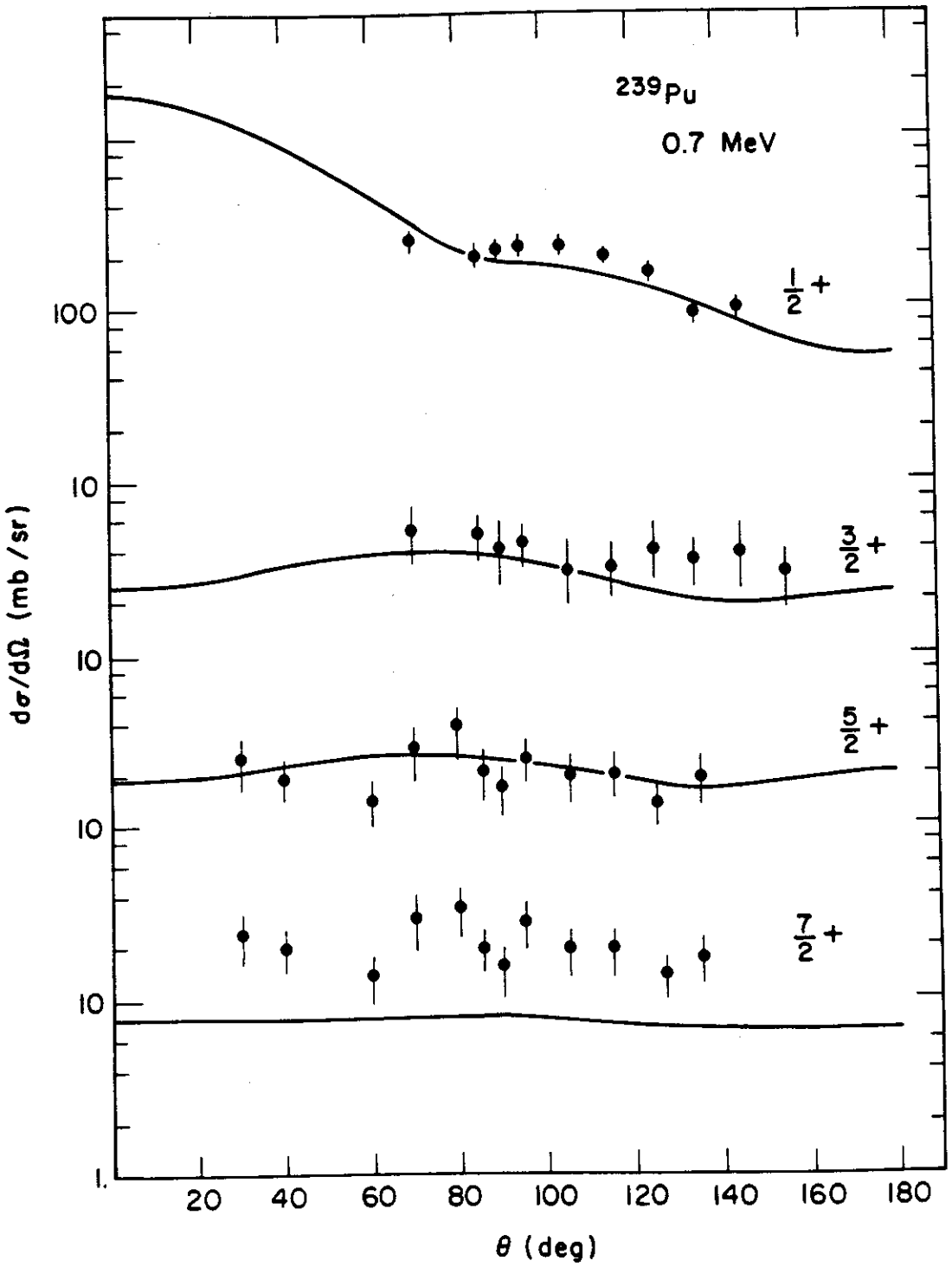


Fig. 2.

Calculated angular distributions compared with recent measurements (Ref. 4) of elastic and inelastic scattering on $^{239}Pu$ at a neutron energy of 0.7 MeV.

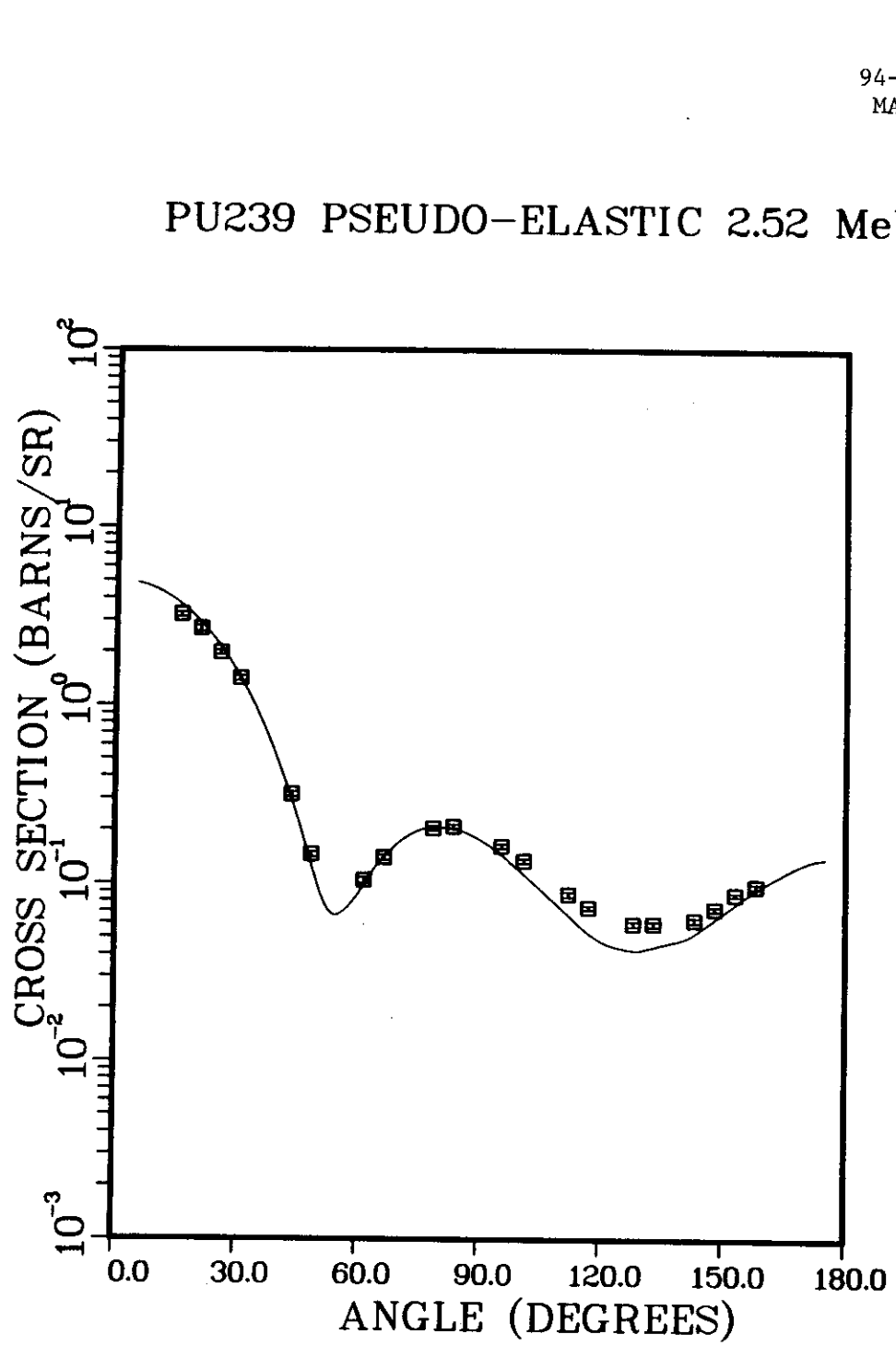


Fig. 3.

Calculations of cross sections for scattering reactions that excite $^{239}Pu$ states having energies ≦ 200 keV are compared with the data of Smith and Guenther (Ref. 15) for 2.5-MeV incident neutrons.

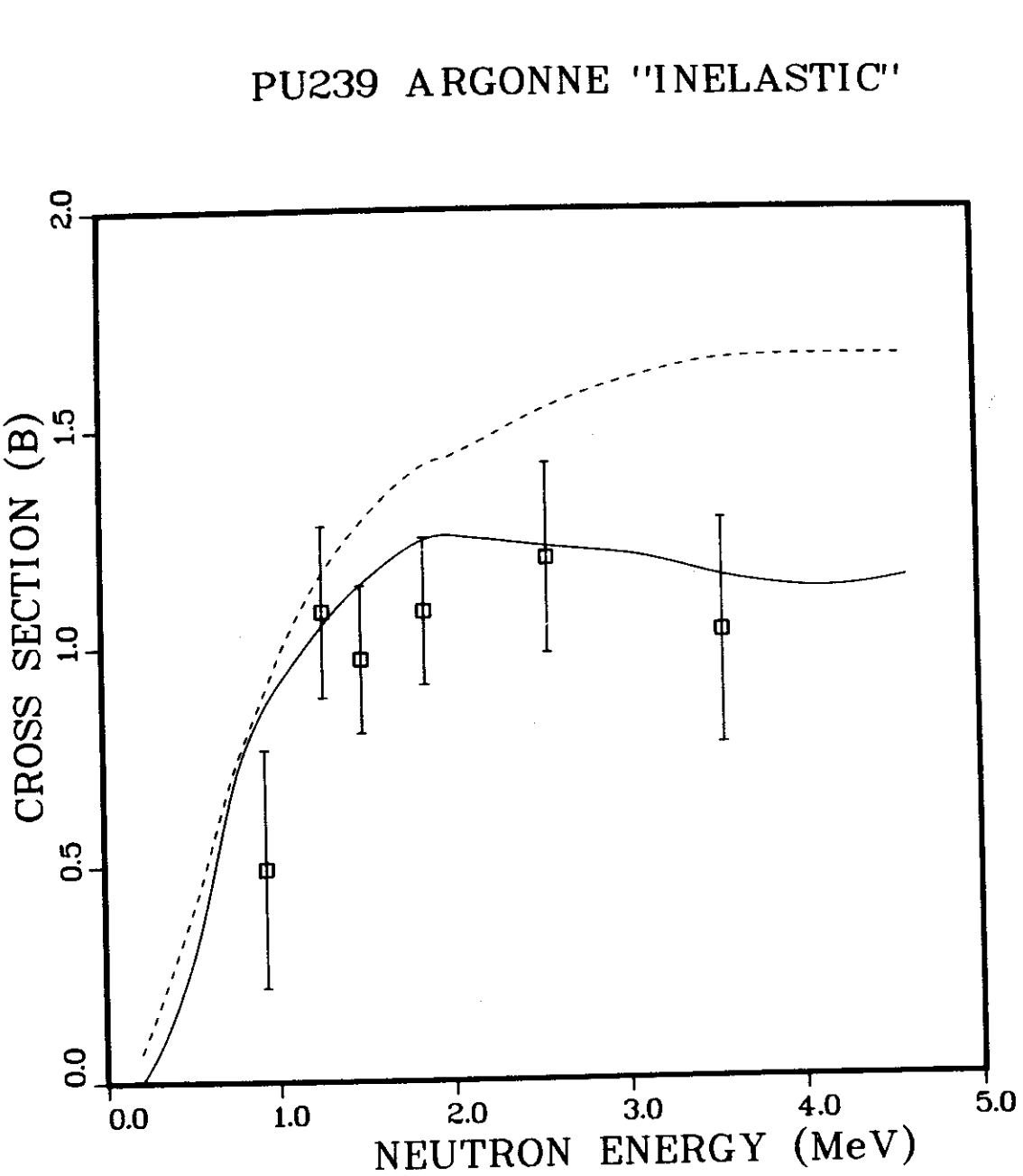


Fig. 4.

Comparison of calculated inelastic cross sections (solid curve) for production of $^{239}$Pu states above a given excitation energy (0.08 to 0.3 MeV) with cross sections inferred from measurements by Smith and Guenther (Ref. 15). The dashed curve is ENDF/B-V.

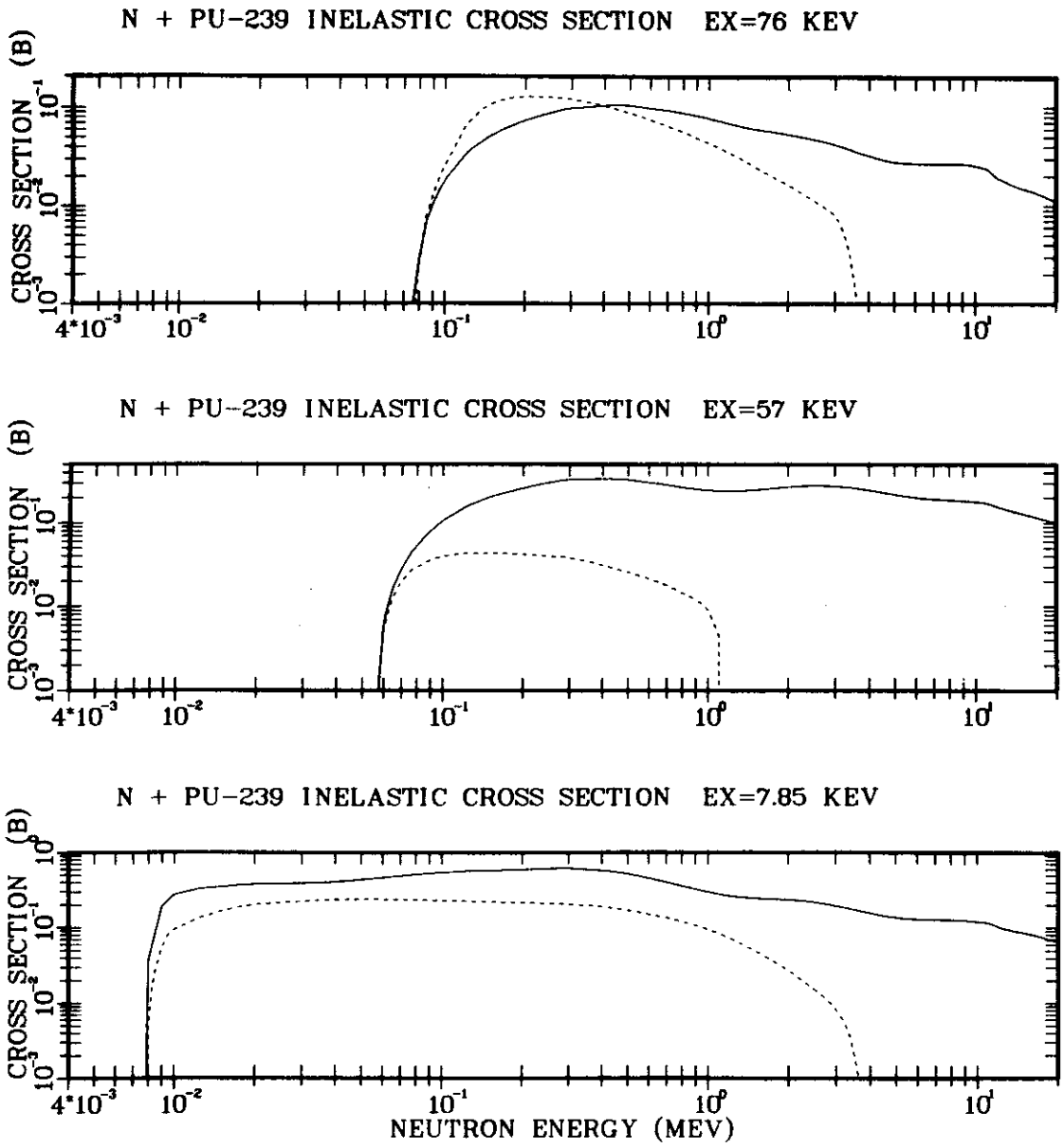


Fig. 5.

Evaluated (n,n') excitation cross sections for the first, second, and third excited states of $^{239}Pu$. The curves are defined in the caption of Fig. 1.

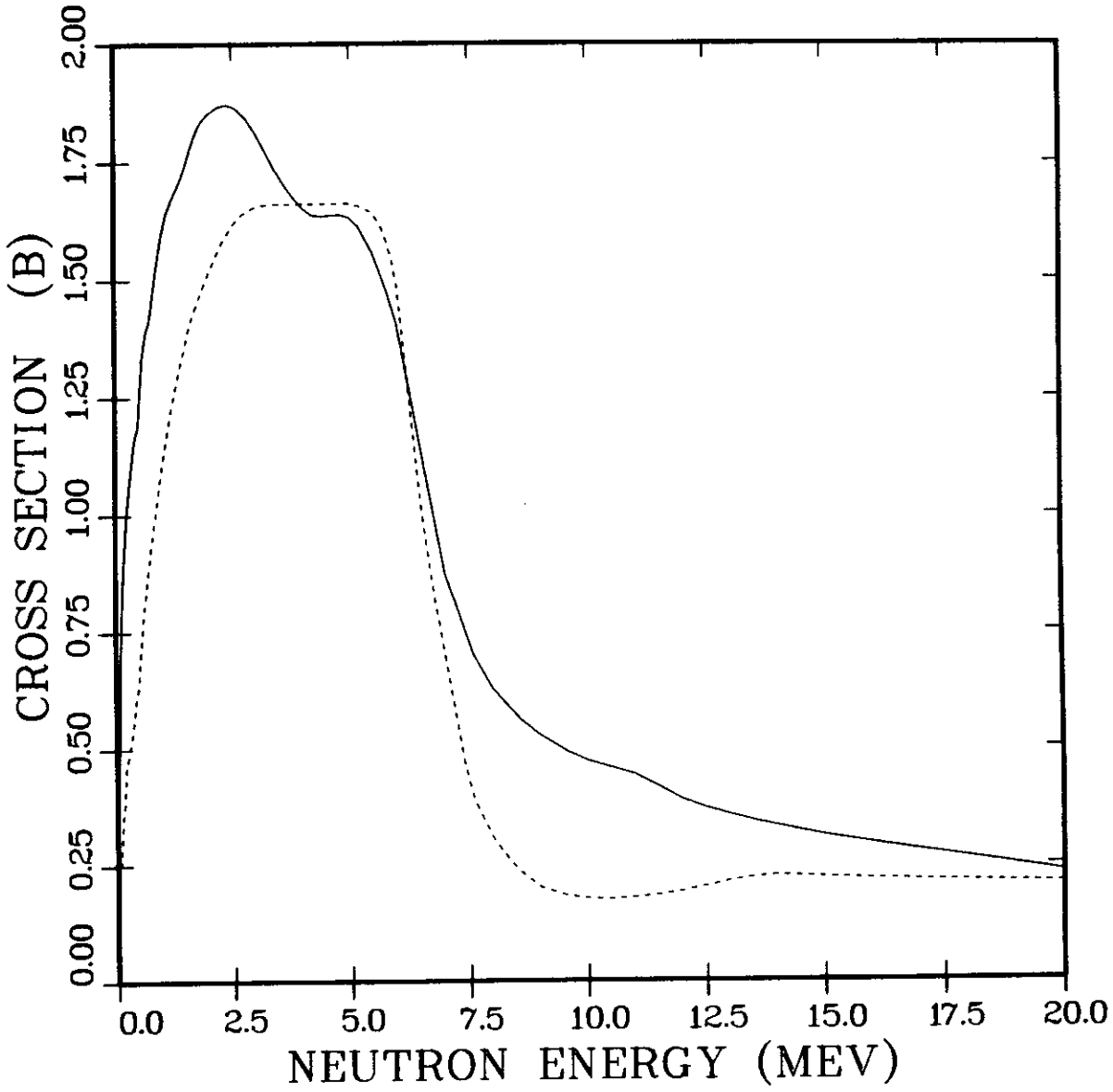


Fig. 6.

Total inelastic neutron cross section for $^{239}$Pu from threshold to 20 MeV. The solid curve is the present revision, and the dashed curve is ENDF/B-V.

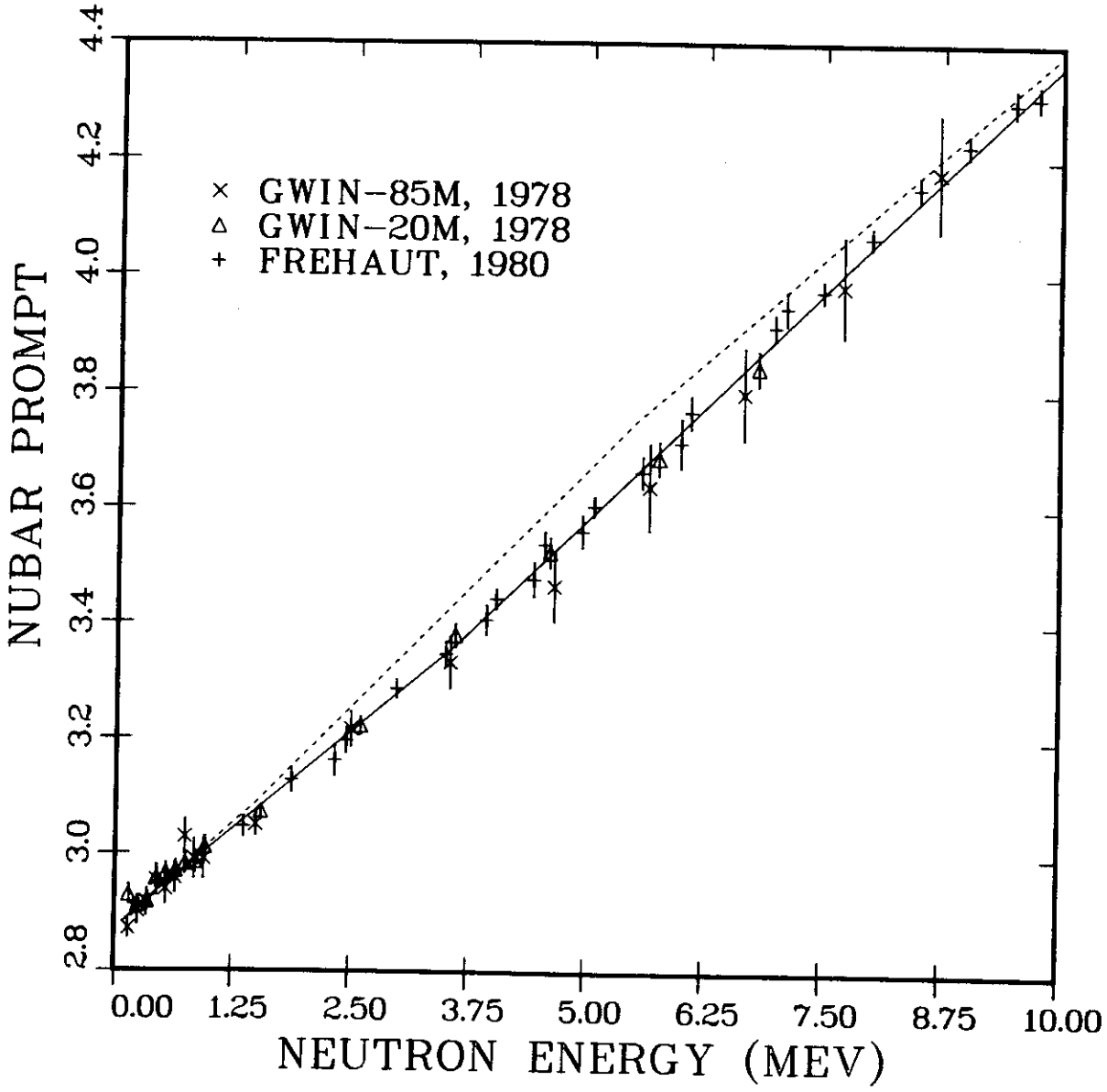


Fig. 7.

Evaluated prompt fission multiplicity $\bar{\nu}_p(E_n)$ between $E_n$ = 0.1 and 10 MeV compared with the experimental data of Gwin et al. (Ref. 20) and Frehaut et al. (Ref. 19). The curves are defined in the caption to Fig. 6.

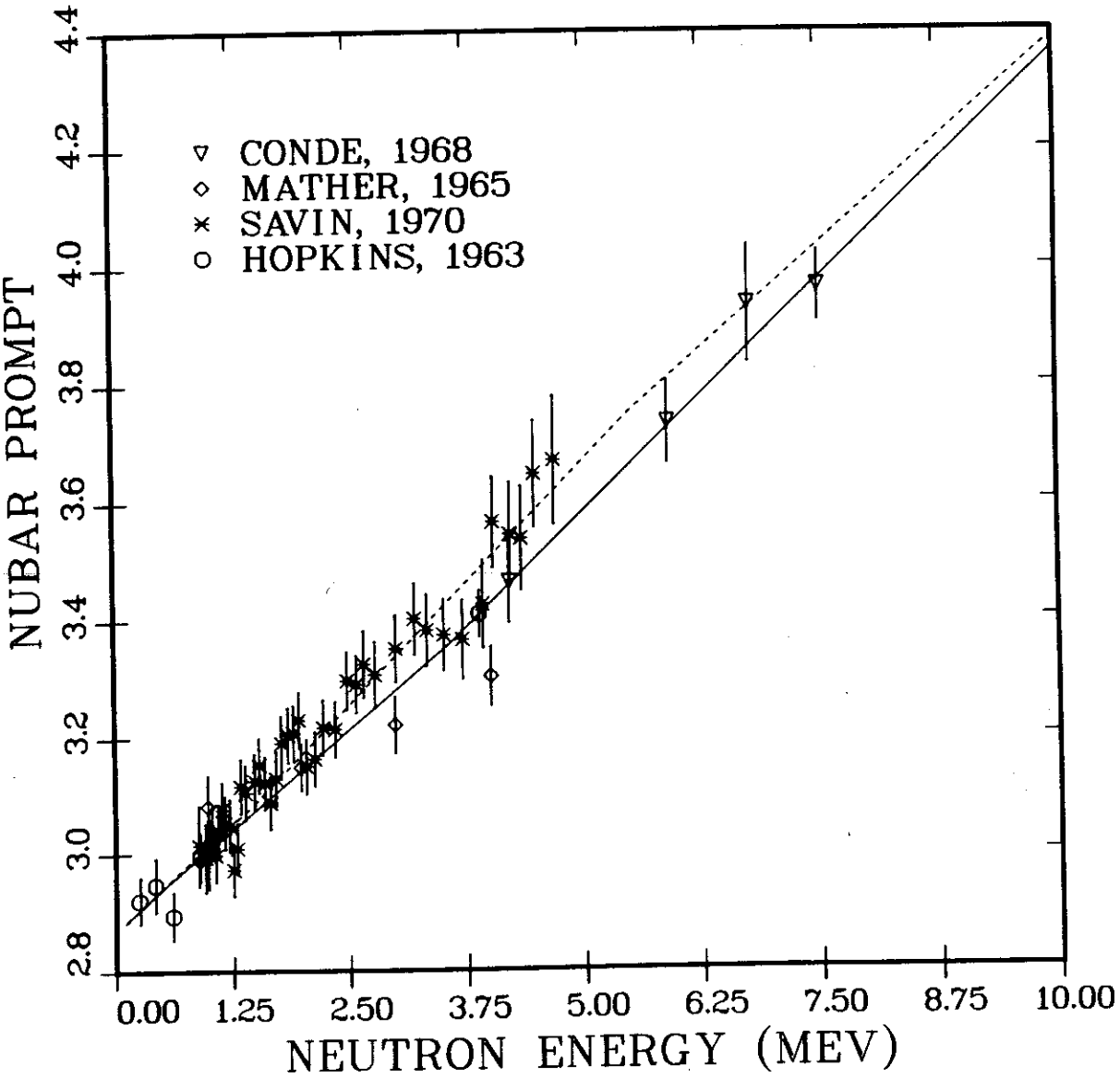


Fig. 8.

Evaluated prompt fission multiplicity $\bar{\nu}_p(E_n)$ between $E_n$ = 0.1 and 10 MeV compared with the experimental data of Condé et al. (Ref. 24), Mather et al. (Ref. 23), Savin et al. (Ref. 21), and Hopkins and Diven (Ref. 22). The curves are defined in the caption to Fig. 6.

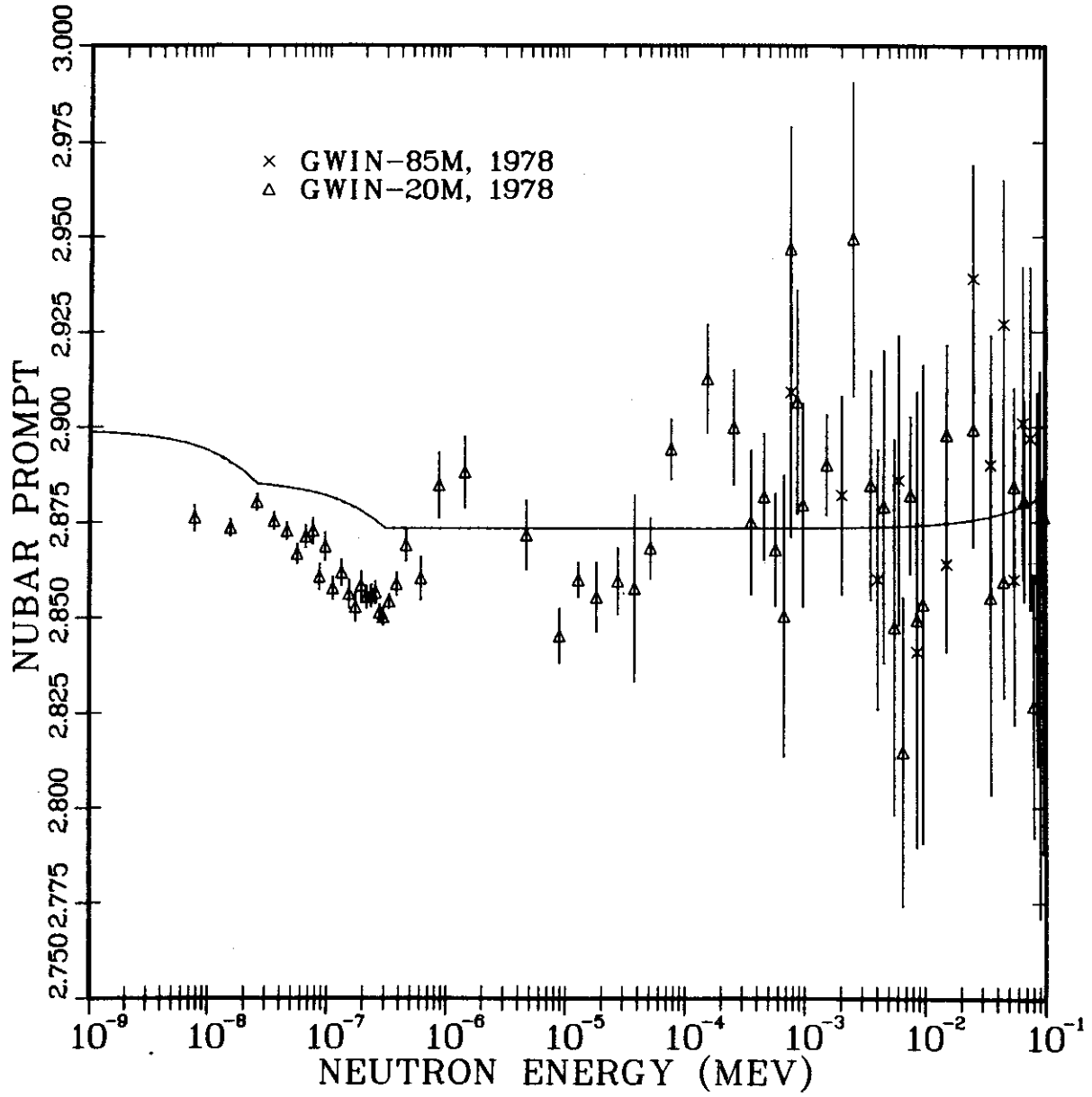


Fig. 9.

Evaluated and experimental (Ref. 20) $\bar{\nu}_p(E_n)$ for $E_n$ = 0.001 eV to 100 keV. The solid curve represents both ENDF/B-V and the present revision.

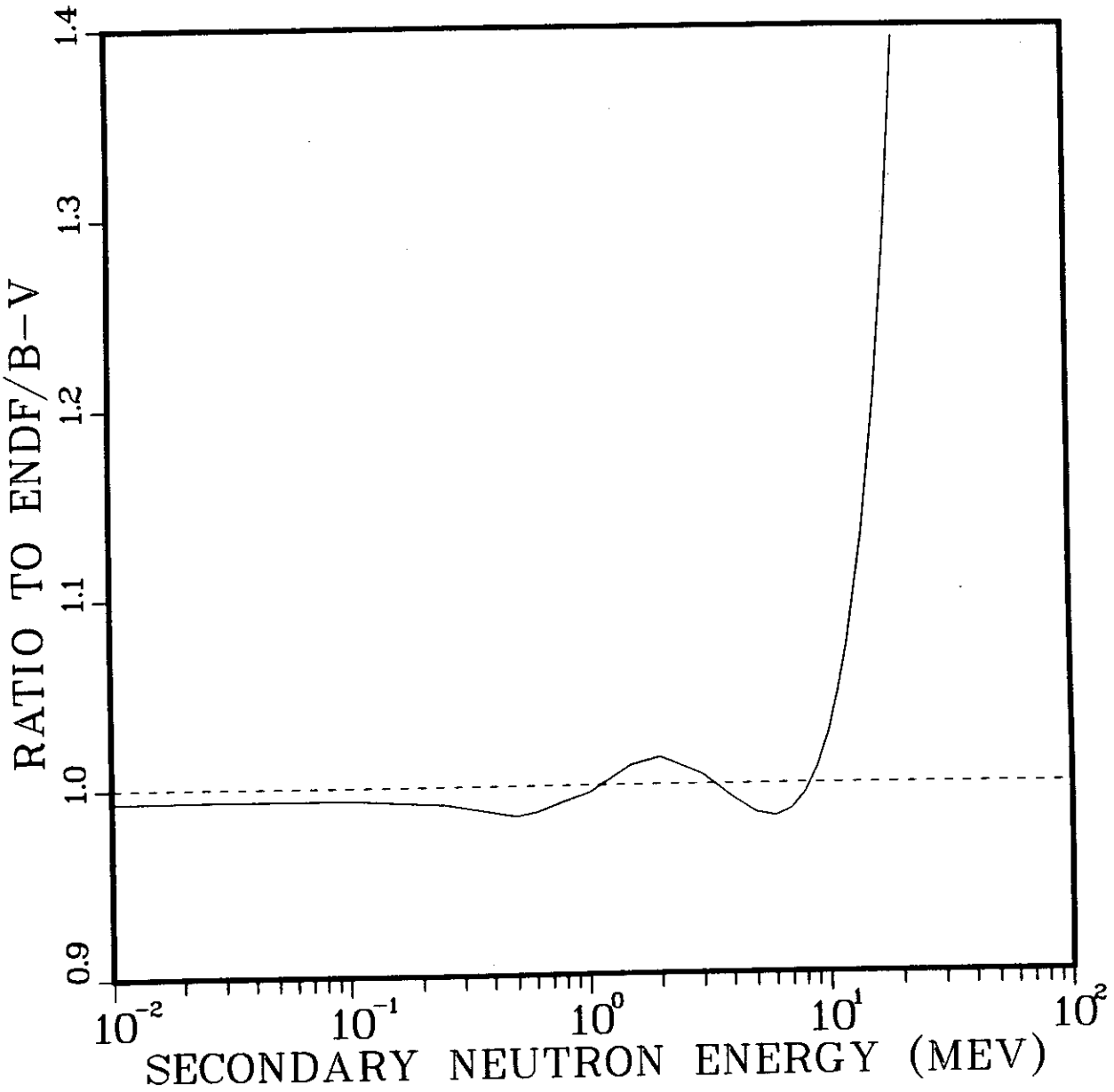


Fig. 10.

Ratio of the revised fission neutron spectrum to ENDF/B-V for thermal incident neutrons.

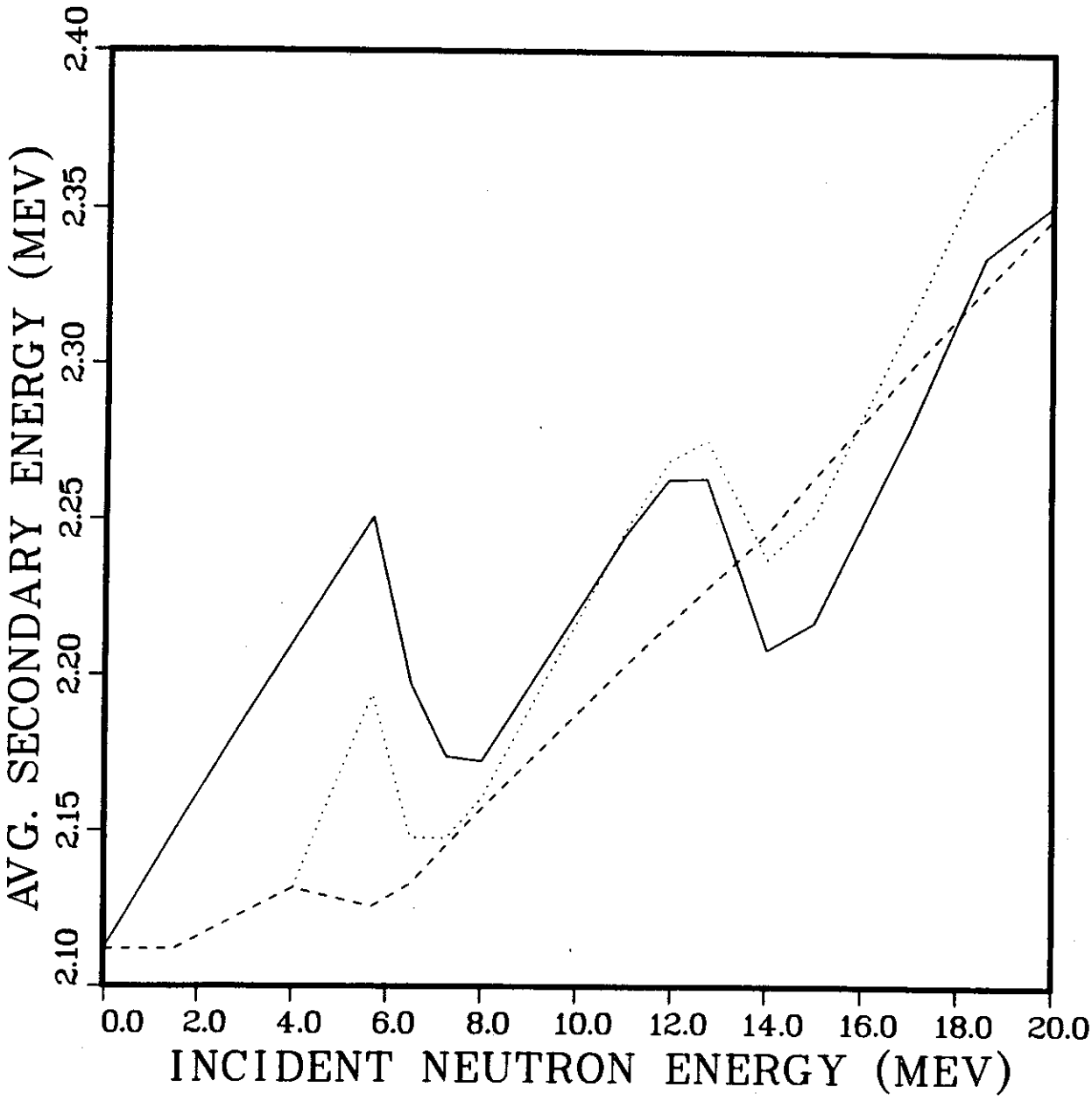


Fig. 11.

Evaluated average secondary neutron energies from fission for incident neutron energies between 0 and 20 MeV. The solid and dashed curves represent average neutron energies from all fission reactions calculated from the present revision and from ENDF/B-V, respectively. The dotted curve is the average fission neutron energy from ENDF/B-V obtained by summing the first-, second-, and third-chance fission contributions. See text for an explanation of the structure.

# REVISION 2 OF ENDF/B-V AMERICIUM

by

F. M. Mann
Hanford Engineering Development Laboratory
Richland, Washington 99352

The major change in Revision 2 is the normalization of the smooth $(n,\gamma)$ reaction to experimental data. In ENDF/B-V, the evaluation was calculated using Hauser-Feshbach calculations with $(\Gamma/D)$ based on systematics. The Revision 2 evaluation has the calculation ($E_n$>10 KeV) renormalized to the data of K. Wisshak and F. Kappeler (Proc. Nucl. Data for Science and Technology, Antwerp, Belgium, 1982). The elastic cross section was adjusted to take the difference.

## III CORRECTIONS AND MINOR REVISIONS

## Corrections and Minor Modifications

Tritium (MAT 1169)

File 8. Radioactive Decay and Fission Product Yield Data.

MT=457. Radioactive Decay Data. ENDF/B-V.0 section updated. Q(Beta) from Wapstra and Bos, AT. Data and Nuc. Data Tables 19, 177 (77) and $\beta^-$ from M. J. Martin, Nuclear Decay Properties for Selected Radionuclides, ORNL-5114, (76).

Sodium-23 (MAT 1311)

File 13. Photon Production Cross Section.

MT=3. Nonelastic Cross Section. Correction in the interpolation scheme; record 3594, field 1, replaced integer 1 with integer 2, i.e. replaced histogram with linear-linear interpolation.

File 15. Continuous Photon Energy Spectrum.

MT=3. Nonelastic Cross Section. Correction in the interpolation scheme; record 3612, field 1, replaced integer 1 with integer 2 (see File 13 above).

Chromium-Nat (MAT 1324)

File 12. Photon Production Multiplicities and Transition Probability Arrays.

MT=102. (n,$\gamma$). Replaced the $\gamma$ spectrum.

File 15. Continuous Photon Energy Spectrum.

MT=102. (n,$\gamma$). Replaced the spectrum at 200 keV.

Tantalum-181 (MAT 1285)

File 4. Angular Distributions of Secondary Neutrons.

MT=2. (n,n). Replaced portions of the 14 MeV angular distribution (records 951-958 and 970-976).

Tantalum-182 (MAT 1127)

File 8. Radioactive Decay and Fission Product Yield Data.

MT=457. Radioactive Decay Data. ENDF/B-V.0 updated to ENDF/B-V.2 with the addition of MT=457, evaluated by Reich, INEL, April 1978, $\beta^-$ from P. C. ENSDF Decay Data File, W. B. Eubank, ORNL, NDP, 10/78.

Lead-Nat (MAT 1382)

File 3. Neutron Cross Sections.

MT=1. Total Cross Section. Replaced records 474 and 508 (minor correction to cross section values at 2.98 MeV and 14.18 MeV).

MT=2. (n,n). Replaced records 724-727; corrections to the elastic cross sections from 14-20 MeV.

File 12. Photon Production Multiplicities and Transition Probability Arrays.

MT=102. (n,$\gamma$). Corrected interpolation scheme, records 3304, 3305, i.e. replaced linear-linear with histogram for the last 2 values.

File 33. Covariances of Neutron Cross Sections.

MT=2. (n,n). Added covariance subsection for E=1-730 keV.

## IV MODIFICATIONS OF FISSION ENERGY RELEASE

# FISSION ENERGY RELEASE FOR 16 FISSIONING NUCLIDES*

R. Sher
Stanford University
Stanford, California 94305

Tables I and II are corrected sets of data that originally appeared as an EPRI report in March 1981 (ref. 1). The corrections in Table I consist of the inclusion of the delayed neutron energy (END) in the total energy release (QG) and accounting for the covariance terms in computing the errors in the LSQ values of QG and EP. This reduces these errors considerably and makes them comparable to the uncertainties in QG's obtained by mass difference. The LSQ values of QG and EP can therefore be adopted as the recommended values and are the ones used in ENDF/B-V. For each of the "primary" isotopes (Th-232, U-233, U-235, U-238, Pu-239 and Pu-241), there now exists a consistent set of recommended values.

Two major corrections have been applied to the "non-primary" isotopes in Tables I and II. In the original Tables (ref. 1) the values of EP should have had EINC subtracted from them. This has now been done. In addition, in order to force the sum of the component energies to equal QG, the values of EPG have been changed. There is no good basis for determining EGP; the original value (ref. 1) was simply the measurements on other isotopes and had been used for want of anything better.

*The above text was condensed and edited by B. A. Magurno. The material was extracted from ref. (2, 3).

For the "non-fissile" isotopes, Table II, the fission energy release components were corrected to zero incident neutron energy according to the prescription of W. H. Walker (communication to CSEWG, November 1979).

The prescription is as follows:

$$E_i(0) = E_i(EINC) + \delta E_i$$

where $E_i$ is any of the energy release components, $E_i(0)$ is the value at EINC=0, and $E_i(EINC)$ is the value at an incident energy EINC. It should be recognized that the values at EINC=0 are strictly fictitious and represent an artifice by which it is possible to recover the values at any EINC.

The $\delta E_i$'s are given by the following:

$\delta QG = EINC - (1.057\ EINC - 8.07(\nu(EINC) - \nu(0)))$

$= - 0.057\ EINC + 8.07(\nu(EINC) - \nu(0))$.

$\delta EB = 0.075\ EINC$.

$\delta EGD = 0.075\ EINC$.

$\delta ENU = 0.100\ EINC$.

$\delta EFR = 0$.

$\delta ENP = -(1.307\ EINC - 8.07(\nu(0))$.

$\delta EGP = 0$ (but see remark below).*

$\nu(EINC) - \nu(0)$ was estimated for each isotope, based on the linear fits of Manero and Konshin (Atomic Energy review, 10, No. 4, p. 637 (1972)). For those isotopes not evaluated by Manero and Konshin, $\nu(EINC) - \nu(0)$ was taken to be 0.15 EINC.

*For the non-primary isotopes, the values of EGP were slightly adjusted where necessary, to account for round off errors in the sums, i.e. they were changed to force ED+EP+END to equal QG.

The error limits were not changed, so that if one starts with the values at EINC=0 and computes the values at the actual EINC, one will obtain the correct errors on those results.

Finally, the values of END for Am-241, Am-243 and Cm-244 have been added to the table.

## REFERENCES

1. R. Sher, EPRI NP-1771, Electric Power Research Institute, Palo Alto (March 1981).

2. R. Sher, EPRI NP-1771 (Revision), Electric Power Research Institute, Palo Alto (January 1983).

3. R. Sher, Fission Energy Release: Correction to Zero Incident Neutron Energy, Private Communication to B. A. Magurno (February 1983).

Table I

Energy Release Parameters for the Fissile Isotopes

| | U-233 | U-235 | Pu-238 | Pu-239 | Pu-241 | Am-241 | Cm-244 |
|---|---|---|---|---|---|---|---|
| QG | 197.97±0.21 | 202.49±0.13 | 204.66±0.24 | 207.06±0.21 | 210.84±0.25 | 209.51±0.24 | 211.52±0.87 |
| ED | 17.10±0.21 | 21.60±0.17 | 18.01±1.50 | 17.62±0.21 | 21.84±0.30 | 18.68±1.50 | 21.03±1.50 |
| EP | 180.84±0.22 | 180.88±0.18 | 186.65±2.30 | 189.44±0.22 | 188.99±0.33 | 190.83±2.30 | 190.49±2.30 |
| EB | 5.16±0.06 | 6.50±0.05 | 5.42±0.50 | 5.31±0.06 | 6.58±0.09 | 5.62±0.50 | 6.33±0.50 |
| EGD | 5.01±0.06 | 6.33±0.05 | 5.31±0.75 | 5.17±0.06 | 6.40±0.09 | 5.51±0.75 | 6.20±0.75 |
| ENU | 6.93±0.09 | 8.75±0.07 | 7.28±1.10 | 7.14±0.09 | 8.85±0.12 | 7.54±1.10 | 8.50±1.10 |
| EFR | 168.22±0.50 | 169.12±0.49 | 173.60±2.00 | 175.78±0.10 | 175.36±0.68 | 176.40±2.00 | 178.50±2.00 |
| EGP | 7.72±0.52 | 6.97±0.50 | 7.13±1.00 | 7.76±0.22 | 7.64±0.69 | 7.90±1.00 | 4.37±1.00 |
| ENP | 4.90±0.10 | 4.79±0.07 | 5.92±0.34 | 5.90±0.10 | 5.99±0.13 | 6.53±0.36 | 7.62±0.58 |
| EINC | (thermal) | (thermal) | (thermal) | (thermal) | (thermal) | (thermal) | (thermal) |
| END | 0.031±15% | 0.0074±15% | 0.002±20% | 0.0028±15% | 0.005±20% | 0.002±20% | 0.002±20% |

Table II

Energy Release Parameters for the Non-Fissile (Threshold) Isotopes*

| | Th-232 | Pa-233 | U-234 | U-236 | U-238 | Np-237 | Pu-240 | Pu-242 | Am-243 |
|---|---|---|---|---|---|---|---|---|---|
| EINC | 3.35±0.10 | 2.50±0.30 | 2.36±0.10 | 2.82±0.10 | 3.10±0.10 | 2.37±0.10 | 2.39±0.10 | 2.32±0.10 | 2.50±0.50 |
| $\nu$(EINC)-$\nu$(0) | 0.51 | 0.38 | 0.32 | 0.37 | 0.47 | 0.36 | 0.35 | 0.35 | 0.38 |
| $\delta$QG | 3.90 | 2.88 | 2.44 | 2.82 | 3.58 | 2.73 | 2.69 | 2.68 | 2.88 |
| $\delta$EB | 0.25 | 0.19 | 0.18 | 0.21 | 0.23 | 0.18 | 0.18 | 0.17 | 0.19 |
| $\delta$EGD | 0.25 | 0.19 | 0.18 | 0.21 | 0.23 | 0.18 | 0.18 | 0.17 | 0.19 |
| $\delta$ENU | 0.34 | 0.25 | 0.24 | 0.28 | 0.31 | 0.24 | 0.24 | 0.23 | 0.25 |
| $\delta$ENP | -0.29 | -0.24 | -0.51 | -0.71 | -0.30 | -0.23 | -0.29 | -0.22 | -0.24 |
| QG(0) | 199.74±0.28 | 199.50±0.66 | 200.22±0.65 | 204.64±0.12 | 209.45±0.30 | 204.97±0.80 | 208.35±0.23 | 212.15±0.82 | 212.68±0.88 |
| ED(0) | 27.81±0.31 | 23.92±1.50 | 20.76±1.50 | 25.13±1.50 | 28.12±1.50 | 21.29±1.50 | 21.99±1.50 | 26.16±1.50 | 22.43±1.50 |
| EP(0) | 171.91±0.31 | 175.57±2.30 | 179.45±2.30 | 179.50±2.30 | 181.31±2.30 | 183.67±2.30 | 186.36±2.30 | 185.98±2.30 | 190.25±2.30 |
| EB(0) | 8.38±0.10 | 7.20±0.50 | 6.25±0.50 | 7.56±0.50 | 8.48±0.08 | 6.41±0.50 | 6.62±0.50 | 7.87±0.50 | 6.75±0.50 |
| EGD(0) | 8.16±0.10 | 7.06±0.75 | 6.13±0.75 | 7.42±0.75 | 8.25±0.07 | 6.28±0.75 | 6.49±0.75 | 7.72±0.75 | 6.62±0.75 |
| ENU(0) | 11.27±0.13 | 9.66±1.10 | 8.38±1.10 | 10.15±1.10 | 11.39±0.10 | 8.60±1.10 | 8.88±1.10 | 10.57±1.10 | 9.06±1.10 |
| EFR(0) | 160.39±0.92 | 163.50±2.00 | 167.10±2.00 | 167.50±2.00 | 169.57±0.49 | 170.60±2.00 | 173.70±2.00 | 174.00±2.00 | 176.30±2.00 |
| EGP(0) | 7.11±0.90 | 7.03±1.00 | 7.50±1.00 | 7.30±1.00 | 6.53±0.53 | 7.13±1.00 | 6.18±1.00 | 5.22±1.00 | 6.42±1.00 |
| ENP(0) | 4.41±0.12 | 5.04±0.40 | 4.85±0.43 | 4.70±0.29 | 5.21±0.10 | 5.94±0.48 | 6.48±0.36 | 6.76±0.54 | 7.53±0.59 |
| END | 0.022±20% | 0.01±25% | 0.005±20% | 0.01±20% | 0.018±15% | 0.005±25% | 0.004±20% | 0.01±20% | 0.004±20% |

*The error values included here are those calculated for the EINC values listed above and not for EINC=0.

## V MODIFICATIONS OF THE COVARIANCE FILES

## Modification of the Covariance File

The modifications to the Covariance File were done in two parts. The first part (below) consisted of minor corrections done at the NNDC. The second part by L. W. Weston follows as a separate report.

File 33 Covariances of Neutron Cross Sections

Nitrogen-14 (MAT 1275)

MT=102. Changed covariance value at 20 MeV to 0.0 (record 6022).

Carbon-Natural (MAT 1306)

MT=4. Corrected AWRI (record 2482).

MT=91. Changed lower limit of the energy range from 7.887 MeV to 8.296 MeV (record 2594).

MT=103. Changed covariance value at 20 MeV to 0.0 (record 2612).

MT=104. Changed covariance value at 20 MeV to 0.0 (record 2617).

Fluorine-19 (MAT 1309)

MT=51. Extended the file from 15 to 20 MeV (record 4704).

MT=52. Added covariance values between 4.5 keV and 1.1 MeV (after record 4709). Extended the file from 15-20 MeV (record 4711).

Silicon-Natural (MAT 1314)

MT=2. Replaced section.

MT=3. Replaced section.

MT=4. Replaced section.

Chromium-Natural (MAT 1324)

MT=4. Corrected mispunched exponent (record 12865).

MT=58. Corrected mispunched exponent (record 13041).

# COVARIANCE FILE CHANGES

by

L. W. Weston
Oak Ridge National Laboratory

These changes were brought about when Chuck Weisbin's group (ORNL) found that the uncertainties for broad group averages for the fuel isotopes did not yield reasonable results in some cases. Changes were carried out which were agreed upon with the evaluators. In going through the files in detail, other problems were found such that in some cases the changes are more extensive than originally intended.

Tables 1 and 2 give the original 5 group averages of ENDF/B-V and the values for Revision 2. The attached plots show the standard deviations and the correlation matrix derived with 52 group averages. Since these group averages do not necessarily correspond to the group structure in the evaluated File 33, there are some anomalies introduced, however, these should be obvious to the viewer. The blocked structure of the correlation matrix is brought about by the fact that certain types of measurements tend to cover essentially fixed neutron energy ranges so that the data in these neutron energy ranges are highly correlated.

## U-235 FISSION AND CAPTURE

The uncertainties in the fission and capture cross sections of U-235 were not changed but are listed in Table 2 for comparison purposes.

The only change in File 33 for U-235 was the addition of the fact that the Pu-240 and Pu-241 fission cross sections above 200 keV were evaluated as ratio measurements with U-235 as the standard.

## U-238 CAPTURE

The uncertainty in the U-238 capture cross sections in the neutron energy range from 4 keV to 20 MeV was found to be lower than the evaluator intended when large group averages were taken. The problem was that there were no long range correlations included in the file. This situation was modified by adding long range correlations in a manner to reproduce the long range uncertainties desired by the evaluator (W. P. Poenitz) and to retain the structure previously indicated in the files.

In the resonance region, 1 eV to 4 keV, uncertainties were derived from the uncertainties in the resonance parameters. This was done to give an indication of the values of these uncertainties for the infinitely dilute case. These results were derived by B. L. Broadhead (ORNL) and are preliminary. For Revision 2 these results were placed in File 1 for those who may be interested. The available processing codes will not handle uncertainties in resonance parameters at the present time, however, this would be necessary to derive highly self-shielded group cross sections for U-238. Below 1 eV the uncertainties in File 33 were unchanged.

U-238 FISSION

In the process of studying File 33 for U-238 it was noticed that the uncertainties for the fission cross section had no long range component. The effect of this would be that if large group cross sections are calculated the uncertainties would be unreasonably small. Because of this deficiency, a fully correlated uncertainty of 1.5% from 1 eV to 20 MeV was added to the file. This will solve the problem with large group averages and will make the uncertainties on the U-238 fission cross section more reasonable in relation to those for U-235 fission.

Pu-239 FISSION

The range of a 2% uncertainty from 0.2 to 15 MeV was changed to a range of from 1 eV to 15 MeV. This was based on a long range uncertainty brought about by normalization procedures. The uncertainty in the thermal region was increased from 0.3 to 1.5% at the suggestion of W. P. Poenitz because of the change in the evaluated Pu-239 half-life which affects the normalization of part of the data.

Pu-239 CAPTURE

In the original File 33 it was indicated that the capture cross section above 200 keV was based on ratio measurements to the fission cross section. The author did not think this was the case so this dependance was removed. The uncertainty in the 1 to 20 MeV range was essentially unchanged. The uncertainty in the 20 keV to 1 MeV range was reduced from about 20% to about 12%.

Below 200 keV the fact that the evaluation of the capture cross section was based on ratio measurements to the fission cross section was retained. The estimated uncertainties in the evaluation of the alpha measurements were reduced somewhat as can be seen in Table 2. The uncertainties below 1 eV were unchanged.

Pu-240 FISSION

There was no uncertainty file for this cross section in ENDF/B-V. Since there was to be a Revision for the uncertainties of the capture cross section, an uncertainty file for the fission cross section was added for Revision 2.

Pu-240 CAPTURE

The uncertainty file for Pu-240 capture was redone. The uncertainty file for ENDF/B-V was done by the author and was carried over from ENDF/B-IV which was a "quickie" effort to get something into the uncertainty files. The uncertainty file did not correspond to the ENDF/B-V evaluation. The proposed File 33 for Pu-240 capture is considered to be much more realistic.

From thermal through the resonance region, part of the uncertainty file for ENDF/B-V consisted of uncertainties in the resonance parameters and this feature is retained in Revision 2. Since the 1 eV resonance is normally highly self-shielded, this is the only way to properly handle this situation.

Pu-241 FISSION

The uncertainty file for Pu-241 fission in ENDF/B-V was redone except in the neutron energy range from 100 eV to 200 keV. The uncertainty file of ENDF/B-V was carried over from ENDF/B-IV, was done by the author, and did not correspond to the ENDF/B-V evaluation.

There were previously no uncertainties below 100 eV and these were added. Above 200 keV the evaluation was based on the ratio measurements to the fission cross section of U-235 and Revision 2 reflects this fact as well as containing more reasonable uncertainty estimates.

Pu-241 CAPTURE

The Pu-241 capture cross section uncertainty file was not part of the 5 group uncertainty study, however, it was reevaluated for this Revision. The status of this uncertainty file was essentially the same as for the Pu-241 fission cross section. Revision 2 is considered to be much more realistic than the previous uncertainty file in ENDF/B-V.

Table 1 - The Five Energy Group Structure.

| Group Number | Group Bounds | Weighting |
|---|---|---|
| 1 | 0.498 - 20 MeV | "Fission and FUSION"* |
| 2 | 24.8 keV - .498 MeV | 1/E |
| 3 | 1.23 keV - 24.8 keV | 1/E |
| 4 | 0.414 eV - 1.23 keV | 1/E |
| 5 | 0.00001 - .414 eV | Maxwellian |

*For further information see: C. R. Weisbin et al., "Vitamin-E: An ENDF/B-V Multigroup Cross Section Library for LMFBR Core and Shield, LWR Shield, Dosimetry and Fusion Blanket Technology," p. 14, ORNL-5505, ENDF-274 (1979).

Table 2
Standard Deviation (%)

| File | Group | ENDF/B-V | Revision 2 |
|---|---|---|---|
| U-235 Fission | 1 | 3.8 | same |
| | 2 | 2.4 | |
| | 3 | 5.0 | |
| | 4 | 2.0 | |
| | 5 | 0.3 | |
| U-235 Capture | 1 | 43.7 | same |
| | 2 | 9.8 | |
| | 3 | 7.5 | |
| | 4 | 2.9 | |
| | 5 | 0.9 | |
| U-238 Fission | 1 | 4.1 | 4.2 |
| | 2 | 18.8 | 18.9 |
| | 3 | 28.6 | 28.6 |
| | 4 | - | - |
| | 5 | 25.0 | 25.0 |
| U-238 Capture | 1 | 8.3 | 9.7 |
| | 2 | 1.4 | 4.7 |
| | 3 | 3.1 | 4.0 |
| | 4 | 5.0 | 3.4 |
| | 5 | 0.7 | same |
| Pu-239 Fission | 1 | 6.8 | 4.4 |
| | 2 | 3.6 | 4.1 |
| | 3 | 6.0 | 6.3 |
| | 4 | 1.6 | 3.4 |
| | 5 | 0.3 | 1.5 |
| Pu-239 Capture | 1 | 20.4 | 19.0 |
| | 2 | 20.4 | 12.8 |
| | 3 | 15.8 | 10.1 |
| | 4 | 4.7 | 7.1 |
| | 5 | 2.6 | 2.3 |
| Pu-240 Fission | 1 | - | 5.2 |
| | 2 | - | 12.6 |
| | 3 | - | 31.6 |
| | 4 | - | 23.3 |
| | 5 | - | 31.6 |
| Pu-240 Capture | 1 | 2.0 | 50.3 |
| | 2 | 26.1 | 11.5 |
| | 3 | 10.4 | 8.2 |
| | 4 | 4.6* | same |
| | 5 | 1.0* | same |
| Pu-241 Fission | 1 | 0.3 | 5.4 |
| | 2 | 2.9 | 2.8 |
| | 3 | 5.5 | 5.8 |
| | 4 | - | 4.6 |
| | 5 | - | 0.5 |
| Pu-241 Capture | 1 | | 50.2 |
| | 2 | | 11.8 |
| | 3 | | 10.0 |
| | 4 | | 8.3 |
| | 5 | | 4.5 |

*Corrected for mistake in ENDF/B-V evaluation

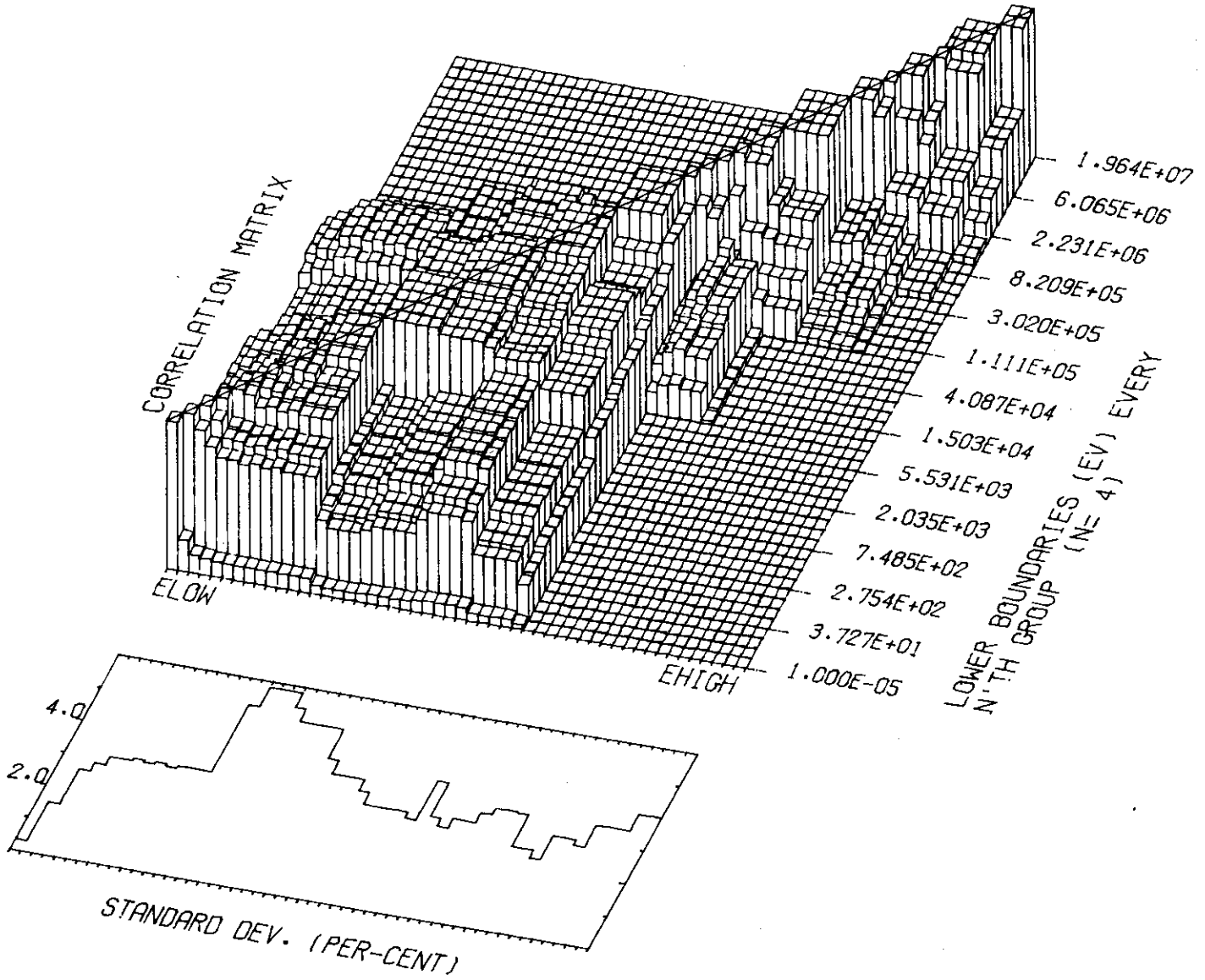


Fig. 1. U-235 FISSION CORRELATION MATRIX

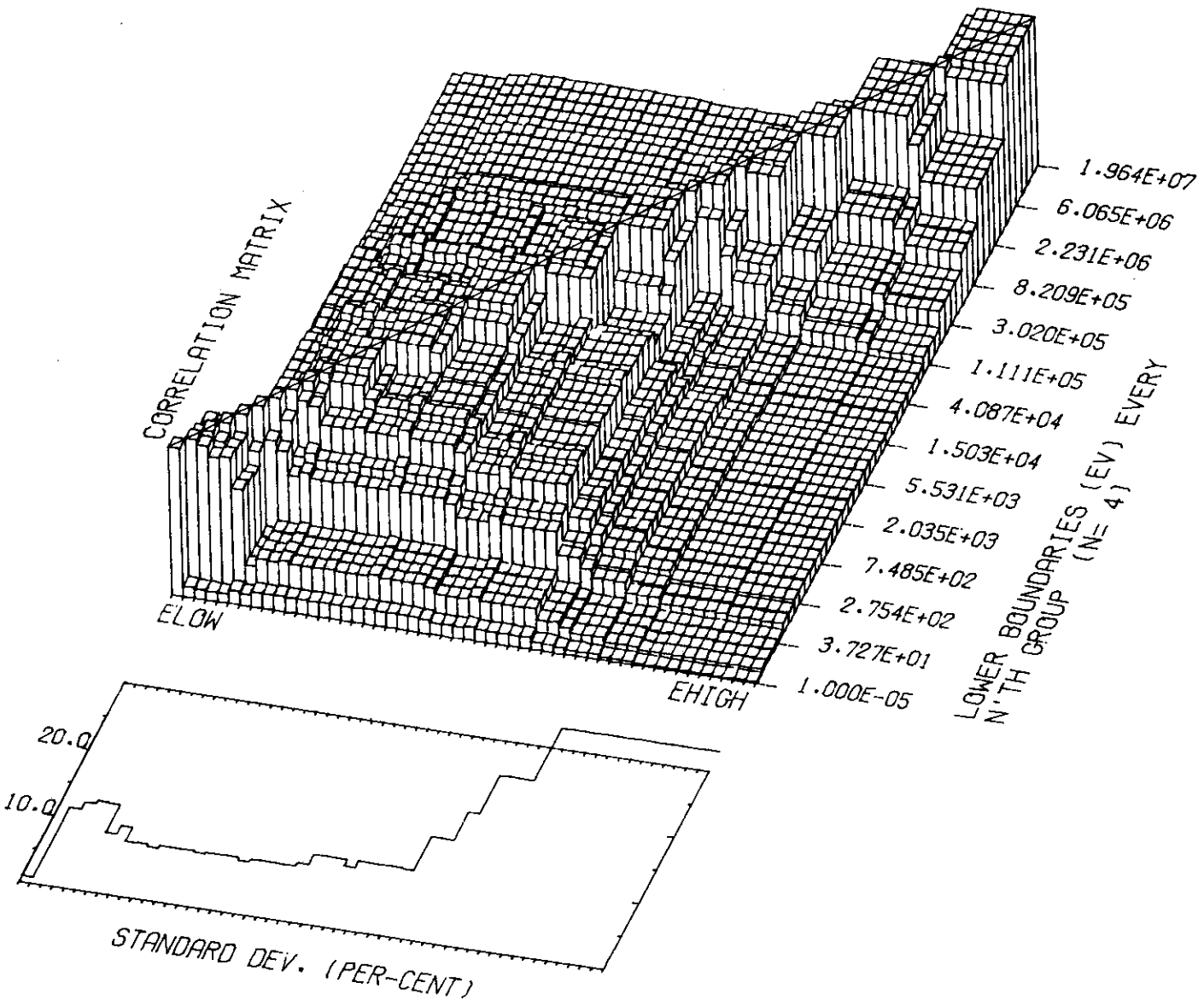


Fig. 2. U-235 CAPTURE CORRELATION MATRIX

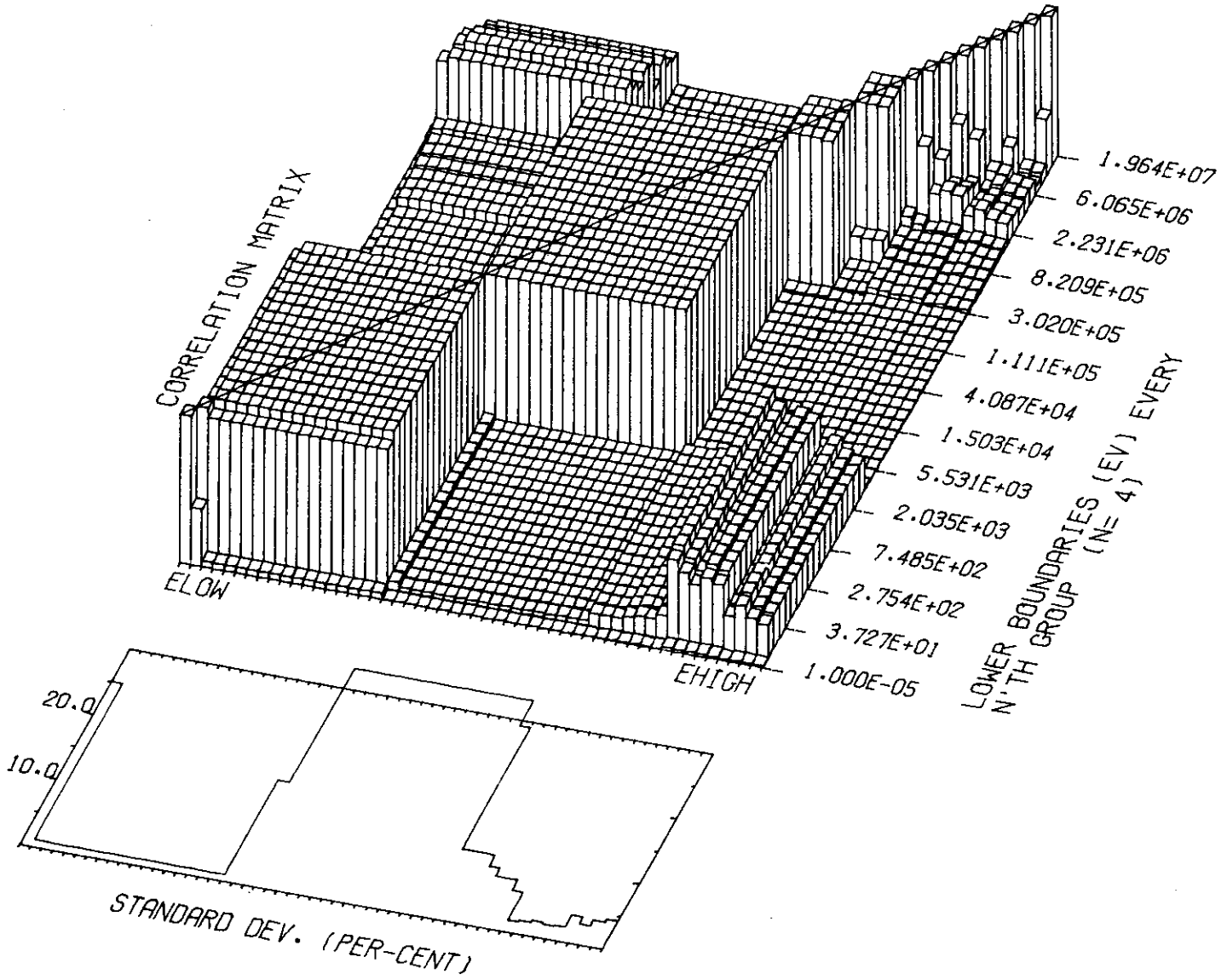


Fig. 3. U-238 FISSION CORRELATION MATRIX

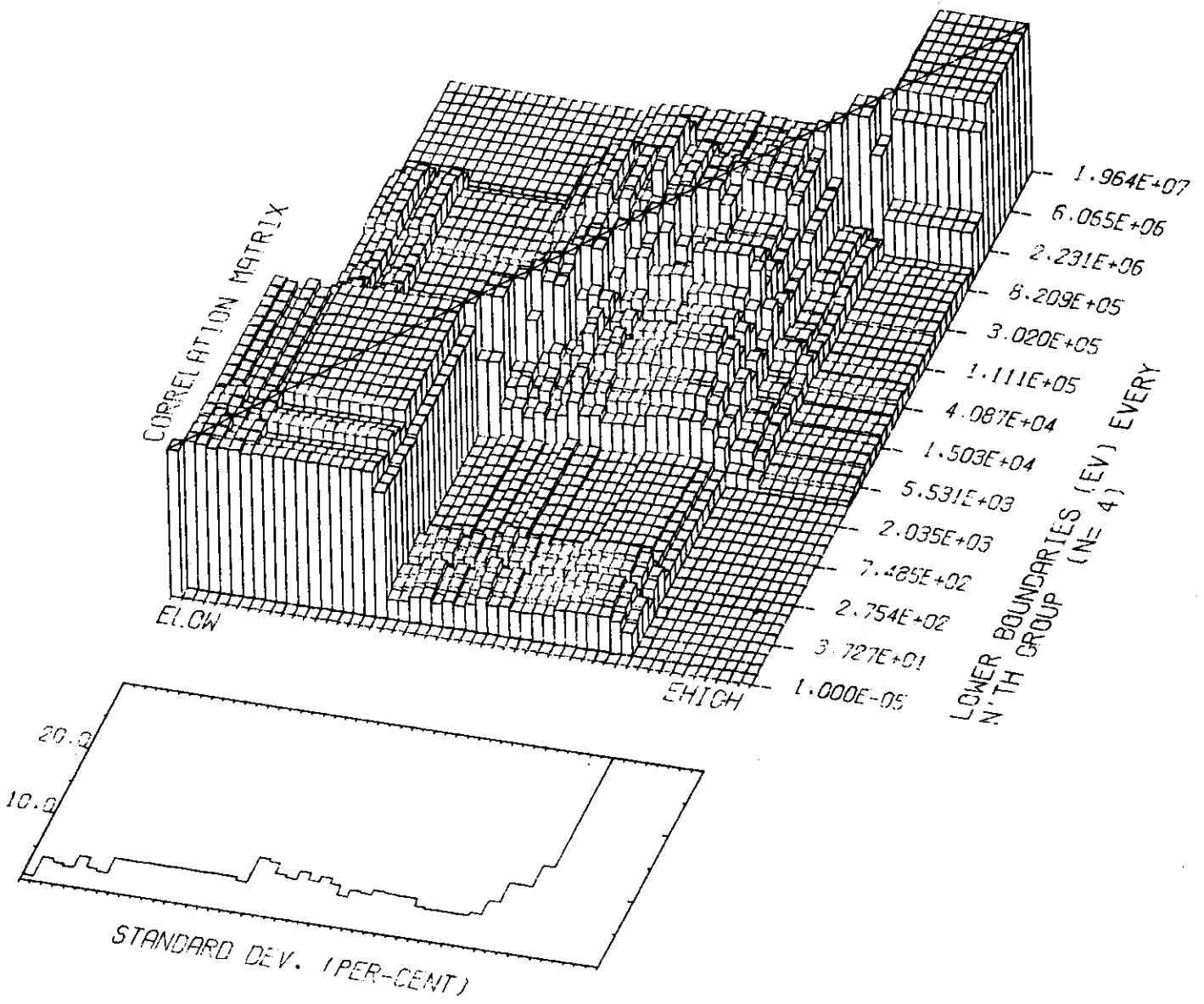


Fig. 4. U-238 CAPTURE CORRELATION MATRIX

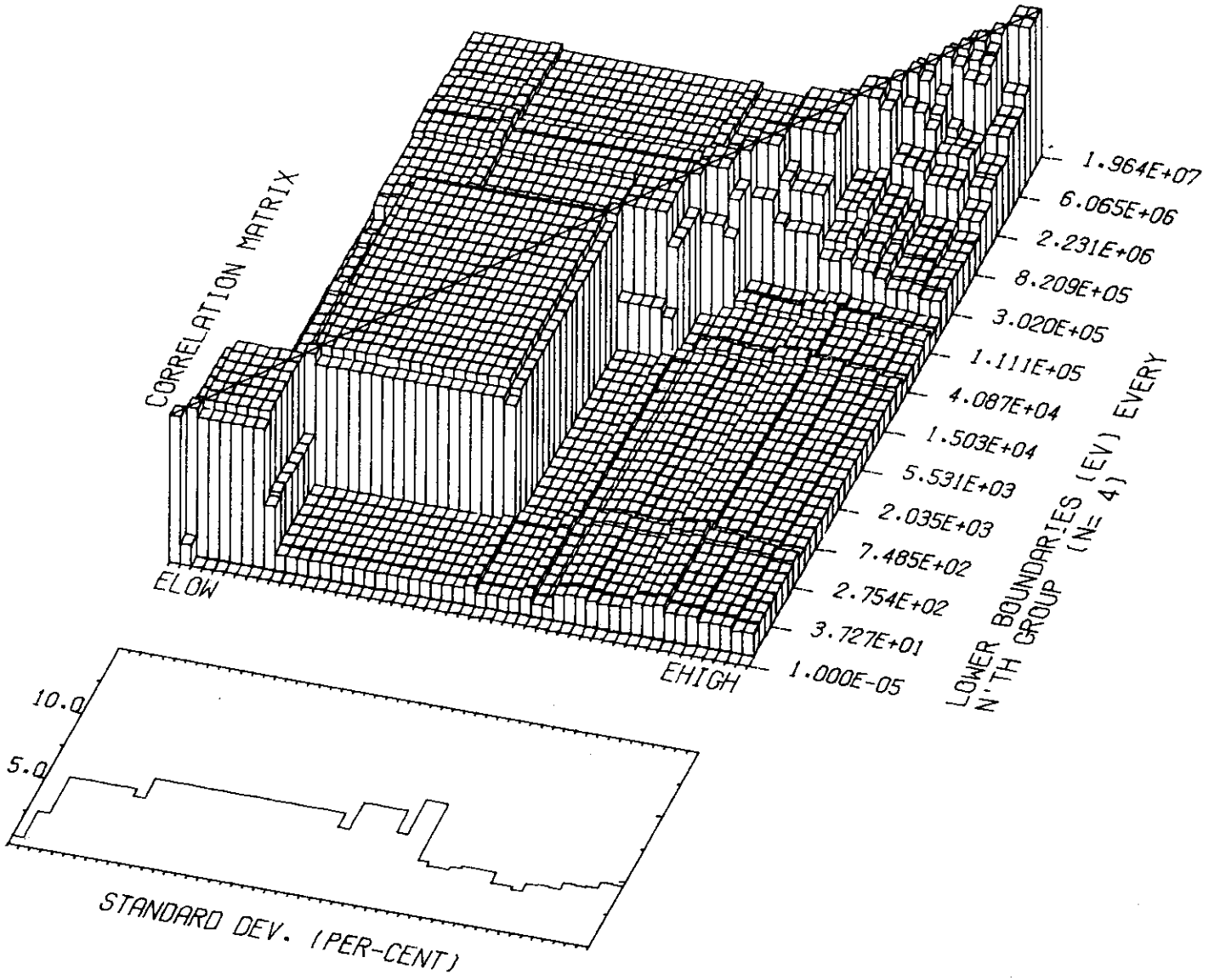


Fig. 5. PU-239 FISSION CORRELATION MATRIX

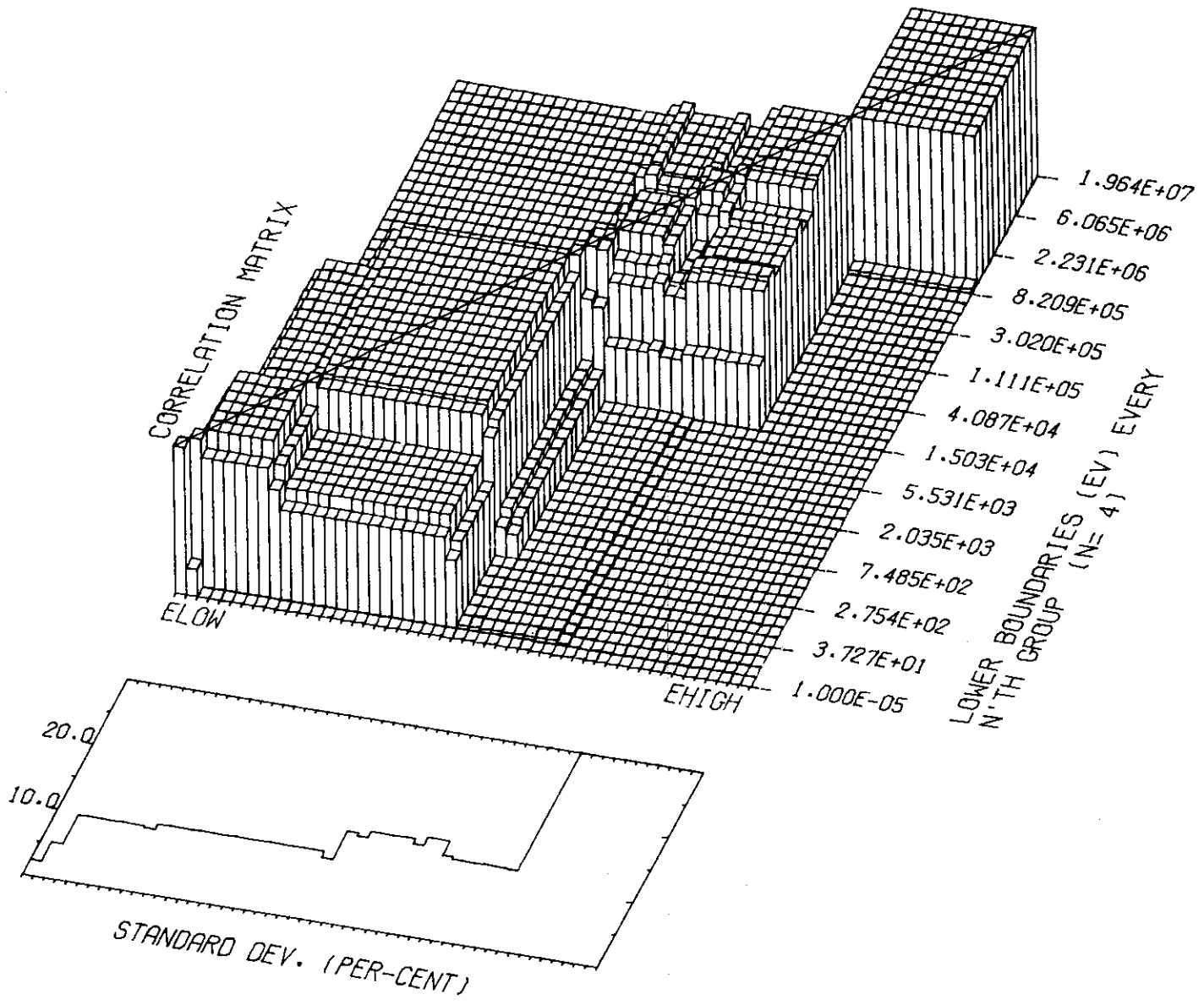


Fig. 6. PU-239 CAPTURE CORRELATION MATRIX

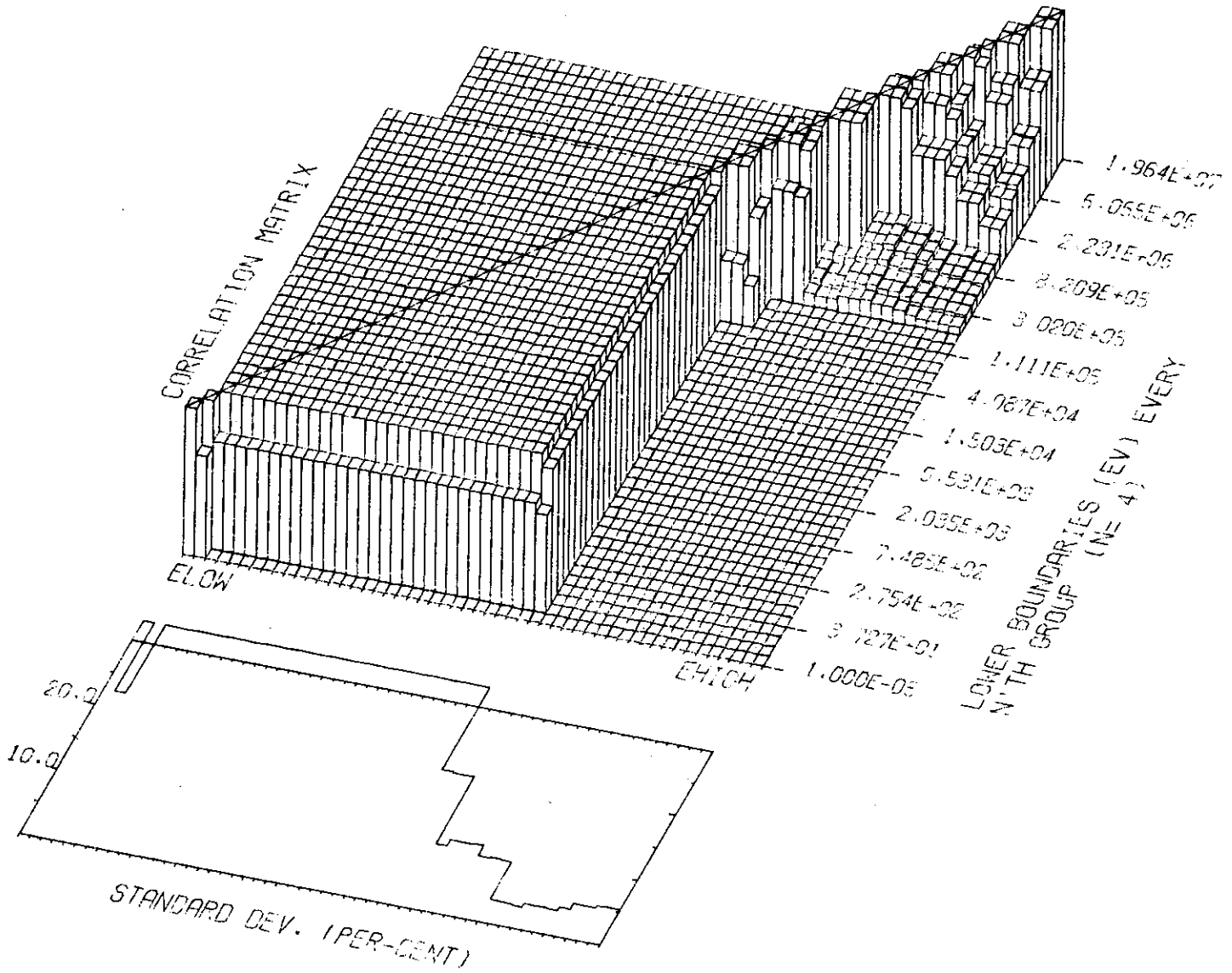


Fig. 7. PU-240 FISSION CORRELATION MATRIX

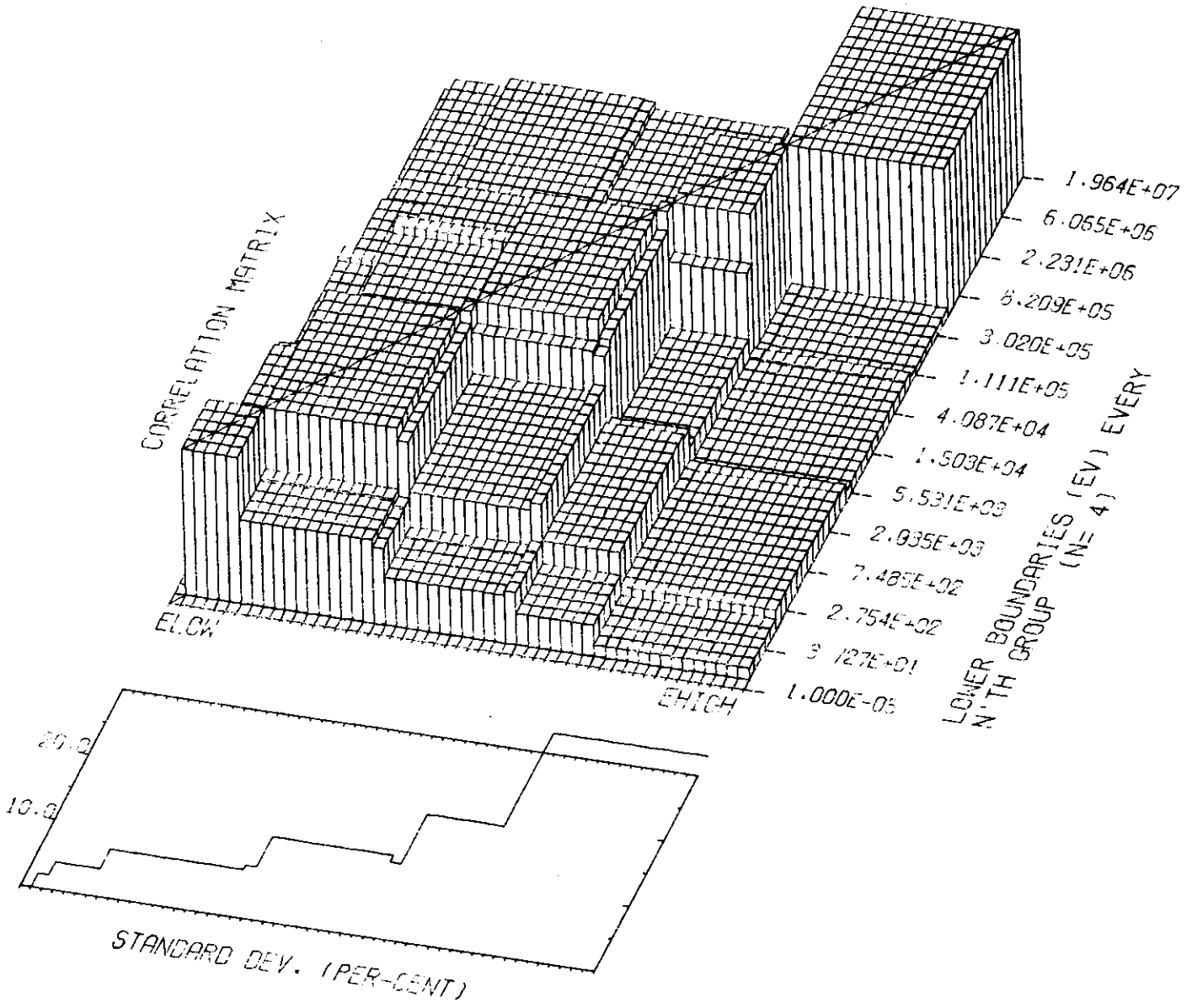


Fig. 8. PU-240 CAPTURE CORRELATION MATRIX

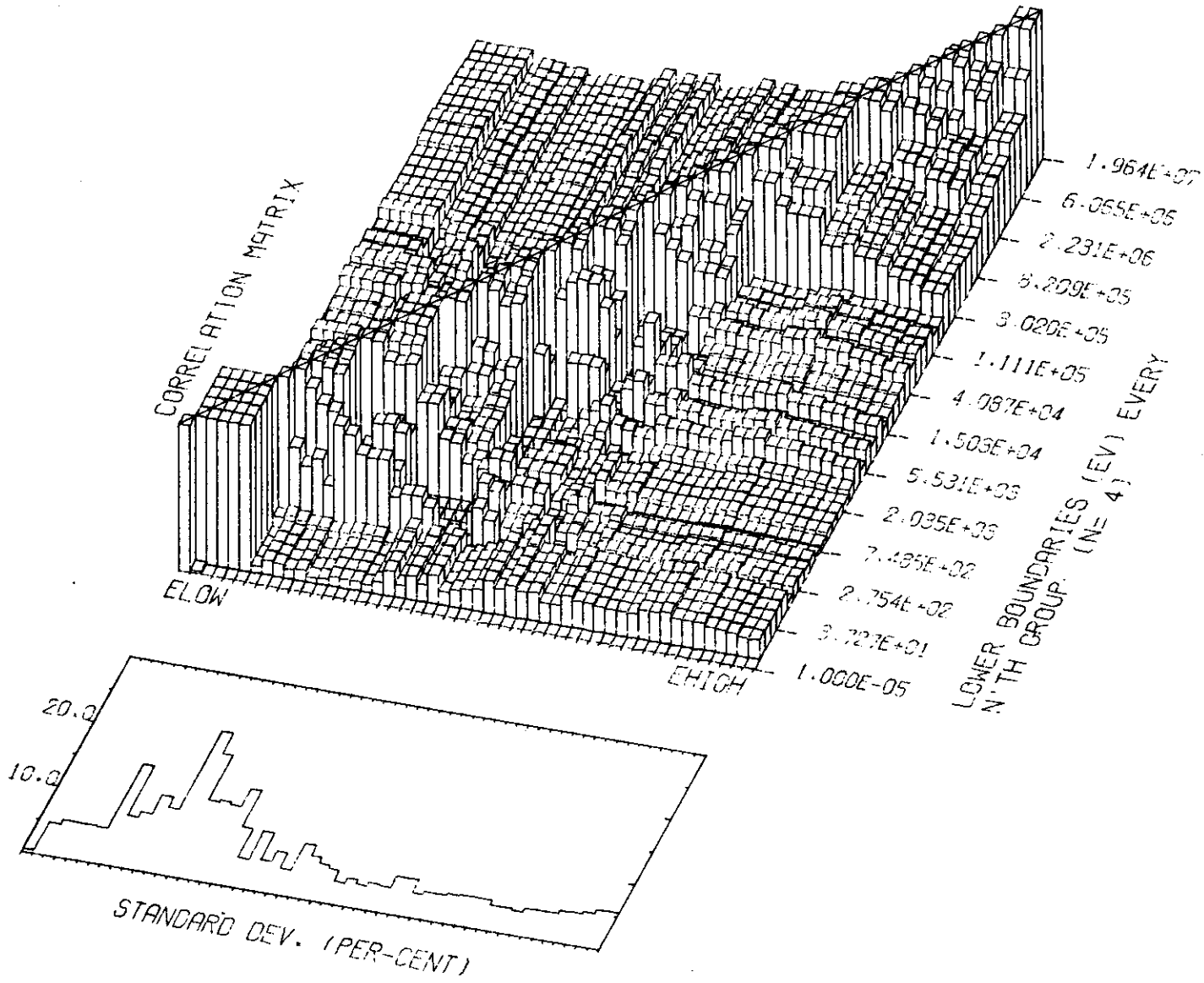


Fig. 9. PU-241 FISSION CORRELATION MATRIX

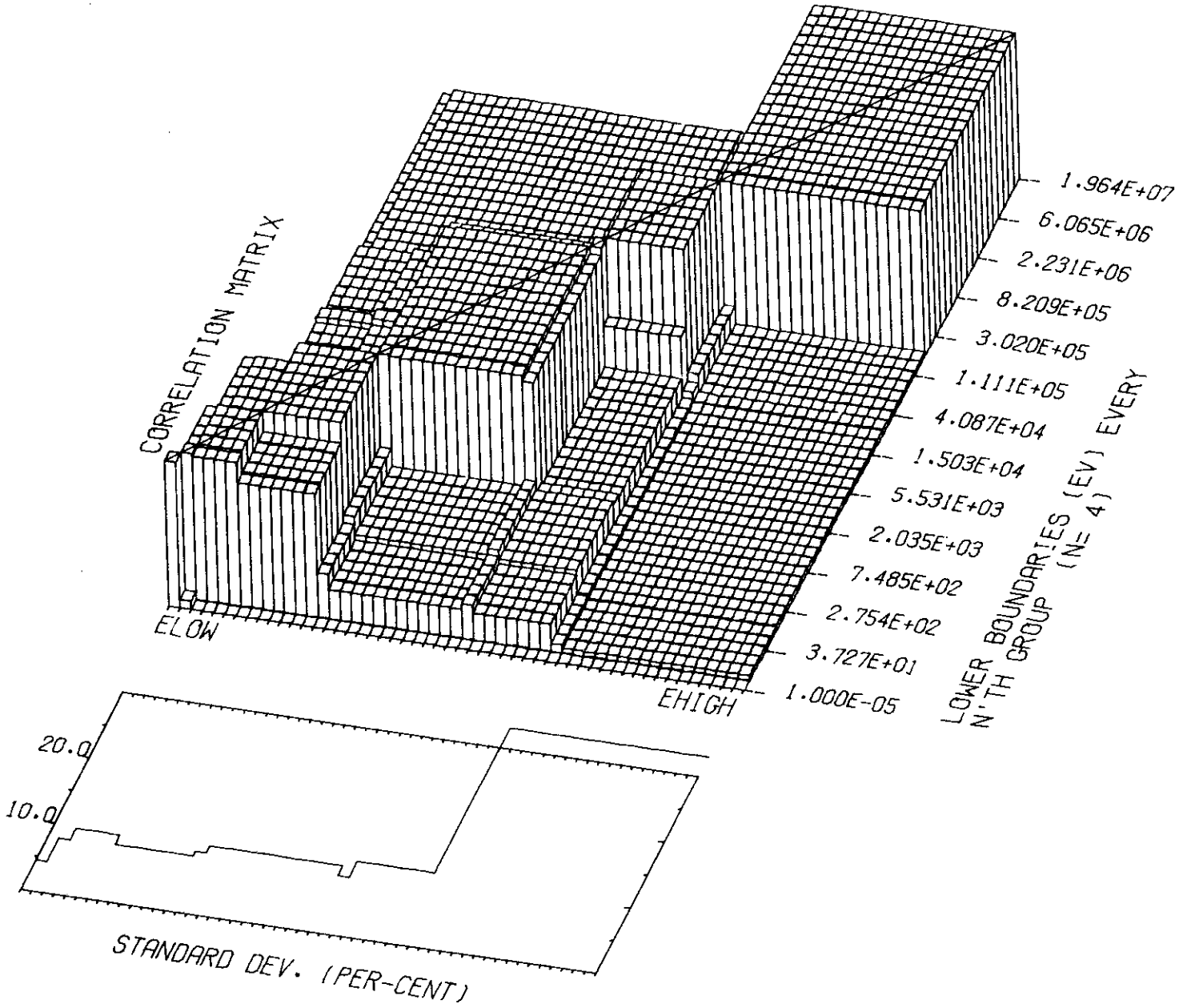


Fig. 10. PU-241 CAPTURE CORRELATION MATRIX